SYNTHESIS AND BIOLOGICAL STUDIES OF N,N'-DIARYLFORMAMIDINE DITHIOCARBAMATE METAL COMPLEXES

BY

SEGUN DANIEL OLADIPO

(Student No 217077545)

Submitted in fulfilment of the academic requirements for the degree of Doctor of Philosophy in Chemistry, School of Chemistry and Physics, University of KwaZulu-Natal (Westville campus), Durban 4000, South Africa

As the candidate's supervisor, I have approved this thesis for examination.

Date: 25th September 2019 Signature: [redacted]

Supervisor: Prof. B. O. Owaga

DECLARATION 1: PLAGIARISM

I, Segun Daniel Oladipo, declare that:

(i) the research reported in this dissertation, except where otherwise indicated or acknowledge, is my original work;

(ii) this dissertation has not been submitted in full or in part for any degree or examination to any other university;

(iii) this dissertation does not contain other persons' data, pictures, graphs or other information, unless specifically acknowledged as being sourced from other persons;

(iv) this dissertation does not contain other persons' writing, unless specifically acknowledged as being sourced from other researchers. Where other written sources have been quoted, then:

  (a) their words have been re-written but the general information attributed to them has been referenced;

  (b) where their exact words have been used, their writing has been placed inside quotation marks and referenced;

(v) where I have used material for which publication followed, I have indicated in detail my role in the work;

(vi) this dissertation is primarily a collection of material, prepared by myself, published as journal articles or presented as a poster and oral presentation at conferences. In some cases additional material has been included;

(vii) this dissertation does not contain text, graphics or tables copied and pasted from the Internet, unless specifically acknowledged, and the source being detailed in the dissertation and in the Reference sections.

Signed: Segun Daniel Oladipo

DECLARATION 2: PUBLICATIONS

DETAILS OF CONTRIBUTION TO PUBLICATION that form part and /or include research presented in this thesis (include papers published and in preparation). My role in each paper is indicated. The * indicates corresponding author.

Paper 1

Segun D. Oladipo, Bernard Omondi* and Chunderika Mocktar. Synthesis and structural studies of nickel(II)- and copper(II)-N,N'-diarylformamidine dithiocarbamate complexes as antimicrobial and antioxidant agents, *Polyhedon* **2019**, 170, 722.

My contribution:

The research reported is based on the data I collected from the experimental study I did on the synthesis and structural study of nickel(II)- and copper(II)-N,N'-diarylformamidine dithiocarbamate complexes as antimicrobial and antioxidant agents and drafted the article. These were achieved under the supervision of my supervisor.

Paper 2

Segun D. Oladipo, Bernard Omondi* and Chunderika Mocktar. Novel Co(III) N,N'-diarylformamidine dithiocarbamate complexes: synthesis, characterization, crystal structures and biological studies. Manuscript submitted to *Applied Organometallic Chemistry*.

My contribution:

I synthesized the complexes, carried out the characterization and screened the complexes and ligands for antimicrobial and antioxidant studies and wrote the first manuscript and did the necessary corrections towards publication of the paper under the supervision of my supervisor.

Paper 3

Segun D. Oladipo, Fisayo A. Olotu, Mahmoud Soliman, and Bernard Omondi. Formamidine thiurams as potential anticancer drugs; synthesis, *in silico* insights and chemoinformatics evaluation. Manuscript submitted to *Future Medicinal Chemistry*, FMC-2019-0195.

My contribution:

I synthesized the compounds, carried out the characterization and wrote the section that entails the synthesis and characterization in the manuscript and carried out subsequent modifications towards publication of the paper under the supervision of my supervisors.

Paper 4

Segun D. Oladipo, Bernard Omondi* and Chunderika Mocktar. Novel Heteroleptic Cu(I) N,N'-diarylformamidine dithiocarbamate PPh_3 complexes: Synthesis, Structural characterization, Optical properties and *in vitro* biological studies. Manuscript in preparation

My contribution:

I synthesized the complexes, carried out the characterization and screened the complexes for biological studies and wrote the initial draft of the manuscript and carried out subsequent modifications towards publication of the paper. These were achieved under the direction of my supervisors.

Other contributions related to this work

Paper 5

Segun D. Oladipo and Bernard Omondi*. Novel Mercury (II) N,N'-diarylformamidine dithiocarbamate complexes: Synthesis, structural characterization and their use as a single source-precursor for the preparation of Oleylamine capped HgS nanoparticle. Manuscript in preparation.

My contribution:

I synthesized the complexes, carried out the characterization, thermolyzed the mercury (II) complexes to HgS nanoparticles, characterized the as-synthesized HgS nanoparticles and wrote the initial draft of the manuscript as well as carrying out subsequent modification towards publication of the paper. These were achieved under the guidance of my supervisor.

Paper 6

Segun D. Oladipo, Sizwe J. Zamisa and Bernard Omondi*. Synthesis and structural studies of Ag(I) N,N-diarylformamidine dithiocarbamate complexes. Manuscript in preparation.

My contribution:

I synthesized the complexes, carried out the characterization, wrote the initial draft of the manuscript and did the necessary corrections towards the publication of the paper. These were achieved under the supervision of my supervisor.

Paper 7

Segun D. Oladipo and Bernard Owaga*. Cadmium (II) N,N'-diarylformamidine dithiocarbamate and it's 2,2-Bipyridine adducts complexes: Synthesis, structural characterization and their use as a single-source precursor for the preparation of TOPO caped CdS nanoparticles. Manuscript in preparation.

My contribution:

I synthesized the Cd(II) dithiocarbamate complexes and it's 2,2-bipyridine adducts, carried out the characterization, thermolyzed the complexes to CdS nanoparticles and drafted the articles. These were achieved under the supervision of my supervisor.

[redacted]

Signed: Segun Daniel Oladipo

CONFERENCE PARTICIPATION

1. Segun D. Oladipo and Bernard Omondi

Dithiocarbamates to Thiuram disulfides: Synthesis, characterization and antioxidant studies. (Poster presentation at the college of Agriculture, Engineering and Science research day, 25th October 2018, Westville campus, UKZN).

2. Segun D. Oladipo and Bernard Omondi

Dithiocarbamates to Thiuram disulfides: Synthesis, characterization and antioxidant studies. (Poster presentation at the postgraduate research colloquium , 6th March, 2019, Durban University of Technology, Ritson Campus).

PREFACE

The experimental work described in this thesis is carried out in the School of Chemistry and Physics, University of Kwazulu-Natal, Westville campus, Durban from July 2017 to July 2019, under the supervision of Prof Bernard Owaga.

These studies represent the original work of the author and have not been submitted in any form for any diploma or degree to any tertiary institution. In any case where the work of others have been used, it has been acknowledged accordingly in the main text.

The chapters in this thesis are written as a set of discrete research papers, with an overall introduction, experimental procedures and final conclusion. All the chapters have been submitted for publication in internationally recognised peer-reviewed journals while some have been accepted and published.

ABSTRACT

In this work, N,N'-diarylformamidine dithiocarbamate metal complexes were synthesized and investigated for their antimicrobial and antioxidant properties. Eight symmetrical and unsymmetrical N,N'-diarylformamidine dithiocarbamates **DL1** – **DL8** were used to synthesize thiuram disulfide **1** – **6**, Ni(II) dithiocarbamate metal complexes **7** – **12**, Cu(II) dithiocarbamate metal complexes **13** – **18**, Co(III) dithiocarbamate metal complexes **19** – **24** and heteroleptic Cu(I) dithiocarbamate-PPh_3 complexes **25** – **32**. All ligands and the complexes were characterized using FT-IR, UV-vis, ^{1}H and ^{13}C NMR, mass spectrometry and by elemental analysis. The electronic and steric properties of the dithiocarbamate ligands were varied in a bid to investigate their effects biologically. All compounds synthesised were tested against Gram – positive bacteria *viz*; *S. aureus* and MRSA and Gram - negative bacteria *viz*; *S typhimurium*, *P aeruginosa*, *E coli* and *K pneumoniae*. In addition, DPPH and nitric oxide assay were used to investigate their antioxidant activities.

Compounds **1** – **6** were obtained in good yields with single X-ray crystal structures revealing the coupling of N,N'-diarylformamidine dithiocarbamates moieties with S—S covalent bond. **1 - 6** displayed better antimicrobial activity against *E. coli*, *S. typhimurium* and *P. aeruginosa* than **DL1** – **DL6** except against *K. pneumoniae* whereas **DL1** – **DL6** are more active than **1** – **6**. Compounds **1** – **6** and **DL1** – **DL6** were active against *S.typhimurium* with compounds **4** and **5** surpassed ciprofloxacin with MIC value of 0.2 µg/mL. **DL1** – **DL6** and **1** – **6** showed poor DPPH free radical scavenging ability when compare to ascorbic acid. *In silico* investigation and cheminformatics evaluation of 1 – 6 showed that **1** and **4** exhibited dual selective inhibitory activities towards the inflammatory machineries of cancer, Cyclooxygenase -1 and 2 and all the compounds had minimal violations of the Lipinski's rule.

Compounds **7** – **24** were obtained in good yields and the single crystal X-ray diffraction analysis of **7**, **11**, **12**, **14**, **17** and **18** revealed mononuclear neutral species in which the geometry around the metal centers is distorted square planar for Ni(II) and Cu(II) complexes and octahedral for Co(III) complexes (**19**, **20**, **22** and **23**). All complexes showed moderate to good antibacterial activities against Gram-negative, *Salmonella typhimurium*, *Pseudomonas aeruginosa*, *Escherichia coli* and *Klebsiella pneumoniae* and gram-positive, *Staphylococcus aureus* (methicillin resistant) and *Staphylococcus aureus* bacteria. Complexes **23** and **24** were more active than the standard, ciprofloxacin against *S. typhimurium E. coli*, *P. aeruginosa* and *K. pneumoniae*. **7 - 24** were more efficient than **DL1** – **DL6** as antioxidant agents. of found to

be. Complex **20** with an IC_{50} values of 2.84 x 10^{-4} mM and 0.27 mM displayed the highest DPPH and NO free radicals scavenging activities of all the compounds tested and along with **20**, even outdoing ascorbic acid.

Heteroleptic Cu(I) complexes **25** – **32** were obtained as a stable yellow powder with good luminescent properties and the structures confirmed by single crystal structures of **25** – **32**. The coordination is such that the copper atom is bound to two sulfur atoms from the dithiocarbamate ligand and two phosphorus atoms of the PPh_3 units resulting in distorted tetrahedral geometry. **25 - 32** showed low to moderate antibacterial potential against all the bacteria strains and moderate to good DPPH and NO free radical scavenging abilities. .

ACKNOWLEDGMENTS

I give glory, honour and adoration to God of all universe who has given me the strength, grace, love, joy and courage to the completion of this research work. To him alone all be the glory. I am highly grateful for and sincerely appreciate the unflinching support, unalloyed guidance, constructive criticisms, extremely love, and spirit uplifting assistance I received from my supervisor Prof B. O. Owaga which all together made this work achievable in due time. May the almighty God bless you abundantly sir. I extend my sincere appreciation to the administration staff and technical staff in the School of Chemistry and Physics (UKZN) for their assistance.

My special appreciation goes to my parents Late Mr A. O. Oladipo and Mrs C. F. Oladipo for raising me in the way of the Lord, believing in my dream and ensure I become a successful man in life, I say thank you so much. I love you Mum! I am indebted to my sibling; Mr & Mrs Adenika, Mr & Mrs Ibukun Oladipo and Mr & Mrs Seun Oladipo which all played a major role in my upbringing, I say thank you all. To all my extended family member, I also appreciate your love and prayers.

I thank all my lab mates in synthetic laboratory for the ideas shared, support and fun we had together. My profound gratitude to Mr Zamisa for his supports during this research work most especially in the area of crystallography. You are a rare gem bro, I say thank you.

Special thanks to School of Chemistry and Physics (UKZN) for providing lab space and equipment, which allowed me to carry out this research work successfully. I also thank Nano-Chemistry research group for their inputs to this work, most especially their criticisms and corrections during group presentation.

I owe the following a lot of gratitude for being there for me at one point or the other, Dr Kunle, Dr Olatunji, Dr Habeeb, Dr Fisayo, Dr Andrew, Dr Gideon, Dr & Mrs Aibinu, Dr Labulo, Dr James, Dr Segun, Mr Ejalonibu, Mrs Adesola, Miss Bimbo, Miss Lara, Mrs Iwalaye, Mr Damilola, Mr Bakare, Mr Silver, Mr Tosin, Miss Bukky, Mr Lewis, Mr Mosuru, Mr Bakare, Miss Maxime, Miss Denisha, Mr Vicent, Mr Joshua, Mr Gideon, Mr Femi, Mrs Regina, Mr Shoyiga, Mr Mhkize, Mr Segun, Miss Kareen, Mr & Mrs Joseph, Miss Nike, Miss Damilola, Miss Thandeka, Miss Esther, Miss Isabel, Mr Attairuh and Miss Abimbola Awodire.

My prayer is that, may the Almighty God bless you all and may we all have reasons to celebrate in all the areas of our life. Amen.

DEDICATION

This work is dedicated to the KING OF KINGS, the LORD OF LORDS and the ALMIGHTY GOD. And to my LOVING MOTHER for her love, care and invaluable contributions towards my academic pursuit.

.

LIST OF ABBREVIATIONS AND SYMBOLS

Contents	**Page**
Å	Ångstrom
AEAC	Ascorbic acid equivalent antioxidant capacity
Calcd	Calculated
$CDCl_3$	Deuterated chloroform
$(CD_3)_2SO$	Deuterated dimethyl sulfoxide
COX-1/2	Cyclooxygenase-1/2
°C	Degree Celsius
δ	Delta representing a chemical shift
d	Doublet
DCM	Dichloromethane
DFT	Density function theory
DPPH	2,2-Diphenyl-1-picrylhydrazyl
DMF	Dimethylformamide
DMSO	Dimethylsulfoxide
DNA	Deoxyribonucleic acid
DTCs	Dithiocarbamates
ESI-MS	Electrospray ionization mass spectroscopy
FT-IR	Fourier transform infrared spectroscopy
g	Gram(s)
g mol^{-1}	Gram per mole
h	Hour(s)
HIV	Human Immune-deficiency Virus
Hz	Hertz

IC_{50}	Inhibitory concentration 50 %
^{i}Pr	Isopropyl
J	Coupling constant
L	Litre
m	Multiplet
Me	Methyl
MHZ	Mega hertz
mM	Millimolar
mL	Millilitres
µL	Microlitre
MIC	Minimum inhibitory concentration
min	Minutes(s)
mmol	Millimoles
mol	Moles
MRSA	Methicillin-resistance staphylococcus aureus
MW	Molecular weight
NMR	Nuclear Magnetic resonance
PPh_3	Triphenylphosphine
PDB	Protein data bank
ppm	Parts per million
ppt	Precipitates
ROS	Reactive oxygen species
Rof	Rule of five
s	Singlet

t	Triplet
UV-vis	Ultraviolet-visible
THF	Tetrahydrofuran
υ	Wavenumber
σ_{rt}	Electrical conductivity at room temperature
Ω cm	Ohm-centimeter
SCm^{-1}	Siemen per centimeter

TABLE OF CONTENT

LIST OF TABLES

LIST OF FIGURES

LIST OF SCHEMES

CHAPTER ONE

INTRODUCTION AND LITERATURE REVIEW

1.0 General Introduction

In living systems metal ions have significant functions and has become key in research for medicinal purpose. The deficiency of electrons in metal ions allows them to attract, bind and interact with electron rich biological molecules such as DNA and proteins. Such interactions enable metal ions to carry out tasks such as transporting oxygen in the body, regulating the functions of genes in cell nuclei and controlling sugar metabolism. Futhermore they are one of the vital components in metalloenzymes [1, 2]. With such important roles, it is not a surprise that study of metal complexes is significant in the field of medical sciences [3]. Although the use of metal complexes, as both therapeutic and diagnostic agents, can be traced back as far as 3500 BC [4], medicinal inorganic chemistry as a specific discipline came gained prominence when the anti-tumour activity of cisplatin was discovered. This breakthrough stimulated research interest in finding new metal complexes that could serve as modern diagnostic agents, such as bismuth(III) complexes for the treatment of ulcers, silver(I) complexes as antimicrobial agents and gold(I) complexes as anti-arthritic agents [5, 6]. In designing metal complexes for the specific pharmaceutical purpose of diagnostic or therapeutic agents, important factors such as the types of ligands, coordination geometry and choice of oxidation state are often considered [7] in order to control their thermodynamic and kinetic properties [8]. The mechanism through which the therapeutic agents work can also be affected by their lipophilicity, electric charge and redox behaviour [3].

Dithiocarbamates (DTCs), together with their metal complexes have been known to possess biological properties [9-12] and, in the past decades, those with a broad spectrum of biological activities have been a major research field [13]. DTCs are often synthesized by the reaction of either primary or secondary amines with carbon disulfide in the presence of a base, while their metal complexes are prepared via simple ligand displacement reactions following the addition of the dithiocarbamate salt to a metal precursor in the appropriate ratio [10, 14, 15]. The electronic properties of DTCs, and their structural architectures and applications, are influenced by the easily electronically tunable amines used in making the dithiocarbamate metal complexes [16]. Organic compounds such as imidazole [17], indoline [18], piperazine [19, 20], 1,2,3,4-tetrahydroisoquinone [19], N-methylbenzylamine [21], thalidomide [9], propranolol

[11], cyclohexylamine [22] and pyrrolidine [23], among others with a primary or secondary amine functional group have been used to synthesize DTC metal complexes for different purposes. For this study, symmetrical and unsymmetrical N,N'-diarylformamidine will be used as a source of secondary amine. Formamidines belong to a class of organic compound with the general molecular formula $R^1N=C(H)NHR^2$ where R^1 and R^2 can be either an alkyl or an aryl substituent. If $R^1 = R^2$ we have symmetrically substituted formamidines, and when $R^1 \neq R^2$ we have unsymmetrically substituted formamidine. While different methods have been employed to synthesize formamidines [24-27], to prepare bulky N,N'-diaryl formamidines the reaction of choice has been that between amines and triethyl orthoformate, using the appropriate molar ratio in the presence of glacial acetic acid as catalyst [28, 29]. In solution formamidines exist as four isomers (**Scheme 1**) [9, 22], and this phenomenon leads to complex, and seldom accurate, NMR spectra reported in the literature [11].

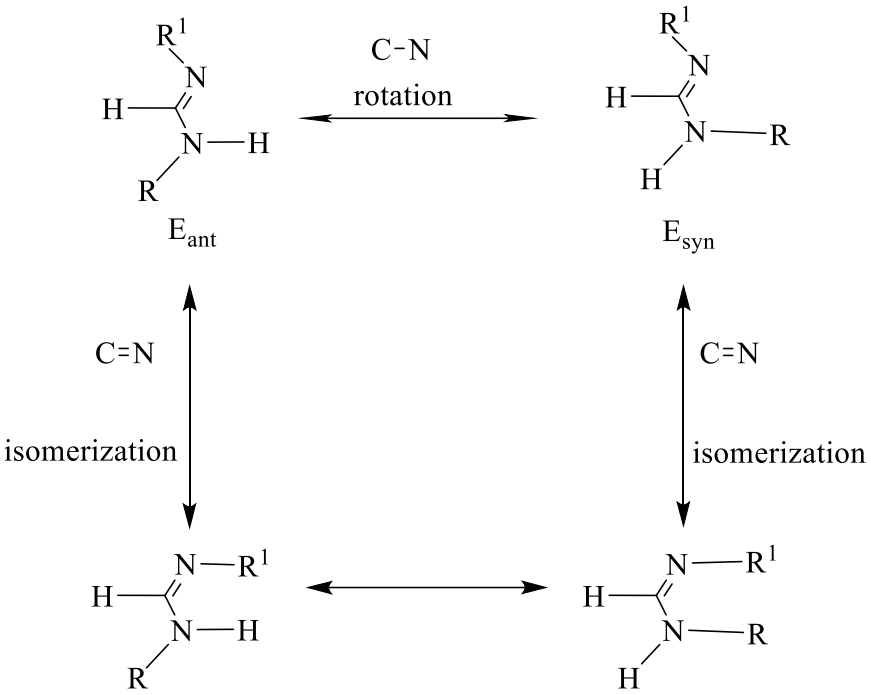

Scheme 1.1: Isomerism of formamidines in solution **[24]**

Formamidines have shown antimicrobial activity against chloroquino-resistant strain of bacteria [30]. It can, therefore, be envisaged that using them as a source of a secondary amine in preparing DTC metal complexes would enhance their biological activity, due to an increase in the electronic conjugation of the formamidine system in the dithiocarbamate metal complexes.

Biological activities of DTC metal complexes have been reported [31, 32] and their versatile pharmacological properties can be associated with presence of sulfur as well as metal chelate formation in their structures [33, 34]. The resemblance between the metal-sulfur system in DTCs and those present in biomolecules, especially metal-sulfur enzymes [35], drew the attention of researchers to dithiocarbamate metal complexes, in order to to gain insight into them [33]. In medicine, they are used as anticancer [9, 36], antimicrobial [22, 37], antioxidant [38, 39] and anti-HIV [40] agents. We next focus on studies concerning the antibacterial and antioxidant properties of dithiocarbamate metal complexes.

DTC complexes have been extensively used as antibacterial agents [34, 41-43]; their antibacterial properties being possibly associated with their ability to interfere with vital metabolic processes taking place in the cells [18]. An advantage of DTC complexes is the presence of functional groups that help transport them to important physiological enzymes or co-enzymes having H—S group, where the enzymes are inhibited, as well as interfering with cellular processes, thereby leading to lysis [44]. Generally, the transition metal of DTC complexes displayed better antibacterial activities than DTC as free ligands [39, 45]. Exceptions included a few cases where the ligand exhibited higher activity than some of the complexes, including fluconazole, one of the standards used in the study [43]. The enhanced antibacterial activity of the complexes can be best elucidated using chelation theory. To elaborate, upon coordination of the free ligand to metal ions, the polarity of the metal ions is reduced as a result of delocalization of the p-electrons over the chelate ring, as well from partial sharing of ions' positive charge with the donor group, which leads to the increase in lipophilic properties of the central metal ions, thereby favouring the permeability of complexes through the lipid layer of cell membrane [11, 46].

Another important property of DTC metal complexes is the antioxidant activity, which has been researched and reported in literatures [38, 47]. The antioxidant activity potential of DTCs and their metal complexes may be attributed to the electron donating ability of the transition metals ions and sulfur atoms in their various complexes, which resulted in their scavenging free radicals and hydroxyl ions [47]. Antioxidants protect organisms and cells from damage induced by oxidative stress [48]. Oxidative stress is caused by the presence of reactive oxygen species (ROS), such as the superoxide radical anion ($O_2^{\bullet-}$), hydroxyl radical ($OH^{\bullet}$) and hydrogen peroxide (H_2O_2). ROS species are known to cause damages such as cancerous inflammations, angiocardiopathy, diabetes, Parkinson's disease, Alzheimer's disease, and

other neurodegenerative diseases [49]. Apart from their health benefits, antioxidants are also used in the food processing and cosmetics industries [50].

Apart from DTC metal complexes, the oxidized form of dithiocarbamates, known as thiuram disulfides, have been reported to have excellent biological applications [51-54]. Iodine oxidation of appropriate dithiocarbamate salts produces thiuram disulfide compounds [51]. Thiuram disulfides are known to be active biologically and have been used in anticancer treatments [51, 55], as fungicides [56], for antibacterial purposes [54, 57], to arrest HIV infections and acquired immunodeficiency syndrome (AIDS) [58] and also in treating alcoholism because of their inhibitory effect upon liver alcohol dehydrogenase [54]. These versatile biological applications have been attributed to a combination of at least two factors. These are, firstly, the tendency of thiuram disulfides to undergo reversible redox reaction at an appropriate potential, and secondly, their ability to fit in into receptor sites in targeted cells [59]. In this study, we investigated the potency of N,N'-diarylformamidine-based thiuram disulfide as anticancer agents, using computational modelling, and pre- determined their drug-likeness and oral bioavailability using cheminformatics methods.

In the literature, it has been reported that Cu(I) complexes, with phosphine as auxiliary ligand, displayed good biological activity [60-66]. With this in mind, we synthesized heteroleptic Cu(I) dithiocarbamate-PPh_3 complexes and probed their biological activity. In addition, photoluminescence properties of the synthesized Cu(I) complexes were also investigated.

1.1 Dithiocarbamates

Dithiocarbamates ($R_2CNS_2^-$) belong to a class of compound known as 1,1-dithiolates [10, 67]. This group of compounds includes, among others, dithiocarboxylates, xanthates, and dithiophosphinates (**Table 1**) [68]. Dithiolates are generally formed by reacting suitable nucleophiles with carbon disulfide under appropriate experimental conditions. Due to their simple method of preparation, an extensive chemistry has developed around these compounds [69], which has led to their diverse applications as agrochemicals [12, 22], pharmaceuticals [9, 70], intermediates in organic synthesis [71-73], as protecting groups in peptide synthesis [74, 75], as chelators in material chemistry [76].and in synthesis of ionic liquids [77]. DTCs coordinate to metal ions in a unique way, due to their S—C—S delocalized electronic system [78]. They can stabilize metal ions in various oxidation state and coordination geometry [79], due to the characteristic dithiocarbamate and thiouride tautomers that are formed [80].

Table 1.1: Typical examples of 1,1-dithiolate ligands

Composition	Structure	Name
$R_2NCS_2^-$	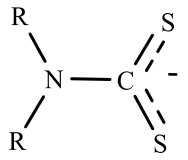	dithiocarbamate
$ROCS_2^-$	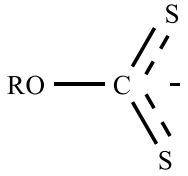	Xanthate
RCS_2^-	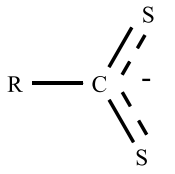	dithiocarboxylate
OCS_2^{2-}	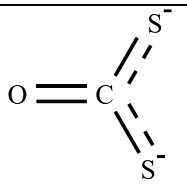	dithiocarbonate
CS_3^{2-}	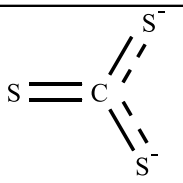	trithiocarbonate
$R_2PS_2^-$	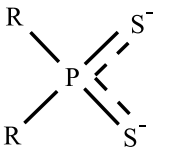	dithiophoshinate
$(RO)_2PS_2^-$	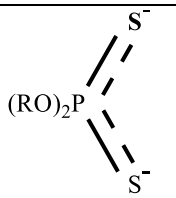	dithiophosphate

The dithiocarbamate complex is a soft ligand and stabilizes soft metals centre at low oxidation state. The lone pair of electrons localized on the nitrogen atom, which leads to substituents being arranged in a pyramidal fashion. This form of complex contains a single bond between the nitrogen atom and the carbon atom bonded to sulfur, and delocalization of -1 charge among the carbon and two sulfur atoms. Thiouride is a hard ligand and stabilizes hard metals centre

with high oxidation states. It is planar, with the lone pair of electrons on the nitrogen atom being delocalized, resulting in double bond character between nitrogen and the CS_2 carbon, while the two sulfur atoms both possess negative charges [80-83]. The structure of DTCs can be described by four resonance structures as shown in (**Fig 1.1**) [17]. In elucidating the overall structure of DTCs, the contribution of structure (IV) is considered significant due to the predominant υ(C—N) band that appears in the region 1480 - 1550 cm^{-1} of the IR spectra of dithiocarbamate [20, 84, 85].

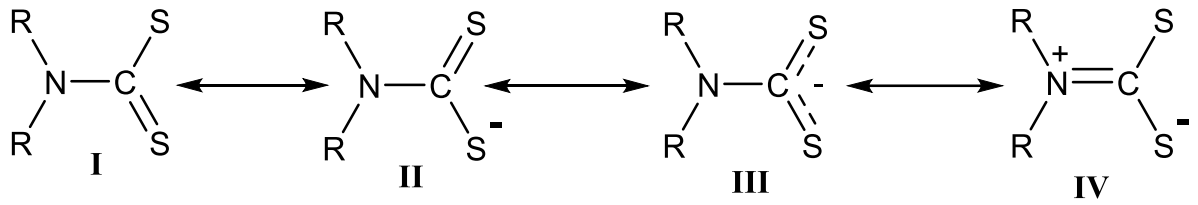

Figure 1.1: Resonance structures of dithiocarbamate moiety

The consequence of the above resonance behaviour is that DTCs can be strong or weak field ligands, depending on the substituents. If the 'dithiocarbamate' form (**III**) dominates then it is considered a strong field ligand and if 'thiouride' form (**IV**) dominates it is considered a weak field ligand [69]. The significances of both forms arise when the ligand is bound to metal ions such as Fe(III), where the electronic configuration of the low spin is different from that of high spin, according to crystal field theory [86].

1.1.1 Synthesis and properties of dithiocarbamate salts

Dithiocarbamates are generally prepared by the nucleophilic addition reaction of primary or secondary amines (nucleophiles) and carbon disulfide (CS_2) in the presence of a base as a proton acceptor, which is usually sodium hydroxide, potassium hydroxide [11, 85, 87] or ammonium hydroxide [88, 89] (**Equations 1.1** & **1.2**). Reactions are usually carried out in an appropriate solvent, such as water, methanol , ethanol or tetrahydrofuran (THF) [51, 90, 91]. To prepare dithiocarbamate salts of aromatic amines, strong bases such as sodium hydride (NaH) in THF and potassium hydroxide in dimethyl sulfoxide (DMSO) can be used because carbon disulfides reacts less readily with aromatic amines (especially diarylamine) [92]. These reactions are best carried out at a low temperature using an ice bath; under such conditions, they usually proceed with no side product. At high temperatures, undesirable side products are unavoidable. Purification can be achieved by crystallization and in some cases washing with a suitable solvent has been used to remove impurities from DTCs [92, 93]. DTCs synthesized

from primary amines are less stable than their secondary amine counterparts, and can decompose to give the corresponding isothiocyanate [94].

$$RNH_2 + CS_2 + MOH \longrightarrow RNHCS_2^-M^+ + H_2O \quad (1)$$

$$R_2NH + CS_2 + MOH \longrightarrow R_2NCS_2^-M^+ + H_2O \quad (2)$$

M = K, Na or NH_4

Apart from primary and secondary amines, many other organic compounds with an N—H bond can also serve as a source of amine for the preparation of dithiocarbamates. These reactions commonly involve the addition of carbon disulfide to the N—H group in an organic compound under suitable experimental conditions [17]. Such amino compounds have been used to synthesize dithiocarbamates, as is shown next.

- Synthesis from diamines

The nucleophilic addition reaction of CS_2 with diamines, in a 1:1 ratio, results in dithiocarbamate ligands with one DTC moiety (—NCS_2) [95], while the bis(dithiocarbamate) compound will be formed if the ratio of the CS_2 to diamine is in 2:1 as in Scheme 1.2 [96].

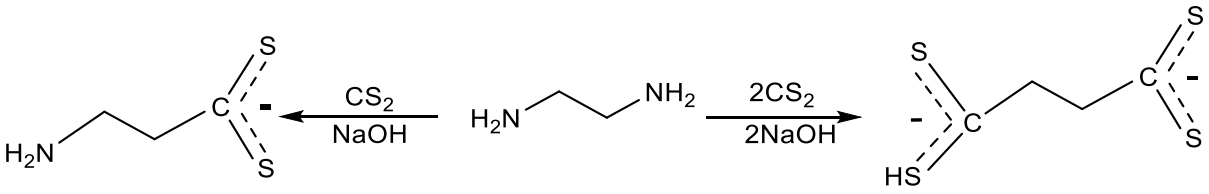

Scheme 1.2: Preparation of dithiocarbamates ligands from diamines

Fabretti *et al.* [97], showed that a similar transformation can be effected with piperazine as in Scheme 1.3.

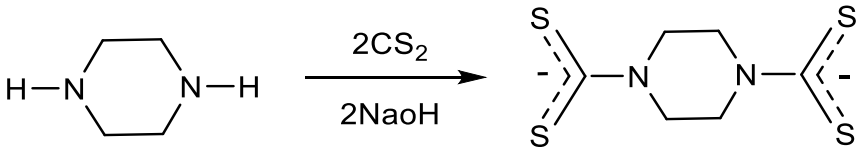

Scheme 1.3: Preparation of piperazine bis(dithiocarbamate) ligand

❖ From hydrazine

Hydrazine had been used to synthesize dithiocarbamate salts (**Scheme 1.4**). In the presence of a base (MOH), it reacts with carbon disulfide to afford a dithiocarbamate salt, NaS_2CNHNH_2 [98], and if a greater proportion of base and carbon disulfide are used, $Na_3S_2CNHCS_2$ can be formed as a second product as seen in Scheme 1.4 [99].

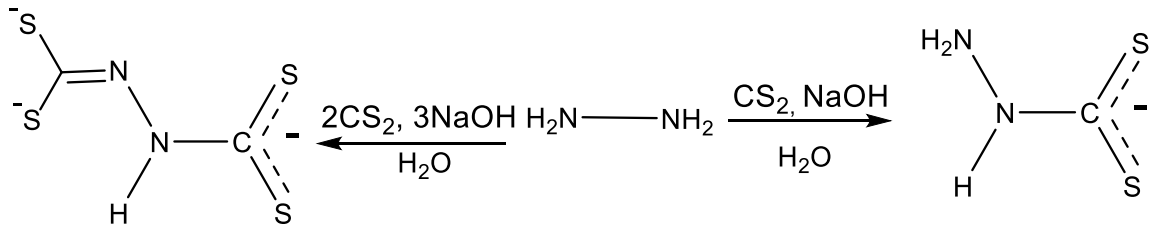

Scheme 1.4: Preparation of dithiocarbamate from hydrazine

In water, potassium and sodium salts of dithiocarbamate display good solubility, whereas they are mostly insoluble in common organic solvents. However, the ammonium salts are much more soluble in organic solvents than in water [69]. Studies have also shown that DTCs obtained from primary amines readily decompose under basic conditions to form isothiocyanates (**Scheme 1.5a**) [17, 92, 100], while in acidic condition, most DTCs decompose to form an amine and CS_2 (**Scheme 8b**) [11]. Meanwhile, those obtained from secondary amines are stable under basic and neutral conditions.

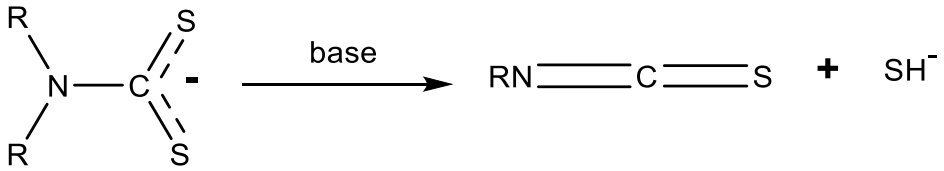

(**a**)

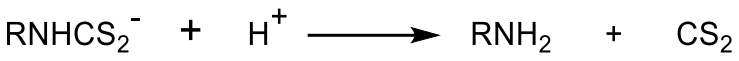

(**b**)

Scheme 1.5: Decomposition of dithiocarbamates (a) in basic medium (b) in acidic medium

1.1.2 Thiuram disulfide (oxidized form of dithiocarbamate salts)

Dithiocarbamates are readily oxidized by suitable oxidizing agents such as hydrogen peroxide, iodine or bromine, to form corresponding radicals, which then combine very fast to give

thiuram disulfides (**Scheme 1.6**) [10]. This process can be carefully monitored by cyclic voltammetry [101].

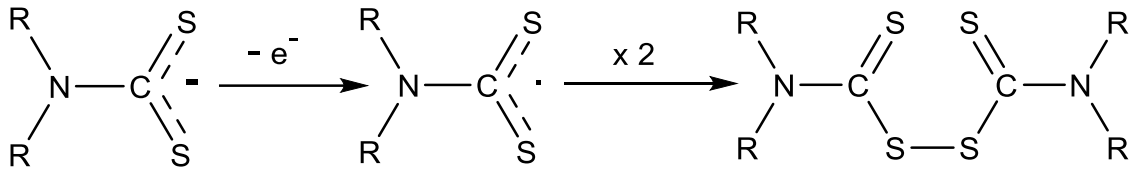

Scheme 1.6: Oxidation of dithiocarbamate to thiuram disulfide

For example, the oxidation of N'N-dibenzyldithiocarbamate using iodine as oxidizing agent produces tetrabenzylthiuram disulfides (**Scheme 1.7**) [102].

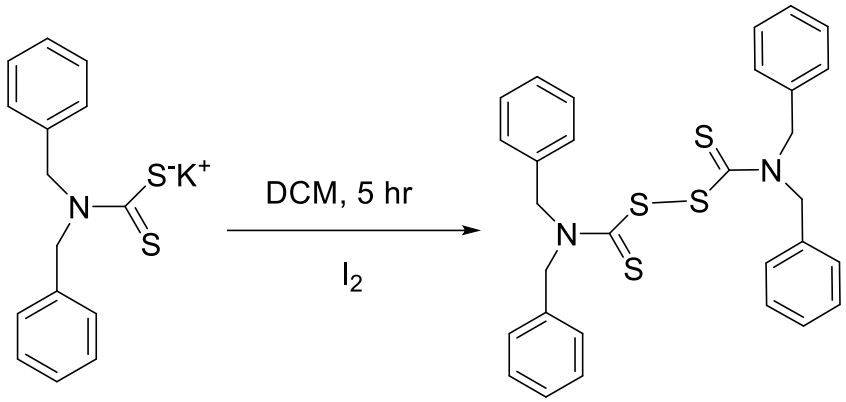

Scheme 1.7: Oxidation of N'N-dibenzyldithiocarbamate to give tetrabenzylthiuram disulfide.

1.2 Transition metal dithiocarbamate complexes

Transition metal dithiocarbamate complexes were first prepared in 1907 by Delépine [103] and over the years they have been prepared in a wide range of oxidation states [69]. The ability of dithiocarbamate ligands to form complexes with all metals is attributed to the presence of the sulfur atoms and the delocalization of a positive charge from the metal to the periphery of the complex [59, 100, 104]. They are reported to have versatile applications in several areas, such as agriculture [12, 78], analytical chemistry [105, 106] and solar energy [107]. They also possess good biological activity against certain pathogens, medicinal and botanical ; hence their use as anticancer, antioxidant, antifungal and antibacterial agents [9, 22, 36, 38]. Organically capped semiconductor metal sulfide nanoparticles of various sizes and shapes have been prepared, using dithiocarbamate metal complexes as a single-source precursor [23, 88, 91, 108, 109]. The complexes have also been used extensively as fungicides, scavengers for heavy metals, accelerators for vulcanization in rubber industries and as photo-sensitizer in photosensitized solar cells [110, 111].

1.2.1 Synthesis of transition metal dithiocarbamate complexes

Different methods have been utilized to prepare transition metal dithiocarbamate complexes. Among all these methods, the direct addition of the dithiocarbamate ligand to the metal salt precursor, will often, but not necessarily, result in the loss of the coordinated anionic ligand (**Scheme 1.8**). This route has few limitations and so complexes of all the transition metals have been prepared using it [69]. Importantly, the oxidation state of the metal does not change in the course of the reaction [10].

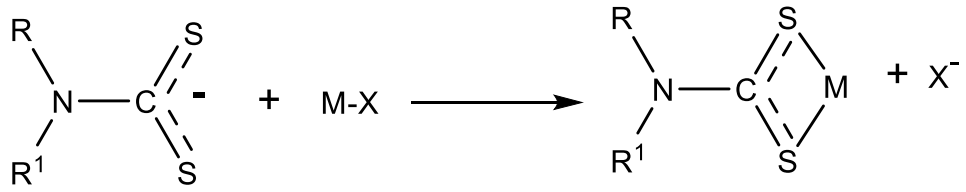

Scheme 1.8: Preparation of dithiocarbamate metal complexes by direct ligand addition.

Transition metal dithiocarbamate complexes can also be prepared using one pot synthesis, where the DTC complex is prepared in a single step (**Scheme 1.9**). The carbon disulfide and amine, dissolved in an appropriate solvent, are allowed to react for a short period of time followed by the addition of an aqueous solution of metal salt precursor [112]. The mixture is stirred vigorously and the metal complex precipitates upon refluxing for several hours [113, 114] or stirring at room temperature [115].

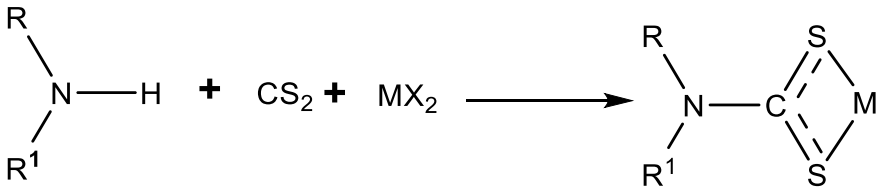

Scheme 1.9: One-pot synthesis of dithiocarbamate metal complexes**.**

Numerous other preparation methods include, cleavage of dithioesters [116], insertion of organic isothiocyanates into metal-thiolates [117] or metal hydride [118], and addition of a secondary amine to the relevant alkyltrithiocarbonate [119] or xanthate [120].

1.2.2 Binding modes of dithiocarbamate metal complexes

Dithiocarbamates are versatile ligands, capable of coordinating with up to four transition metal atoms in different ways, as illustrated in Figure **1.2 [69]**.

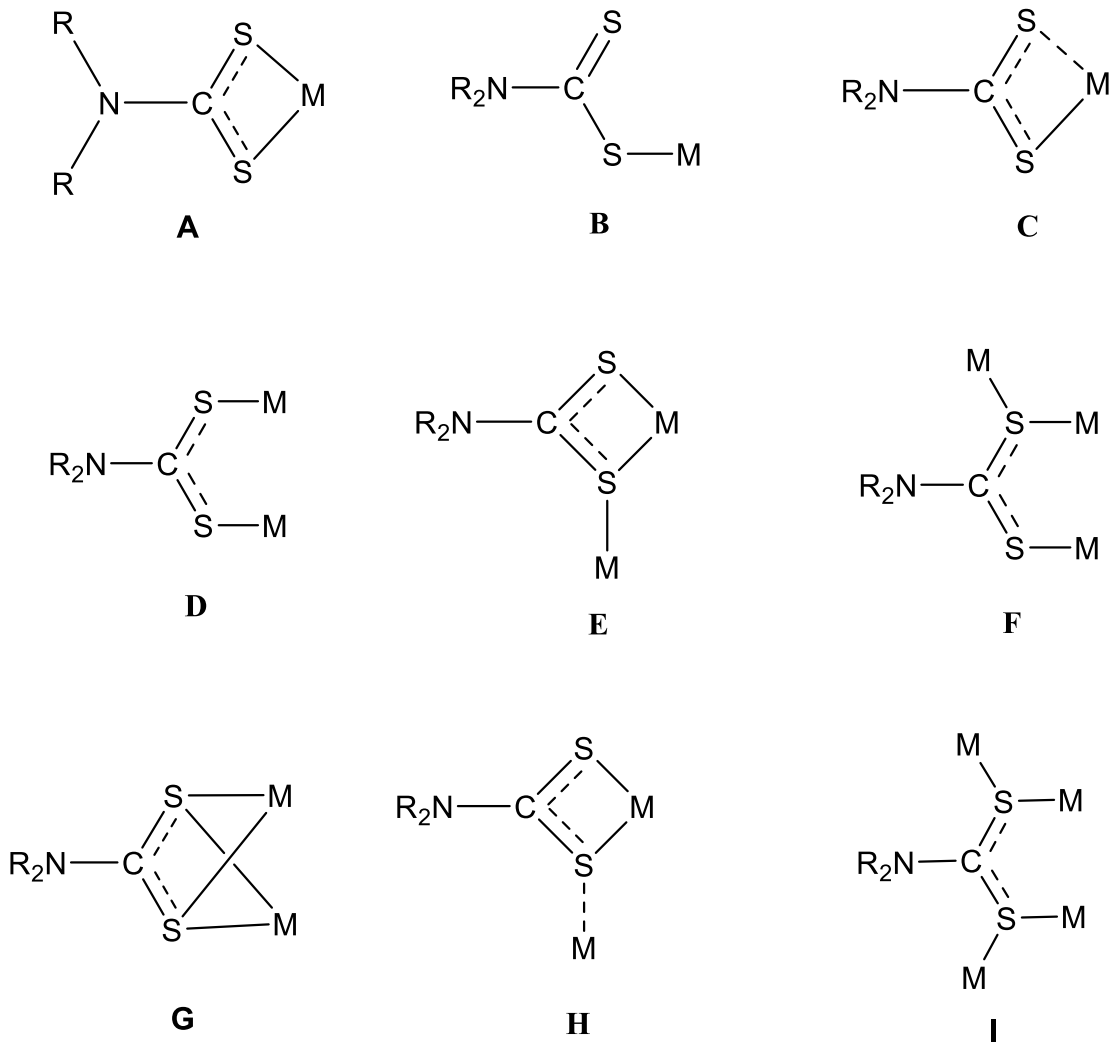

Figure 1.2: Dithiocarbamate binding modes.

Chelating mode **A** is the most common and is found in most transition metal complexes and allows the metal to be in a variety of oxidation states [10]. In coordination mode of **A**, the two metal-sulfur interactions are approximately equal and the ligand can be considered to be a net four-electron donor [69]. In doing so, it forms a S—M—S bond angle between 65 – 80 °, the angle being dependent on the size of the metal ion [69]. Coordination mode (B) is monodentate and is formed when electronic and steric demands of the second sulfur atom are high to coordinate to the metal centre. It could also arise from the electronic demands of the metal centre. For example, when the lone pair of electrons on the second sulfur atom cannot be used for bonding because the metal centre has no vacant orbitals of either correct symmetry or energy to accept it. This coordination mode is relatively common, especially in gold chemistry, where, for example, gold (III) complexes,$[Au(S_2CNR_2)_3]$, contain one chelating and two monodentate dithiocarbamate ligands [121]. Anisobidentate coordination mode (**C**) is another

binding mode commonly displayed by dithiocarbamates. In this mode, the two metal-sulfur bonds are relatively different, but nevertheless within the expected range for such bond length [122, 123].

All other coordination modes are seldom mentioned in the literature and have not been tested biologically. While, modes (**D, E** and **F**) are more common than are (**G**, **H** and **I**), they all involve the dithiocarbamate coordinating to two, three or four metal atoms, as seen in the face-capped copper cube, $[Cu_8(\mu_4\text{-}S_2CNPr_2)_6ClO]_2$ [10, 124]. In binding mode **D**, each sulfur atom of the —NCS_2 moiety of the dithiocarbamate ligand binds to a single metal centre in an η^1, η^1-manner. Although mode **D** is not particularly common, a significant number of complexes have been characterized structurally in this mode [69, 125, 126]. In binding mode **E**, one sulfur atom coordinates with the two metal atoms, such that all the three metal—sulfur bond length are often similar. This mode of bonding is common in ruthenium [127-129], osmium [130, 131] and other late transition metal dithiocarbamates [132-134]. In mode **F** the dithiocarbamate caps three metal atoms while, in mode **I**, the dithiocarbamate caps four metal atoms. These two binding modes are uncommon and limited to late transition metals [69]. In **G**, the two sulfur atoms in –NCS_2 of the dithiocarbamate unit bind to each metal atom as shown in Figure 1.2. Only a few examples of this mode of binding can be found in the literature and it seems to be restricted to only dirhodium complexes [69]. Mode **H** is similar to **E**, but the interaction is not symmetrical as in **E** it is usually seen only in the solid state and the structure is lost upon dissolution [69].

1.3 Heteroleptic copper(I) complexes with phosphine compound as coligand

Heteroleptic complexes is comprised of a metal centre coordinated to two or more type of ligands.and they receive current interest in coordination chemistry due to the usefulness and structural diversity among coordination compounds [135]. In bio-inorganic chemistry, they possess a unique role due to their ability to mimic biological molecules in their tendency to compete among millions of potential ligands for metal ions *in vivo* [136]. Heteroleptic complexes have been reported to display properties such as non-linear optical application [137], electrical conductivities [138] and antimicrobial activities [139, 140]. Heteroleptic Cu(I) complexes with phosphine compound as coligand have been studied, due to their biological activity [141-143] and interesting photoluminescent properties. These properties have possible technological application related to imaging in probing biological cells [144], energy conversion in solar cells [145-149], and as light emmiters in electrochemical devices [150-

154]. The excellent luminescent properties of Cu(I) complexes could be attributed to their $3d^{10}$ configuration with no low-energy ligand-field transition, which enables low-energy transfer excited state [155]. In Cu(I) complexes with phosphine as coligand, their electronic and luminescence properties are influenced by the nature of substituents, which in turn affects the conjugation of charge in the complexes. Copper(I) salts form clusters with dithiocarbamate, xanthate, and dithiophosphate ligands. However, the coordination sphere around Cu(I) can be controlled by the use of bidentate nitrogen or sulfur atoms together with the strong σ-donor and π-acceptor bulky phosphine ligand, which makes their coordination tend towards tetrahedral geometry [156].

1.4 Mechanism of antimicrobial drugs and resistance to them by pathogenic bacteria

In 1670s, a Dutch scientist Antonie van Leeuwenhoek was the first to observe and describe microscopic bacteria, with the help of microscope. However, the ability of these bacteria to cause diseases was not known until the middle of nineteenth century when Robert Koch was able to explain the occurrence bacterial infectious diseases such as typhoid, tuberculosis and cholera [157, 158]. At the time, diseases such as tuberculosis and bacteraemia, caused by bacteria had high mortality rates. Survival rates for patients infected with such diseases remained very low until antimicrobial drugs were introduced in the 1940s [159, 160]. These antibiotics radically changed such a bleak prognosis and new antimicrobial drugs continue to be developed [161]. The main class of antibiotics and typical examples of each are given in **Table 1.2**.

Table 1.2: Main classes of antibiotics [161]

Class	Examples
β-Lactams	
Penicillin	Penicillin G, penicillin V, dicloxacillin oxacillin, nafcillin, ampicillin, amoxicillin, methicillin, cloxacillin
Carbapenems	Meropenem, imipenem
Monobactams	Astreonam
β-Lactamase inhibitors	Tazobactam, sulbactam, clavulanate
Aminoglycosides	Paromycin, gentamicin, streptomycin, tobramycin, amikacin, netilmicin, spectinomycin, neomycin, kanamycin

Tetracyclines	Tetracycline, demeclocycline, minocycline chlortetracycline, oxytetracycline, methacycline, doxycycline
Rifamycins	Rifampicin, rifapentine, rifabutin, rifaximin, benzoxazinorifamycin
Macrolides	Azithromycin, clarithromycin, Erythromycin
Lincosamides	Lincomycin, clindamycin
Glycopeptides	Vancomycin, teicoplanin
Streptogramins	Deflopristin, quinupristin
Oxazolidinones	Linezolid
Quinolones	Nalidixic acid, oxolinic acid, norfloxacin, pefloxacin, enoxacin, ciprofloxacin, temafloxacin, lomefloxacin, sitafloxacin
Sulfonamides	Sulfanilamide, para-aminobenzoic acid, sulfadiazine, sulfisoxazole, sulfamethoxazole, sulfathalidine
Others	Metronidazole, polymyxin, trimethoprim

Antibiotics have different effects on bacteria; hence they act in various capacities and some of the major antibacterial target are depicted in **Figure 1.3**. Some are bacteriostatic, acting by inhibiting bacterial growth, whilst others are bactericidal and act by killing bacteria [161]. The drugs achieve these outcomes by targeting vital components that bacteria make use of during their metabolism and so render the bacteria inactive [162, 163]. The main antibiotics target bacterial cell-wall synthesis, bacterial protein synthesis and bacterial DNA replication and repair processes [163]. For example, quinolones, such as norfloxacin, target DNA gyrase, which is an enzyme with a vital role in DNA replication [164], while β-lactam antibiotics, such as cephalosporins or penicillin, target the process of cell-wall synthesis [165]. Rifampicin targets DNA-directed RNA polymerase [166] and macrolides inhibit protein synthesis [167].

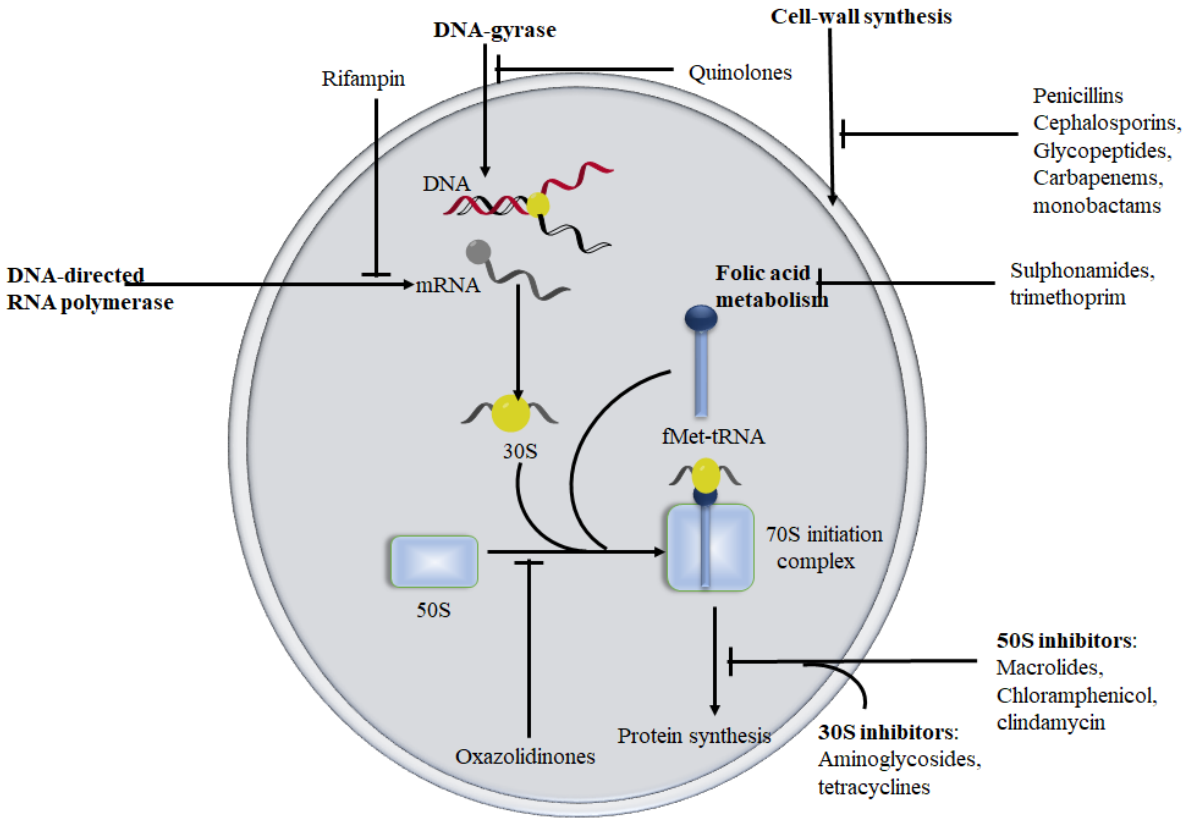

Figure 1.3: The five major antibacterial drug targets

Despite the different mechanisms used by different antimicrobial agents to combat bacteria, their resistant towards these agents keeps increasing [168]. Bacterial resistance to drugs arises through different means but depends mainly on the mechanism by which the antibacterial agents act, as well as their chemical structure. The bacterial mechanisms include altering the site of action [169], by-passing inhibiting steps, reducing the intracellular concentration of the antibacterial agents [170], modifying the structure of the drug thereby rendering it inactive [171] and extensive multiplication of the target enzymes by the bacteria [161]. Different ways at which antimicrobial agents are rendered inactive are illustrated in **Figure 1.4**.

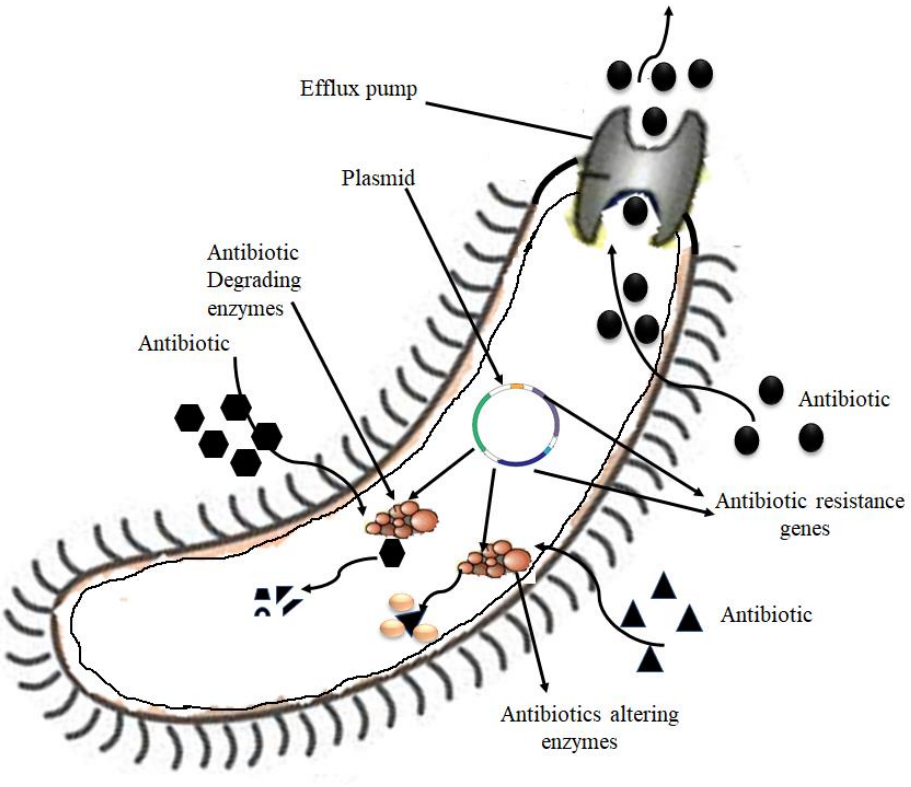

Figure 1.4: Diagram showing how some antimicrobial agents are rendered ineffective [168].

1.5 Free radicals and antioxidants in biological systems

Compounds with antioxidant activity are frequently suggested at the preliminary stage in developing new drugs for the treatment of pathological disorders that are caused by oxidative damage resulting from free radicals interacting with proteins [49]. The term 'free radical' refers to molecules or molecular fragments containing one or more unpaired electrons in their atomic or molecular orbitals [172]. The presence of unpaired electron(s) in free radicals makes them energetic and highly reactive [173]. Their generation by ordinary cellular digestion or exogeneous agents have been reported [174]. Reactive oxygen species (ROSs) are examples of free radicals which include hydroxyl radicals ($OH^{\bullet}$), hydrogen peroxide (H_2O_2), and superoxide anions ($O_2^{\bullet-}$). The superoxide anion ($O_2^{\bullet-}$) is formed by the addition of one electron to O_2 which occurs during metabolic processes or physical irradiation of O_2 [173]. The reduction of $O_2^{\bullet-}$ by the addition of a second electron gives hydrogen peroxide H_2O_2, which is formed as a by-product of lipid metabolism of peroxisomes with the help of certain enzymes. The hydroxyl radical ($OH^{\bullet}$) is thought to be formed through one-electron reduction of hydrogen peroxide (H_2O_2), a reaction that is facilitated by reduced transition metals i.e. reduced iron. [49]. ROSs can be either beneficial or harmful to biological systems [49, 175] One beneficial role is to

induce mitogenic response at low concentration. They also play physiological roles in cellular responses to *noxia*, such as enhancing cellular signals needed for good functioning and defending living system by killing infectious agents [176]. However, in high concentrations, ROS are deleterious to living systems. They contribute to damaging cell structures such as proteins and nucleic acid, lipids and cell membranes [177]. $OH^{\bullet}$ also interacts with different parts of the DNA molecule, damaging the deoxyribose backbone, purine and pyrimidine bases [172]. All these harmful effects of free radicals increase the risk of diseases such as asthma, cancer, angiocardiopathy, diabetes, Alzheimer's and Parkinson's diseases in human [177, 178].

In order to protect organisms and cells from damage induced by oxidative stress, scientific researchers have isolated natural compounds and developed synthetic compounds with antioxidant properties. For example, ascorbic acid, α-tocopherol, carotenoids, flavonoids etc. have been known to have good antioxidant activity [179]. Research is ongoing to develop compounds with better activity than the existing ones. Dithiocarbamates and their metal complexes have been reported to exhibit antioxidant properties [41, 180, 181]. Their free radical scavenging ability could be explained based on the electron donating ability of sulfur, as well as the nature of the central metal ions in their various complexes, both of which lead to stabilization of free radicals [41].

1.6 Application of dithiocarbamates and their metal complexes

DTCs and their metal complexes have been used in analytical chemistry [182-184], industry [185], biology [9, 33, 186], and as a source of single precursor to prepare semiconductor nanoparticles [90, 187-189]. Biologically, they have been tested as anticancer [9, 36], antimicrobial [22, 37], and antioxidant agents [38, 39], anti-alcoholic drug [190, 191], and as co-adjuvant in AIDS treatment [192]. In this section, the application of DTC metal complexes for biological purpose (primarily as antibacterial and antioxidant agents) shall be reviewed and their use as a source of metal sulfide nanoparticles shall be briefly discussed in the later part of this section.

1.6.1 Biological application of dithiocarbamate metal complexes

1.6.1.1 Dithiocarbamate metal complexes as antimicrobial agents

Several publications in the literature have reported the antimicrobial activities of DTC metal complexes, with first row transition metals. In this subsection, we focus on Ni(II), Cu(II) and Co(III) complexes and give their geometry as reported in the literature. Bobinihi *et al*. [193]

reported the synthesis of Ni(II), Pd(II) and Pt(II) complexes of dithiocarbamates derived from N-phenylaniline, 4-methylaniline and 4-ethylaniline as seen in **Figure 1.5**. Single X-ray crystal analysis of some of the complexes, namely bis(N-phenyldithiocarbamate)platinum(II), bis(4-ethylphenyldithiocarbamate)platinum(II) and bis(N-phenyldithiocarbamate)palladium(II), showed that they have distorted square planar geometry due to the small bite bond angle for (S—M—S) of 74.75(3)°, 74.93(2)° and 75.134(17)° respectively. The complexes were screened for their antimicrobial activities with bacteria species such as *S. aureus*, *K. Pneumonia*, *B. cereus*, *E. coli* and *P. aeruginosa* and fungi species *C. Albican* and *A. flavus* and the results showed that the metal complexes of sodium p-ethylphenyldithiocarbamates are the most active of those tested [193].

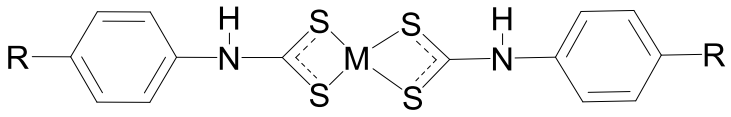

R = H, CH_3, and C_2H_5

M = Ni(II), Pd(II) and Pt(II)

Figure 1.5: Dithiocarbamate metal complexes of aniline derivatives.

Mambal *et al*. [22] conveyed the preparation of Ni(II), Co(II), Cu(II) and Zn(II) complexes of the type $[M(L)_2]$, **Figure 1.6** and the adduct containing monodentate phosphine of the type $[M(L)_2(PPh_3)]$, where L represents cyclohexylamine-N-dithiocarbamate and PPh_3 represents triphenylphosphine. Antimicrobial activities of the ligands as well as the complexes were evaluated against six bacteria and four fungi. Their results showed that the metal complexes displayed better antimicrobial activity compared to the dithiocarbamate ligands and the nickel complexes $[Ni(L)_2]$ was more active against the growth of fungi when 100—400 µg/mL were loaded at laboratory condition.

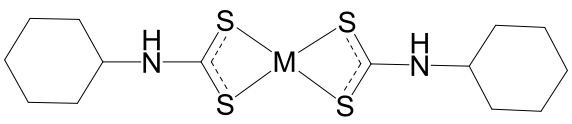

M = Ni. Co, Cu and Zn

Figure 1.6: Metal complexes of cyclohexylamine-N-dithiocarbamate

Islam *et al*. [194] reported the synthesis, characterization and biological activity of Ni(II) and Pd(II) with pyrrolidine-based dithiocarbamate ligand (**Figure 1.7**). Antibacterial activities of the complexes and the pyrrolidine dithiocarbamate ligand have been tested against four bacteria strains; viz, *Streptococcus pneumonia*, *E.coli*, *Vibrio cholerae* and *Bacillus cereus*. The complexes showed better antimicrobial activities compared to the ligand but not as active as the standard used, chloramphenicol. They attributed the higher antimicrobial activities of the complexes to the increase in delocalization of pi electron into the whole chelate ring of the complexes thus increasing their lipophilicity.

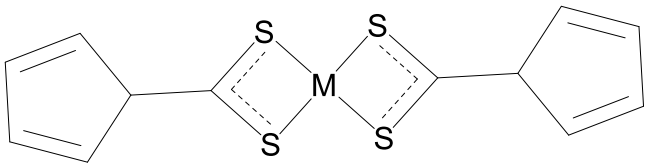

M = Ni and Pd

Figure 1.7: Metal complexes of pyrrolidine dithiocarbamate

A series of 3d transition metal dithiocarbamates formulated as $M(pdtc)_2$ [where M represents Mn(II), Fe(II), Co(II), Ni(II) or Cu(II)] and pdtc represents 1,4-phenyldiaminobis(pyrrole-1-sulfino)dithioate (**Figure 1.8**) have been synthesized and screened for their biological activities by Nami *et al.* [41]. They proposed tetrahedral geometry for all the complexes except Cu(II) which was found to be square planar. The ligand and the complexes were tested against *E.coli*, *Bacillus subtilis*, *Streptococcus pyogenes*, *Klebsiella pneumoniae*, *Staphylococcus aureus* and *Pseudomonas aeruginosa* using a disc diffusion method and chloramphenicol as a standard. Compounds have moderate to good antimicrobial activities and Cu(pdtc) was found to be as active as chloramphenicol. Molecular docking study showed that $Cu(pdtc)_2$ interacts effectively with the receptor molecule (amino acids), which is responsible for its high antimicrobial activities compared to other compounds.

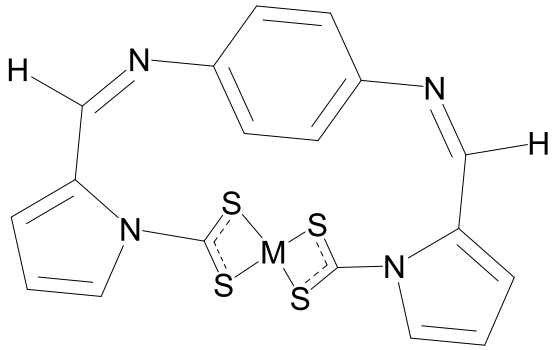

M = Mn(II), Fe(II), Co(II), Ni(II) and Cu(II)

Figure 1.8: Metal complexes of self-assembled 1,4-phenyldiaminobis(pyrrole-1-sulfino)dithioate.

Synthesis, characterization and biological studies of Cr(III), Mn(II), Co(II), Cu(II) and Pd(II) dithiocarbamate metal complexes using sodium N-ethyl-N-phenyldithiocarbamate were reported by Onwudiwe *et al.* [181]. Tetrahedral geometry was proposed for Mn(II), Co(II), Cu(II), while square planar and octahedral geometry were proposed for Pd(II) and Cr(III), respectively (**Figure 1.9**). The antimicrobial potential of each compound were evaluated against four bacteria, *E.coli*, *Staphylococcus aureus*, *Pseudomonas aeruginosa* and *Salmonella typhi* and two fungi, *Aspergillus flavus* and *Fasiparium oxysporium*. All the complexes showed moderate to good antimicrobial activities at a concentration of 100 µg/mL against the bacteria strains and fungi organism, apart from the Cr(III) complex, which showed no antibacterial activities. Their results also revealed that the complexes exhibited better activities as antibacterial agents than they did as antifungal agents.

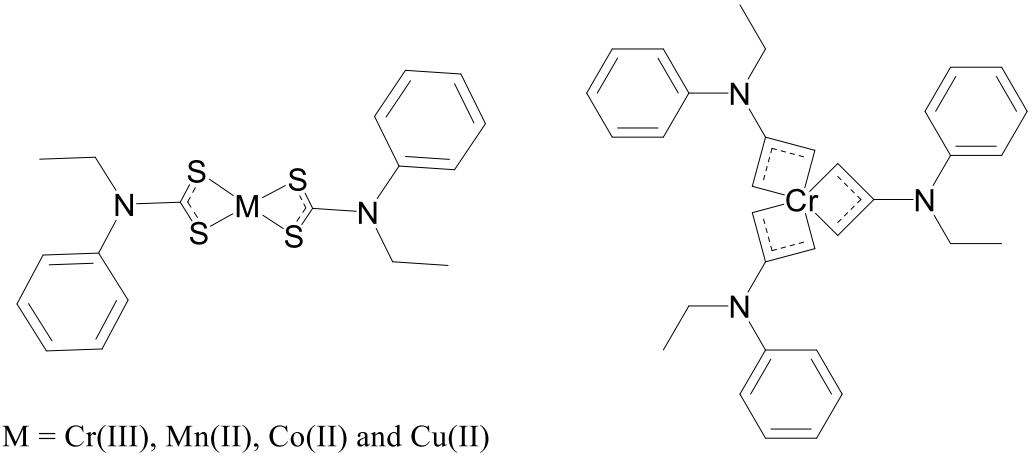

M = Cr(III), Mn(II), Co(II) and Cu(II)

Figure 1.9: Metal complexes of sodium N-ethyl-N-phenyldithiocarbamate.

Hussain *et al.* [195] described the preparation of nickel(II) bis(N,N-diethyldithiocarbamate) as seen in Figure **1.10** by the reaction of $NiL(ClO_4)_2$ with sodium salt of diethyldithiocarbamate [where L represents 3,7-bis(2-aminoethyl)-1,3,5,7-tetraazabicyclo(3.3.1) nonane]. The isolated single crystal of the complex showed it to have a square planar geometry and they were able to improve on the refinement factor R, from 10.6 % to 2.99 %, as previously reported in the literature. Antimicrobial activities of the complex was screened against three bacteria strains, viz *Pseudomonas aeruginosa, Bacillus thuringiensis* and *Escherichia coli* and three fungi strains, viz *Penicillium chrysogenum*, *Aspergillus nigrus* and *Fusarium oxysporum*. Their

results showed that the complex showed better activity against the fungi and bacteria than did known antibiotics, nystatin and tetracycline.

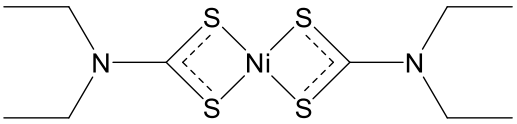

Figure 1.10: Ni(II) bis(N,N-diethyldithiocarbamate)

The Co(II), Cu(II), Fe(II), Mn(II), Ni(II) and Zn(II) complexes of phenylpiperazine-based dithiocarbamate, (**Figure 1.11**) derived from potassium salts of phenylpiperazine (Phpzdtc), fluorophenylpiperazine (F-Phpzdtc) and nitrophenylpiperazine (N-Phpzdtc), have been synthesized and screened against three Gram-negative bacteria strains (*Escherichia coli*, *Salmonella styhimurium* and *Pseudomonas aeruginosa*) two Gram-positive bacteria strains (*Bacillus pumilus*, and *Staphylococcus aureus*) and two fungi strains (*Candida albicaus* and *Aspergillus niger*) [196]. The phenylpiperazine dithiocarbamate ligand was found to be more active against the bacteria and fungi strains compared to its fluoro and nitro derivatives, and the biological activity of the dithiocarbamate ligands was not enhanced on complexation with metal ions.

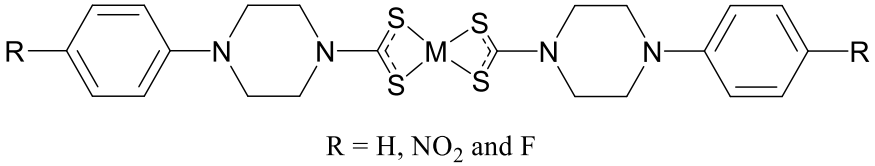

R = H, NO_2 and F

Figure 1.11: Metal complexes of phenylpiperazine-based dithiocarbamate

Mohammad *et al.* [33] reported the synthesis, characterization and antifungal activities of 1-acetylpiperazinyldithiocarbamate metal complexes of the type $M(acpdtc)_2$ [where M represents Co(II), Cu(II), Fe(II), Mn(II) or Ni(II)], **Figure 1.12**. Distorted-tetrahedral geometry was proposed for the Co(II), Fe(II) and Mn(II) complexes, based on the UV-Visible spectra and magnetic susceptibility measurement, while square planar geometry was proposed for the Ni(II) and Cu(II) complexes. All the complexes were screened against two fungi strains, *Fusarium sp* and *Sclerotina sp*. The ligand showed no antifungal activity while the complexes displayed strong antifungal activity at higher loading of test solution (200 and 300 µL) with $Ni(acpdtc)_2$ having the highest zone of inhibition.

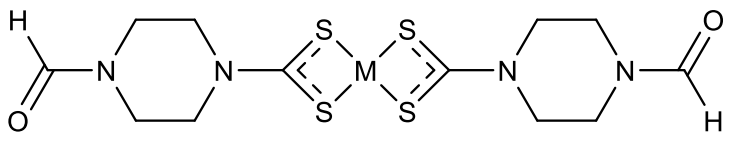

Figure 1.12: Metal complexes of 1-acetylpiperazinyldithiocarbamate.

Hassan *et al*. [45] reported one-pot synthesis of macrocyclic bimetallic dithiocarbamate based complexes (**Figure 1.13**) via the reaction involving bis-amine Schiff bases as the secondary amine, KOH, CS_2 and metal chloride. Spectrometry studies and other measurements revealed binuclear complexes of the formula of $M_2(L)_2$ [where M represents Co(II), Cu(II), Ni(II) or Zn(II) and L represents 2,2'-(1E, 1'E)(1,2-diphenylethane-1,2-diylidene) bis(azan-1-yl-1-ylidene)bis(2,1-phenylene)dicarbamodithioate]. Square planar geometry was proposed for the Ni(II) and Cu(II) complexes while tetrahedral geometry was proposed for their Co(II) and Zn(II) equivalents. Antimicrobial activity evaluation of the ligand and the complexes against *Escherichia coli, Staphylococcus aureus* and *Pseudomonas aeruginosa* showed that the complexes have higher antibacterial activities than do the corresponding free ligands.

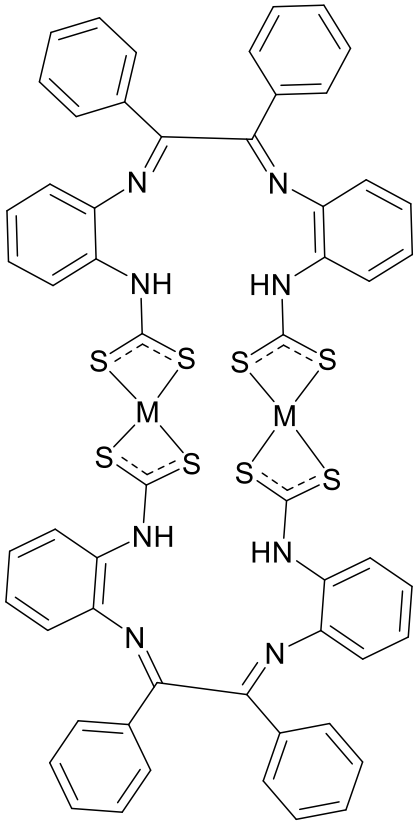

Figure 1.13: Bimetallic Schiff base macrocyclic dithiocarbamate-based complexes.

Verma *et al*. [43] also used a multifunctional secondary amine ligand, 2-chloro-3{2-(piperazinyl)ethyl1-amino-1,4-naphthoquinone, to synthesize mononuclear dithiocarbamate metal complexes of the type $[M\{\kappa^2S,S\text{-}S_2C\text{-piperazine-}C_2H_4N(H)\}ClNQ_n]$ [where M represents Co(III), Cu(II), Mn(III), Ni(II) or Zn(II), and ClNQ represents 2-chloro-1,4-naphthoquinone, and n = 2 or 3]. UV-visible spectra together with magnetic moment values

revealed octahedral geometry for the Mn(III) and Co(III) complexes and square planar geometry for Co(II), Cu(II) and Zn(II) complexes (**Figure 1.14**). The complexes were all subjected to antimicrobial, fluorescence and electrochemical studies. The antimicrobial potential of equivalent ligands and complexes were evaluated against six pathogens, viz; *E. coli*, *P. aeruginosa*, *B. subtilis*, *S.aureus*, *C. albicans*, and *A. niger*. All compounds showed moderate to excellent activities, while the copper complexes and ligand showed better activities against *S. aureus* compared to others and to the antibiotic drug ciprofloxacin.

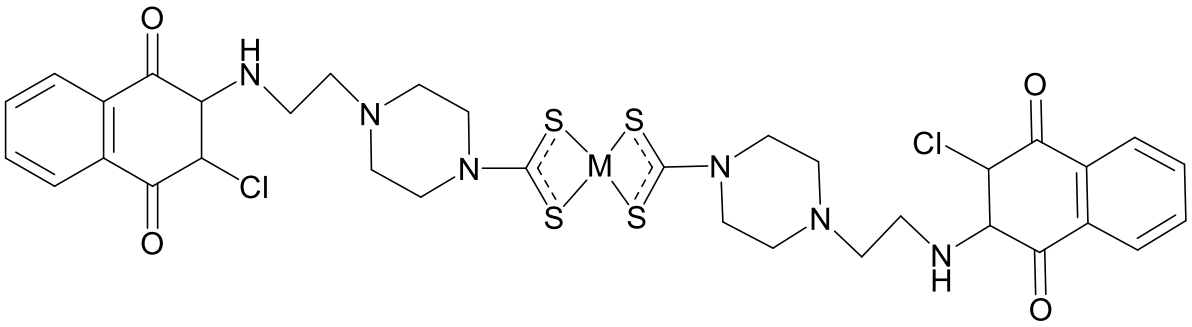

M = Ni(II), Cu(II), Zn(II)

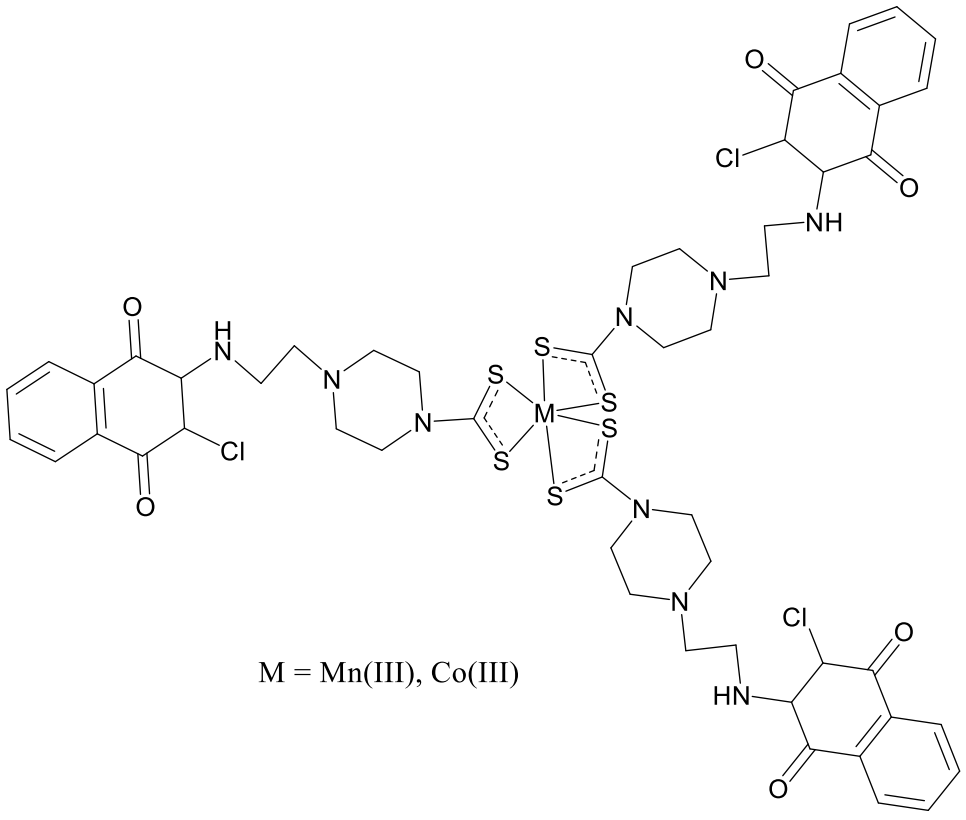

M = Mn(III), Co(III)

Figure 1.14: Dithiocarbamate metal complexes derived from 2-chloro-3{2-(piperazinyl)ethyl}-amino-1,4-naphthoquinone.

Copper(II) dithiocarbamate metal complexes of the sort $Cu\{S_2CNR(CH_2CH_2OH\}$, where R represents Me, Et, Pr or CH_2CH_2OH as seen in **Figure 1.15** have been synthesized, characterized and screened for antimicrobial activity against *P. aeruginosa*, *S. aureus* and *C. albicans* [197]. The presence of the hydrophilic group, CH_2CH_2OH in the dithiocarbamate backbone of the complexes, which could be expected to enhance their biological activity was found to have no influence. Complexes with Me and Et substituents had no antimicrobial activity against all pathogens, while those with Pr and CH_2CH_2OH displayed good antifungal activities against *C. albicans* with MIC values of 26.5×10^{-3} $mmolL^{-1}$ and 36.3×10^{-3} $mmolL^{-1}$, respectively; almost equivalent to that of fluconazole (control drug), which was 32.9×10^{-3} $mmolL^{-1}$. Both complexes displayed smaller antibacterial activity towards *S. aureus* compared to tetracycline (standard drug) and they were inert against *P. aeruginosa*.

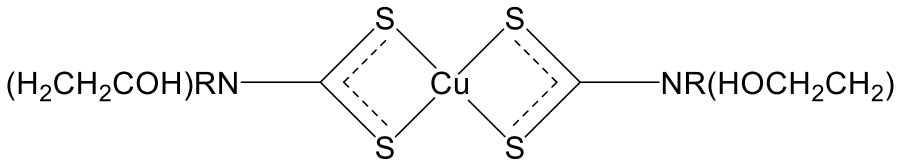

R = Me, Et, Pr and CH_2CH_2OH

Figure 1.15: Cu(II) dithiocarbamate metal complexes of the form $Cu\{S_2CNR(CH_2CH_2OH\}$

Ferreira and co-workers [12] also synthesized dithiocarbamate metal complexes of the type $[M\{S_2CNCH_3(R^1)\}_2]$ and $[M\{S_2CNCH_3(R^2)\}_2]$ where R^1 represents $CH_2CH(OCH_3)_2$, R^2 represents 2-methyl-1,3-dioxolane and M represents Ni(II), Pd(II) or Pt(II) as seen in **Figure 1.16**. Spectroscopy characterization and single X-ray crystallography diffraction of some of the complexes confirmed their square planar geometry. The compounds were screened against *Penicillium citrinum*, *Aspergillus flavus*, *Aspergillus parasiticus* as well as *Aspergillus niger* and the minimum inhibitory concentration (MIC) results showed that all the complexes had better activity than the drug nystatin but were less active than miconazole nitrate, another control drug. The Ni(II) complexes were more active against *A. niger* than the other complexes or nystatin.

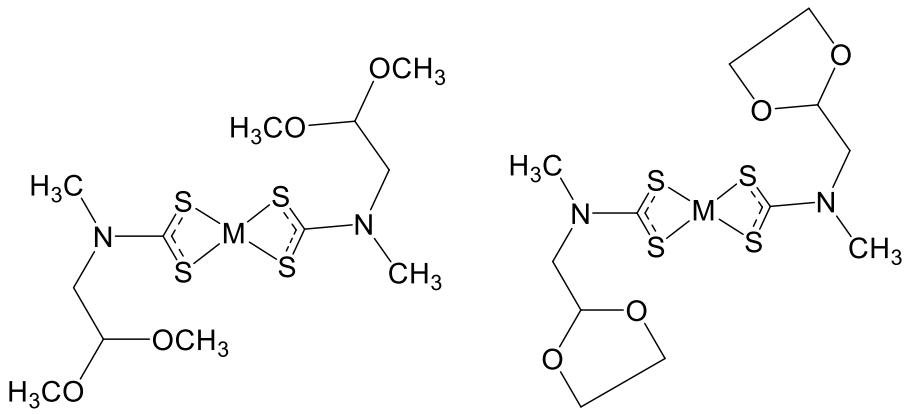

M = Ni(II), Pd(II) and Pt(II)

Figure 1.16: M(II) dithiocarbamate metal complexes of the form $[M\{S_2CNCH_3(R^2)\}_2]$

Verma *et al.* [42] reported the antimicrobial studies and electrochemical properties of ferrocene functionalized dithiocarbamate complexes formulated as $[M\{\kappa^2S,S\text{-}S_2CN(CH_2R)CH_2Fe\}_n]$, as illustrated in **Figure 1.17**, where M represents Co(III), Ni(II), Cu(II), Zn(II), R represents 1-napthyl, or 3-pyridyl or 2-furyl and n = 3 for Co(III) and n = 2 for Ni(II), Cu(II) and Zn(II). All the compounds were tested against four bacteria strains, namely *P. aeruginosa*, *B. subtilis*, *S. aureus* and *E. coli* and the two fungi strains of *C. albicans* and *A. niger*. The Ni(II) complex with 1-napthyl and Cu(II) complex with 2-furyl derivatives were found to be more active against *S. aureus* than were ciprofloxacin and the other compounds while Co(III), Ni(II) and Cu(II) complexes with 3-pyridyl as well as 2-furyl derivatives were found to be less active relative to ciprofloxacin. The Ni(II) complex with 3-pyridyl derivative had MIC value of 50µg/mL, which is almost equivalent antifungal capacity to that of the standard drug, flucanazole, which has MIC value of 40 µg/mL.

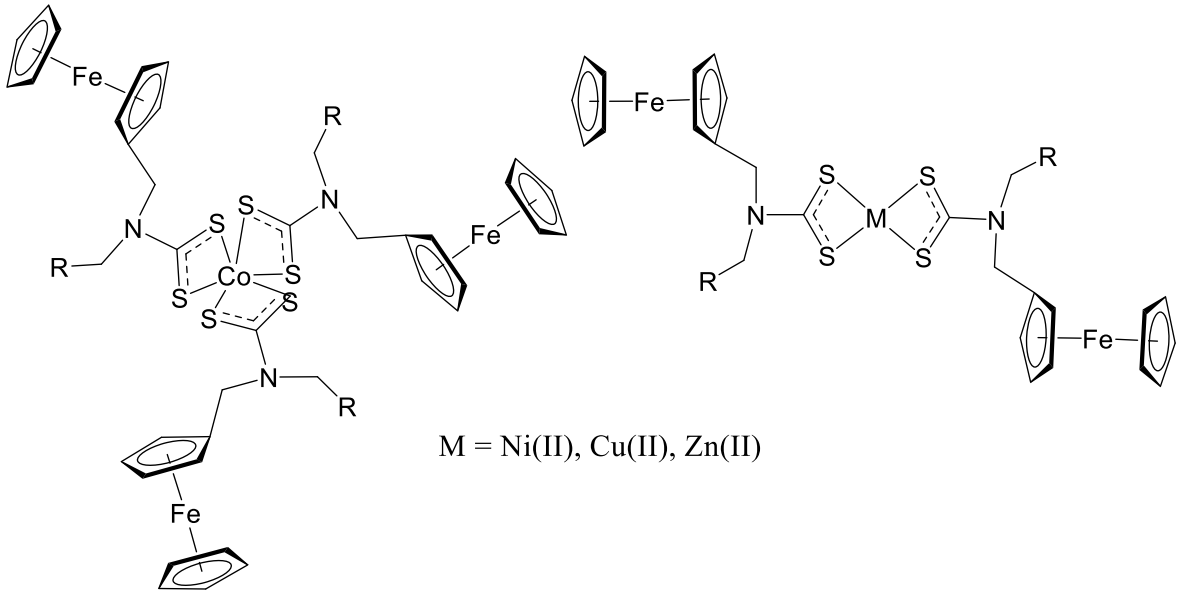

Figure 1.17: Ferrocene functionalized dithiocarbamate-based metal complexes

Khan *et al.* [39] have synthesized diphenyldithiocarbamate metal complexes of Ni(II), Cu(II), Zn(II) as seen in **Figure 1.18** and evaluated their biological application. They proposed a distorted square planar geometry for Ni(II) complexes and distorted tetrahedral geometry for Cu(II) and Zn(II) complexes. The antibacterial studies of the complexes investigated their activity against *B. subtilis*, *Rhodococcus sp*, *E. coli* and *P. aeruginosa*. The metal complexes displayed better antibacterial activity than did the free ligand, while the Ni(II) complex had the least activity compared to Zn(II) and Cu(II) complexes, with zone of inhibition 23±1.6, 14±1.4, 23±0.9 and 21±1.2 against *E. coli*, *P. aeruginosa*, *Rhodococcus sp* and *B. subtilis*.

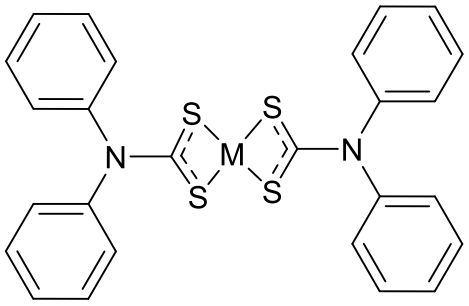

Figure 1.18: Diphenyldithiocarbamate-based metal complexes of Ni(II), Cu(II) and Zn(II)

Onwudiwe and co-workers [198] have reported the synthesis and potential antimicrobial ability of three Ni(II) dithiocarbamate complexes of the type $[Ni(buphdtc)_2]$, $[Ni(buphdtc)(PPh_3)(NCS)]$ and $[Ni(buphdtc)(PPh_3)(NC)]$ where bu represents butyl and ph

represents phenyl (**Figure 1.19**). X-ray crystal structures of two of the complexes showed that they have distorted square planar geometry. Antimicrobial evaluation of the compounds against *P. aeruginosa, E. coli, B. subtilis, S. aureus, S. pneumonia, K oxytoca, A. niger* and *F. oxysporum* showed that Ni(buphdtc)$_2$ displayed better activities compared to others. However, it was less active relative to the standard drugs fluconazole and streptomycin. The outcome of their results was in agreement with other reported literature [22, 199], which indicated that antimicrobial activity of N-substituted dithiocarbamate-based Ni(II) complexes reduces on the introduction of PPh_3, CN and SCN moieties to the compound.

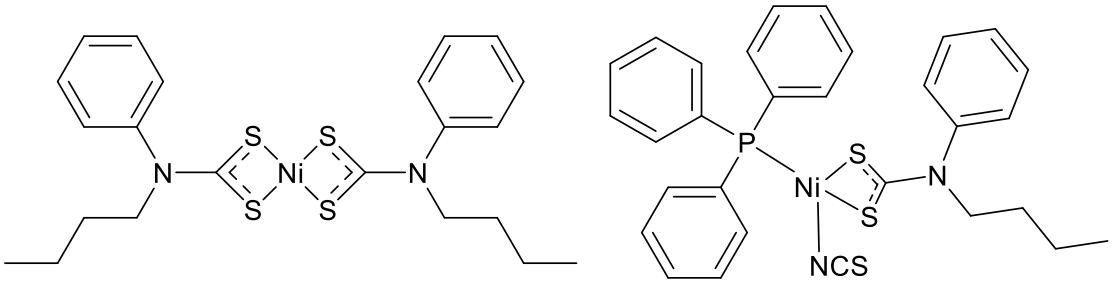

Figure 1.19: Ni(II) dithiocarbamate complexes containing NiS_4 and NiS_2PN moieties

1.6.1.2 Dithiocarbamate metal complexes as antioxidant agents

Antioxidant activities of DTC metal complexes have been reported in the literature [38, 41, 186] and their ability to scavenge free radicals as well as hydroxyl ions can be attributed to the electron donating ability of sulfur atoms and transition metal ions in their various complexes [41]. Onwudiwe *et al*. [38] reported the antioxidant activity of sodium N-ethyl-N-phenyldithiocarbamate and its Cu(II) complex. Their results showed that the complex had a scavenging activity of 75 % at 500 µg/ml compared to that of the ligand, which was 42 % at the same concentration. Recently, the antioxidant potential of pyridine-3-carboxamide dithiocarbamate-based metal complexes of Co(II), Ni(II), Cu(II) and Zn(II) as illustrated in **Figure 1.20** have been reported by Kareem *et al.* [186]. Their study showed that metal complexes had better antioxidant activity than did free dithiocarbamate ligands, and Cu(II) complexes was found to be most potent of the four, with about 40 % scavenging activity.

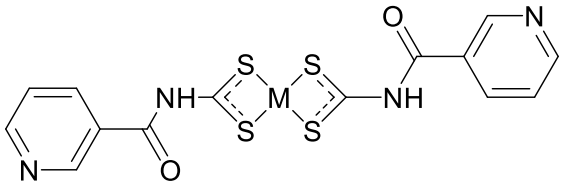

Co(II), Ni(II), Cu(II) and Zn(II)

Figure 1.20: Pyridine-3-carboxamide dithiocarbamate metal complexes

DPPH radical and hydroxy ion scavenging activities of dithiocarbamate metal complexes derived from substituted pyrrole-2-carboxaldehyde have been reported by Nami *et al.* [41], see **Figure 1 8**. The antioxidant activity of the dithiocarbamate ligand increased upon chelation with metal ions. The Cu(II) complex was found to have the highest antioxidant potential compared to ligand and other complexes, with IC50 values for DPPH radical and hydroxyl ion scavenging activity of of 0.52 µg/mL and 0.22 µg/mL, respectively. Khan *et al.* [39] also reported the free radical scavenging ability of diphenyldithiocarbamate metal complexes of Ni(II), Cu(II) and Zn(II) using DPPH assay. Their study showed that the ligand, as well as the complexes, had good antioxidant activity, with all the complexes showing better antioxidant activity compared to ligand and the standard butylated hydroxytoluene. The IC_{50} values for diphenyldithiocarbamate complexes of Zn(II), Ni(II) and Cu(II) were, respectively, 31.45±0.31 µM, 33.55±0.30 µM and 39.12±0.41 µM.

1.6.2 Dithiocarbamate metal complexes as a single-source precursor to synthesize semiconductor nanoparticles

Dithiocarbamate metal complexes have been used as a single-source precursor to prepare metal sulfide nanoparticles [88, 108, 200, 201]. Single-source precursors are an integral part of synthesis methods for metal sulfide nanoparticles based on chemical precipitation [202, 203], micro emulsions [204, 205], sol-gels [206, 207], chemical vapour deposition [210, 211] and sputtering [216, 217] and for processes that are electrochemical [208, 209], hydrothermal [212, 213] or solvothermal [214, 215]. Notably, the technique of thermolysis of single-source precursor produces nanocrystals with reasonable monodispersity [218]. Furthermore, reports have shown the size and morphology of the resulting nanocrystals to be highly dependent on temperature, precursor, concentration and the capping agent/injection solvent mixture [219]. DTC metal complexes are commonly used as single-source precursors for metal sulfide nanoparticles due to both their ability to stabilize a wide range of oxidation states and the ease of breaking the C—S bonds in the DTCs. The latter is a crucial step during thermolysis, providing a decomposition pathway that leaves the metal and sulfur behind [86].

1.7 Thiuram disulfide as a potential anticancer drug

DTCs are of interest as anticancer agents [220, 221] and research had shown that their sulfur—sulfur dimer , such as thiuram disulfide, have better anticancer activity [51, 55] compared to

them. For example, diethyldithiocarbamate is known to be a good anticancer agent [222], while the oxidized form tetraethylthiuram disulfide (disulfiram) has a profound anticancer property [55] as well as a safety record that has been proved by extensive pharmacokinetic studies [223]. Mechanisms such as proteasome pathway inhibition [224], DNA topoisomerase inhibition [220] as well as angiogenesis reduction [225] have been proposed for the action of disulfram as anticancer agent.

Keter *et al.* [51] reported the synthesis and anticancer studies of thiuram disulfide compounds of the type $\{R^1C(S)S—S(S)CR^1\}$ where R^1 represents pyrazolyl, 3,5-dimethylpyrazolyl and indazolyl (see **Figure 1 21**). Compared with the other two, the pyrazolyl derivative showed better anticancer activity and greater selectivity against HeLa cells. However, the dithiocarbamate salts that formed the disulfides showed no growth inhibition for HeLa cells.

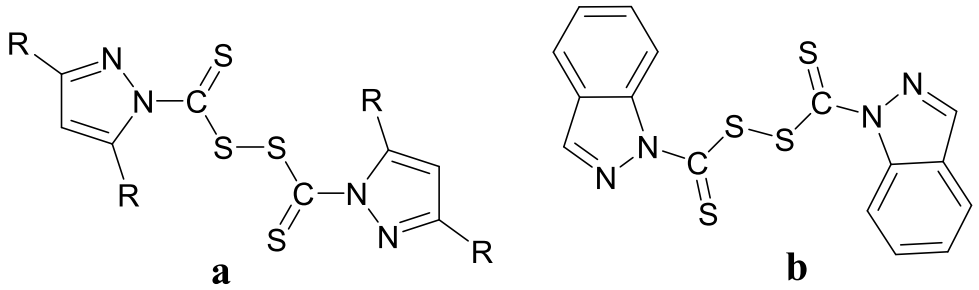

Figure 1.21: (a) bis(pyrazol-1-ylthiocarbonyl)disulfides (b) bis(indazolyl-1-thiocarbonyl)disulfide

Wiggins *et al.* [226] also reported the anticancer activity of disulfiram and its derivative bis(N-benzylethylthiocarbamoyl)disulfide (see **Figure 1.22**) against breast cancer. Their study showed that disulfiram kills MCF-7 and BT474 breast cancer cell lines under appropriate growth conditions and has no effect on the non-cancerous breast epithelial MCF-10A cell line. Also they found out that addition of zinc to the extracellular media of disulfiram and its derivative increases their potency against cancer cells.

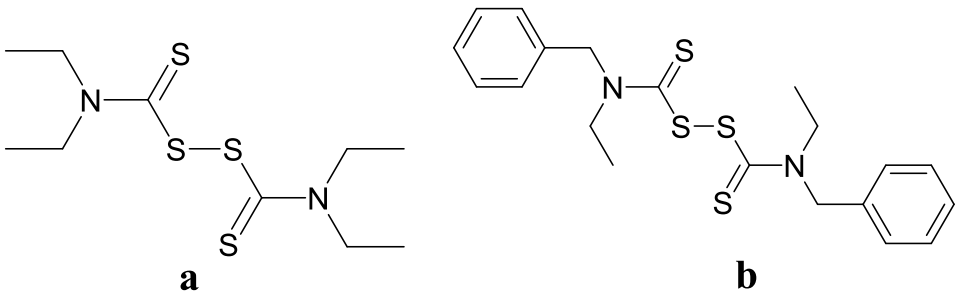

Figure 1.22: **(a)** Disulfiram (b) bis(N-benzylethylthiocarbamoyl)disulfides

The series of disulfiram derivatives, carbamo(dithioperoxo)thioates (**Figure 1.23**), have been synthesized and selected ones were screened against the human breast cancer cell lines, MCF-7 (BCA2-positive), MDA-MD-231 (BCA2-negative) and MCF-10A (non-cancerous control) [227]. The results showed that the compounds were active against MCF-7 cells at a selective sub-micromolar IC_{50} activity.

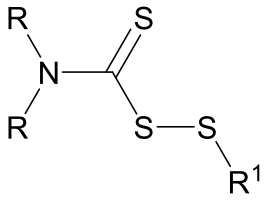

$R = (CH_2)_4$-, $R^1 = CH_2CH_2OH$
$R = (CH_2)_4$-, R^1 = n-Hex
$R = (CH_2)_5$-, R^1 = n-Hex
$R = (CH_2)_2O(CH_2)_2$, R^1 = n-Hex
$R = (CH_2)_2NMe(CH_2)_2$, R^1 = n-Hex

Figure 1.23: Selected carbamo(dithioperoxo)thioates screened against human breast cancers

Disulfiram derivatives bis(dialkylthiocarbamoyl)disulfides (**Figure 1.24**), have been synthesized and tested by Brahemi *et al.* [228] for anticancer activity against the breast cancer associated protein (BCA2). Their results showed that bis(dialkylthiocarbamoyl)disulfides displayed good activity in submicromolar IC_{50} against BCA2 positive viz; MCF-7 and T47D. . However, they were inactive against the normal epithelial cell line MCF10A.

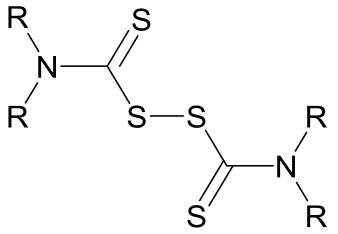

R = piperidine, pyrrolidine, N-methylpiperazine

Figure 1.24: Disulfiram derivative of bis(dialkylthiocarbamoyl)disulfide

Apart from disulfiram and its derivatives being used as anticancer agent, their use as radio-sensitizers during radiotheraputic treatment of human cancers has been reported, both *in vivo* and *in vitro* [229, 230]. Rae *et al.* [231] reported the enhanced radiosensitivity of human neuroblastoma cells, which is not only useful in external-beam radiation but also in radiopharmaceutical therapies with ^{131}I-metaliodobenzylguanidine [231] The inhibition of mammary primary tumor growth and metastasis to the lung by disulfiram adjuvant irradiation had also been reported by Wang *et al.* [232]. They presumed that disulfiram-copper complex targeted the NF-Kappa B pathway by blocking the irradiation-induced stemness in breast cancer cells [233].

1.8 Cu(I) complexes with phosphine ligand as antimicrobial agent

Despite the extensive work on the antimicrobial activity of copper (II) complexes [22, 33, 41, 234] reported above, the potential of copper(I) complexes as antimicrobial agent has been scarce [235], most especially the literature is thin regarding Cu(I) complexes with auxiliary phosphine ligands [236].

Sabounchei *et al.* [236] reported the synthesis of dimeric phosphine ylide Cu(I) complexes of the type $[Cu(\mu\text{-}Cl)\{Ph_2P(CH_2)_nPPh_2C(H)C(O)PhR\}]_2$ as shown in **Figure 1 25** and they were screened against six Gram -positive and negative bacteria strains. Their study showed that the complexes were more active against the bacteria than were the free ligands and displayed better activity against *S. aureus* (+) and *S. marcesceus* (-) than did cephalexin, which was the standard drug used for the study.

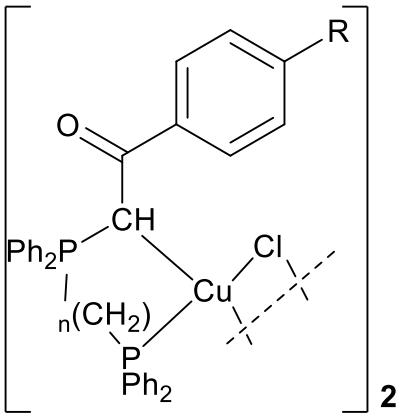

Figure 1.25: Dimeric phosphine ylide of Cu(I) complexes

The synthesis of heteroleptic Cu(I) complexes derived from 2,9-dimethyl-1,10-phenanthroline and tris(aminomethyl)phosphine derived from morpholine and thiomorpholine with I^- or NCS^- as counter ion (see **Figure 1.26)** had been synthesized and screened against *Staphylococcus aureus*, *Escherichia coli* and *Candida albicans* for their antimicrobial and antifungal activity [237]. The complexes showed outstanding antimicrobial activity towards *C. albicans* and *S. aureus*, with MIC values ranging from 1 to 5 µg/ml and results comparable to the standard used (gentamicin), while *E. coli* showed resistance to the complexes.

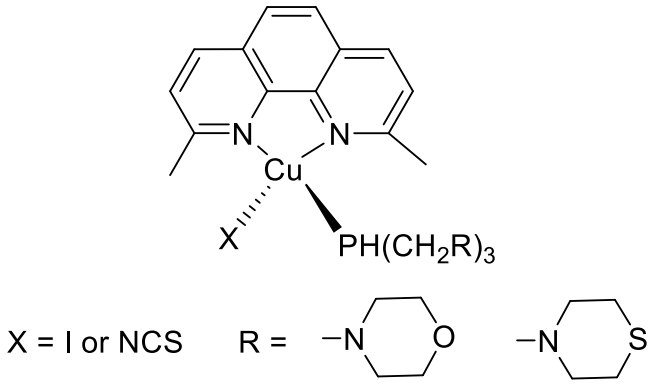

Figure 1.1: Cu(I) complexes derived from 2,9-dimethyl-1.10-phenanthroline and tris(aminomethyl)phosphine

Starosta *et al.* [238] also reported on the heteroleptic Cu(I) diimines, 2,2-bipyridines and 1,10-phenathroline complexes with aminophosphine $PCH_2N(CH_2CH_2)_2NCH_3)_3$, $P(CH_2N(CH_2CH_2NCH_2CH_3)_3$ and $P(CH_2N(CH_2CH_2)_2O)_3$ as coligands, and all were screened for their activity against *E. coli, P. aeruginosa, S. aureus* and *Candida albicans*. All the complexes displayed excellent activity against *S. aureus* but showed little or no activity against

other bacteria or the *Candida* strains. They also revealed that the Cu(I) complexes with 1,10-phenanthroline exhibited better activity than did those with 2,2-bipyridine as substituent.

Complexes of Cu(I) and Ag(I) with mixed ligands of triphenylphosphine and heterocyclic pyrimidine thione (pyrimidine-2-thione or 4,6-dimethyl-pyrimidine-2-thione) of the type $[Cu(PPh_3)_2$(pyrimidine-type thione)$_{1\ or\ 2}]BF_4$ have been synthesized and screened against Gram-negative *E. coli* and Gram-positive *B. subtilis*, *B. cereus* and *S. aureus*, to evaluate their antimicrobial activity [239]. The Cu(I) complexes showed selective antibacterial activity against *B. subtilis* and *S. aureus*. In particular, *S. aureus* was the most susceptible to all the Cu(I) complexes, with MIC value ranging from 12 to 28 µg/mL.

1.9 Research Problem statements

A problem creating serious worldwide concern today is the continuous spread of infectious diseases, which goes beyond borders of countries and even continents [240]. This spread has been exacerbated by the increasing numbers of multi-drug resistant microbial pathogens and the emergence of new infectious diseases, which have made treatment of diseases a challenge, particularly in the last decade [241]. Despite their being several antibiotic drugs available for medical use, the emergence of new and remaining old antibiotic resistance indicates an urgent medical need for new antibiotic agents endowed with excellent antibacterial activities, whose mechanism of action is distinct from those of established antibiotic agents, to which relevant clinical pathogens have become resistant [161]. In addition to infectious diseases, other new threats to living organism have emerged.

The effect of overproduction of reactive oxygen species (ROS) such as the superoxide radical anion ($O_2^{\bullet-}$)., hydroxyl radical ($OH^{\bullet}$), and hydrogen peroxide (H_2O_2) pose a great treat. They are considered to be the main cause of oxidative damage to biomolecules such as proteins, lipids and DNA, thereby accelerating ageing, cancer inflammation, cardiovascular and neurodegenerative diseases [49]. Compounds with antioxidant properties are known to protect organisms and cells from oxidative damage [48, 49], therefore driving the need to discover new compounds with better antioxidant activity than the well-known standards such as ascorbic acid, gallic acid, and thiols, among others.

1.10 Justification

Diseases caused by pathogenic bacteria pose great threat to human lives and their treatment remains a challenging problem because, as discussed above, factors including new infectious disease outbreaks and antibiotic resistance developed by the bacteria [241]. Owing to these challenges, researchers are searching new drugs with excellent antibacterial activities, whose mechanism of action is distinct from that of well-known drugs [161]. The potential antimicrobial activities of metal complexes have been established and are used in medical treatments, such as bismuth for treatment of cancer, metal cluster as anti-HIV drug and silver bandages for treatment of burns [242]. The use of formamidine pharmacological agents have been extensively reported [243-246]. It was projected that synthesizing dithiocarbamates, thiuram disulfides and metal complexes using bioactive ligands such as formamidines as a source of secondary amine could provide solution to the problem of multi-drug resistance in bacteria, becasue their mode of action may be different from the well-known drugs. Dithiocarbamates and their metal complexes are known for their use in medicine as antibacterial [22, 37, 193, 247], and antioxidant agents [38, 39]. The use of N'N-diaryformamidines as a secondary amine will enable us to vary the substituent R group, which may be different or similar, on the -NCS_2 of the synthesized compounds (see **Figure 1.27**). These possible modifications in the chemical structure of the dithiocarbamates backbone could improve the chemotherapeutic properties of the proposed compounds as antibacterial agents and as antioxidant agents. Also it will allow a comparative study to see the effect of substituents on the compounds' antibacterial and antioxidant properties.

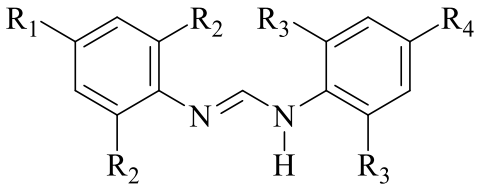

Figure 1.27: General structure of N'N-diarylamine formamidine.

1.11 Aims and objectives

The aim of this research work is to synthesize and characterize N,N'-diarylformamidine-based dithiocarbamate, thiuram disulfide, metal complexes (Ni(II), Cu(II) and Co(III)) and heteroleptic Cu(I) dithiocarbamate-PPh_3 complexes for antibacterial and antioxidant use.

The objectives of this research work are stated below:

- To synthesize and characterize a series of symmetrical and unsymmetrical N'N-diarylformamidine dithiocarbamate ligands
- To oxidize the dithiocarbamate ligands above to form their thiuram disulfide derivatives and characterize them.
- To synthesize the metal complexes of Co(III), Ni(II) and Cu(II) from the dithiocarbamate ligands and characterize them
- To synthesize and characterize heteroleptic Cu(I) dithiocarbamate-PPh_3 complexes.
- To evaluate the anticancer potential of synthesized thiuram disulfide using *in silico* and chemoinformatic computational tools.
- To evaluate the *in vitro* antibacterial and antioxidant activity of all the synthesized compounds.

REFERENCES

1. C. Orvig and M. J. Abrams, *Chemical Reviews*, **1999**, 99, 2201-2204.
2. R. H. Holm, P. Kennepohl and E. I. Solomon, *Chemical Reviews*, **1996**, 96, 2239-2314.
3. D. Chen, V. Milacic, M. Frezza and Q. P. Dou, *Current Pharmaceutical Design*, **2009**, 15, 777-791.
4. P. J. Sadler, in *Advances in Inorganic Chemistry*, Academic Press, **1991**, 36, 1-48.
5. R. W.-Y. Sun, D.-L. Ma, E. L.-M. Wong and C.-M. Che, *Dalton Transactions*, **2007**, 43, 4884-4892.
6. S. J. Lippard, *Nature Chemical Biology*, **2006**, 2, 504.
7. P. Sadler, *The Journal of Rheumatology. Supplement*, **1982**, 8, 71-78.
8. P. Sadler, *Journal of Inorganic Biochemistry*, **1997**, 67, 1-4.
9. I. Ali, W. A. Wani, K. Saleem and M.-F. Hseih, *Polyhedron*, **2013**, 56, 134-143.
10. H. Graeme, *Mini-Reviews in Medicinal Chemistry*, **2012**, 12, 1202-1215.
11. A. Gölcü, *Transition metal Chemistry*, **2006**, 31, 405-412.
12. I. Ferreira, G. de Lima, E. Paniago, J. Takahashi and C. Pinheiro, *Inorganica Chimica Acta*, **2014**, 423, 443-449.
13. S. Ozkirimli, T. I. Apak, M. Kiraz and Y. Yegenoglu, *Archives of Pharmacal Research*, **2005**, 28, 1213-1218.
14. B. Macías, M. V. Villa, E. Chicote, S. Martín-Velasco, A. Castiñeiras and J. n. Borrás, *Polyhedron*, **2002**, 21, 1899-1904.
15. M. Shahid, T. Rüffer, H. Lang, S. A. Awan and S. Ahmad, *Journal of Coordination Chemistry*, **2009**, 62, 440-445.
16. K. K. Manar, M. K. Yadav, Anamika, M. G. B. Drew and N. Singh, *Polyhedron*, **2016**, 117, 592-599.
17. S. M. Mamba, Masters Thesis, University of Johannesburg, South-Africa, **2010**, pp 20-89.
18. S. Khan, S. A. Nami and K. Siddiqi, *Journal of Organometallic Chemistry*, **2008**, 693, 1049-1057.
19. F. Shaheen, A. Badshah, M. Gielen, G. Croce, U. Florke, D. de Vos and S. Ali, *Journal of Organometallic Chemistry*, **2010**, 695, 315-322.
20. F. P. Andrew and P. A. Ajibade, *Journal of Molecular Structure*, **2018,** 1155, 843 - 855.

21. F. P. Andrew and P. A. Ajibade, *Journal of Coordination Chemistry*, **2018**, 71, 2776 - 2786.
22. S. M. Mamba, A. K. Mishra, B. B. Mamba, P. B. Njobeh, M. F. Dutton and E. Fosso-Kankeu, *Spectrochimica Acta Part A: Molecular and Biomolecular Spectroscopy*, **2010**, 77, 579-587.
23. R. M. Nirmal, K. Pandian and K. Sivakumar, *Applied Surface Science*, **2011**, 257, 2745-2751.
24. T. Peddarao, A. Baishya, M. K. Barman, A. Kumar and S. Nembenna, *New Journal of Chemistry*, **2016**, 40, 7627-7636.
25. K. Kaji, H. Matsubara, H. Nagashima, Y. Kikugawa and S. Yamada, *Chemical and Pharmaceutical Bulletin*, **1978**, 26, 2246-2249.
26. C.-H. Lin, C.-H. Tsai and H.-C. Chang, *Catalysis Letters*, **2005**, 104, 135-140.
27. A. Mekhalfia, R. Mutter, W. Heal and B. Chen, *Tetrahedron*, **2006**, 62, 5617-5625.
28. M. L. Cole and P. C. Junk, *Zeitschrift für anorganische und allgemeine Chemie*, **2015**, 641, 2624-2629.
29. R. M. Roberts, *The Journal of Organic Chemistry*, **1949**, 14, 277-284.
30. S. Delarue, S. Girault, F. D. Ali, L. Maes, P. Grellier and C. Sergheraert, *Chemical and Pharmaceutical Bulletin*, **2001**, 49, 933-937.
31. H. Zhang, J.-s. Wu and F. Peng, *Anti-cancer Drugs*, **2008**, 19, 125-132.
32. P. J. Rani and S. Thirumaran, *European Journal of Medicinal Chemistry*, **2013**, 62, 139-147.
33. A. Mohammad, C. Varshney and S. A. Nami, *Spectrochimica Acta Part A: Molecular and Biomolecular Spectroscopy*, **2009**, 73, 20-24.
34. K. Siddiqi, S. Khan, S. A. Nami and M. El-Ajaily, *Spectrochimica Acta Part A: Molecular and Biomolecular Spectroscopy*, **2007**, 67, 995-1002.
35. C. G. Young, *Journal of Inorganic Biochemistry*, **2007**, 101, 1562-1585.
36. B. Cvek, V. Milacic, J. Taraba and Q. P. Dou, *Journal of Medicinal Chemistry*, **2008**, 51, 6256-6258.
37. F. Shaheen, A. Badshah, M. Gielen, M. Dusek, K. Fejfarova, D. de Vos and B. Mirza, *Journal of Organometallic Chemistry*, **2007**, 692, 3019-3026.
38. D. C. Onwudiwe and A. C. Ekennia, *Research on Chemical Intermediates*, **2017**, 43, 1465-1485.
39. S. Khan, W. Ahmad, K. Munawar and S. Kanwal, *Indian Journal of Pharmaceutical Sciences*, **2018**, 80, 480-488.

40. N. Takamune, S. Misumi and S. Shoji, *Biochemical and Biophysical Research Communications*, **2000**, 272, 351-356.
41. S. A. Nami, I. Ullah, M. Alam, D.-U. Lee and N. Sarikavakli, *Journal of Photochemistry and Photobiology B: Biology*, **2016**, 160, 392-399.
42. S. K. Verma and V. K. Singh, *Journal of Organometallic Chemistry*, **2015**, 791, 214-224.
43. S. K. Verma and V. K. Singh, *RSC Advances*, **2015**, 5, 53036-53046.
44. S. Sanchez-Cortes, M. Vasina, O. Francioso and J. Garcıa-Ramos, *Vibrational Spectroscopy*, **1998**, 17, 133-144.
45. H. A. Hasan, E. I. Yousif and M. J. Al-Jeboori, *Global Journal of Inorganic. Chemistry*, **2012**, 3, 1-7.
46. G. G. Mohamed, N. A. Ibrahim and H. A. Attia, *Spectrochimica Acta Part A: Molecular and Biomolecular Spectroscopy*, **2009**, 72, 610-615.
47. S. A. A. Nami, I. Ullah, M. Alam, D.-U. Lee and N. Sarikavakli, *Journal of Photochemistry and Photobiology B: Biology*, **2016**, 160, 392-399.
48. A. Corona-Bustamante, J. M. Viveros-Paredes, A. Flores-Parra, A. L. Peraza-Campos, F. J. Martínez-Martínez, M. T. Sumaya-Martínez and Á. Ramos-Organillo, *Molecules*, **2010**, 15, 5445-5459.
49. I. Kostova and L. Saso, *Current Medicinal Chemistry*, **2013**, 20, 4609-4632.
50. K. Svoboda, J. Brooker and J. Zrustova, *International Symposium on National Preservatives in Food Systems*, **2005**, 709, 35-44.
51. F. K. Keter, M. J. Nell, I. A. Guzei, B. Omondi and J. Darkwa, *Journal of Chemical Research*, **2009**, 5, 322-325.
52. D. Cen, R. I. Gonzalez, J. A. Buckmeier, R. S. Kahlon, N. B. Tohidian and F. L. Meyskens, *Molecular Cancer Therapeutics*, **2002**, 1, 197-204.
53. D. Chen, Q. C. Cui, H. Yang and Q. P. Dou, *Cancer Research*, **2006**, 66, 10425-10433.
54. Y. Horita, T. Takii, T. Yagi, K. Ogawa, N. Fujiwara, E. Inagaki, L. Kremer, Y. Sato, R. Kuroishi and Y. Lee, *Antimicrobial Agents and Chemotherapy*, **2012**, 75. 6445-6411.
55. M. Wickström, K. Danielsson, L. Rickardson, J. Gullbo, P. Nygren, A. Isaksson, R. Larsson and H. Lövborg, *Biochemical Pharmacology*, **2007**, 73, 25-33.
56. V. K. Sharma, J. Aulakh and A. K. Malik, *Journal of Environmental Monitoring*, **2003**, 5, 717-723.

57. J.-P. Visapää, J. Tillonen and M. Salaspuro, *Alcohol and Alcoholism*, **2002**, 37, 322-326.
58. P. K. Gessner, *Principles of Medical Biology*, **1992**, 8, 829-854.
59. L. I. Victoriano, *Coordination Chemistry Reviews*, **2000**, 196, 383-398.
60. M. Fereidoonnezhad, M. Niazi, M. Shahmohammadi Beni, S. Mohammadi, Z. Faghih, Z. Faghih and H. R. Shahsavari, *ChemMedChem*, **2017**, 12, 456-465.
61. M. Frezza, Q. P. Dou, Y. Xiao, H. Samouei, M. Rashidi, F. Samari and B. Hemmateenejad, *Journal of Medicinal Chemistry*, **2011**, 54, 6166-6176.
62. H. Samouei, M. Rashidi and F. W. Heinemann, *Journal of the Iranian Chemical Society*, **2014**, 11, 1207-1216.
63. H. Samouei, M. Rashidi and F. W. Heinemann, *Journal of Organometallic Chemistry*, **2011**, 696, 3764-3771.
64. T. S. Kamatchi, N. Chitrapriya, H. Lee, C. F. Fronczek, F. R. Fronczek and K. Natarajan, *Dalton Transactions*, **2012**, 41, 2066-2077.
65. A. A. Nazarov and P. J. Dyson, *Phosphorus Compounds*, Springer, **2011**, 445-461**.**
66. K. Sampath, S. Sathiyaraj, G. Raja and C. Jayabalakrishnan, *Journal of Molecular Structure*, **2013**, 1046, 82-91.
67. F. A. Cotton and G. Wilkinson, *Advanced Inorganic Chemistry*, Wiley New York, **1988**, 6.
68. D. Coucouvanis, *Progress in Inorganic Chemistry*, **1970**, 11, 233-371.
69. G. Hogarth, *Progress in Inorganic Chemistry*, **2012**, 53, 71-561.
70. R. P. TRIPATHI, A. R. KHAN, B. SRINIVASAN SETTY and A. P. BHADURI, *Acta Pharmaceutica*, **1996**, 46, 169-176.
71. F. Aryanasab, A. Z. Halimehjani and M. R. Saidi, *Tetrahedron Letters*, **2010**, 51, 790-792.
72. S. V. Amosova, M. V. Penzik, V. A. Potapov, A. S. Filippov, V. A. Shagun, A. I. Albanov, T. N. Borodina and V. I. Smirnov, *Synlett*, **2016**, 27, 1653-1658.
73. E. N. Esfahani, M. Mohammadi-Khanaposhtani, Z. Rezaei, Y. Valizadeh, R. Rajabnia, M. Hassankalhori, F. Bandarian, M. A. Faramarzi, N. Samadi, M. R. Amini, M. Mahdavi and B. Larijani, *Research on Chemical Intermediates*, **2019**, 45, 223-236.
74. D. Chaturvedi and S. Ray, *Tetrahedron Letters*, **2006**, 47, 1307-1309.
75. T. W. Greene and P. G. Wuts, *Protective Groups in Organic Synthesis*, Wiley, **1999**.
76. D. C. Onwudiwe and P. A. Ajibade, *International Journal of Molecular Sciences*, **2011**, 12, 1964-1978.

77. D. Zhang, J. Chen, Y. Liang and H. Zhou, *Synthetic Communications*, **2005**, 35, 521-526.
78. I. P. Ferreira, G. M. de Lima, E. B. Paniago, J. A. Takahashi, K. Krambrock, C. B. Pinheiro, J. L. Wardell and L. C. Visentin, *Journal of Molecular Structure*, **2013**, 1048, 357-366.
79. F. Jian, Z. Wang, Z. Bai, X. You, H.-K. Fun, K. Chinnakali and I. A. Razak, *Polyhedron*, **1999**, 18, 3401-3406.
80. F. P. Andrew and P. A. Ajibade, *Journal of Molecular Structure*, **2018**, 1170, 24–29.
81. S. Gorai, D. Ganguli and S. Chaudhuri, *Crystal Growth & Design*, **2005**, 5, 875-877.
82. H. Nabipour, S. Ghammamy and A. Rahmani, *IET Micro & Nano Letters*, **2011**, 6, 217-220.
83. D. Vojta, A. Višnjevac, Z. Leka, M. Kosović and M. Vazdar, *Journal of Molecular Structure*, **2016**, 1103, 245-253.
84. B. Arul Prakasam, M. Lahtinen, A. Peuronen, M. Muruganandham, E. Kolehmainen, E. Haapaniemi and M. Sillanpää, *Inorganica Chimica Acta*, **2015**, 425, 239-246.
85. D. J. Price, M. A. Wali and D. W. Bruce, *Polyhedron*, **1997**, 16, 315-320.
86. A. R. Roffey, UCL (University College London), **2014**.
87. A. Z. Halimehjani, K. Marjani, A. Ashouri and V. Amani, *Inorganica Chimica Acta*, **2011**, 373, 282-285.
88. P. A. Ajibade, J. Z. Mbese and B. Omondi, *Inorganic and Nano-Metal Chemistry*, **2017**, 47, 202-212.
89. D. C. Onwudiwe, T. Arfin and C. A. Strydom, *Electrochimica Acta*, **2014**, 127, 283-289.
90. P. A. Ajibade, D. C. Onwudiwe and M. J. Moloto, *Polyhedron*, **2011**, 30, 246-252.
91. A. A. Nejo, P. Ndifonb and N. Revaprasadu, *New Journal of. Chemistry*, **2011**, 35, 1133-1139.
92. W.-D. Rudorf, *Journal of Sulfur Chemistry*, **2007**, 28, 295-339.
93. P. Giboreau and C. Morin, *The Journal of Organic Chemistry*, **1994**, 59, 1205-1207.
94. G. Li, H. Tajima and T. Ohtani, *The Journal of Organic Chemistry*, **1997**, 62, 4539-4540.
95. Y.-P. Tian, C.-Y. Duan, Z.-L. Lu, X.-Z. You, H.-K. Fun and B.-C. Yip, *Polyhedron*, **1996**, 15, 1495-1502.
96. T. C. Mak, K. S. Jasim and C. Chieh, *Canadian Journal of Chemistry*, **1984**, 62, 808-813.

97. A. C. Fabretti, F. Forghieri, A. Giusti, C. Preti and G. Tosi, *Spectrochimica Acta Part A: Molecular Spectroscopy*, **1984**, 40, 343-346.
98. G. Gattow and S. Lotz, *Zeitschrift für anorganische und allgemeine Chemie*, **1985**, 531, 101-107.
99. G. Gattow and S. Lotz, *Zeitschrift für anorganische und allgemeine Chemie*, **1985**, 531, 97-100.
100. L. I. Victoriano, *Polyhedron*, **2000**, 19, 2269-2275.
101. A. M. Bond, R. Colton, A. F. Hollenkamp, B. F. Hoskins and K. McGregor, *Journal of the American Chemical Society*, **1987**, 109, 1969-1980.
102. J. Zhai, H.-D. Yin, F. Li, S.-W. Chen and D.-Q. Wang, *Acta Crystallographica Section E: Structure Reports Online*, **2007**, 63, 1969-1970.
103. M. Delepine, *Comptes Rendus*, **1907**, 144, 1125-1127.
104. R. Sharma and N. Kaushik, *Journal of Thermal Analysis and Calorimetry*, **2004**, 78, 953-964.
105. S. Tiwari and A. Bajpai, *Reactive and Functional Polymers*, **2005**, 64, 47-54.
106. S. Farhadi and F. Siadatnasab, *Chinese Journal of Catalysis*, **2016**, 37, 1487-1495.
107. R. Yadav, Y. Waghadkar, G. Kociok-Köhn, A. Kumar, S. B. Rane and R. Chauhan, *Optical Materials*, **2016**, 62, 176-183.
108. T. Mthethwa, V. R. Pullabhotla, P. S. Mdluli, J. Wesley-Smith and N. Revaprasadu, *Polyhedron*, **2009**, 28, 2977-2982.
109. D. C. Onwudiwe and P. A. Ajibade, *International Journal of Molecular Sciences*, **2011**, 12, 5538-5551.
110. S. Kanchi, P. Singh and K. Bisetty, *Arabian Journal of Chemistry*, **2014**, 7, 11-25.
111. P. Pitchaimani, K. M. Lo and K. P. Elango, *Polyhedron*, **2015**, 93, 8-16.
112. B. Arul Prakasam, K. Ramalingam, R. Baskaran and G. Bocelli, *Polyhedron*, **2007**, 26, 1133-1138.
113. Z. Trávníček, R. Pastorek and V. Slovák, *Polyhedron*, **2008**, 27, 411-419.
114. K. S. Siddiqi, S. A. Nami and Y. Chebude, *Journal of the Brazilian Chemical Society*, **2006**, 17, 107-112.
115. N. Thammakan and E. Somsook, *Materials Letters*, **2006**, 60, 1161-1165.
116. D. Montagner and P. J. S. Miguel, *Dalton Transactions*, **2011**, 40, 10809-10811.
117. I. Kovács, A.-M. Lebuis and A. Shaver, *Organometallics*, **2001**, 20, 35-41.
118. C. Bianchini, C. A. Ghilardi, A. Meli, S. Midollini and A. Orlandini, *Inorganic Chemistry*, **1985**, 24, 932-939.

119. J. P. Fackler Jr and W. C. Seidel, *Inorganic Chemistry*, **1969**, 8, 1631-1639.
120. A. Vizi-Orosz and L. Markó, *Transition Metal Chemistry*, **1986**, 11, 408-410.
121. J. Noordik, *Crystal Stucture Communication,* **1973**, 2, 81–84.
122. E. J. Fernandez, J. M. Lopez-de-Luzuriaga, M. Monge, E. Olmos, M. C. Gimeno, A. Laguna and P. G. Jones, *Inorganic Chemistry*, **1998**, 37, 5532-5536.
123. H.-D. Yin, J. Zhai, Y.-Y. Sun and D.-Q. Wang, *Polyhedron*, **2008**, 27, 663-670.
124. D. Cardell, G. Hogarth and S. J. I. c. a. Faulkner, *Inorganic Chimica Acta*, **2006**, 359, 1321-1324.
125. A. Bino, F. A. Cotton, Z. Dori and J. C. J. I. C. Sekutowski, *Inorganic Chemistry*, **1978**, 17, 2946-2950.
126. S.-F. Lu, J.-Q. Huang, R.-M. Yu, X.-Y. Huang, Q.-J. Wu, Y. Peng, J. Chen, Z.-X. Huang, Y. Zheng and D.-X. J. P. Wu, *Polyhedron*, **2001**, 20, 2339-2352.
127. W.-H. Leung, J. L. C. Chim, H. Hou, T. S. M. Hun, I. D. Williams and W.-T. Wong, *Inorganic Chemistry*, **1997**, 36, 4432-4437.
128. C. Landgrafe and W. S. Sheldrick, *Journal of the Chemical Society, Dalton Transactions*, **1994**, 1885-1893.
129. T. Furuhashi, M. Kawano, Y. Koide, R. Somazawa and K. Matsumoto, *Inorganic Chemistry*, **1999**, 38, 109-114.
130. L. Maheu, G. Miessler, J. Berry, M. Burow and L. Pignolet, *Inorganic Chemistry*, **1983**, 22, 405-410.
131. S. Wheeler and L. Pignolet, *Inorganic Chemistry*, **1980**, 19, 972-979.
132. M. Ebihara, K. Tokoro, M. Maeda, M. Ogami, K. Imaeda, K. Sakurai, H. Masuda and T. Kawamura, *Journal of the Chemical Society, Dalton Transactions*, **1994**, 3621-3635.
133. M. Ebihara, K. Tokoro, K. Imaeda, K. Sakurai, H. Masuda and T. Kawamura, *Journal of the Chemical Society, Chemical Communications*, **1992**, 21, 1591-1592.
134. H. Brunner, A. Hollman, M. Zabel and B. Nuber, *Journal of Organometallic Chemistry*, **2000**, 609, 44-52.
135. A. C. Ekennia, D. C. Onwudiwe, A. A. Osowole, L. O. Olasunkanmi and E. E. Ebenso, *Journal of Chemistry*, **2016**, 16, 1-12.
136. A. A. El-Sherif and B. J. Jeragh, *Spectrochimica Acta Part A: Molecular and Biomolecular Spectroscopy*, **2007**, 68, 877-882.
137. H.-Y. Bie, J.-H. Yu, J.-Q. Xu, J. Lu, Y. Li, X.-B. Cui, X. Zhang, Y.-H. Sun and L.-Y. Pan, *Journal of Molecular Structure*, **2003**, 660, 107-112.

138. Y. Aydogdu, F. Yakuphanoglu, A. Aydogdu, E. Tas and A. Cukurovali, *Materials Letters*, **2003**, 57, 3755-3760.
139. X. Y. Xu, T. T. Xu, J. Gao, M. Y. Wang, S. R. Niu, S. S. Ni and G. X. Xu, *Synthesis and Reactivity in Inorganic, Metal-Organic and Nano-Metal Chemistry*, **2006**, 36, 681-686.
140. A. R. Sarkar and S. Mandal, *Synthesis and Reactivity in Inorganic and Metal-Organic Chemistry*, **2000**, 30, 1477-1488.
141. W. Villarreal, L. Colina-Vegas, G. Visbal, O. Corona, R. S. Corrêa, J. Ellena, M. R. Cominetti, A. A. Batista and M. Navarro, *Inorganic chemistry*, **2017**, 56, 3781-3793.
142. S. J. Berners-Price, R. K. Johnson, C. K. Mirabelli, L. F. Faucette, F. L. McCabe and P. J. Sadler, *Inorganic Chemistry*, **1987**, 26, 3383-3387.
143. R. J. Bowen, M. Navarro, A.-M. J. Shearwood, P. C. Healy, B. W. Skelton, A. Filipovska and S. J. Berners-Price, *Dalton Transactions*, **2009**, 10861-10870.
144. J. G. Małecki, A. Maroń, J. Palion, J. E. Nycz and M. Szala, *Transition Metal Chemistry*, **2014**, 39, 755-762.
145. M. Sandroni, L. Favereau, A. Planchat, H. Akdas-Kilig, N. Szuwarski, Y. Pellegrin, E. Blart, H. Le Bozec, M. Boujtita and F. Odobel, *Journal of Materials Chemistry A*, **2014**, 2, 9944-9947.
146. M. Sandroni, M. Kayanuma, A. Planchat, N. Szuwarski, E. Blart, Y. Pellegrin, C. Daniel, M. Boujtita and F. Odobel, *Dalton Transactions*, **2013**, 42, 10818-10827.
147. C. E. Housecroft and E. C. Constable, *Chemical Society Reviews*, **2015**, 44, 8386-8398.
148. T. E. Hewat, L. J. Yellowlees and N. Robertson, *Dalton Transactions*, **2014**, 43, 4127-4136.
149. B. Bozic-Weber, S. Y. Brauchli, E. C. Constable, S. O. Fürer, C. E. Housecroft and I. A. Wright, *Physical Chemistry Chemical Physics*, **2013**, 15, 4500-4504.
150. N. Armaroli, G. Accorsi, M. Holler, O. Moudam, J. F. Nierengarten, Z. Zhou, R. T. Wegh and R. Welter, *Advanced Materials*, **2006**, 18, 1313-1316.
151. R. D. Costa, D. Tordera, E. Ortí, H. J. Bolink, J. Schönle, S. Graber, C. E. Housecroft, E. C. Constable and J. A. Zampese, *Journal of Materials Chemistry*, **2011**, 21, 16108-16118.
152. Y.-M. Wang, F. Teng, Y.-B. Hou, Z. Xu, Y.-S. Wang and W.-F. Fu, *Applied Physics Letters*, **2005**, 87, 233512.

153. M. Elie, F. Sguerra, F. Di Meo, M. D. Weber, R. Marion, A. l. Grimault, J.-F. o. Lohier, A. l. Stallivieri, A. Brosseau and R. B. Pansu, *ACS Applied Materials & Interfaces*, **2016**, 8, 14678-14691.
154. R. D. Costa, E. Orti, H. J. Bolink, F. Monti, G. Accorsi and N. Armaroli, *Angewandte Chemie International Edition*, **2012**, 51, 8178-8211.
155. G. Rajput, V. Singh, S. K. Singh, L. B. Prasad, M. G. Drew and N. Singh, *European Journal of Inorganic Chemistry*, **2012**, 24, 3885-3891.
156. A. N. Gupta, V. Singh, V. Kumar, L. B. Prasad, M. G. Drew and N. Singh, *Polyhedron*, **2014**, 79, 324-329.
157. H. Gest, *Notes and Records of the Royal Society*, **2004**, 58, 187-201.
158. L. P. Graham, *An Introduction to Medicinal Chemistry*, **1995**, 7, 336.
159. R. Austrian and J. Gold, *Annals of internal medicine*, **1964**, 60, 759-776.
160. P. Dineeen, W. P. Homan and W. R. Grafe, *Annals of Surgery*, **1976**, 184, 717.
161. A. Coates, Y. Hu, R. Bax and C. Page, *Nature Reviews Drug discovery*, **2002**, 1, 895.
162. J. Heitman, *Mycopathologia*, **2000**, 149, 47-48.
163. C. Walsh, *Nature*, **2000**, 406, 775.
164. J. Smith, *Journal of Antimicrobial Chemotherapy*, **1986**, 18, 21-29.
165. B. G. Spratt, *Philosophical Transaction of the Royal Society of London B. Biological Sciences*, **1980**, 289, 273-283.
166. W. Wehrli, F. Knüsel, K. Schmid and M. Staehelin, *Proceedings of the National Academy of Sciences of the United States of America*, **1968**, 61, 667-670.
167. R. C. Goldman, S. Fesik and C. Doran, *Antimicrobial agents and chemotherapy*, **1990**, 34, 426-431.
168. E. Yousif, A. Majeed, K. Al-Sammarrae, N. Salih, J. Salimon and B. Abdullah, *Arabian Journal of Chemistry*, **2017**, 10, 1639-1644.
169. S. Amyes and J. Smith, *Microbiology*, **1978**, 107, 263-271.
170. D. M. Livermore, *Antimicrobial agents and chemotherapy*, **1992**, 36, 2046-2048.
171. G. A. Jacoby and A. A. Medeiros, *Antimicrobial Agents and Chemotherapy*, **1991**, 35, 1697.
172. B. Halliwell and J. M. Gutteridge, *Free radicals in biology and medicine*, Oxford University Press, USA, **2015**.
173. D. M. Miller, G. R. Buettner and S. D. Aust, *Free Radical Biology and Medicine*, **1990**, 8, 95-108.

174. M.-F. Wang, Z.-Y. Yang, Z.-C. Liu, Y. Li and H.-G. Li, *Synthesis and Reactivity in Inorganic, Metal-Organic, and Nano-Metal Chemistry*, **2013**, 43, 483-494.
175. M. Valko, M. Izakovic, M. Mazur, C. J. Rhodes and J. Telser, *Molecular and Cellular Biochemistry*, **2004**, 266, 37-56.
176. G. Poli, G. Leonarduzzi, F. Biasi and E. Chiarpotto, *Current Medicinal Chemistry*, **2004**, 11, 1163-1182.
177. M. Valko, C. Rhodes, J. Moncol, M. Izakovic and M. Mazur, *Chemico-Biological Interactions*, **2006**, 160, 1-40.
178. R. Abreu, S. Falcão, R. C. Calhelha, I. C. Ferreira, M.-J. R. Queiroz and M. Vilas-Boas, *Journal of Electroanalytical Chemistry*, **2009**, 628, 43-47.
179. M. Valko, D. Leibfritz, J. Moncol, M. T. Cronin, M. Mazur and J. Telser, *The International Journal of Biochemistry & Cell Biology*, **2007**, 39, 44-84.
180. J. Liu, M. K. Shigenaga, Y. Liang-Junyan, A. Mori and B. N. Ames, *Free radical research*, **1996**, 24, 461-472.
181. D. Onwudiwe and A. Ekennia, *Research on Chemical Intermediates*, **2017**, 43, 1465-1485.
182. Y. Chia-Fu, C. Sun-Dsong, C. Wei-Shi, F. Jia-Der and L. Chuen-Ying, *Journal of Chromatography A*, **1993**, 630, 275-285.
183. R. Cremlyn, *Pesticides: Preparation and mode of action*, Wiley Chichester, **1978**.
184. A. K. Malik and W. Faubel, *Pesticide Science*, **1999**, 55, 965-970.
185. E. Reid, *Organic Chemistry Of Bivalent Sulfur*,Chemical Publishing, **1962**, 14.
186. A. Kareem, S. A. A. Nami, M. S. Khan, S. A. Bhat, A. U. Mirza and N. Nishat, *New Journal of Chemistry*, **2019**, 43, 4413–4424.
187. P. Ajibade and A. Nqombolo, *Chalcogenide Letters*, **2016**, 13, 427-434.
188. G. Gomathi, S. H. Dar, S. Thirumaran, S. Ciattini and S. Selvanayagam, *Comptes Rendus Chimie*, **2015**, 18, 499-510.
189. M. Bochmann, *Chemical Vapor Deposition*, **1996**, 2, 85-96.
190. T. Kitson, *Ed Chem*, **1985**, 43-45.
191. G. Vettorazzi, W. F. Almeida, G. J. Burin, R. B. Jaeger, F. R. Puga, A. F. Rahde, F. G. Reyes and S. Schvartsman, *Teratogenesis, carcinogenesis, and mutagenesis*, **1995**, 15, 313-337.
192. P. Gøtzsche, *Lancet*, **1988**, 8618, 1024-1024.
193. F. F. Bobinihi, D. C. Onwudiwe, A. C. Ekennia, O. C. Okpareke, C. Arderne and J. R. Lane, *Polyhedron*, **2019**, 158, 296-310.

194. S. I. Islam, S. B. Das, S. Chakrabarty, S. Hazra, A. Pandey and A. Patra, *Advances in Chemistry*, **2016**, 9, 524-530.
195. A. Husain, S. A. Nami, S. P. Singh, M. Oves and K. Siddiqi, *Polyhedron*, **2011**, 30, 33-40.
196. V. T. Yilmaz, T. K. Yazıcılar, H. Cesur, R. Ozkanca and F. Z. Maras, *Synthesis and reactivity in inorganic and metal-organic chemistry*, **2003**, 33, 589-605.
197. G. M. De Lima, D. C. Menezes, C. A. Cavalcanti, J. A. Dos Santos, I. P. Ferreira, E. B. Paniago, J. L. Wardell, S. M. Wardell, K. Krambrock and I. C. Mendes, *Journal of Molecular Structure*, **2011**, 988, 1-8.
198. D. C. Onwudiwe, A. C. Ekennia and E. Hosten, *Journal of Coordination Chemistry*, **2016**, 69, 2454-2468.
199. P. J. Rani, S. Thirumaran and S. Ciattini, *Journal of Sulfur Chemistry*, **2014**, 35, 106-116.
200. M. Green, P. Prince, M. Gardener and J. Steed, *Advanced Materials*, **2004**, 16, 994-996.
201. P. Bera, C.-H. Kim and S. I. Seok, *Solid State Sciences*, **2010**, 12, 1741-1747.
202. V. Singh and P. Chauhan, *Journal of Physics and Chemistry of Solids*, **2009**, 70, 1074-1079.
203. K. Petcharoen and A. Sirivat, *Materials Science and Engineering: B*, **2012**, 177, 421-427.
204. M. H. Entezari and N. Ghows, *Ultrasonics sonochemistry*, **2011**, 18, 127-134.
205. M. A. Malik, M. Y. Wani and M. A. Hashim, *Arabian Journal of Chemistry*, **2012**, 5, 397-417.
206. H. Cao, Y. Xu, J. Hong, H. Liu, G. Yin, B. Li, C. Tie and Z. Xu, *Advanced Materials*, **2001**, 13, 1393-1394.
207. F. Gu, S. F. Wang, M. K. Lü, G. J. Zhou, D. Xu and D. R. Yuan, *The Journal of Physical Chemistry B*, **2004**, 108, 8119-8123.
208. X.-J. Xu, G.-T. Fei, W.-H. Yu, X.-W. Wang, L. Chen and L.-D. Zhang, *Nanotechnology*, **2005**, 17, 426.
209. D. Xu, Y. Xu, D. Chen, G. Guo, L. Gui and Y. Tang, *Advanced Materials*, **2000**, 12, 520-522.
210. J. J. Wu and S. C. Liu, *Advanced Materials*, **2002**, 14, 215-218.
211. S. Y. Bae, H. W. Seo and J. Park, *The Journal of Physical Chemistry B*, **2004**, 108, 5206-5210.

212. H. Zhang, L. Wang, H. Xiong, L. Hu, B. Yang and W. Li, *Advanced Materials*, **2003**, 15, 1712-1715.
213. H.-C. Chiu and C.-S. Yeh, *The Journal of Physical Chemistry C*, **2007**, 111, 7256-7259.
214. Y. Li, H. Liao, Y. Ding, Y. Fan, Y. Zhang and Y. Qian, *Inorganic Chemistry*, **1999**, 38, 1382-1387.
215. K. B. Tang, Y. T. Qian, J. H. Zeng and X. G. Yang, *Advanced Materials*, **2003**, 15, 448-450.
216. S. Kumar, V. Gupta and K. Sreenivas, *Nanotechnology*, **2005**, 16, 1167.
217. M. Nie, K. Sun and D. D. Meng, *Journal of Applied Physics*, **2009**, 106, 5431-5439.
218. N. Pradhan, B. Katz and S. Efrima, *The Journal of Physical Chemistry B*, **2003**, 107, 13843-13854.
219. A. L. Abdelhady, M. A. Malik, P. O'Brien and F. Tuna, *The Journal of Physical Chemistry C*, **2012**, 116, 2253-2259.
220. J. S. Yakisich, Å. Sidén, P. Eneroth and M. Cruz, *Biochemical and Biophysical Research Communications*, **2001**, 289, 586-590.
221. Y.-J. Kim, J. Y. Kim, N. Lee, E. Oh, D. Sung, T.-M. Cho and J. H. Seo, *Biochemical and Biophysical Research Communications*, **2017**, 486, 1069-1076.
222. A. Spath and K. Tempel, *Chemico-Biological Interactions*, **1987**, 64, 151-166.
223. Z. E. Sauna, S. Shukla and S. V. Ambudkar, *Molecular Biosystems*, **2005**, 1, 127-134.
224. H. Lövborg, F. Öberg, L. Rickardson, J. Gullbo, P. Nygren and R. Larsson, *International Journal of Cancer*, **2006**, 118, 1577-1580.
225. S.-G. Shian, Y.-R. Kao, F. Y.-H. Wu and C.-W. Wu, *Molecular Pharmacology*, **2003**, 64, 1076-1084.
226. H. L. Wiggins, J. M. Wymant, F. Solfa, S. E. Hiscox, K. M. Taylor, A. D. Westwell and A. T. Jones, *Biochemical Pharmacology*, **2015**, 93, 332-342.
227. V. Cilibrasi, K. Tsang, M. Morelli, F. Solfa, H. L. Wiggins, A. T. Jones and A. D. Westwell, *Tetrahedron Letters*, **2015**, 56, 2583-2585.
228. G. Brahemi, F. R. Kona, A. Fiasella, D. Buac, J. Soukupová, A. Brancale, A. M. Burger and A. D. Westwell, *Journal of Medicinal Chemistry*, **2010**, 53, 2757-2765.
229. N. M. Gandhi, U. V. Gopalaswamy and C. K. K. Nair, *Journal of Radiation research*, **2003**, 44, 255-259.
230. R. Taylor, A. Maners, H. Salari, M. Baker and E. Walker, *Annals of Clinical & Laboratory Science*, **1986**, 16, 443-449.

231. C. Rae, M. Tesson, J. W. Babich, M. Boyd, A. Sorensen and R. J. Mairs, *Journal of Nuclear Medicine*, **2013**, 54, 953-960.
232. Y. Wang, W. Li, S. S. Patel, J. Cong, N. Zhang, F. Sabbatino, X. Liu, Y. Qi, P. Huang and H. Lee, *Oncotarget*, **2014**, 5, 3743.
233. Y. Jiao, B. N Hannafon and W.-Q. Ding, *Anti-Cancer Agents in Medicinal Chemistry (Formerly Current Medicinal Chemistry-Anti-Cancer Agents)*, **2016**, 16, 1378-1384.
234. A. Osowole, G. Kolawole and O. Fagade, *Journal of Coordination Chemistry*, **2008**, 61, 1046-1055.
235. R. A. Khan, M. Usman, R. Dhivya, P. Balaji, A. Alsalme, H. AlLohedan, F. Arjmand, K. AlFarhan, M. A. Akbarsha, F. Marchetti, C. Pettinari and S. Tabassum, *Scientific Reports*, **2017**, 7, 45229.
236. S. J. Sabounchei, M. Pourshahbaz, A. Hashemi, M. Ahmadi, R. Karamian, M. Asadbegy and H. R. Khavasi, *Journal of Organometallic Chemistry*, **2014**, 761, 111-119.
237. R. Starosta, A. Bykowska, A. Kyzioł, M. Płotek, M. Florek, J. Król and M. Jeżowska-Bojczuk, *Chemical Biology & Drug Design*, **2013**, 82, 579-586.
238. R. Starosta, M. Florek, J. Król, M. Puchalska and A. Kochel, *New Journal of Chemistry*, **2010**, 34, 1441-1449.
239. P. A. Papanikolaou, A. G. Papadopoulos, E. G. Andreadou, A. Hatzidimitriou, P. J. Cox, A. A. Pantazaki and P. Aslanidis, *New Journal of Chemistry*, **2015**, 39, 4830-4844.
240. V. Vuksanović, Z. Leka and N. Terzić, *Fresenius Environmental Bulletin*, **2013**, 22, 3803-3807.
241. M. Rizzotto, in *A search for antibacterial agents*, InTechopen, **2012**, chapter 5.
242. R. S. Joseyphus and M. S. Nair, *Mycobiology*, **2008**, 36, 93-98.
243. S. A. Aziz and C. O. Knowles, *Nature*, **1973**, 242, 417.
244. R. Beeman and F. Matsumura, *Nature*, **1973**, 242, 273.
245. A. Meyers and T. R. Elworthy, *The Journal of Organic Chemistry*, **1992**, 57, 4732-4740.
246. R. Hollingworth, *Environmental Health Perspectives*, **1976**, 14, 57-69.
247. J. O. Adeyemi, D. C. Onwudiwe, A. C. Ekennia, C. P. Anokwuru, N. Nundkumar, M. Singh and E. C. Hosten, *Inorganica Chimica Acta*, **2019**, 485, 64-72.

CHAPTER TWO

EXPERIMENTAL METHODOLOGY

2.1 Preface

This chapter gives the list of materials (reagents and chemicals) and also describes the instruments used for characterization techniques in this study. It also details the experimental procedure for the synthesis of symmetrical and unsymmetrical N,N-diarylformamidine, dithiocarbamate ligands, thiuram disulfides, Ni(II), Cu(II) and Co(III) dithiocarbamate metal complexes as well as heteroleptic Cu (I) dithiocarbamate-phosphine complexes. This chapter also outlines the computational methodology utilized to give an *in silico* insight and cheminformatics evaluation of the thiuram disulfides synthesized in this study. The methodology for the *in vitro* antibacterial studies and antioxidant assay for all the compounds are also presented in Sections 2.11 and 2.12, respectively.

2.2 Reagents and chemicals

All reagents and chemicals were obtained from Sigma Aldrich Corporation and, being of analytical grade, they were used as obtained without further purification. Reagents used as the preparation source of secondary amine (N,N'-diarylformamidine), potassium dithiocarbamate salts and heteroleptic copper(I) metal complexes were 2,6-dimethylaniline (99 %), 2,6-diisopropylaniline (97 %), 2,4,6-trimethylaniline (98 %), 2,6-dichloroaniline (98 %), 2-bromoaniline (98 %), triphenylphosphine (99 %), triethyl orthoformate (99 %), potassium hydroxide (85 %) and carbon disulfides (≥99 %).

Metal salts used for complexation were $CuCl_2{\cdot}2H_2O$ (97 %), $NiCl_2{\cdot}6H_2O$ (98 %), $CoCl_2$ (97 %) and $Cu(NO_3)_2{\cdot}3H_2O$ and they were all obtained from Promark Chemicals, South Africa. The media for antibacterial studies [Nutrient Agar (NA), Nutrient Broth (NB) and Mueller-Hinton Agar (MHA)] were all obtained from Biolab, South Africa, while reagents used for antioxidant studies, that is 2,2-Diphenyl-1-picrylhydrazyl (DPPH), ascorbic acid, sodium nitroprusside and Griess reagent, were obtained from Merck Chemicals (Pty) Ltd.

Solvents used were acetonitrile, ethanol, methanol, dichloromethane, hexane, chloroform, ether, tetrahydrofuran, diethylether, acetone and dimethyl sulfoxide (DMSO), which were also obtained from Promark Chemicals, South Africa.

2.3 Physical measurement and spectroscopy techniques

The melting point of the ligands and metal complexes were recorded using Electrothermal (9100). Infrared spectra were obtained on a PerkinElmer Universal ATR spectrum 100 FT-IR spectrometer in the region of 4000 – 300 cm^{-1}. Ultraviolet-Visible absorption spectra of the ligands and complexes were recorded on Shimadzu UV-Vis-NIR spectrophotometer in the region of 800 – 200 nm. The ^{1}H and ^{13}C NMR spectra were recorded at 25 °C on a Bruker Avance^{III} 400 MHz spectrometer. Both ^{1}H NMR and ^{13}C NMR data were recorded in either $CDCl_3$ referenced to the residual $CDCl_3$ peaks at δ 7.26 and δ 77.00 ppm or $(CD_3)_2SO$ (DMSO) referenced to the residual $(CD_3)_2SO$ peaks at δ 2.50 and δ 39.52 ppm, respectively.

Elemental analyses were recorded on a Vario elemental EL cube CHNS analyzer. Mass spectra of the compounds were obtained from a Water synaptic GR electrospray positive spectrometer and the emission spectra were recorded using a PerkinElmer LS 55 fluorescence spectrometer.

2.4 Synthesis of N,N'-diarylformamidine (source of secondary amine)

The symmetrical N,N'-diarylformamidine (**L1** – **L3**) and unsymmetrical N,N'-diarylformamidines (**L4** – **L8**) are shown in **Figure 2.1**.

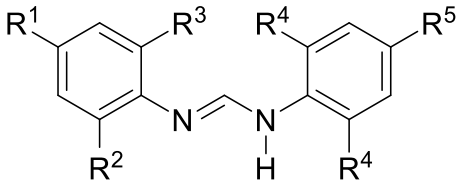

$R^1 = R^5 = H$, $R^2 = R^3 = R^4 = Me$**: L1**
$R^1 = R^5 = H$, $R^2 = R^3 = R^4 = iPr$**: L2**
$R^1 = R^2 = R^3 = R^4 = R^5 = Me$**: L3**
$R^1 = R^5 = H$, $R^2 = R^3 = Cl$, $R^4 = Me$**: L4**
$R^1 = R^5 = H$, $R^2 = R^3 = Cl$, $R^4 = iPr$**: L5**
$R^1 = H$, $R^2 = R^3 = Cl$, $R^4 = R^5 = Me$**: L6**
$R^1 = R^3 = R^5 = H$, $R^2 = Br$, $R^4 = Me$**: L7**
$R^1 = R^3 = H$, $R^2 = Br$, $R^4 = R^5 = Me$**: L8**

Figure 2.1: Symmetrical and unsymmetrical N,N'-diarylformamidines used for this study.

2.4.1 Synthesis of symmetrical N,N'-diarylformamidine (L1 - L3)

N,N'-bis(2,6-dimethyphenyl)formamidine (L1), N,N'-bis(2,6-diisopropylphenyl)formamidine (L2) and N,N`-bis(2,4,6-trimethylphenyl)formamidine (L3) were synthesized following the published procedure, with a slight modification [1, 2]. Three or four drops of acetic acid were added to the reaction mixture in a round-bottom flask charged with the aniline (2 mole equivalents) and triethyl orthoformate (1 mole equivalent). The reaction mixture was heated under reflux and temperature maintained at 130 - 150 °C. After 3 hours, the temperature was increased to 160 °C to remove all the volatiles via distillation. The reaction was allowed to cool and the crude product was triturated with hexane and collected by gravity filtration. The solids obtained were recrystallized in 50 cm^3 of hot acetone and stored at 4 °C to yield the pure products.

2.4.2 Synthesis of unsymmetrical N,N'-diarylformamidine (L4 - L8)

Unsymmetrical formamidine was synthesized as follows. Three or four drops of acetic acid was added to the reaction mixture containing aniline (30 mmol) and triethyl orthoformate (30 mmol) in a round-bottom flask. The mixture was refluxed at 140 °C for 30 min with stirring followed by distillation (2 mmol of EtOH collected). A second amount of aniline (30 mmol) was then added to the reaction mixture and heating continued until 1 mmol of ethanol was collected. Upon cooling to 25 °C, the solution solidified. The crude product was triturated with cold hexane and collected by filtration. Solids were then washed with 50 cm^3 of dichloromethane to completely remove traces of symmetrical formamidine by-products, which had formed during the reaction, to afford N-(2,6-dichlorophenyl)-N-(2,6-dimethylphenyl)formamidine, (L4), N-(2,6-dichlorophenyl)-N-(2,6-dimethylphenyl)formamidine (L5), N-(2,6-dichlorophenyl)-N-mesitylformamidine (L6), N-(2-bromophenyl)-N-(2,6-dimethylphenyl)formamidine, (L7) and N-(2-bromophenyl)-N-mesitylformamidine (L8).

2.5 Synthesis of potassium salt of dithiocarbamate ligands

An equimolar ratio of the N,N'-diarylformamidines and KOH in 20 mL of acetonitrile was stirred for 20 min in an ice bath at 0 – 5 °C to form a white coloured solution. To the resulting solution, carbon disulfide of the same molar ratio was added drop-wise and stirring continued for 3 hours over an ice bath and another one hour at 25 °C to give a yellow solution. The solvent was removed using a rotary evaporator and a crude yellow solid product was obtained. The

crude product was rinsed three times with ethanol to remove unreacted formamidine, resulting in a pure yellow solid product, which was stored in a desiccator.

2.5.1 Synthesis of N,N'-bis(2,6-dimethylphenyl) formamidine dithiocarbamate potassium salt (DL1)

The reaction of L1 (1.00 g, 4 mmol), KOH (0.22 g, 4 mmol) and CS_2 (0.24 mL, 4 mmol) in 20 mL of acetonitrile furnished dithiocarbamate ligand **DL1** as a yellow powder. Yield 87 %. Decomposition temp. range, 237 – 242 °C. ^{1}H NMR (DMSO, 400 MHz): δ (ppm) 1.90 (s, 6H, CH_3-Ar), 1.99 (s, 6H, CH_3-Ar), 6.91 (s, 3H, Ar-H), 6.85 (d, 2H, J_{HH} = 7.48 Hz, Ar-H), 6.70 (t, 1H, J_{HH} = 7.48 Hz, Ar-H) 9.86 (s, 1H, -CH=N) . ^{13}C NMR (DMSO, 100 MHz) δ (ppm) 16.7, 17.3, 116.9, 121.0, 124.9, 126.0, 126.4, 126.5, 126.6, 134.1, 140.9, 148.3, 151.5, 217.62. IR υ (cm^{-1}) 2918(w), 1640(s), 1467(s), 1000(s), 921(w). UV-Vis ($CHCl_3$, λ_{max}, nm), 292, 340. Anal. calcd for $C_{18}H_{22}KN_2OS_2$: C, 56.21; H, 5.50; N, 7.28; S, 16.67. Found: C, 56.06; H, 5.75; N, 7.22; S, 16.20.

2.5.2 Synthesis of N,N'-bis(2,6-diisopropylphenyl) formamidine dithiocarbamate potassium salt (DL2)

The reaction of L2 (1.46 g, 4 mmol), KOH (0.22 g, 4 mmol) and CS_2 (0.16 mL, 4 mmol) in 20 mL of acetonitrile furnished dithiocarbamate ligand **DL2** as a yellow powder. Yield 74.18%. Decomposition temp. range, 244 – 249 °C. ^{1}H NMR (DMSO, 400 MHz) : δ (ppm) 1.06 (d, 12H, J_{HH} = 6.88 Hz, -CH_3-CH-), 2.84 (m, 2H, J_{HH} = 6.72 Hz, CH-CH_3), 2.97 (m, 2H, J_{HH} = 6.84 Hz, CH-CH_3), 6.94 (t, 1H, J_{HH} = 6.76 Hz, Ar-H), 7.02 (d, 2H, J_{HH} = 7.12 Hz, Ar-H), 7.11 (d, 2H, J_{HH} = 7.5 Hz, Ar-H), 7.21 (t, 1H, J_{HH} = 7.00 Hz, Ar-H), 10.15 (s, 1H, -CH=N). ^{13}C NMR (DMSO, 100 MHz) δ (ppm): 23.80, 24.00, 24.86, 26.58, 28.24, 122.47, 122.86, 127.08, 138.61, 138.87, 145.23, 147.49, 154.21, 220.94. IR υ (cm^{-1}) :2959(s), 2865(w) 1639(s), 1452(s), 1152(s), 999(s). UV-Vis ($CHCl_3$, λ_{max}, nm), 293, 339. Anal. calcd for $C_{26}H_{35}KN_2S_2$: C, 66.08; H, 7.69; N, 5.85; S, 13.39. Found: C, 65.92; H, 7.37; N, 5.85; S, 12.20.

2.5.3 Synthesis of N,N'-bis(2,4,6-trimethylphenyl) formamidine dithiocarbamate potassium salt (DL3)

The reaction of L3 (1.12 g, 4 mmol), KOH (0.22 g, 4 mmol) and CS_2 (0.21 mL, 4 mmol) in 20 mL of acetonitrile furnished dithiocarbamate ligand **DL3** as a yellow powder. Yield 93.63%. Decomposition temp. range, 258 – 263 °C. ^{1}H NMR (DMSO, 400 MHz) δ (ppm) 1.94 (s, 6H,

CH_3-Ar), 2.03 (s, 6H, CH_3-Ar), 2.15 (s, 3H, CH_3-Ar), 2.22 (s, 3H, CH_3-Ar) 6.75 (s, 2H, Ar-H), 6.81 (s, 2H, Ar-H), 9.92 (s, 1H, CH=N). ^{13}C NMR (DMSO, 100 MHz) δ (ppm): 13.92, 17.70, 18.32, 20.29, 20.58, 127.26, 127.90, 128.30, 130.51, 134.82, 139.55, 147.10, 152.79, 218.95. IR υ (cm^{-1}) 2951 (m), 1629(s), 1477(m), 1023(s), 956(w). UV-Vis ($CHCl_3$, λ_{max}, nm), 289, 338. Anal. calcd for $C_{20}H_{23}KN_2S_2$: C, 60.87; H, 5.87; N, 7.10; S, 16.25. Found: C, 60.41; H, 5.93; N, 6.95; S, 15.97.

2.5.4 Synthesis of N-(2,6-dichlorophenyl)-N-(2,6-dimethylphenyl) formamidine dithiocarbamate potassium salt (DL4)

The reaction of L4 (1.17 g, 4 mmol), KOH (0.22 g, 4 mmol) and CS_2 (0.25 g, 4mmol) in 20 mL of acetonitrile furnished dithiocarbamate ligand **DL4** as a yellow powder. Yield 77%. Decomposition temp. range, 245 – 248 °C. ^{1}H NMR (DMSO, 400 MHz): δ (ppm): 2.13 (s, 6H, CH_3-Ar), 7.02 (s, 4H, Ar-H), 7.39 (d, 2H, J_{HH} = 8.08 Hz, Ar-H) 10.12 (s, 1H, -CH=N). ^{13}C NMR (DMSO, 100 MHz) δ (ppm): 17.76, 124.13, 126.37, 126.40, 127.26, 127.52, 127.73, 128.34, 135.23, 135.42, 141.29, 146.08, 154.81, 218.82. IR υ (cm^{-1}): 3177(w), 1614(s), 1432(s), 1128(s), 1033(s). UV-Vis ($CHCl_3$, λ_{max}, nm), 293, 345. Anal. calcd for $C_{16}Cl_2H_{15}KN_2OS_2$: C, 45.67; H, 3.95; N, 6.58; S, 15.20. Found: C, 45.52; H, 3.81; N, 6.29; S, 15.19.

2.5.5 Synthesis of N-(2,6-dichlorophenyl)-N-(2,6-diisopropylphenyl) formamidine dithiocarbamate potassium salt (DL5)

The reaction of L5 (1.40 g, 4 mmol), KOH (0.22 g, 4 mmol) and CS_2 (0.21 g, 4 mmol) in 20 mL of acetonitrile furnished dithiocarbamate ligand **DL5** as a yellow powder. Yield 91%. Decomposition temp. range, 250 – 260 °C. ^{1}H NMR (DMSO, 400 MHz): δ (ppm): 1.14 (t, 12H, J_{HH} = 7.28 Hz, CH_3-CH), 2.87 (m, 2H, J_{HH} = 6.76 Hz, CH-Ar), 6.98 (t, 1H, J_{HH} = 8.08 Hz, Ar-H), 7.10 (d, 2H, J_{HH} = 7.56 Hz, Ar-H), 7.21 (t, 1H, J_{HH} = 7.24 Hz, Ar-H), 7.38 (d, 2H, J_{HH} = 8.08 Hz, Ar-H) 10.39 (s, 1H, -CH=N-Ar). ^{13}C NMR (DMSO, 100 MHz) δ (ppm): 26.81, 27.75, 27.98, 132.87, 133.98, 137.90, 138.48, 145.31, 146.14, 146.33, 151.41, 156.87, 217.02. IR υ (cm^{-1}): 2960 (w), 1603(s), 1430(s), 1145(s), 1036(s). UV-Vis ($CHCl_3$, λ_{max}, nm), 300, 345. Anal. calcd for $C_{20}Cl_2H_{27}KN_2O_3S_2$: C, 46.61; H, 5.62; N, 5.41; S, 12.63. Found: C, 46.53; H, 5.55; N, 5.05; S, 12.59.

2.5.6 Synthesis of N-(2,6-dichlorophenyl)-N-mesityl formamidine dithiocarbamate potassium salt (DL6)

The reaction of L6 (1.23 g, 4 mmol), KOH (0.22 g, 4 mmol) and CS_2 (0.24 g, 4 mmol) in 20 mL of acetonitrile furnished dithiocarbamate ligand **DL6** as a yellow powder. Yield 83%. Decomposition temp. range, 255 – 258 °C. ^{1}H NMR (DMSO, 400 MHz): δ (ppm): 2.07 (s, 6H, CH_3-Ar-N-), 2.23 (s, 3H, CH_3-Ar), 6.81 (s, 2H, Ar-H) 7.00 (t, 1H, J_{HH} = 8.4 Hz, Ar-H), 7.35 (d, 2H, J_{HH} = 8.04 Hz, Ar-H), 10.11 (s, 1H,CH=N-Ar). ^{13}C NMR (DMSO, 100 MHz) δ (ppm): 17.68, 20.59, 124.04, 126.34, 127.97, 128.32, 135.02, 135.12, 138.71, 146.17, 154.83, 219.04. IR υ (cm^{-1}) 2915(w), 1612(s), 1435(s), 1141(s), 1032(s). UV-Vis ($CHCl_3$, λ_{max}, nm), 295 343. Anal. calcd for $C_{17}Cl_2H_{17}KN_2OS_2$: C, 46.46; H, 3.90; N, 6.37; S, 14.59. Found: C, 46.29; H, 4.05; N, 6.33; S, 14.26.

2.5.7 Synthesis of N-(2-bromophenyl)-N-(2,6-dimethylphenyl) formamidine dithiocarbamate potassium salt (DL7)

The reaction of L7 (1.27 g, 4 mmol), KOH (0.23 g, 4 mmol) and CS_2 (0.30 g, 4 mmol) in 20 mL of acetonitrile furnished dithiocarbamate ligand **DL7** as a yellow powder. Yield 77%. Decomposition temp. range, 230 - 233°C. ^{1}H NMR (DMSO, 400 MHz): δ (ppm): 1.99(s, 3H, CH_3-Ar), 2.09(s, 3H, CH_3-Ar), 6.79(t, 1H, $J_{H,H}$ = 7.40, Ar-H), 6.89(d, 1H, $J_{H,H}$ = 7.60, Ar-H), 6.95(d, 2H, $J_{H,H}$ = 7.88, Ar-H), 7.29(t, 1H, $J_{H,H}$ = 7.48, Ar-H), 7.35(t, 1H, $J_{H,H}$ = 7.32, Ar-H), 7.52(d, 1H, $J_{H,H}$ = 7.92, Ar-H), 10.08(s, 1H, -CH=N). ^{13}C NMR (DMSO, 100 MHz) δ (ppm): 18.24, 18.33, 18.86, 121.95, 122.76, 125.11, 125.34, 126.68, 126.82, 127.71, 128.03, 128.24, 128.99, 129.12, 132.88, 133.04, 135.64, 135.71, 142.33, 142.48, 149.86, 150.44, 152.81 and 219.19. IR υ (cm^{-1}) 2976(w), 1613(s), 1467(s), 1023(s), 870. UV-Vis ($CHCl_3$, λ_{max}, nm), 303 and 337. Anal. calcd for $BrC_{16}H_{14}KN_2S_2$: C, 46.04; H, 3.38; N, 6.71; S, 15.36. Found: C, 45.99; H, 3.15; N, 6.39; S, 15.21.

2.5.8 Synthesis of N-(2-bromophenyl)-N-mesityl formamidine dithiocarbamate potassium salt (DL8)

The reaction of L8 (1.26 g, 4 mmol), KOH (0.22 g, 4 mmol) and CS_2 (0.31 g, 4 mmol) in 20 mL of acetonitrile furnished dithiocarbamate ligand **DL8** as a yellow powder. Yield 70%. Decomposition temp. range, 239 - 241°C. ^{1}H NMR (DMSO, 400 MHz): δ (ppm): 2.01(s, 6H, CH_3-Ar), 2.22(s, 3H, CH_3-Ar), 6.80(s, 1H, Ar-H), 6.87(t, 1H, $J_{H,H}$ = 7.80, Ar-H), 6.96(t, 1H,

$J_{H,H}$ = 7.56, Ar-H), 7.28(t, 1H, $J_{H,H}$ = 7.64, Ar-H), 7.51(d, 1H, $J_{H,H}$ = 7.92, Ar-H), 10.07(s, 1H, -CH=N). ^{13}C NMR (DMSO, 100 MHz) δ (ppm):18.17, 18.26, 21.08, 25.57, 117.30, 121.98, 125.28, 128.44, 129.11, 132.87, 135.26, 135.56, 139.75, 150.55, 152.88 and 219.43. IR υ (cm^{-1}) 2915(w), 1614(s), 1465(s), 1024(s), 852. UV-Vis ($CHCl_3$, λ_{max}, nm), 306 and 342. Anal. calcd for $BrC_{16}H_{14}KN_2S_2$: C, 47.33; H, 3.74; N, 6.49; S, 14.86. Found: C, 46.99; H, 3.52; N, 6.16; S, 14.99.

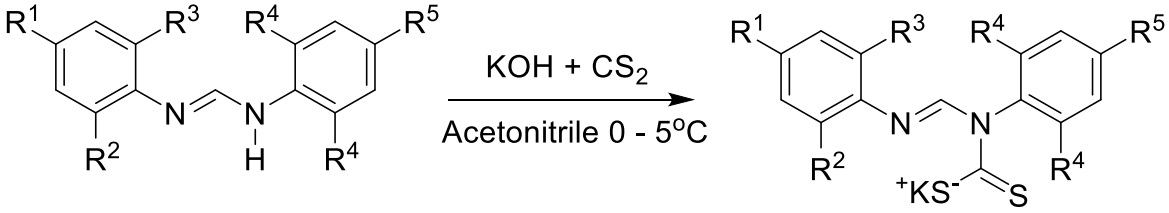

$R^1 = R^5 = H$, $R^2 = R^3 = R^4 = Me$**: L1, DL1**
$R^1 = R^5 = H$, $R^2 = R^3 = R^4 = iPr$**: L2, DL2**
$R^1 = R^2 = R^3 = R^4 = R^5 = Me$**: L3, DL3**
$R^1 = R^5 = H$, $R^2 = R^3 = Cl$, $R^4 = Me$**: L4, DL4**
$R^1 = R^5 = H$, $R^2 = R^3 = Cl$, $R^4 = iPr$**: L5, DL5**
$R^1 = H$, $R^2 = R^3 = Cl$, $R^4 = R^5 = Me$**: L6, DL6**
$R^1 = R^3 = R^5 = H$, $R^2 = Br$, $R^4 = Me$**: L7, DL7**
$R^1 = R^3 = H$, $R^2 = Br$, $R^4 = R^5 = Me$**: L8, DL8**

Scheme 2.1: Synthesis of potassium salt of N,N'-diarylformamidines dithiocarbamates **DL1 - DL8**

2.6 Synthesis of thiuram disulfides

The general procedure for the synthesis of the thiuram disulfides is as follows. Firstly, 2 moles of the appropriate dithiocarbamate salt was dissolved in acetonitrile. To the resulting yellow solution, 1 mole of iodine was added. Thereafter, the reaction mixture was stirred at room temperature for 20 min. After all the iodine has reacted, a less intense yellow precipitate was formed. The resulting solids were collected by filtration, washed with diethyl ether three times and dried at room temperature.

2.6.1 Synthesis of N,N'-(disulfanne-1,2-dicarbonothioyl)bis(N,N'-bis(2,6-dimethylphenyl) formamidine (1)

The reaction of **DL1** and iodine in 20 mL of acetonitrile furnished thiuram disulfide **1** as a yellow powder. Yield 65%. Melting point 189–190 °C ^{1}H NMR ($CDCl_3$, 600 MHz): δ (ppm) 2.12 (s, 12H, CH_3-Ar), 2.46 (s, 12H, CH_3-Ar), .6.93 (t, 2H, $J_{H,H}$ = 7.38, Ar-H), 7.02 (d, 4H, $J_{H,H}$ = 7.32, Ar-H), 7.29 (d, 4H, $J_{H,H}$ = 7.02, Ar-H), 7.34 (t, 2H, $^{2}J_{H,H}$ = 7.38, Ar-H), 9.84 (s, 2H, -CH=N). ^{13}C NMR (DMSO, 150 MHz) δ (ppm) 18.05, 18.73, 124.01, 127.75, 128.18, 129.06, 130.75, 132.68, 137.69, 147.01, 150.80 and 198.44. IR υ (cm^{-1}) 2920(w), 1645(s), 1469(s), 1256(s), 859(m). ESI-TOF MS: m/z (%); $[M + 4H – DL1 – K]^+$ 331.17. UV-Vis ($CHCl_3$, λ_{max}, nm): 268, 312 (shoulder). Anal. calcd for $C_{36}H_{40}N_4OS_4$: C, 64.25; H, 6.30; N, 8.33; S, 19.06. Found: C, 64.17; H, 6.24; N, 8.32; S, 18.78.

2.6.2 Synthesis of N,N'-disulfanne-1,2-dicarbonothioyl)bis(N,N'-bis(2,6-diisopropylphenyl) formamidine (2)

The reaction of **DL2** and iodine in 20 mL of acetonitrile furnished thiuram disulfide **2** as a yellow powder. Yield 61%. Melting point 210–211 °C ^{1}H NMR ($CDCl_3$, 600 MHz): δ (ppm) 1.15 (d, 28H, $J_{H,H}$ = 6.18, CH_3-CH), 1.27 (d, 20H, $^{1}J_{H,H}$ = 6.72, -CH_3-CH), 3.01 (m, 8H, $^{3}J_{H,H}$ = 6.54, CH-CH_3), 7.13 (t, 6H, $J_{H,H}$ = 6.72, Ar-H), 7.37 (d, 4H, $^{1}J_{H,H}$ = 7.44, Ar-H), 7.55 (d, 2H, $^{1}J_{H,H}$ = 6.72, Ar-H), 9.46 (s, 2H, -CH=N). ^{13}C NMR ($CDCl_3$, 150 MHz) δ (ppm) : 23.63, 24.07, 24.65, 24.79, 27.61, 29.11, 123.17, 124.61, 124.80, 137.24, 139.08, 144.40, 147.59, 151.71 and 198.97. IR υ (cm^{-1}) 2927(w), 1645(s), 1463(s), 1256(s), 858(m). ESI-TOF MS: m/z (%) $[M + Li]^+$. 886.97. UV-Vis ($CHCl_3$, λ_{max}, nm): 271, 314 (shoulder). Anal. calcd for $C_{52}H_{70}N_4S_4$: C, 71.02; H, 8.32; N, 6.37; S, 14.58. Found: C, 70.12; H, 8.29; N, 6.09; S, 14.72.

2.6.3 Synthesis of N,N-(disulfanne-1,2-dicarbonothioyl)bis(N,N'-dimesityl) formamidine (3)

The reaction of **DL3** and iodine in 20 mL of acetonitrile furnished thiuram disulfide **3** as a yellow powder. Yield 70%. Melting point 186–187 °C. ^{1}H NMR ($CDCl_3$, 600 MHz) δ (ppm): 2.10 (s, 12H, CH_3-Ar), 2.27 (s, 6H, CH_3-Ar), 2.41 (s, 18H, CH_3-Ar), 6.85 (s, 4H, Ar-H), 7.11 (s, 4H, Ar-H), 9.42 (s, 2H, CH=N). ^{13}C NMR ($CDCl_3$, 150 MHz) δ (ppm): 17.95, 18.67, 20.67, 21.36, 127.60, 129.87, 133.23, 133.57, 137.26, 140.87, 144.73, 151.07 and 198.85. IR υ (cm^{-1}) 2963(w), 1643(s), 1478(s), 1251(s), 849(m). ESI-TOF MS: m/z (%); $[M + 3H – DL3 + K]^+$

359.20. UV-Vis ($CHCl_3$, λ_{max}, nm): 262, 309 (shoulder). Anal. calcd for $C_{40}H_{52}N_4O_3S_4$: C, 62.79; H, 6.55; N, 7.32; S, 16.77. Found: C, 62.55; H, 6.21; N, 7.09; S, 16.77.

2.6.4 Synthesis of N,N-(disulfane-1,2-dicarbonothioyl)bis(N-(2,6-dichlorophenyl)-N'-(2,6-dimethylphenyl) formamidine (4)

The reaction of **DL4** and iodine in 20 mL of acetonitrile furnished thiuram disulfide **4** as a yellow powder. Yield 73%. Melting point 225–226 °C. ^{1}H NMR($CDCl_3$, 600 MHz): δ (ppm): 2.49 (s, 12H, CH_3-Ar), 6.97 (t, 2H, $^2J_{H,H}$ = 8.16 Ar-H), 7.30 (d, 8H, $J_{H,H}$ = 8.40, Ar-H) 7.05 (t, 2H, $^2J_{H,H}$ = 7.44 Ar-H), 9.56 (s, 2H, -CH=N) . ^{13}C NMR ($CDCl_3$, 150 MHz) δ (ppm) 18.03, 125.09, 126.74, 127.74, 128.08, 128.20, 128.28, 129.07, 131.02, 135.51, 138.04, 144.09, 153.46 and 198.73. IR υ (cm^{-1}) 2918(w), 1649(s), 1433(s), 1265(s), 865(m). ESI-TOF MS: m/z (%); $[M + 4K - 4H]^+$. 887.06. UV-Vis ($CHCl_3$, λ_{max}, nm): 270, 315 (shoulder). Anal. calcd for $C_{32}Cl_4H_{26}N_4S_4$: C, 54.38; H, 3.56; N, 7.61; S, 18.41. Found: C, 54.29; H, 3.49; N, 7.59; S, 18.20.

2.6.5 Synthesis of N,N'-(disulfanne-1,2-dicarbonothioyl)bis(N-(2,6-dichlorophenyl)-N-(2,6-diisopropylphenyl) formamidine (5)

The reaction of **DL5** and iodine in 20 mL of acetonitrile furnished thiuram disulfide **5** as a yellow powder. Yield 69%. Melting point 234–235 °C ^{1}H NMR ($CDCl_3$, 600 MHz): δ (ppm): 1.32 (d, 12H, $J_{H,H}$ = 6.60 CH_3-CH), 1.43 (d, 12H, $J_{H,H}$ = 6.54 CH_3-CH),3.11 (m, 4H, $^3J_{H,H}$ = 6.48, CH-CH_3), 6.97 (t, 2H, $J_{H,H}$ = 7.86, Ar-H), 7.32 (d, 4H, $^1J_{H,H}$ = 8.10, Ar-H), 7.39 (d, 2H, $^1J_{H,H}$ = 7.68, Ar-H), 7.59 (t, 2H, $J_{H,H}$ =8.04, Ar-H) 9.81 (s, 2H, -CH=N). ^{13}C NMR ($CDCl_3$, 150 MHz) δ (ppm):24.48, 25.25, 28.92, 124.89, 125.09, 127.04, 128.59, 131.55, 144.13, 147.89, 155.57 and 199.65. IR υ (cm^{-1}) 2930(w), 1630(s), 1433(s), 1259(s), 864(w). ESI-TOF MS: m/z (%); $[M + K]^+$ 887.05. UV-Vis ($CHCl_3$, λ_{max}, nm): 271, 324. Anal. calcd for $C_{40}H_{42}Cl_4N_4S_4$: C, 56.90; H, 4.99; N, 6.60; S, 15.11. Found: C, 56.81; H, 4.99; N, 6.42; S, 15.01.

2.6.6 Synthesis of N,N-(disulfanne-1,2-dicarbonothioyl)bis(N-(2,6-dichlorophenyl)-N-mesityl formamidine (6)

The reaction of **DT6** and iodine in 20 mL of acetonitrile furnished thiuram disulfide **6** as a yellow powder. . Yield 75%. Melting point 239–240 °C ^{1}H NMR ($CDCl_3$, 600 MHz): δ (ppm): 2.41 (s, 6H, CH_3-Ar), 2.46 (s, 12H, CH_3-Ar), 6.98 (t, 2H, $J_{H,H}$ = 8.04, Ar-H), 7.12 (s, 4H, Ar-H), 7.31 (d, 4H, $J_{H,H}$ = 8.10, Ar-H), 9.56 (s, 2H, -CH=N). ^{13}C NMR ($CDCl_3$, 150 MHz) δ (ppm):

17.94, 21.42, 125.06, 126.78, 128.26, 129.93, 132.90, 137.62, 141.25, 144.25, 153.66, and 199.25. IR υ (cm^{-1}) 2972(w), 1633(s), 1436(s), 1256(s), 863(m). ESI-TOF MS: m/z (%) [M – DL6 – K]$^+$ 381.01. UV-Vis ($CHCl_3$, λ_{max}, nm): 272, 318. Anal. calcd for $C_{34}H_{30}Cl_4N_4S_4$: C, 53.81; H, 3.95; N, 7.33; S, 17.98. Found: C, 53.79; H, 3.82; N, 7.17; S, 17.33.

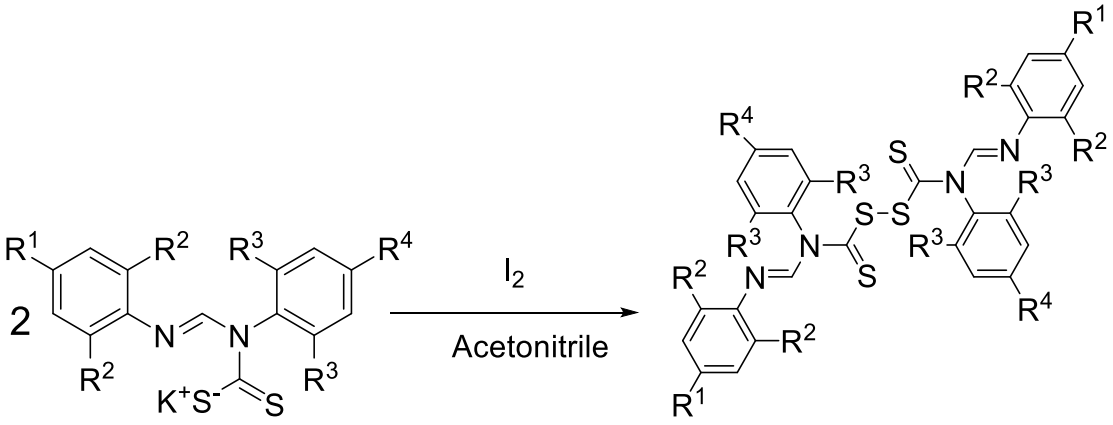

$R^1 = R^4 = H$, $R^2 = R^3 =$ Me**: DL1**, **1**
$R^1 = R^4 = H$, $R^2 = R^3 =$ iPr**: DL2**, **2**
$R^1 = R^2 = R^3 = R^4 =$ Me**: DL3**, **3**
$R^1 = R^4 = H$, $R^2 =$ Cl, $R^3 =$ Me**: DL4**, **4**
$R^1 = R^4 = H$, $R^2 =$ Cl, $R^3 =$ iPr**: DL5**, **5**
$R^1 = H$, $R^2 =$ Cl, $R^3 = R^4 =$ Me**: DL6**, **6**

Scheme 2.2: Synthesis of thiuram disulfide **1 - 6**

2.7 Synthesis of N,N'-diarylformamidine dithiocarbamate metal complexes

The respective dithiocarbamate salts, 2 mmol or 3 mmol, were dissolved in 15 mL of acetonitrile. To the resulting mixture, 1 mmol of the metal chloride salt dissolved in 10 ml of water was added drop-wise and stirred for about 30 min at room temperature. A sudden change in colour was observed, according to the metal salt used and a precipitate was formed immediately. The product formed was collected by filtration. The complexes were then recrystallized in hot ethanol at 80 °C to remove any unreacted ligand. The solid precipitate was then collected by filtration and dried in the oven at 50 °C.

2.7.1 Synthesis of [Ni-(DL1)$_2$] (7)

The reaction of DL1 (0.30 g, 0.8 mmol) and $NiCl_2 \cdot 6H_2O$ (0.10 g 0.4 mmol) in acetonitrile furnished complex **7** as a purple-red powder. Yield 72%. Decomposition temp. range, 265-267 °C. ^{1}H NMR ($CDCl_3$, 400 MHz) δ (ppm): 2.09 (s, 12H, CH_3-Ar), 2.29 (s, 12H, CH_3-Ar), 6.91

(t, 2H, J_{HH} = 7.24 Hz, Ar-H), 7.00 (d, 5H, J_{HH} = 7.32 Hz, Ar-H), 7.19 (d, 5H, J_{HH} = 7.28 Hz, Ar-H), 8.85 (s, 2H, -CH=N) : ^{13}C NMR ($CDCl_3$, 100 MHz) δ (ppm): 17.62, 18.64, 18.71, 124.32, 126.33, 127.61, 128.24, 128.85, 129.91, 133.96, 135.91, 145.04, 146.66, 216.95. IR υ (cm^{-1}): 2949(m), 1647(s), 1474(m), 1126(m), 999(m), 376(s). ESI-TOF MS: m/z (%); $[M]^+$ 713.14. UV-Vis ($CHCl_3$, λ_{max}, nm), 262, 341, 457. Anal. calcd for $C_{36}H_{40}N_4NiS_4$: C, 60.42; H, 5.63; N, 7.83; S, 17.92. Found: C, 60.28; H, 5.29; N, 7.71; S, 17.35

2.7.2 Synthesis of [Ni-(DL2)$_2$] (8)

The reaction of DL2 (0.3 g, 0.6 mmol) and $NiCl_2 \cdot 6H_2O$ (0.07 g, 0.3 mmol) in acetonitrile furnished complex **8** as an orange powder. Yield 68.25%. Decomposition temp. range, 280 – 282 °C. ^{1}H ($CDCl_3$, 400 MHz) : δ (ppm) 1.14 (d, 26H, J_{HH} = 5.2 Hz, -CH_3-CH), 1.32 (s, 10H, CH_3-), 1.40 (s, 12H, -CH_3), 2.83 (m, 8H CH-CH_3) 7.10 (s, 5H, Ar-H), 7.15 (s, 7H, Ar-H), 8.88 (s, 2H, -CH=N). ^{13}C NMR ($CDCl_3$, 100 MHz) δ (ppm): 24.05, 24.10, 25.26, 27.61, 29.26, 30.93, 123.19, 124.61, 124.85, 130.57, 138.74, 145.14, 146.26, 206.98 IR υ (cm^{-1}) 2961(s), 2867(w) 1651(s), 1460(s), 1178(s), 996(s), 378(s). ESI-TOF MS: m/z (%); $[M + K]^+$. 973.30. UV-Vis ($CHCl_3$, λ_{max}, nm), 261, 341, 457. Anal. calcd for $C_{52}H_{74}N_4NiOS_4$: C, 65.73; H, 7.80; N, 5.85; S, 13.38. Found: C, 65.60; H, 7.80; N, 5.70; S, 13.06.

2.7.3 Synthesis of [Ni-(DL3)$_2$] (9)

The reaction of DL3 (0.3 g, 0. 8mmol) and $NiCl_2 \cdot 6H_2O$ (0.08 g, 0.4 mmol) in acetonitrile furnished complex **9** as a purple-red powder. Yield 70%. Decomposition temp. range, 270-272 °C. ^{1}H NMR ($CDCl_3$, 400 MHz): δ (ppm) 2.05 (s, 10H, CH_3-Ar), 2.24 (s, 18H, CH_3-Ar), 2.30 (s, 3H, CH_3-Ar), 6.82 (s, 4H, Ar-H), 7.00 (s, 4H, Ar-H), 8.81 (s, 2H, CH=N). ^{13}C NMR ($CDCl_3$, 150 MHz) δ (ppm): 17.58, 17.57, 18.52, 19.26, 20.63, 21.21, 127.47, 128.73, 128.87, 129.06, 129.50, 129.61, 133.61, 135.43, 144.79, 217.92. IR υ (cm^{-1}) 2914(w), 1644(s), 1477(m) 1145(m), 955(w), 318(s). ESI-TOF MS: m/z (%); $[DL3 - CH_3]^+$ 340.18. UV-Vis ($CHCl_3$, λ_{max}, nm), 258, 340, 454. Anal. calcd for $C_{40}H_{48}N_4NiS_4$: C, 62.25; H, 6.27; N, 7.26; S, 16.62. Found: C, 61.90; H, 6.11; N, 7.09; S, 16.60.

2.7.4 Synthesis of [Ni-(DL4)$_2$] (10)

The reaction of DL4 (0.20 g, 0.50 mmol) and $NiCl_2 \cdot 6H_2O$ (0.06 g 0.25 mmol) in acetonitrile furnished complex **10** as a purple-red powder. Yield 78%. Decomposition temp. range 260-262 °C. ^{1}H NMR ($CDCl_3$, 400 MHz) δ (ppm): 2.31 (s, 12H, CH_3-Ar-), 6.96 (t, 3H, J_{HH} = 8.16

Hz, Ar-H), 7.16 (d, 4H, J_{HH} = 7.4 Hz, Ar-H), 7.28 (s, 3H, Ar-H), 8.94 (s, 2H, -CH=N). : ^{13}C NMR ($CDCl_3$, 100 MHz) δ (ppm): 17.59, 125.42, 126.57, 128.32, 128.78, 130.09, 133.36, 136.20, 143.61, 147.33, 219.32. IR υ (cm^{-1}) 2968(w), 1642(s), 1435(m), 1096(m), 887(s).371(s). ESI-TOF MS: m/z (%); $[M - 2Cl]^+$. 723.03. UV-Vis ($CHCl_3$, λ_{max}, nm), 263, 341, 462. Anal. calcd for $C_{32}Cl_4H_{34}N_4NiO_3S_4$: C, 45.52; H, 4.03; N, 6.58; S, 15.19. Found: C, 45.47; H, 3.95; N, 6.42; S, 15.18.

2.7.5 Synthesis of [Ni-(DL5)$_2$] (11)

The reaction of DL5 (0.20 g, 0.4 mmol) and $NiCl_2 \cdot 6H_2O$ (0.05 g 0.20 mmol) in acetonitrile furnished complex **11** as an orange powder. Yield 78%. Decomposition temp. Range, 274-276 °C. ^{1}H NMR ($CDCl_3$, 400 MHz) δ (ppm): 1.25 (s, 16H, CH_3-CH), 1.34 (s, 8H, CH_3-CH), 2.85 (s, 4H, CH-CH_3, 6.93 (s, 2H, Ar-H), 7.55 (s, 2H, Ar-H), 9.10 (s, 2H, -CH=N). ^{13}C NMR ($CDCl_3$, 100 MHz) δ (ppm): 17.51, 29.26, 30.93, 123.16, 124.61, 124.85, 130.56, 138.75, 146.26, 218.76. IR υ (cm^{-1}) 2961(w), 1639(s), 1435(m), 1084(m), 888(s).372(s). ESI-TOF MS: m/z (%); $[M - 2Cl]^+$. 835.15. UV-Vis ($CHCl_3$, λ_{max}, nm), 262, 343, 467. Anal. calcd for $C_{40}Cl_4H_{46}N_4NiOS_4$: C, 51.80; H, 5.00; N, 6.04; S, 13.38. Found: C, 51.21; H, 4.63; N, 5.84; S, 13.43.

2.7.6 Synthesis of [Ni-(DL6)$_2$] (12)

The reaction of DL6 (0.20 g, 0.50 mmol) and $NiCl_2 \cdot 6H_2O$ (0.06 g 0.25 mmol) in acetonitrile furnished complex **12** as a purple-red powder. Yield 80%. Decomposition temp. Range, 268-270 °C. ^{1}H NMR ($CDCl_3$, 400 MHz) δ (ppm): 2.26 (s, 12H, CH_3-Ar), 2.29 (s, 6H, CH_3-Ar), 6.93 (d, 2H, J_{HH} = 7.7, Ar-H), 6.98 (s 4H, Ar-H), 8.91 (s, 2H, -CH=N). ^{13}C NMR ($CDCl_3$, 100 MHz) δ (ppm): 17.51, 29.26, 30.93, 123.19, 124.61, 124.85, 130.56, 138.75, 146.26, 218.76. IR υ (cm^{-1}) 2970(w), 1644(s), 1436(m), 1098(m), 889(s).317(s). ESI-TOF MS: m/z (%); $[M - 2Cl]^+$. 752.38. UV-Vis ($CHCl_3$, λ_{max}, nm), 263, 343, 465. Anal. calcd for $C_{34}H_{32}Cl_4N_4NiS_4$: C, 49.48; H, 3.91; N, 6.79; S, 15.54. Found: C, 49.02; H, 3.47; N, 6.61; S, 15.27.

2.7.7 Synthesis of [Cu-(DL1)$_2$] (13)

The reaction of DL1 (0.3 g, 0.8 mmol) and $CuCl_2 \cdot 2H_2O$ (0.07 g, 0.4 mmol) in acetonitrile furnished complex **13** as a deep brown powder. Yield 89%. Decomposition temp. Range, 280–282 °C. IR υ (cm^{-1}) 2918(w), 1645(s), 1470(m), 1186(s), 999(m), 374(w). ESI-TOF MS: m/z (%); $[M]^+$ 718.13. UV-Vis ($CHCl_3$, λ_{max}, nm), 300, 316 (shoulder), 449. Anal. calcd for

$C_{36}CuH_{46}N_4O_3S_4$: C, 56.21; H, 5.99; N, 7.33; S, 17.26. Found: C, 56.04; H, 5.99; N, 7.27; S, 17.15.

2.7.8 Synthesis of [Cu-(DL2)$_2$] (14)

The reaction of DL2 (0.3 g, 0.6 mmol) and $CuCl_2 \cdot 2H_2O$ (0.50 g, 0.3 mmol) in acetonitrile furnished complex **14** as a reddish-brown powder. Yield 84%. Decomposition temp. Range, 294–296 °C. IR υ (cm^{-1}) 2960(m), 2915(m), 1639(s), 1477(m), 1143(m) 957(w), 395(w). ESI-TOF MS: m/z (%); $[M + K – (DL2 – 5H)]^+$ 537.09. UV-Vis ($CHCl_3$, λ_{max}, nm), 301, 319 (shoulder), 449. Anal. calcd for $C_{52}CuH_{72}N_4S_4$: C, 60.69; H, 5.98; N, 8.18; S, 18.50. Found: C, 60.38; H, 5.97; N, 8.12; S, 18.11.

2.7.9 Synthesis of [Cu-(DL3)$_2$] (15)

The reaction of DL3 (0.3 g, 7.3mmol) and $CuCl_2 \cdot 2H_2O$ (0.06 g, 3.6mmol) in acetonitrile furnished complex **15** as a deep brown powder. Yield 86%. Decomposition temp. range, 290–293 °C. IR υ (cm^{-1}) 2913(m), 1638(s), 1478(m), 1143(m), 957(w), 358(w). ESI-TOF MS: m/z (%); $[M – 3H]^+$ 773.19. UV-Vis ($CHCl_3$, λ_{max}, nm), 300, 317 (shoulder), 449. Anal. calcd for $C_{40}CuH_{52}N_4O_2S_4$: C, 59.12; H, 6.45; N, 6.89; S, 15.78. Found: C, 59.80; H, 6.08; N, 6.81; S, 15.85.

2.7.10 Synthesis of [Cu-(DL4)$_2$] (16)

The reaction of DL4 (0.2 g, 0.50 mmol) and $CuCl_2 \cdot 2H_2O$ (0.04 g, 0.25 mmol) in acetonitrile furnished complex **16** as a deep brown powder. Yield 89%. Decomposition temp. range, 268–270 °C. ESI-TOF MS: m/z (%); $[M]^+$. 798.99. IR υ (cm^{-1}) 2973(w), 1641(s), 1471(m), 1125(m), 883(m).370(w). UV-Vis ($CHCl_3$, λ_{max}, nm), 301, 321 (shoulder), 449. Anal. calcd for $C_{32}Cl_4CuH_{34}N_4O_3S_4$: C, 44.89; H, 4.00; N, 6.54; S, 14.98. Found: C, 44.60; H, 3.87; N, 6.29; S, 15.05.

2.7.11 Synthesis of [Cu-(DL5)$_2$] (17)

The reaction of DL5 (0.20 g, 0.40 mmol) and $CuCl_2 \cdot 2H_2O$ (0.40 g 0.20 mmol) in acetonitrile furnished complex **17** as a reddish-brown powder. Yield 84%. Decomposition temp. range, 285 – 287 °C. IR υ (cm^{-1}) 2964(w), 1640(s), 1434(m), 1130(m), 885(s).390(w). ESI-TOF MS: m/z (%); $[M]^+$.911.13. UV-Vis ($CHCl_3$, λ_{max}, nm), 301, 323 (shoulder), 449. Anal. calcd for

$C_{40}Cl_4CuH_{50}N_4O_3S_4$: C, 49.61; H, 5.20; N, 5.79; S, 13.24. Found: C, 49.44; H, 4.94; N, 5.61; S, 12.80.

2.7.12 Synthesis of [Cu-(DL6)$_2$] (18)

The reaction of DL6 (0.20 g, 0.50 mmol) and $CuCl_2 \cdot 2H_2O$ (0.04 g, 0.25 mmol) in acetonitrile furnished complex **18** as a deep brown powder. Yield 86%. Decomposition temp. range, 274 – 276 °C. ESI-TOF MS: m/z (%); $[M - H]^+$, 827.03. IR υ (cm^{-1}) 2971(w), 1639(s), 1436(m), 1125(m), 883(s).354(w). UV-Vis ($CHCl_3$, λ_{max}, nm), 300, 321 (shoulder), 449. Anal. calcd for $C_{34}Cl_4CuH_{32}N_4S_4$: C, 49.19; H, 3.89; N, 6.75; S, 15.45. Found: C, 48.89; H, 3.60; N, 6.59; S, 15.26.

2.7.13 Synthesis of [Co-(DL1)$_3$] (19)

The reaction of **DL1** (0.30 g, 0.80 mmol) and $CoCl_2$ (0.04 g, 0.27mmol) in acetonitrile furnished complex **19** as a green powder. Yield 81%. Decomposition temp. range 279 - 281 °C. . ^{1}H NMR ($CDCl_3$, 600MHz): δ (ppm): 2.18 (s, 36H, CH_3-Ar), 6.89 (t, 3H, Ar-H), 6.98 (d, 6H, Ar-H), 7.19 (m, 6H, Ar-H) 7.31 (m, 3H, Ar-H) 8.85 (s, 2H, CH=N), 8.99 (s, 1H, CH=N). ^{13}C NMR ($CDCl_3$, 150MHz) δ (ppm): 17.85, 17.93, 18.75, 124.01, 127.82, 128.18, 128.91, 129.76, 134.19, 136.45, 144.44, 147.15, and 212.97. IR υ (cm^{-1}): 2955(m), 1648(s), 1472(m), 1186(s), 888(s), 419(w). UV-Vis ($CHCl_3$, λ_{max}, nm), 277 (shoulder), 309, 389, 490 (shoulder), 621. ESI-TOF MS: m/z (%); $[M + 2Na - 2DL1]^+$ 435.93. Anal. calc. for $C_{54}CoH_{64}N_6O_2S_6$: C, 60.03; H, 5.97; N, 7.78; S, 17.80. Found C, 59.31; H, 5.58; N, 7.52; S, 17.25.

2.7.14 Synthesis of [Co-(DL2)$_3$] (20)

The reaction of **DL2** (0.30 g, 0.60 mmol) and $CoCl_2$ (0.03 g, 0.2 mmol) in acetonitrile furnished complex **20** as a green powder. Yield 77%. Decomposition temp. range 287 - 289 °C. ^{1}H NMR ($CDCl_3$, 600MHz): 1.19 (m, 72H, CH_3-CH), 2.85 (m, 12H, CH-CH_3), 7.10 (t, 10H, Ar-H), 7.28 (t, 5H, Ar-H), 7.47 (t, 5H, Ar-H), 8.99 (t, 3H, CH=N). ^{13}C NMR ($CDCl_3$, 150MHz) δ (ppm): 24.07, 24.25, 25.09, 25.32, 25.72, 27.59, 29.12, 29.26, 123.08, 123.17, 124.55, 130.42, 130.81, 138.94, 139.06, 145.07, 145.23, 145.42, 146.75, 146.88, and 214.81. IR υ (cm^{-1}): 2961(m), 1647(s), 1469(m), 1185(s), 888(s), 418(w). UV-Vis ($CHCl_3$, λ_{max}, nm), 278 (shoulder), 307, 388, 494 (shoulder), 632. ESI-TOF MS: m/z (%); $[M - DL2]^+$ 939.40. Anal. calc. for $C_{78}CoH_{108}N_6S_6$: C, 67.84; H, 7.88; N, 6.09; S, 13.93. Found C, 67.51; H, 7.44; N, 5.88; S, 13.43.

2.7.15 Synthesis of [Co-(DL3)$_3$] (21)

The reaction of **DL3** (0.30 g, 0.80 mmol) and $CoCl_2$ (0.04 g, 0.27 mmol) in acetonitrile furnished complex **21** as a green powder. Yield 79%. Decomposition temp. range 269 - 271 °C. . ^{1}H NMR ($CDCl_3$, 600MHz): 2.19 (m, 72H, CH_3-CH), 6.79 (t, 6H, Ar-H), 6.97 (s, 1H, Ar-H), 7.03 (d, 5H, Ar-H), 8.82 (d, 2H, CH=N) 8.96 (s, 1H, CH=N) ^{13}C NMR ($CDCl_3$, 150MHz) δ (ppm): 17.75, 17.83, 18.66, 20.66, 21.32, 127.66, 128.78, 129.75, 131.56, 133.22, 135.94, 139.62, 144.85, 213.07. IR υ (cm^{-1}): 2920(m), 1646(s), 1473(m), 1190(s), 890(s), 420(w). UV-Vis ($CHCl_3$, λ_{max}, nm), 275 (shoulder), 305, 387, 497 (shoulder), 618. ESI-TOF MS: m/z (%); [M - DL3]$^+$ 771.21. Anal. calc. for $C_{60}CoH_{72}N_6S_6$: C, 63.86; H, 6.43; N, 7.45; S, 17.04. Found C, 63.22; H, 6.17; N, 7.36; S, 16.57.

2.7.16 Synthesis of [Co-(DL4)$_3$] (22)

The reaction of **DL4** (0.30 g, 0.80 mmol) and $CoCl_2$ (0.04 g, 0.27 mmol) in acetonitrile furnished complex **22** as a green powder. Yield 84%. Decomposition temp. range 284 - 286 °C. ^{1}H NMR ($CDCl_3$, 600MHz): 2.24 (m, 18H, CH_3-CH), 6.93 (m, 3H, Ar-H), 7.27 (m, 15H, Ar-H), 8.96 (s, 2H, -CH=N) 9.10 (s, 1H, -CH=N) ^{13}C NMR ($CDCl_3$, 150MHz) δ (ppm): 17.78, 21.37, 125.09, 126.86, 128.89, 129.78, 130.88, 136.27, 136.69, 139.99, 144.20, 147.45, 213.94. IR υ (cm^{-1}): 2919(m), 1645(s), 1474(m), 1191(s), 882(s), 417 (w). UV-Vis ($CHCl_3$, λ_{max}, nm), 278 (shoulder), 309, 385, 487, 631 ESI-TOF MS: m/z (%); [M + 2K]$^+$ 1242.85. Anal. calc. for $C_{48}Cl_6CoH_{42}N_6S_6$: C, 49.41; H, 3.63; N, 7.20; S, 16.48. Found C, 48.96; H, 3.39; N, 7.18; S, 16.14.

2.7.17 Synthesis of [Co-(DL5)$_3$] (23)

The reaction of **DL5** (0.30 g, 0.70 mmol) and $CoCl_2$ (0.03 g, 0.24 mmol) in acetonitrile furnished complex **23** as a green powder. Yield 79%. Decomposition temp. range 305 - 307 °C. ^{1}H NMR ($CDCl_3$, 600MHz): 1.25 (m, 36H, CH3-CH), 2.79 (m, 6H, CH-CH_3), 6.94 (t, 3H, Ar), 7.28 (d, 11H, Ar-H), 7.48 (s, 4H, Ar-H), 9.20 (s, 3H, CH=N). ^{13}C NMR ($CDCl_3$, 150MHz) δ (ppm): 24.28, 24.76, 25.49, 28.95, 124.79, 125.04, 126.95, 128.44, 130.19, 130.58, 144.37, 147.03, 148.84, 215.80. IR υ (cm^{-1}): 2921(m), 1646(s), 1469(m), 1194(s), 889(s), 418 (w). UV-Vis ($CHCl_3$, λ_{max}, nm), 277 (shoulder), 313, 388, 482 (shoulder), 629. ESI-TOF MS: m/z (%) [M + H]$^+$ 1371.12. Anal. Calc. for $C_{60}Cl_6CoH_{66}N_6S_6$: C, 53.97; H, 4.98; N, 6.29; S, 14.41. Found C, 53.61; H, 4.41; N, 6.21; S, 14.26.

2.7.18 Synthesis of [Co-(DL6)$_3$] (24)

The reaction of DL6 (0.30 g, 0.80 mmol) and $CoCl_2$ (0.04 g, 0.26 mmol) in acetonitrile furnished complex **24** as a green powder. Yield 79%. Decomposition temp. range 290 - 292 °C. ^{1}H NMR ($CDCl_3$, 600MHz): 2.24 (m, 27H, CH_3-Ar), 6.97 (m, 10H, Ar-H), 7.27 (s, 3H, Ar-H), 9.01 (d, 3H, CH=N). ^{13}C NMR ($CDCl_3$, 150MHz) δ (ppm): 17.77, 21.36, 125.07, 126.85, 128.24, 129.76, 130.85, 136.23, 139.98, 144.19, 147.46, and 213.92. IR υ (cm^{-1}): 2921(m), 1647(s), 1468(m), 1193(s), 889(s), 419 (w). UV-Vis ($CHCl_3$, λ_{max}, nm), 277 (shoulder), 310, 387, 490 (shoulder), 625. ESI-TOF MS: m/z (%) $[M + H]^+$ 1244.85. Anal. calc. for $C_{48}Cl_6CoH_{42}N_6S_6$: C, 50.67; H, 4.00; N, 6.95; S, 15.91. Found C, 50.38; H, 3.53; N, 6.64; S, 15.78.

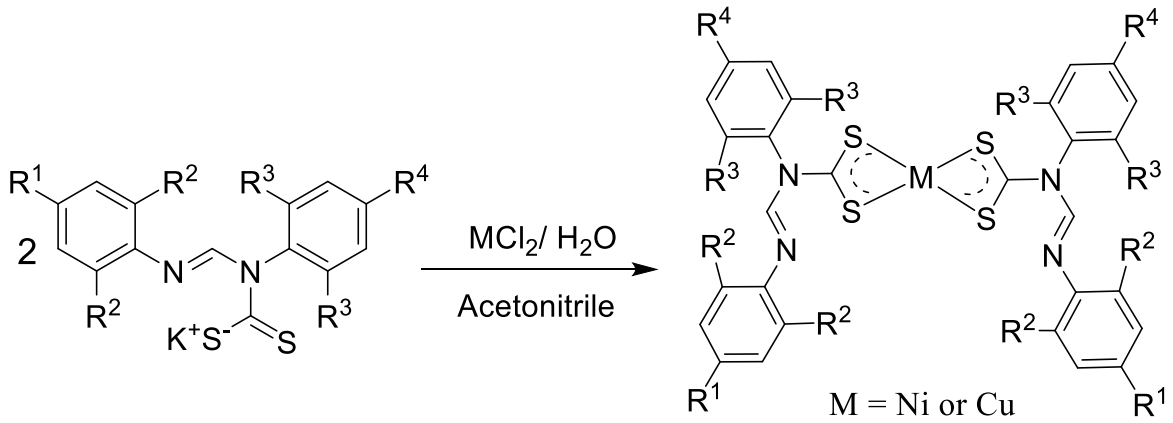

$R^1 = R^4$= H, $R^2 = R^3$ = Me, M = Ni **: DL1**, **7**
$R^1 = R^4$= H, $R^2 = R^3$ = iPr, M = Ni **: DL2**, **8**
$R^1 = R^2 = R^3 = R^4$ = Me, M = Ni **: DL3**, **9**
$R^1 = R^4$ = H, R^2 = Cl, R^3 = Me, M = Ni **: DL4**, **10**
$R^1 = R^4$ = H, R^2 = Cl, R^3 = iPr, M = Ni **: DL5**, **11**
R^1 = H, R^2 = Cl, $R^3 = R^4$ = Me, M = Ni **: DL6**, **12**
$R^1 = R^4$= H, $R^2 = R^3$ = Me, M = Cu **: DL1**, **13**
$R^1 = R^4$= H, $R^2 = R^3$ = iPr, M = Cu **: DL2**, **14**
$R^1 = R^2 = R^3 = R^4$ = Me, M = Cu **: DL3**, **15**
$R^1 = R^4$ = H, R^2 = Cl, R^3 = Me, M = Cu **: DL4**, **16**
$R^1 = R^4$ = H, R^2 = Cl, R^3 = iPr, M = Cu **: DL5**, **17**
R^1 = H, R^2 = Cl, $R^3 = R^4$ = Me, M = Cu **: DL6**, **18**

Scheme 2.3: Synthesis of Ni(II) dithiocarbamate metal complexes **7 - 12** and Cu(II) dithiocarbamate metal complexes **13 -1 8.**

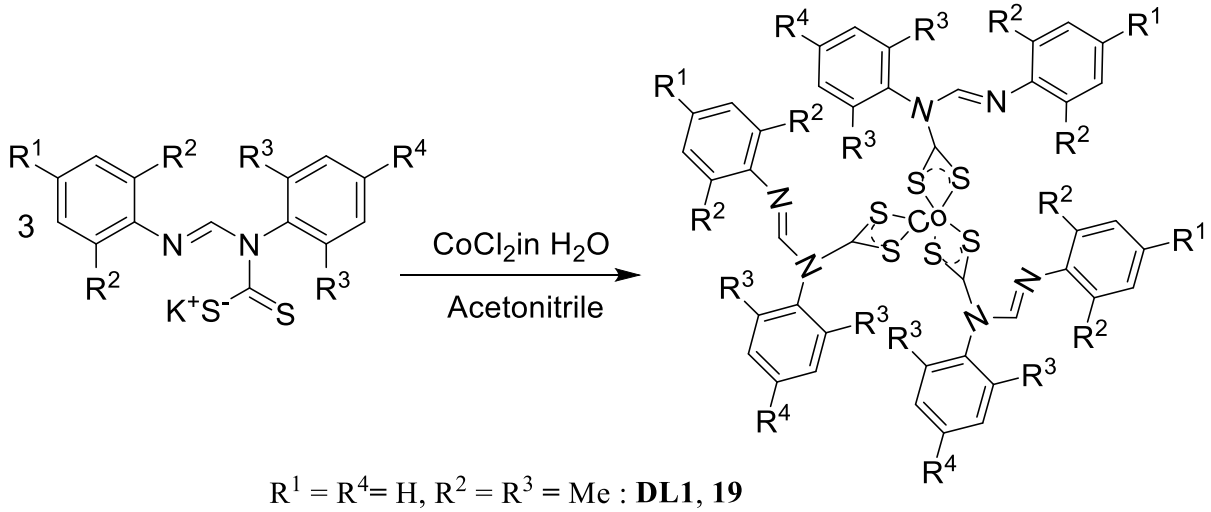

$R^1 = R^4$= H, $R^2 = R^3$ = Me : **DL1**, **19**
$R^1 = R^4$= H, $R^2 = R^3$ = iPr : **DL2**, **20**
$R^1 = R^2 = R^3 = R^4$ = Me : **DL3**, **21**
$R^1 = R^4$ = H, R^2 = Cl, R^3 = Me : **DL4**, **22**
$R^1 = R^4$ = H, R^2 = Cl, R^3 = iPr : **DL5**, **23**
R^1 = H, R^2 = Cl, $R^3 = R^4$ = Me : **DL6**, **24**

Scheme 2.4: Synthesis of Co(III) dithiocarbamate metal complexes **19 - 24.**

2.8 Synthesis of Nitratobis(triphenylphosphine) copper(I) [$Cu(PPh_3)_2NO_3$]

The metal salt, $Cu(PPh_3)_2NO_3$, used in this study was synthesized following a procedure from the literature [3] with slight modification. A solid portion of 2.5 g (0.01 mol) of $Cu(NO_3)_2{\cdot}3H_2O$ was added to a solution of 10.5 g (0.04 mol) of triphenylphosphine in 100 mL of hot methanol. The copper (II) salt dissolves spontaneously forming a colourless solution, but almost at the end of the addition, a cloudy white precipitate was formed. Thereafter, the resulting solution was refluxed for 10 minutes and then cooled to ambient temperature. The solution was filtered and the resulting white precipitate was washed thoroughly with ethanol three times and then with diethylether two times. The white precipitate (product) was air dried to give 5.3 g (75 %) of $Cu[P(C_6H_5)_3]_2(NO_3)$ (**Equation 2.1**).

$$2Cu(NO_3)_2.3H_2O + 5(C_6H_5)_3P \longrightarrow \underset{\text{White ppt (product)}}{2[Cu[P(C_6H_5)_3]_2(NO_3)]} + (C_6H_5)OP + 2HNO_3 + 5H_2O \quad (2.1)$$

Equation 2.1: Synthesis of potassium salt of Nitratobis(triphenylphosphine) copper(I)

2.9 Synthesis of heteroleptic copper(I) dithiocarbamate-PPh_3 complexes

The complexes were prepared by following general procedure from the literature [4, 5]. Firstly, 1 mmol of the respective potassium dithiocarbamate salts were dissolved in 30 ml acetonitrile

in a round bottom flask. To the resultant solution, 1 mmol of $Cu(PPh_3)_2NO_3$, dissolved in 15 ml of dichloromethane, was added drop-wise and stirred for 30 min (**Equation 2.2**). The resultant yellow solids were collected by filtration, washed three times with ethanol and then twice with ether. The pure products were dried in the oven at 40 °C and stored in a desiccator.

2.9.1 Synthesis of [$Cu(PPh_3)_2$DL1] (25)

The reaction of **DL1** (0.37 g, 1 mmol) $Cu(PPh_3)_2$DL (0.65 g, 1 mmol) in acetonitrile furnished complex **25** as a yellow powder. Yield 80%. Melting point: 244 – 245 °C. ^{1}H NMR ($CDCl_3$, 400 MHz): δ (ppm) 2.12 (s, 6H, CH_3-Ar), 2.18 (s, 6H, CH_3-Ar), 6.83 (t, 1H, , J_{HH} = 7.48 Hz, Ar-H), 6.95 (d, 2H, J_{HH} = 7.48 Hz, Ar-H), 7.11 (d, 2H, J_{HH} = 7.44 Hz, Ar-H), 7.17 (t, 13H, J_{HH} = 7.40 Hz, PPh_3), 7.30 (t, 18H, J_{HH} = 7.92 Hz, PPh_3), 9.56 (s, 1H, -CH=N) . ^{13}C NMR ($CDCl_3$, 100 MHz) δ (ppm) 17.91, 18.89, 123.10, 127.89, 128.12, 128.22, 129.43, 133.69, 135.82, 148.65 149.59. 215.90. ^{13}P NMR (121.50 MHZ, $CDCl_3$): δ = 0.0027. IR υ (cm^{-1}): 3042(w), 1643(s), 1476(s), 1092(s), 880(s), 492. ESI-TOF MS: m/z (%); $[M + 3Na – 5H]^+$ 979.21, $[M – DL1]^+$ 587.15. UV-Vis ($CHCl_3$, λ_{max}, nm): 272 and 330. Anal. calcd for $C_{54}CuH_{50}N_2P_2S_2$: C, 70.76; H, 5.50; N, 3.06; S, 7.00. Found: C, 69.71; H, 5.32; N, 2.89; S, 7.01.

2.9.2 Synthesis of [$Cu(PPh_3)_2$DL2] (26)

The reaction of **DL2** (0.48 g, 1 mmol) $Cu(PPh_3)_2$DL (0.65 g, 1 mmol) in acetonitrile furnished complex **26** as a yellow powder. Yield 74%. Melting point: 218 – 220 °C. ^{1}H NMR ($CDCl_3$, 400 MHz): δ (ppm) 0.98 (d, 6H, , J_{HH} = 6.80 Hz, CH_3-CH), 1.19 (d, 12H, , J_{HH} = 6.80 Hz, CH_3-CH), 1.23 (d, 6H, J_{HH} = 6.76 Hz, CH_3-CH), 2.85 (m, 2H, , J_{HH} = 6.72 Hz, CH-CH_3), 3.07 (m, 2H, , J_{HH} = 6.64 Hz, CH-CH_3), 7.01 (s, 1H, Ar-H), 7.07 (t, 3H, , J_{HH} = 6.60 Hz, Ar-H), 7.16 (t, 12H, J_{HH} = 7.48 Hz, PPh_3), 7.21 (s, 1H, PPh_3), 7.29 (d, 18H, J_{HH} = 7.00 Hz, PPh_3), 7.36 (t, 1H, J_{HH} = 7.72 Hz, Ar-H), 9.77 (s, 1H, -CH=N). ^{13}C NMR ($CDCl_3$, 100 MHz) δ (ppm): 10.98, 14.07, 23.00, 23.77, 24.15, 24.26, 24.97, 27.43, 28.97, 30.39, 30.93, 38.76, 122.85, 123.67, 124.04, 128.31, 128.82, 129.04, 129.36, 130.91, 133.70, 134.18, 139.33, 146.04, 146.49, 151.12, and 217.47. ^{13}P NMR (121.50 MHZ, $CDCl_3$): δ = -0.8479 IR υ (cm^{-1}): 3042(w), 1643(s), 1476(s), 1092(s), 880(s), 492. ESI-TOF MS: m/z (%); $[M + 3Na]^+$ 1099, $[M – DL2]^+$ 587.09. UV-Vis ($CHCl_3$, λ_{max}, nm): 274 and 333. Anal. calcd for $C_{62}CuH_{66}N_2P_2S_2$: C, 72.38; H, 6.47; N, 2.72; S, 6.23. Found: C, 72.18; H, 6.34; N, 2.63; S, 6.30.

2.9.3 Synthesis of [Cu(PPh$_3$)$_2$DL3] (27)

The reaction of **DL3** (0.39 g, 1 mmol) Cu(PPh$_3$)$_2$DL (0.65 g, 1 mmol) in acetonitrile furnished complex **27** as a yellow powder. Yield 75%. Melting point: 214 – 216 °C. ^{1}H NMR ($CDCl_3$, 400 MHz): δ (ppm) 2.09 (s, 6H, CH_3-Ar), 2.14 (d, 6H, CH_3-Ar), 2.20 (s, 3H, CH_3-CH), 2.27 (s, 3H, CH_3-Ar), 6.76 (s, 2H, Ar-H), 6.93 (s, 2H, Ar-H), 7.17 (t, 12H, J_{HH} = 7.40 Hz, PPh_3), 7.29 (s, 2H, PPh_3), 7.31 (d, 16H, J_{HH} = 8.28 Hz, PPh_3), 9.53 (s, 1H, -CH=N). ^{13}C NMR ($CDCl_3$, 100 MHz) δ (ppm): 17.83, 18.84, 20.73, 21.33, 128.04, 128.35, 128.54, 129.78, 129.09, 129.21, 129.44, 129.76, 132.16, 133.73, 134.08, 135.38, 135.89, 137.81, 146.29, 150.17 and 216.05. ^{13}P NMR (121.50 MHZ, $CDCl_3$): δ = 0.1251 IR υ (cm^{-1}): 3055(w), 1633(s), 1478(s), 1024(s), 844(s), 494. ESI-TOF MS: m/z (%); $[M - 3CH_3]^+$ 900.08. UV-Vis ($CHCl_3$, λ_{max}, nm): 274 and 333. Anal. calcd for $C_{56}CuH_{54}N_2P_2S_2$: C, 71.20; H, 5.76; N, 2.97; S, 6.79. Found: C, 70.75; H, 5.60; N, 2.79; S, 6.94.

2.9.4 Synthesis of [Cu(PPh$_3$)$_2$DL4] (28)

The reaction of **DL4** (0.41 g, 1 mmol) Cu(PPh$_3$)$_2$DL (0.65 g, 1 mmol) in acetonitrile furnished complex **28** as a yellow powder. Yield 81%. Melting point: 234 – 236 °C. ^{1}H NMR ($CDCl_3$, 400 MHz): δ (ppm) 2.23 (s, 6H, CH_3-Ar), 6.86 (t, 1H, J_{HH} = 8.08 Hz, Ar-H), 7.11 (d, 2H, J_{HH} = 7.36 Hz, Ar-H), 7.18 (t, 15H, J_{HH} = 7.52 Hz, PPh_3), 7.24 (t, 4H, J_{HH} = 7.96 Hz, PPh_3), 7.32 (d, 11H, J_{HH} = 7.20 Hz, PPh_3), 9.67 (s, 1H, -CH=N). ^{13}C NMR ($CDCl_3$, 100 MHz) δ (ppm) : 17.88, 124.13, 127.35, 128.04, 128.09, 128.39, 128.56, 129.48, 133.67, 136.13, 152.33 and 215.30. ^{13}P NMR (121.50 MHz, $CDCl_3$): δ = 0.1976 IR υ (cm^{-1}): 3053(w), 1632(s), 1477(s), 1027(s), 879(s), 495. ESI-TOF MS: m/z (%); $[M - 2CH_3]^+$ 927.29. UV-Vis ($CHCl_3$, λ_{max}, nm): 277 and 336. Anal. calcd for $C_{52}Cl_2CuH_{44}N_2P_2S_2$: C, 65.23; H, 4.63; N, 2.93; S, 6.70. Found: C, 65.35; H, 4.61; N, 2.83; S, 6.79.

2.9.5 Synthesis of [Cu(PPh$_3$)$_2$DL5] (29)

The reaction of **DL5** (0.46 g, 1 mmol) Cu(PPh$_3$)$_2$DL (0.65 g, 1 mmol) in acetonitrile furnished complex **29** as a yellow powder. Yield 77%. Melting point: 209 – 211 °C. ^{1}H NMR ($CDCl_3$, 400 MHz): δ (ppm) 0.97 (d, 6H, J_{HH} = 6.80 Hz, CH_3-CH), 1.23 (d, 6H, J_{HH} = 6.76 Hz, CH_3-CH), 2.89 (m, 2H, J_{HH} = 6.48 Hz, CH-CH_3), 6.86 (t, 1H, J_{HH} = 8.16 Hz, Ar-H), 7.18 (m, 15H, J_{HH} = 7.64 Hz, PPh_3), 7.29 (m, 15H, J_{HH} = 8.24 Hz, PPh_3), 7.32 (d, 4H, J_{HH} = 8.00 Hz, Ar-H), 7.37 (t, 1H, J_{HH} = 8.18 Hz, PPh_3), 10.02 (s, 1H, -CH=N). ^{13}C NMR ($CDCl_3$, 100 MHz) δ (ppm): 24.60, 24.72, 28.75, 124.03, 124.08, 127.47, 128.29, 128.38, 129.22, 129.45, 133.67, 133.96,

134.32, 145.95, 146.21, 154.47 and 218.04. ^{13}P NMR (121.50 MHZ, $CDCl_3$): δ = -0.2015. IR υ (cm^{-1}): 2963(w), 1632(s), 1479(s), 1025(s), 880(s), 490. ESI-TOF MS: m/z (%); $[M + 3Na – 5H]^+$ 1075.06, $[M – DL5]^+$ 587.09. UV-Vis ($CHCl_3$, λ_{max}, nm): 275 and 334. Anal. calcd for $C_{56}Cl_2CuH_{52}N_2P_2S_2$: C, 66.36; H, 5.17; N, 2.76; S, 6.33. Found: C, 66.31; H, 4.98; N, 2.64; S, 6.51.

2.9.6 Synthesis of [Cu(PPh$_3$)$_2$DL6] (30)

The reaction of **DL6** (0.30 g, 1 mmol) $Cu(PPh_3)_2DL$ (0.65 g, 1 mmol) in acetonitrile furnished complex **30** as a yellow powder. Yield 72%. Melting point: 211 – 213 °C. ^{1}H NMR ($CDCl_3$, 400 MHz): δ (ppm) 2.19 (s, 6H, CH_3-Ar), 2.27 (s, 3H, CH_3-Ar), 6.85 (t, 1H, J_{HH} = 8.00 Hz, Ar-H), 6.93 (s, 2H, Ar-H), 7.17 (t, 12H, J_{HH} = 7.40 Hz, PPh_3), 7.24 (t, 3H, J_{HH} = 8.18 Hz, PPh_3), 7.30 (t, 15H, J_{HH} = 7.44 Hz, PPh_3), 9.69 (s, 1H, -CH=N). ^{13}C NMR ($CDCl_3$, 100 MHz) δ (ppm) : 17.81, 18.82, 20.71, 21.35, 124.09, 127.39, 128.01, 128.38, 128.50, 129.07, 129.47, 133.68, 133.94, 135.14, 135.33, 135.66, 137.78, 138.01, 145.82, 152.43 and 216.58. ^{13}P NMR (121.50 MHZ, $CDCl_3$): δ = 0.2015. IR υ (cm^{-1}): 3047(w), 1633(s), 1479(s), 1027(s), 881(s), 490s. ESI-TOF MS: m/z (%); $[M + 2H]^+$ 956.82. UV-Vis ($CHCl_3$, λ_{max}, nm): 274 and 335. Anal. calcd for $C_{53}Cl_2CuH_{46}N_2P_2S_2$: C, 65.53; H, 4.77; N, 2.88; S, 6.60. Found: C, 65.41; H, 4.78; N, 2.75; S, 6.52.

2.9.7 Synthesis of [Cu(PPh$_3$)$_2$DL7] (31)

The reaction of **DL7** (0.42 g, 1 mmol) $Cu(PPh_3)_2DL$ (0.65 g, 1 mmol) in acetonitrile furnished complex **31** as a yellow powder Yield 75 %. Melting point : 196 - 198 °C. ^{1}H NMR ($CDCl_3$, 400 MHz): δ (ppm) 2.20 (s, 6H, CH_3-Ar), 6.83 (t, 1H, J_{HH} = 7.28 Hz, Ar-H), 6.93 (m, 2H, J_{HH} = 7.36 Hz, Ar-H), 7.11 (d, 2H, J_{HH} = 7.08 Hz, Ar-H), 7.18 (t, 15H, J_{HH} = 7.24 Hz, PPh_3), 7.25 (s, 1H, Ar-H), 7.30 (d, 15H, J_{HH} = 7.24 Hz, PPh_3), 7.48 (d, 1H, J_{HH} = 7.88 Hz, Ar-H), 9.53 (s, 1H, -CH=N). ^{13}C NMR ($CDCl_3$, 100 MHz) δ (ppm): 17.89, 18.04, 18.87, 117.91, 121.52, 123.10, 125.29, 127.89, 127.91, 128.04, 128.11, 128.21, 128.38, 129.46, 132.68, 132.88, 133.68, 133.96, 135.79, 138.37, 149.26, 149.37, 149.86 and 216.09. ^{13}P NMR (121.50 MHZ, $CDCl_3$): δ = -0.0078 IR υ (cm^{-1}): 3051(w), 1616(s), 1465(s), 1024(s), 874(s), 495(s). ESI-TOF MS: m/z (%); $[M + 4H – PPh_3]^+$ 735.77 UV-Vis ($CHCl_3$, λ_{max}, nm): 274 and 333. Anal. calcd for $BrC_{52}CuH_{45}N_2P_2S_2$: C, 64.56; H, 4.69; N, 2.90; S, 6.63. Found: C, 64.88; H, 4.82; N, 2.71; S, 6.77.

2.9.8 Synthesis of [Cu(PPh$_3$)$_2$DL8] (32)

The reaction of **DL8** (0.30 g, 1 mmol) Cu(PPh$_3$)$_2$DL (0.65 g, 1 mmol) in acetonitrile furnished complex **32** as a yellow powder. Yield 70%. Melting point : 202 - 204 °C. . ^{1}H NMR (CDCl$_3$, 400 MHz): δ (ppm) 2.16 (s, 6H, CH$_3$-Ar), 2.27 (s, 3H, CH$_3$-Ar), 6.90 (m, 4H, J_{HH} = 7.20 , Ar-H), 7.17 (t, 14H, J_{HH} = 7.52, PPh$_3$), 7.25 (s, 1H, Ar-H), 7.30 (m, 16H, J_{HH} = 7.52, PPh$_3$), 7.48 (d, 1H, J_{HH} = 7.92, Ar-H), 9.67 (s, 1H, -CH=N). ^{13}C NMR (CDCl$_3$, 100 MHz) δ (ppm): 17.81, 17.97, 18.81, 117.79, 121.68, 125.21, 127.87, 128.00, 128.38, 128.99, 129.46, 132.63, 133.68, 133.98, 135.33, 135.67, 137.91, 149.47, 149.59, 216.22. ^{13}P NMR (121.50 MHZ, CDCl$_3$): δ = -0.0899 IR υ (cm^{-1}): 3053(w), 1625(s), 1479(s), 1025(s), 881(s), 492(s). ESI-TOF MS: m/z (%); [M + Li – DL8]$^+$ 673.86. UV-Vis (CHCl$_3$, λ_{max}, nm), 274 and 337. Anal. calcd for $BrC_{53}CuH_{47}N_2P_2S_2$: C, 64.86; H, 4.83; N, 2.85; S, 6.53. Found: C, 64.46; H, 4.63; N, 2.72; S, 6.81.

$$[Cu(PPh_3)_2]NO_3 + KDL(n) \xrightarrow[CH_2Cl_2]{CH_3CN} [Cu(PPh_3)_2DL(n)] + KNO_3 \quad \text{where n = 1-8} \qquad (2.2)$$

[Cu(PPh$_3$)$_2$**DL1**] = **25** [Cu(PPh$_3$)$_2$**DL2**] = **26** [Cu(PPh$_3$)$_2$**DL3**] = **27**

[Cu(PPh$_3$)$_2$**DL4**] = **28** [Cu(PPh$_3$)$_2$**DL5**] = **29** [Cu(PPh$_3$)$_2$**DL6**] = **30**

[Cu(PPh$_3$)$_2$**DL7**] = **31** [Cu(PPh$_3$)$_2$**DL8**] = **32**

Equation 2.2: Synthesis of heteroleptic copper(I) dithiocarbamate-PPh$_3$ complexes **25 - 32.**

2.10 Single-crystal X-ray crystallography

Crystal evaluation and data collection for all the single crystals obtained for some of the compounds was done on a Bruker Smart APEXII diffractometer with Mo Kα radiation (I = 0.71073 Å) equipped with an Oxford Cryostream low temperature apparatus operating at 100K. Reflections were collected at different starting angles and the *APEXII* program suite was used to index the reflections [6]. Data reduction was performed using the *SAINT* [7] software and the scaling and absorption corrections were applied using the *SADABS* [8] multi-scan technique. The structures were solved by the direct method using the *SHELXS* program and refined using *SHELXL* program [9]. Graphics of the crystal structures were drawn using Mercury software [10]. Non-hydrogen atoms were first refined isotropically and then by anisotropic refinement with the full-matrix least square method based on F^2 using *SHELXL*.

Disordered molecules were modelled using PART-1 instruction with a fixed site occupancy factor of 0.5 and in all situations where the molecule was highly disordered and an attempt to model it had been unsuccessful, SQUEZE option [11] in PLATON [12] was utilized to omit it. The crystallographic data and structure refinement parameters for the available structures are given in **Tables 2.1-2.6**.

Table 2.1**:** The summary of X-ray crystal data collection and structure refinement parameters for compounds **1**, **2**, **3**, **4a** and **4b.**

	1	**2**	**3**	**4a**	**4b**
Empirical formula	$C_{36}H_{38}N_4S_4$	$C_{52}H_{70}N_4S_4$	$C_{40}H_{46}N_4S_4$	$C_{33}H_{28}Cl_6N_4S_4$	$C_{32}H_{26}Cl_4N_4S_4$
Formula weight	654.98	879.36	711.05	821.53	736.61
Crystal system	triclinic	monoclinic	monoclinic	Monoclinic	triclinic
Space group	P-1	$P2_1$	$P2_1/n$	$P2_1/c$	P-1
a/Å	11.9450(2)	11.7155(9)	12.2246(2)	17.3326(2)	8.8656(2)
b/Å	13.2690(3)	11.6781(9)	24.1962(4)	17.1686(2)	13.0483(2)
c/Å	13.4674(2)	19.6646(15)	14.1647(2)	12.6861(2)	18.0945(3)
α/°	63.4110(10)	90	90	90	107.3830(10)
β/°	72.388(2)	104.8400(10)	109.4880(10)	98.7150(10)	95.6390(10)
γ/°	67.004(3)	90	90	90	105.8960(10)
Volume/Å^3	1735.84(7)	2600.7(3)	3949.73(11)	3731.50(9)	1883.86(6)
Z	2	2	4	4	2
ρ_{calc}g/cm^3	1.253	1.123	1.196	1.462	1.299
μ/mm^{-1}	0.305	0.219	0.273	0.715	0.563
F(000)	692	948	1512	1680	756
Crystal size/mm^3	0.29x0.17x0.12	0.24×0.18×0.12	0.23×0.14×0.09	0.220 x 0.140 x 0.120	0.35×0.19×0.12
2Θ range for data collection/°	1.712 to 28.379	1.798 to 27.905	2.27 to 28.2	1.679 to 28.236	1.726 to 28.388
Index ranges	$-15 \le h \le 15$	$-15 \le h \le 15$	$-16 \le h \le 16$	$-22 \le h \le 22$	$-11 \le h \le -11$
	$-17 \le k \le 17$	$-15 \le k \le 15$	$-30 \le k \le 32$	$-22 \le k \le 22$	$-17 \le k \le -17$
	$-17s \le l \le 17$	$-25 \le l \le 25$	$-18 \le l \le 17$	$-16 \le l \le 16$	$-24 \le l \le 24$
Reflections collected	5962	20154	49648	47359	30404
Independent reflections	8591 [R_{int} = 0.0399]	11726 [R_{int} = 0.0217]	9806 [R_{int} = 0.0403]	9110 [R(int) = 0.0361]	9177 [R_{int} = 0.0164]
Data/restraints/parameters	8591/0/405	11726 / 1 / 557	9806/0/445	9110 / 0 / 425	9177/204/475
Goodness-of-fit on F^2	1.001	1.011	1.005	0.953	1.061
Final R indexes [I>=2σ (I)]	0.0432, 0.0885	0.0452, 0.1064	0.0406, 0.0867	0.0304, 0.0832	0.0320, 0.0822
Final R indexes [all data]	0.0789, 0.1014	0.0571, 0.1130	0.0681, 0.069	0.0427, 0.0890	0.0378, 0.0856
Largest diff. peak and hole (e Å^{-3})	0.423 and -0.301	1.156 and -0.384	0.388 and -0.293	0.695 and -0.842	0.402 and -0.314

Table 2.2: The summary of X-ray crystal data collection and structure refinement parameters for compounds **5**, **6**, **7**, **11** and **12.**

	5	**6**	**7**	**11**	**12**
Empirical formula	$C_{41}H_{44}Cl_6N_4S_4$	$C_{34}H_{30}Cl_4N_4S_4$	$C_{36}H_{38}N_4NiS_4$	$C_{40}H_{42}Cl_4N_4NiS_4.2(CH_2Cl_2)$	$C_{34}H_{30}Cl_4N_4NiS_4$
Formula weight	933.74	764.66	713.65	1077.38	823.37
Crystal system	Triclinic	orthorhombic	Monoclinic	triclinic	monoclinic
Space group	P-1	Aea2	$P2_1/n$	*P*-1	$P2_1/c$
a/Å	8.4725(2)	11.1007(6)	12.5278(3)	8.55440(10)	7.5570(2)
b/Å	9.5405(3)	51.4730(3)	12.3052(3)	11.2627(2)	29.5198(6)
c/Å	28.6392(8)	12.4967(7)	14.7214(4)	13.0340(2)	10.2393(2)
α/°	91.196(2)	90	90	105.0640(10)	90
β/°	92.5660(10)	90	114.8480(10),	100.016(2)	106.3980(10)
γ/°	105.8440(10)	90	90	94.213(3)	90
Volume/$Å^3$	2223.46(11)	7140.5(7)	2059.32(9)	1184.80(3)	2191.28(9)
Z	2	8	2	1	2
$\rho_{calc}g/cm^3$	1.395	1.423	1.151	1.51	1.248
μ/mm^{-1}	0.609	0.597	0.701	1.073	0.903
F(000)	1380	3152.0	748	554	844
Crystal size/mm^3	0.28×0.14×0.09	0.34 x 0.18 x 0.13	0.190 x 0.120 x 0.080	0.4 × 0.27 × 0.14	0.28 x 0.18 x 0.12
2Θ range for data collection/°	2.137 to 27.499	3.996 to 57.286	1.799 to 27.563	3.302 to 54.00	2.893 to 28.00
Index ranges	$-22 \le h \le 21$	$-14 \le h \le 14$	$16 \le h \le 16$	$-10 \le h \le 8$	$-7 \le h \le 9$
	$-22 \le k \le 19$	$-61 \le k \le 69$	$-14 \le k \le 14$	$-14 \le k \le 14$	$-38 \le k \le 31$
	$-22 \le l \le 22$	$-5 \le l \le 16$	$-15 \le l \le 16$	$-15 \le l \le 16$	$-13 \le l \le 13$
Reflections collected	32965	22438	27584	16602	18040
Independent reflections	10018[R_{int} = 0.0210]	22438[R_{int} = 0]	4729 [R(int) = 0.0421]	5049 [R_{int} = 0.0151]	5222
Data/restraints/parameters	10018/0/504	22438/1/421	4729 / 0 / 205	5049/1/282	5222/2/217
Goodness-of-fit on F^2	1.019	1.015	1.021	1.029	1.039
Final R indexes [I>=2σ (I)]	0.0308, 0.0678	0.0316, 0.0624	0.0359, 0.0860	0.0328, 0.0802	0.0332, 0.0818
Final R indexes [all data]	0.0419, 0.0727	0.0377, 0.0656	0.0552, 0.0929	0.0388, 0.0835	0.0395, 0.0852
Largest diff. peak and hole (e $Å^{-3}$)	0.453 and -0.393	0.22 and -0.21	0.455 and -0.315	0.97 and -1.10	0.515, -0.360

Table 2.3: The summary of X-ray crystal data collection and structure refinement parameters for complexes **14**, **17**, **18**, **19a** and **19b.**

	14	**17**	**18**	**19a**	**19b**
Empirical formula	C_{52} H_{70} Cu N_4 S_4	$C_{40}H_{42}Cl_4CuN_4S_4.(C_6H_5.CH_3)$	$C_{34}H_{30}Cl_4CuN_4S_4$	$C_{54}H_{57}CoN_6S_6$	$C_{54}H_{57}CoN_6S_6.3(CH_2Cl_2)$
Formula weight	942.9	1004.49	828.20	1041.34	1296.12
Crystal system	Triclinic	monoclinic	monoclinic	Trigonal	Trigonal
Space group	*P* -1	$P2_1/c$	$P2_1/c$	R-3:H	R -3 :H
a/Å	9.4674(16)	12.3469(6)	7.5424(8)	18.0869(3)	18.0774(3)
b/Å	12.120(2)	14.0658(8)	29.800(3)	18.0869(3)	18.0774(3)
c/Å	12.249(2)	14.6828(8)	10.0602(10)	32.8086(6)	32.4623(6)
α/°	75.343(5)	90	90	90	90
β/°	68.614(6)	109.835(3)	108.449(2)	90	90
γ/°	77.373	90	90	120	120
Volume/$Å^3$	1253.6(4)	2398.7(2)	2145.0(4)	9294.9(4)	9187.2(3)
Z	1	2	2	6	6
$\rho_{calc}g/cm^3$	1.249	1.391	1.282	1.116	1.406
μ/mm^{-1}	0.64	0.89	0.980	0.295	0.789
F(000)	503	1042	846	3276.0	4032
Crystal size/mm^3	0.210 x 0.150 x 0.080	0.21×0.18×0.08	0.26 x 0.15 x 0.11	0.22×0.15×0.13	0.220 x 0.160 x 0.080
2Θ range for data collection/°	1.754 to 25.498	1.753 to 27.543	2.241 to 28.182	1.44 to 28.39	1.807 to 27.672
Index ranges	$-18 \le k \le 16$	$-16 \le h \le 16$	$-4 \le h \le 9$	$22 \le h \le 24$	$-22 \le h \le 23$
	$-18 \le k \le 16$	$-18 \le k \le 16$	$-39 \le k \le 37$	$-24 \le k \le 18$	$-23 \le k \le 20$
	$-19 \le l \le 18$	$-19 \le l \le 18$	$-12 \le l \le 13$	$-43 \le l \le 42$	$-42 \le l \le 42$
Reflections collected	8942	29811	12486	20111	44468
Independent reflections	4564 [R(int) = 0.0194]	5222 [R_{int} = 0.0186]	5122	5151[R_{int} = 0.0271]	4766 [R(int) = 0.0343]
Data/restraints/parameters	4564 / 1 / 285	5478/123/309	5122/1/217	5151/0/206	4766 / 0 / 233
Goodness-of-fit on F^2	1.043	1.029	1.035	1.110	1.035
Final R indexes [I>=2σ (I)]	0.0820, 0.2009	R_1 = 0.0500, wR_2 = 0.1080	0.0302, 0.0736	0.0421, 0.1088	0.0371, 0.0892
Final R indexes [all data]	0.1027, 0.2172	R_1 = 0.0500, wR_2 = 0.1240	0.0401, 0.0773	0.0506, 0.1123	0.0493, 0.0966
Largest diff. peak and hole (e $Å^{-3}$)	4.469 and -0.753	0.789 and -0.647	0.374 and -0.281	0.39 and -0.36	1.029 and -0.799

Table 2.4: The summary of X-ray crystal data collection and structure refinement parameters for complexes **20**, **22**, and **23.**

	20	**22**	**23**
Empirical formula	$C_{78}H_{105}CoN_6S_6$	$C_{48}H_{39}Cl_6CoN_6S_6$	$C_{60}H_{63}Cl_6CoN_6S_6$
Formula weight	1377.96	1164.32	1332.15
Crystal system	monoclinic	triclinic	Triclinic
Space group	$P2_1/c$	P-1	P-1
a / Å	18.4354(4)	14.3904(9)	16.5248(3)
b/Å	23.9108(5)	14.6123(9)	17.0460(4)
c/Å	18.7970(4)	16.4524(9)	17.2205(5)
α/°	90	91.839(2)	65.378(2)
β/°	111.2040(10)	113.978(2)	63.9490(10)
γ/°	90	116.2640(10)	66.828(3)
V/Å^3	7724.9(3)	2738.2(3)	3827.78(19)
Z	4	2	2
ρ_{calc}g/cm^3	1.185	1.412	1.156
μ/mm^{-1}	0.429	0.874	0.633
F(000)	2952.0	1182	1380
Crystal size/mm^3	0.22×0.14×0.08	0.31×0.18×0.14	0.28×0.14×0.09
2θ range for data collection/°	3.406 to 55.3	1.707 to 28.376	1.694 to 28.272
Index ranges	$-23 \le h \le 24$ $-31 \le k \le 31$ $-24 \le l \le 24$	$-16 \le h \le 19$ $-19 \le k \le 18$ $-21 \le l \le 18$	$-22 \le h \le 21$ $-22 \le k \le 19$ $-22 \le l \le 22$
Reflections collected	91538	38071	55172
Independent reflections	17942[R_{int} = 0.0372]	13330 [R_{int} = 0.018]	18644 [R_{int} = 0.0174]
Data/restraints/parameters	17942/0/844	13330/66/758	18644/3/724
Goodness-of-fit on F^2	1.020	1.087	1.046
Final R indexes [I>=2σ (I)]	0.0374, 0.0802	0.0461, 0.1092	0.0413, 0.1065
Final R indexes [all data]	0.0649, 0.0922	0.0461, 0.1092	0.0578, 0.1092
Largest diff. peak and hole (e Å^{-3})	0.39 and -0.270	0.774 and -1.170	1.996 and -1.379

Table 2.5: The summary of X-ray crystal data collection and structure refinement parameters for complexes **25**, **26**, **27** and **28**

	25	**26**	**27**	**28**
Empirical formula	C_{54} H_{49} Cu N_2 P_2 S_2	$C_{62.68}$ $H_{65.36}$.$Cl_{10.60}$ Cu $N_2P_2S_2$	C_{115} $H_{116}Cl_2Cu_2$ N_4 P_4 S_4O_2	$C_{52}H_{43}$Cl2Cu$N_2P_2S_2$.CH_2Cl_2
Formula weight	915.55	1057.56	2036.24	1041.31
Crystal system	monoclinic	triclinic	triclinic	triclinic
Space group	P 21/n	*P*-1	*P*-1	*P* -1
a/Å	22.4044(4)	11.5681(4)	12.5065(3)	12.2942(6)
b/Å	9.5916(2)	15.9024(5)	13.1610(2)	15.2958(7)
c/Å	22.9024(4)	17.1608(6)	15.9918(2)	15.3366(7)
α/°	90°	104.286(2)	85.803(10)	106.825(2)
β/°	109.010(10)°.	104.050(2)	89.170(2)	108.178(2)
γ/°	90°	105.939(2)	77.974(3)	101.797(2)
Volume/$Å^3$	4653.17(15)	2773.51(17)	2567.55(3)	2481.2(2)
Z	4	2	1	2
$\rho_{calc}g/cm^3$	1.307	1.266	1.317	1.394
μ/mm^{-1}	0.667	0.596	0.663	0.843
F(000)	1912	1113	1066	1072
Crystal size/mm^3	0.370 x 0.230 x 0.140	0.36 × 0.24 × 0.14	0.4 × 0.27 × 0.14	0.26× 0.24× 0.14
2Θ range for data collection/°	1.104 to 28.382°	1.942 to 28.540	1.665 to 28.342	1.66 to 28.24
Index ranges	$-29 \leq h \leq 29$	$-15 \leq h \leq 15$	$-16 \leq h \leq 16$	$-16 \leq h \leq 15$
	$-12 \leq k \leq 12$	$-18 \leq k \leq 21$	$-17 \leq k \leq 17$	$-20 \leq k \leq 20$
	$-30 \leq l \leq 30$	$-22 \leq l \leq 22$	$-21 \leq l \leq 21$	$-19 \leq l \leq 15$
Reflections collected	58617	43604	9988	29938
Independent reflections	11622 [R_{int} = 0.0255]	13740 [R_{int} = 0.0179]	12357 [R_{int} = 0.0151]	11724 [R_{int} = 0.0279]
Data/restraints/parameters	11622/0/550	13740/0/622	12357/1/621	11724/0/577
Goodness-of-fit on F^2	1.041	1.018	1.022	1.011
Final R indexes [I>=2σ (I)]	0.0537, 0.1076	0.0316, 0.0756	0.0436, 0.0814	0.0430, 0.01171
Final R indexes [all data]	0.0537, 0.1166	0.0397, 0.0801	0.0336, 0.0864	0.0538, 0.1242
Largest diff. peak and hole (e $Å^{-3}$)	0.687 and -0.614	0.519 and -0.378	0.97 and -1.10	0.785 and -1.260

Table 2.6: The summary of X-ray crystal data collection and structure refinement parameters for complexes **29**, **30**, **31** and **32**

	29	**30**	**31**	**32**
Empirical formula	$C_{57}H_{53}Cl_4Cu\,N_2P_2S_2$	$C_{53}H_{45}Cl_2CuN_2P_2S_2$	$C_{52}H_{44}BrCuN_2P_2S_2$	$C_{54}H_{48}BrCl_2CuN_2P_2S_2$
Formula weight	1097.71	970.41	946.72	1065.35
Crystal system	triclinic	triclinic	monoclinic	Triclinic
Space group	*P* -1	*P* -1	P 21/n	*P* -1
a/Å	11.4165(2)	12.4084(2)	22.4506(7)	12.3468(2)
b/Å	15.6593(3)	13.3139(2)	9.6562(3)	13.0249(20
c/Å	17.1053(3)	16.01132(2)	22.6611(7)	17.8668(3)
α/°	108.8080(10)	83.3890(10)	90	73.4720(10)
β/°	105.1040(6)	81.1170(10)	108.8560(10)	87.1780(10)
γ/°	77.373	65.0040(10)	90	63.7040(10)
Volume/Å^3	2639.94(9)	2364.95(6)	4649.0(3)	2458.62(7)
Z	4	2	2	2
ρ_{calc}g/cm^3	1.381	1.363	1.353	1.438
μ/mm^{-1}	0.796	0.769	1.319	1.554
F(000)	1136	1004	1948	1.092
Crystal size/mm^3	0.48 x 0.36 x 0.18	0.36 × 0.21× 0.12	0.33 x 0.24 x 0.15	0.34 x 0.220 x 0.170
2Θ range for data collection/°	1.331 to 28.459	1.823 to 28.524	1.899 to 28.390	1.824 to 28.474
Index ranges	$-15 \le k \le 20$ $-20 \le k \le 20$ $-22 \le l \le 16$	$-16 \le h \le 13$ $-17 \le k \le 17$ $-21 \le l \le 21$	$-29 \le h \le 29$ $-6 \le k \le 12$ $-30 \le l \le 30$	$-16 \le h \le 16$ $-16 \le k \le 17$ $-23 \le l \le 23$
Reflections collected	8942	27947	52335	37035
Independent reflections	13077 [R(int) = 0.0157]	11783 [R_{int} = 0.0279]	11617 [R_{int} = 0.0299]	12146 [R_{int} = 0.0187]
Data/restraints/parameters	13077 / 0 / 613	11783/0/559	11617/232/615	12146/0/587
Goodness-of-fit on F^2	1.043	0.962	1.074	0.950
Final R indexes [I>=2σ (I)]	R1 = 0.0298, wR2 = 0.080	R_1 = 0.0403, wR_2 = 0.0883	R_1 = 0.0425, wR_2 = 0.0910	R_1 = 0.0379, wR_2 = 0.0922
Final R indexes [all data]	R1 = 0.0345, wR2 = 0.0829	R_1 = 0.0636, wR_2 = 0.0978	R_1 = 0.0589, wR_2 = 0.0971	R_1 = 0.0479, wR_2 = 0.0978
Largest diff. peak and hole (e Å^{-3})	0.424 and -0.833	0.531 and -0.481	1.117 and -1.305	0.968 and -1.430

2.11 *In vitro* antibacterial studies

2.11.1 Bacterial strains used for this study

The samples were tested against six bacterial strains. There were four Gram-negative bacteria, viz *Salmonella typhimurium* ATCC 14026, *Pseudomonas aeruginosa* ATCC 27853, *Escherichia coli* ATCC 25922 and *Klebsiella pneumoniae* ATCC 31488, and two Gram-positive bacteria, viz, *Staphylococcus aureus* ATCC 700699 (methicillin resistant) and *Staphylococcus aureus* ATCC 25923.

2.11.2 Preparation of Media

Nutrient agar (NA) (Biolab, South Africa) was prepared by dissolving 28 g of NA powder in 1 L of distilled water and then autoclaved at 121^{o}C for 15 mins. After autoclaving, ± 8 ml of NA was poured into sterile disposable petri dishes (65 mm) and allow to solidify at room temperature resulting in a final thickness of ± 4 mm.

Nutrient Broth (NB) (Biolab, South Africa) was prepared by dissolving 16 g of NB powder in 1 L of distilled water. 10 ml of the NB solution was transferred into Mc Carthney bottles and autoclaved at 121^{o}C for 15 min and allow to cool to room temperature.

Mueller-Hinton Agar (MHA) (Biolab, South Africa) was prepared by dissolving 38 g of MHA powder in 1 L of distilled water and autoclaved at 121^{o}C for 15 min. After autoclaving, ± 8 ml of MHA was poured into sterile disposable petri dishes (65mm) and allow to solidify at room temperature resulting in a final thickness of ± 4 mm.

2.11.3 Screening of samples for antibacterial activity

The samples were prepared by dissolving 1000 µg of test sample in 1 mL of dimethyl sulfoxide (DMSO). The bacteria were inoculated onto NA plates using the streak plate technique and incubated at 37^{o}C for 18 hours. A single colony was then isolated and inoculated into 10 mL sterile NB. This was incubated at 37^{o}C for 18 hours in a shaking incubator (100 rpm). The concentration of each bacterial strain was adjusted with sterile distilled water to achieve a final concentration equivalent to 0.5 Mc Farland's Standard (i.e 1.5 x 10^{8} cfu/mL) using a densitometer (Mc Farland, Latvia). Thereafter, the MHA plates were lawn inoculated with the diluted bacteria using a sterile throat swab. Finally, 5 µL of each sample was spotted onto the

MHA plates and the plates were incubated at 37°C for 18 hours and then assessed for antibacterial activity, which was denoted by a clear zone at the point of spotting.

2.11.4 Minimum inhibitory concentration experiments (MIC)

Samples that showed antimicrobial potential during antibacterial screening were tested further to determine their minimum inhibitory concentrations (MICs). The samples were serially diluted 10 times to achieve concentrations ranging from 1000 µg/mL to 0.2 µg/mL. For the samples where their MICs were lower than 0.2 µg/mL, the solutions were further diluted serially 5 times to achieve concentrations ranging from 0.100 µg/mL to 0.00625µg/mL. Then 5 µL of each samples at different concentrations were spotted onto the MHA plates and the plates were incubated at 37°C for 18 hours and then assessed for their MIC. These trails were done in triplicate and the MIC was determined as the lowest concentration of the compounds at which no visible bacterial growth was observed after incubation. The results were compared with those from ciprofloxacin, which was used as a standard antibiotic for this study. The samples were also tested against DMSO.

2.12 Antioxidant assay

2.12.1 2,2-Diphenyl-1-picrylhydrazyl (DPPH) assay

DPPH (1,1-diphenyl-2-picrylhydrazyl) radical scavenging assay of all the compounds was carried out according to the method reported by Chandrika *et al.* [13], with slight modifications. At the start, 100 µL aliquots of varying concentration (1.0 mM, 0.75 mM, 0.50 mM, and 0.25 mM) of the test sample and the standard were added to an equal quantity of 0.1mM solution of DPPH in ethanol. The reaction mixture was mixed thoroughly with care and left in the dark at room temperature for 30 min. After 30 min of incubation at room temperature, the DPPH reduction was measured by reading the absorbance at 517 nm. Ascorbic acid standard of varying concentration (1.0 mM, 0.75 mM, 0.50 mM, and 0.25 mM) was used as the reference compound. The ability of the compounds to scavenge DPPH radical was calculated as shown below.

$$\%\ Scavenging\ Activity\ = \frac{Absorbance\ control - Absorbance\ of\ sample\ x\ 100}{Absorbance\ control}$$

2.12.2 Nitric oxide (NO) scavenging assay.

Nitric oxide scavenging assay is based on the ability of sodium nitroprusside solution at physiological pH 7.2 to produce NO spontaneously. Under aerobic condition, NO could interact with oxygen to produce stable nitrite ions, which can be measured with the Griess reagent. Compounds that scavenge NO compete with oxygen resulting in reduced nitrite ions generation [14]. The assay was carried out by incubating 100 µL of 10 mM sodium nitroprusside in sodium phosphate buffer (7.4) and 100 µL of test samples at different concentrations (0.25 mM, 0.50 mM, 0.75 mM and 1.0 mM) at 37 °C for 2 hours. The same reaction mixture, without the test sample but with an equivalent amount of the solvent used in dissolving the test samples, served as control. Thereafter, 100 µL of Griess reagent was added to the reaction mixture. A chromophore that can be read at 546 nm was formed during the diazotization of the nitrite with sulfanilamide (Griess reagent). The percentage inhibition of NO generated by either the test samples or the standard antioxidant ascorbic acid were calculated relative to the absorbance of the control.

$$\% \ Inhibition \ of \ NO \quad = \frac{Absorbance \ control - Absorbance \ of \ sample \ x \ 100}{Absorbance \ control}$$

2.13 Computational methodology

This section describes how multiple computational software was used to determine the anticancer potential of the thiuram disulfides **1 - 6** synthesized in this study. This methodical integration is a crucial step in defining the therapeutic roles for compounds prior to *in vitro* or *in vivo* studies, as it first narrows down the compounds to those with drug-like potential and so ultimately saves time and cost. The methods as well as the software employed are discussed in the subsections below.

2.13.1 *In silico* preparation of compounds 1-6, optimization and protein target fishing

Compounds **1** to **6** were screened against a big three-dimensional library of proteins to identify possible hits for each of the compounds. Prior to screening, the 2D chemical structures of the **1 - 6** were prepared on a *Graphical User Interface* (GUI) of *MarvinSketch* software [15]. The structures were then optimized geometrically on a *Universal Force Field* (UFF) using the steepest descent algorithm with the aid of Avogadro 1.2.0 [16]. A full optimization of compounds **1 - 6** was done using the Gaussian16 program at a B3LYP/6-311++G(d,p) theoretical level to attain the minimum energy conformation [17]. Thereafter, the optimized

compounds were saved in the appropriate Simplified Molecular-Input Line-Entry System (SMILES), in sdf and mol2 formats for use in subsequent *in silico* studies.

Target-fishing was primarily carried out using the *HitPick* webserver [18, 19] and validated using the *SwissTargetPrediction* tool [20]. *HitPick* is a highly precise webserver for predicting possible targets for chemical compounds and integrates similarity search with methodical machine learning. These methods are descriptive of a 2D molecular fingerprinting approach [21] and they entail a 1-nearest-neighbour similarity search (1NN) and a Laplacian-modified naïve Bayesian target model [22], which ranks potential targets based on their binding interactions with similar compounds. Moreover, the pairwise Tanimoto coefficient (Tc) determines compounds that are similar to the each query from a cohort of known protein-ligand interactions [23]. Overall, *HitPick* achieves a 60.94% sensitivity, 99.99% specificity and 92.11% precision [18]. The SMILES format of compounds **1 to 6** were then loaded into the *HitPick* web server and predicted targets were presented as gene symbols, which were more appropriately identified in their translatable protein forms.

2.13.2 Retrieval of predicted protein targets, molecular docking and post-docking structural minimization.

With the potential protein targets for each query (of section **2.12.2**), we retrieved the correlating 3D X-ray crystal structures of the proteins from the Protein Data Bank (PDB); **1** – PTGS1/PTGS2 (5WBE/5F19) [24, 25], **2** – SCN2A/SCN4A (6J8E/6AGF), **3** – CAII (5N0E), **4** – PTGS1/PTGS2 (5WBE/5F19), **5** – SIGMAR1 (5HK1) and **6** – SIGMAR1 (5HK1). The retrieved proteins were prepared in their monomeric forms prior to molecular docking experiments. This involved the removal of co-crystallized ions, molecules and crystal waters not relevant to this study, which was carried out on the GUI of UCSF Chimera [26]. Molecular docking experiments of each of the thiuram disulfide into the active sites of their respective target proteins was done, and for those that possessed plausible anti-cancer propensities. Gridboxes were defined based on co-crystallized ligands already present at active sites of the potential targets prior to system preparation. The best-docked conformations of the respective compounds were ranked, based on generated docking scores with the highest negative energies. The most appropriate docked complexes were then retrieved and saved using the UCSF Chimera. These complexes, were further optimized on AMBER14 PMEMD engine using its Graphic Processor Unit (GPU) version in congruence with of SANDER and LEAP modules integrated in the AMBER software package [27]. The AMBER FF14SB was utilized to

parameterize and generate topology files for the protein/ligand systems. The LEAP module was used to add hydrogen atoms and appropriate neutral (Na+ and Cl-) ions to the systems in water solvent, which was explicitly done for all atoms via a 10Å-sized TIP3P water box [28]. Histidine residues in the target proteins were protonated at a constant pH (cpH) using the *pdb4amber* script to achieve a suitably modified protein system for the tleap execution. These procedures were then followed by stepwise minimization for 12,500 steps; initiated for 2500 steps in the presence of 500 kcal/mol Å restraint potential and 10,000 steps with no energy restraints. This was essential to remove steric inter-residual/inter-molecular clashes and obtain insights into the binding poses of **1** - **6** at their potential target sites.

2.13.3 *In silico* pharmacological and pharmacokinetic prediction

Cheminformatics methods were further employed to predict the pharmacological properties of compounds **1** to **6**. These were achieved using a cohort of online/offline cheminformatics tools that include Molsoft (http://molsoft.com/mprop/), ProTox webserver [29], OSIRIS DataWarrior property tool [30] and Molinspiration cheminformatics. Multiple tools were used to achieve a high degree of accuracy in our prediction and ensure reproducibility. These tools, all together, were enough to predict the ADMET (absorption, distribution, metabolism, excretion and toxicity) tendencies of the synthesized thiuram disulfides compounds in adherence to the Lipinski's rule of five (Ro5), a threshold used to pre-determine the drug-likeness of small molecules.

REFERENCES

1. E. D. Akpan, S. O. Ojwach, B. Omondi and V. O. Nyamori, *New Journal of Chemistry*, **2016**, 40, 3499-3510.
2. R. M. Roberts, *The Journal of Organic Chemistry*, **1949**, 14, 277-284.
3. H. J. Gysling and G. J. Kubas, *Inorganic Syntheses*, **1979**, 19, 92-97.
4. G. Rajput, V. Singh, S. K. Singh, L. B. Prasad, M. G. Drew and N. Singh, *European Journal of Inorganic Chemistry*, **2012**, 24, 3885-3891.
5. A. N. Gupta, V. Singh, V. Kumar, A. Rajput, L. Singh, M. G. Drew and N. Singh, *Inorganica Chimica Acta*, **2013**, 408, 145-151.
6. Bruker, *APEXII*, APEXII Bruker AXS Inc, Madison, Wisconsin, USA, 2009.
7. Bruker, *SAINT*, SAINT Bruker AXS InC, Madison, Wisconsin, USA, 2009.
8. Bruker, *SADABS*, SADABS Bruker AXS Inc, Madison, Wisconsin, USA, 2009.
9. G. M. Sheldrick, *Acta Crystallographica Section A: Foundations of Crystallography*, **2008**, 64, 112-122.
10. C.F. Macrae, I.J. Bruno, J.A. Chisholm, P.R. Edgington, P. McCabe, E. Pidcock, L. Rodriguez-Monge, R. Taylor, J. Van de Streek and P.A. Wood, *Journal of Applied Crystallography*, **2008**, 41, 466-470.
11. A. L. Spek, *Acta Crystallographica Section C: Structural Chemistry*, **2015**, 71, 9-18.
12. A. L. Spek, *Acta Crystallographica Section D: Biological Crystallography*, **2009**, 65, 148-155.
13. C. M. Liyana-Pathirana and F. Shahidi, *Journal of Agricultural and Food Chemistry*, **2005**, 53, 2433-2440.
14. L. Pari and R. Saravanan, *Diabetes, Obesity and Metabolism*, **2004**, 6, 286-292.
15. ChemAxon, *https:// www.chemaxon.com/products/marvin/*.**2013**.
16. M. D. Hanwell, D. E. Curtis, D. C. Lonie, T. Vandermeersch, E. Zurek and G. R. Hutchison, *Journal of Cheminformatics*, **2012**, 4, 17-25.
17. M. Frisch, G. Trucks, H. Schlegel, G. Scuseria, M. Robb, J. Cheeseman, G. Scalmani, V. Barone, G. Petersson and H. Nakatsuji, *Gaussian 16 Revision A 3*, **2016**.
18. X. Liu, I. Vogt, T. Haque and M. Campillos, *Bioinformatics*, **2013**, 29, 1910-1912.
19. X. Wang, C. Pan, J. Gong, X. Liu and H. Li, *Journal of Chemical Information and Modeling*, **2016**, 56, 1175-1183.
20. D. Gfeller, A. Grosdidier, M. Wirth, A. Daina, O. Michielin and V. Zoete, *Nucleic Acids Research*, **2014**, 42, 32-38.

21. A. Schuffenhauer, P. Floersheim, P. Acklin and E. Jacoby, *Journal of Chemical Information and Computer Sciences*, **2003**, 43, 391-405.
22. Nidhi, M. Glick, J. W. Davies and J. L. Jenkins, *Journal of Chemical Information and Modeling*, **2006**, 46, 1124-1133.
23. P. Willett, J. M. Barnard and G. M. Downs, *Journal of Chemical Information and Computer Sciences*, **1998**, 38, 983-996.
24. G. Cingolani, A. Panella, M. G. Perrone, P. Vitale, G. Di Mauro, C. G. Fortuna, R. S. Armen, S. Ferorelli, W. L. Smith and A. Scilimati, *European Journal of Medicinal Chemistry*, **2017**, 138, 661-668.
25. M. J. Lucido, B. J. Orlando, A. J. Vecchio and M. G. Malkowski, *Biochemistry*, **2016**, 55, 1226-1238.
26. E. F. Pettersen, T. D. Goddard, C. C. Huang, G. S. Couch, D. M. Greenblatt, E. C. Meng and T. E. Ferrin, *Journal of Computational Chemistry*, **2004**, 25, 1605-1612.
27. D. A. Case, T. E. Cheatham III, T. Darden, H. Gohlke, R. Luo, K. M. Merz Jr, A. Onufriev, C. Simmerling, B. Wang and R. J. Woods, *Journal of Computational Chemistry*, **2005**, 26, 1668-1688.
28. W. L. Jorgensen, J. Chandrasekhar, J. D. Madura, R. W. Impey and M. L. Klein, *The Journal of Chemical Physics*, **1983**, 79, 926-935.
29. M. N. Drwal, P. Banerjee, M. Dunkel, M. R. Wettig and R. Preissner, *Nucleic Acids Research*, **2014**, 42, 53-58.
30. T. Sander, J. Freyss, M. von Korff and C. Rufener, *Journal of Chemical Information and Modeling*, **2015**, 55, 460-473.

CHAPTER THREE

Novel N,N'-diarylformamidine based thiuram disulfides: synthesis, characterization, X-ray crystal structures, biological studies and *in silico* investigation as potential anticancer drugs

Abstract

In this study, we present the synthesis and biological evaluation of a series of N,N'-diarylformamidine-based thiuram disulfides. Six compounds were synthesized via the oxidation of six symmetrical and unsymmetrical formamidine-based dithiocarbamates. These were N,N'-bis(2,6-dimethylphenyl)formamidine dithiocarbamate (**DL1**), N,N'-bis(2,6-disopropylphenyl) formamidine dithiocarbamate (**DL2**), N,N'-dimesitylformamidine dithiocarbamate (**DL3**), N'-(2,6-dichlorophenyl-N-(2,6-dimethylphenyl)formamidine dithiocarbamate (**DL4**), N'-(2,6-dichlorophenyl)-N-(2,6-diisopropylphenyl)formamidine dithiocarbamate (**DL5**) and N'-(2,6-dichlorophenyl)-N-mesitylformamidine dithiocarbamate (**DL6**) The oxidation of the dithiocarbamates with iodine produced sulfur-sulfur coupling compounds **1**, **2**, **3**, **4**, **5** and **6**. All the compounds were characterized using UV-vis, FT-IR, ^{1}H and ^{13}C NMR, mass spectrometry and by elemental analysis. In addition, the single crystal structures of compounds **1**, **2**, **3**, **4a**, **4b**, **5**, and **6** are reported and confirm the coupling of N,N'-diarylformamidine dithiocarbamates moieties in **1** – **6**. Using efficient computational methods, therapeutic functionalities were defined for the novel thiuram disulfides **1** to **6**. Compounds **1** and **4** predictively exhibit dual selective inhibitory activities towards the inflammatory agents of cancer, cyclooxygenase -1 and 2. Docking and post-minimization results revealed that these compounds exhibit similar binding patterns at the active sites of both proteins, complemented by the formation of high-affinity interactions. Pharmacological estimations of these compounds revealed that both compounds had minimal violations of the Lipinski's rule but exhibited inclinations to be orally bioavailable and less toxic. *In vitro* antimicrobial study revealed that all the compounds displayed moderate to good activities against Gram-negative bacteria, *Escherichia coli*, *Salmonella typhimurium*, *Klebsiella pneumoniae* and *Pseudomonas aeruginosa*, but none of the twelve were active against Gram-positive bacteria, methicillin-resistant *Staphylococcus aureus* (MRSA) and *Staphylococcus aureus*. Compounds **4** and **5** were found to be more active than ciprofloxacin against *S. typhimurium* while **DL3** and **DL5** were also found to display better activity against *K. pneumoniae* when compared to the others and ciprofloxacin. All compounds exhibited poor antioxidant activity when compared to ascorbic acid but **DL1** – **DL6** displayed better activity relative to **1** – **6**.

Keywords: Thiuram disulfide; cheminformatics; cyclooxygenase 1 and 2; molecular docking; antimicrobial; antioxidant

3.1 Introduction

Although several attempts had been made to prevent, diagnose and treat cancer, the disease still poses a threat to mankind [1]. Reports indicate that cancer is the second most common disease, and of the causes of all worldwide fatalities, it ranks only after cardiovascular disorders [2, 3]. Millions die annually due to cancer and there is daily increase of its incidence due to factors that include those due to modernization of our society [2, 4]. Although different chemotherapy agents have been employed in the treatment of various cancer types, the platinum complex cisplatin and its derivatives are still the most commonly used for some cancer types. However, their use comes along with serious side effects, which include nephrotoxicity, emetogenesis, and neurotoxicity. These side effects limit possible dosage and applications [5]. In addition, inherent resistance is another setback often associated with, not only platinum-based drugs, but other drugs in use or under trials. For these reasons, there is increasing interest among researchers in developing novel non-platinum based metal complexes incorporating useful ligands as anticancer agents [6]. Of importance is also research on the antimicrobial activity of natural and synthetic compounds, due to increase numbers of antibiotic resistant bacterial pathogen microorganisms, which threaten the efficacies of existing antimicrobial drugs. This has become a global concern to public health practitioners [7, 8].

Dithiocarbamates have been used as anticancer agents and even better anticancer activity has been reported for thiuram disulfides, which are generated from the dithiocarbamates. For example, diethyldithiocarbamate is known to be a good anticancer agent [9]. More profound anticancer activity has been shown for its oxidized form, tetraethylthiuram disulfide (disulfram) [10]. Moreover, its safety record has been proven by extensive pharmacokinetic studies [11]. Mechanisms of proteasome pathway inhibition [12], DNA topoisomerase inhibition [13] as well as angiogenesis reduction [14] have been proposed for the action of disulfram as an anticancer agent. Besides anticancer activity, antimicrobial activity of thiuram disulfide as well as dithiocarbamates have also been reported [15, 16]. Horital *et al.* [15] reported the antimycobacterial activities of disulfram (DSF) and diethyldithiocarbamate (DDC) against multi-drug and extensively resistance drug resistance tuberculosis (MDR/XDR-TB). Both compounds exhibited potent anti-tubercular activity against 42 clinical isolates of *M. tuberculosis*, with disulfram showing distinctly remarkable bacterial activity *ex vivo* and *in*

vivo . Furthremore, the ability of disulfram to inhibit the *in vitro* growth of methicillin resistant *Staphylococcus aureus* has been reported by Phillip *et al.* [16]. However, reports on the potential antioxidant ability of both disulfide and dithiocarbamate compounds are scarce.

Generally, the thiuram disulfides are produced by iodine oxidation of the appropriate dithiocarbamate salts [17]. The mechanism of this reaction entails the oxidation of the dithiocarbamates to their corresponding radicals, which then combine at almost the diffusion rate to yield thiuram disulfides [18]. Apart from using them as anticancer and antibacterial agents, other biological application have been reported, such as antifungal activity [11, 19], and in treating alcoholism, the action of which is based on their inhibitory effect upon liver alcohol dehydrogenase [15, 20]. Other uses of disulfide compounds are in the vulcanization of synthetic rubber [21].

Reverse screening has evolved over the years as an important approach to identify hit proteins for novel compounds whose antagonistic or therapeutic roles are yet unknown [22-24]. The potential and effectiveness of *in silico* methods made their application in this study appropriate for defining therapeutic roles for the chosen compounds. This contrasts with the conventional virtual screening methods that are usually employed to identify novel lead compounds for protein targets. The efficacy of this method has been reported in several studies [22-25]. Likewise, molecular docking is a preliminary approach to obtain basic insight into the binding poses and interactions that suggest potential therapeutic inhibitors [26, 27]. This is important because the basis of drug targeting entails a complementary interaction between the ligand molecules and target proteins. This could also provide an avenue to identify non-interacting moieties, which are not essential for ligand-protein binding, hence eliminating them to reduce off-target effects, from a computational drug design perspective [27-29]. Over the years, the use of cheminformatics to gain primary insights into potential drug-ability and drug-likeness of a chemical compounds prior to *in vitro* and *in vivo* studies have been widely used to aid the development of potent drugs with minimal toxicities and off-target activities. This incorporates the possibility of determining active drug properties such as solubility, lipophilicity, surface area, oral bioavailability and toxicities using the standard Lipinski's rule of five (Ro5) threshold [30-32]. Herein, we report the synthesis of six disulfiram derivatives and enumerate their potential as anti-cancer agents as well as reporting their physiochemical and physicochemical properties using efficient *in silico* methods. We also report the antimicrobial and antioxidant activity of the synthesized compounds.

3.2 Results and discussion

3.2.1 Synthesis of N,N'-diarylformamidine dithiocarbamate salts and the respective thiuram disulfides.

The synthesis routes for **DL1** – **DL6** and **1** – **6** are shown in **Schemes 2.1 and 2.2**. The potassium dithiocarbamate salts **DL1 – DL6** were obtained by mixing an equimolar ratio of appropriate N,N`–diarylformamidine (**L1 - L6**) with carbon disulfides in the presence of KOH. The yields were between 74 and 94 % and melting points were 237 – 263 ℃. Compounds **1** – **6** were obtained by the reaction of salts of potassium dithiocarbamates with iodine in a 2:1 ratio. They are air stable yellow solids with sharp melting points between 186 and 235 ℃, which is much lower than those of the dithiocarbamate salts. This could be attributed to the formation of the covalent S—S bond, which is relatively weak.

3.2.2 Spectroscopic studies

(i) *Nuclear magnetic resonance*

The ^{1}H NMR data of **DL1** – **DL6** and **1** – **6** were obtained in dimethyl sulfoxide (DMSO) and $CDCl_3$, respectively, with peak assignments done using 2D NMR. There was an upfield shift of the azomethine proton in comparison to what was observed in the respective spectra of **DL1** – **DL6** (see **Table 3.1**). The methyl protons in **DL3** appeared at 1.94, 2.03, 2.15 and 2.22, but these shifted to 2.10, 2.14 and 2.27 in **3 (Figure 3.1)** and the same pattern was observed in the position of the methyl protons in the spectra of **DL1** – **DL6** when compared to **1** – **6**. Similar observations were made in the ^{13}C NMR spectra of **1** – **6** with a general upfield shift was observed. In particular, the quaternary thiouride carbon peaks (-NCS_2) are more shielded in thiuram disulfides, therefore appearing relatively upfield between 198 and 200 ppm for **1 – 6** compared to 217.6 and 220.9 ppm in **DL1** – **DL6**. This is because the electron-withdrawing power of the sulfur in the disulfide ligands has been reduced, due to the sulfur-sulfur bond formation.

Table 3.1: The -NCS_2 (^{13}C-NMR) and NC(H)=N (^{1}H-NMR) signals for **DL1 – DL6** and **1 – 6**, and the IR bands of thiouride (C—N) and azomethine (C=N) **for DL1 – DL6** and **1 – 6.**

Dithiocarbamates (Thiuram disulfides)	δ (-NCS_2) ppm	Δ δ	δ NC(H)=N ppm	Δ δ	υ(C=N) cm^{-1}	Δυ	υ(C—N) cm^{-1}	Δυ
DL1 (1)	217.62 (198.44)	19.18	9.86(9.84)	0.02	1640 (1645)	5	1467 (1469)	2
DL2 (2)	220.94 (198.67)	22.27	10.15(9.46)	0.69	1639 (1645)	6	1452 (1463)	11
DL3 (3)	218.95 (198.85)	20.10	9.92(9.42)	0.50	1629 (1643)	14	1477 (1478)	1
DL4 (4)	218.82 (198.73)	20.09	10.12(9.56)	0.56	1614 (1649)	35	1432 (1433)	1
DL5 (5)	217.02 (199.65)	17.37	10.13(9.81)	0.32	1603 (1630)	27	1430 (1433)	3
DL6 (6)	219.04 (199.25)	19.79	10.39(9.56)	0.83	1612 (1633)	21	1435 (1436)	1

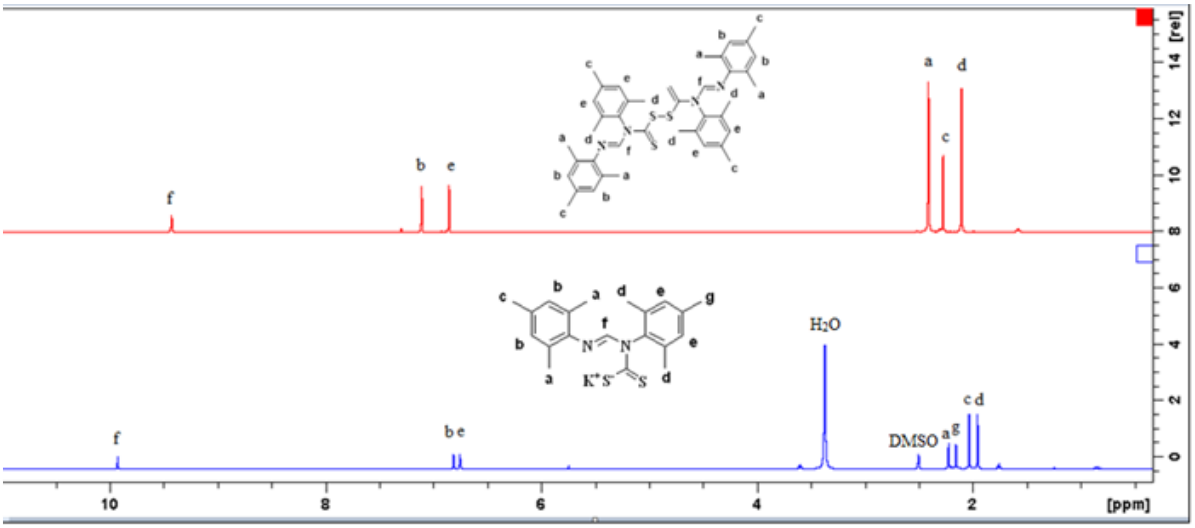

Figure 3.1: Stacked ^{1}H-NMR spectra of **DL3** and **3**

(ii) *Fourier transform infra-red spectroscopy*

The IR spectra of compounds **1 – 6** show all the major vibrational bands associated with the compounds. Of primary interest are bands associated with the thiouride moiety, the C—N, the C—S and the C=S bonds. The C—N_{str} part of the thiouride band in **DL1 - DL6** appears at 1430 – 1467 cm^{-1} is shifted to between 1433 cm^{-1} and 1478 cm^{-1} in **1 – 6**. The positions of the C—N_{str} bands are indicative of a partial double bond character, given that the υ(C=N) is normally between 1640 cm^{-1} and 1690 cm^{-1} while the υ(C–N) is normally between 1250 cm^{-1} and 1360 cm^{-1} in related compounds [33-36]. Similarly, there is a shift to higher frequencies in the υ(C=N_{str}) of the azomethine from 1603 – 1640cm^{-1} in **DLI – DL6** to 1630 – 1649 cm^{-1} in **1** to **6** (**Table 3.1**).

There is an increase in π-electron density in the C=N bond upon oxidation of the dithiocarbamate salts, resulting in a more double bond character in the thiuram disulfides. The ν(C–S_{str}) vibrational mode of **DL1 – DL6** appeared in the region of 921 – 1036 cm^{-1} while it appeared at a lower frequency in **1 – 6,** around 849 – 865 cm^{-1}, owing to the stronger withdrawing effect of electron from the carbon atom on the –NCS_2 moiety, through ionic interactions with the K^+ ion.

(iii) *UV-Visible spectroscopy*

The electronic absorption spectra of the dithiocarbamate ligands **DL1** – **DL6** and thiuram disulfide **1 - 6** were recorded in DMSO and chloroform, respectively. The UV-Visible spectra of all the ligands and the thiuram disulfide are given in Figures **3.2a** – **3.2b**. In all cases, two strong absorption bands were observed in the UV region between 289 nm and 300 nm and 338 nm and 345 nm for **DL1** – **DL6** and it appeared between 262 nm and 272 nm and 309 nm and 318 nm for **1** – **6**. These absorption bands were assigned to π→π* transitions associated with the N-C=S group and π→π* transition within the S-C=S moiety in the -NCS_2 units of the dithiocarbamate salts and thiuram disulfide compounds, respectively [37]. There is a general shift to lower wavelengths of the absorption bands from **1** – **6** when compared to those of the respective dithiocarbamates, **DL1** – **DL6**.

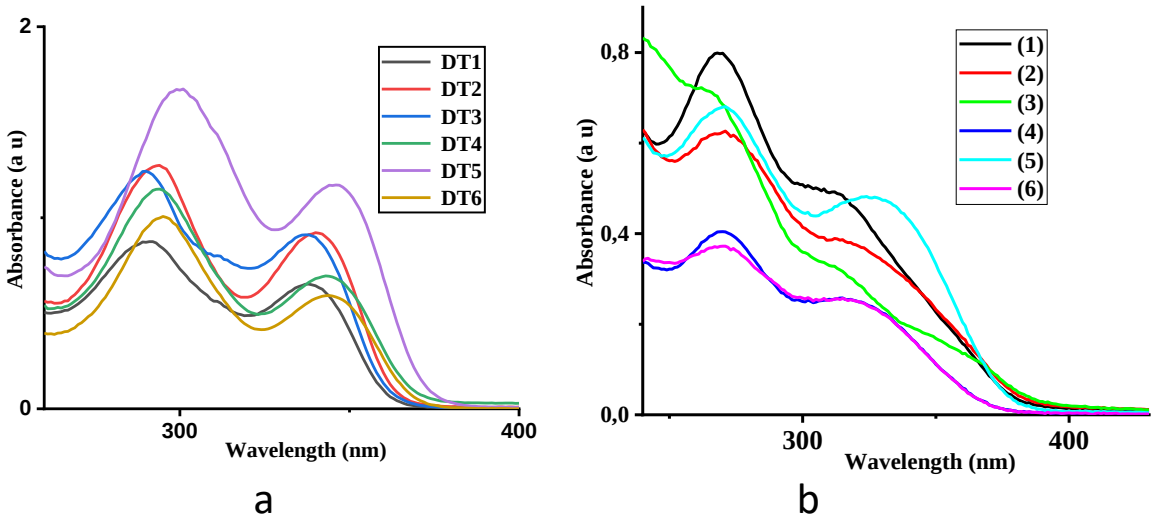

Figure 3.2: **(**a): Electronic absorption spectra of **DL1** – **DL6** (1b): Electronic absorption spectra of **1** – **6**.

3.3 Single crystal X-ray structural analysis

The molecular structures of compound **1 - 6** are given in **Figures 3.3 – 3.9,** while selected interatomic bond distances and bond angles are listed in **Table 3.2**. Crystals suitable for single X-ray structural analysis for **1**, **2**, and **4a** were obtained by slow evaporation from their dichloromethane solution, while those of **3**, **4b**, **5** and **6** were obtained by slow diffusion of ethanol into a dichloromethane solution of the compounds. In **4a**, one of the 2,6-dimethybenzene groups was found to be disordered over 2 positions, with the major component having 50% site occupancy, while in **4b,** the hydrogen atoms on three of the methyl groups were also found to be disordered over the two positions with the same site occupancy as that found in **4a**. For compound **4a**, a solvent mask was calculated and in one void 69.0 electrons was found in volume of 278.0 $Å^3$, which is consistent with the presence of 0.75[CH_2Cl_2] per formula unit to account for 63.0 electrons. The dichloromethane molecule in **4a** was found to be highly disordered and attempts to model it were unsuccessful; thus the *SQUEZE* option [38] in *PLATON* [39] was used.

The structures of **1 - 6** contain their two dithiocarbamate ligand units, which are almost perpendicular to each other, with torsion angles of 90.55º, 87.61º, 88.35º 83.14º, 85.89º, 88.90º and 86.28º for **1**, **2**, **3, 4a**, **4b, 5** and **6,** respectively, and they are linked by an S–S bond. Two sets of significantly different C–S distances were observed with these distances obviously corresponding to single and double bonded C–S distances. That is C(26)—S(1) = 1.6304(4), C(26)—S(2) = 1.798(4), C(27)—S(3) = 1.810(3) and C(27)—S(4) = 1.630(3) for compound 2. The C—N bond in the dithiocarbamate group of the compounds was shorter than C—N single bond and this indicates a considerable partial bond character. For example, C(26)—N(2) = 1.381(4) and C(27)—N(3) = 1.370(4) for **1** and for **4a** C(16)—N(2) = 1.370(2) and C(17)—N(3) = 1.3692(19). The C=S, C–S and C–N bond length measured here are comparable with those observed in the related structures [40-43]. The molecular structure of **4a** and **4b** are polymorphs. The space group of **4a** and **4b** are $P2_1/c$ and P-1 respectively.

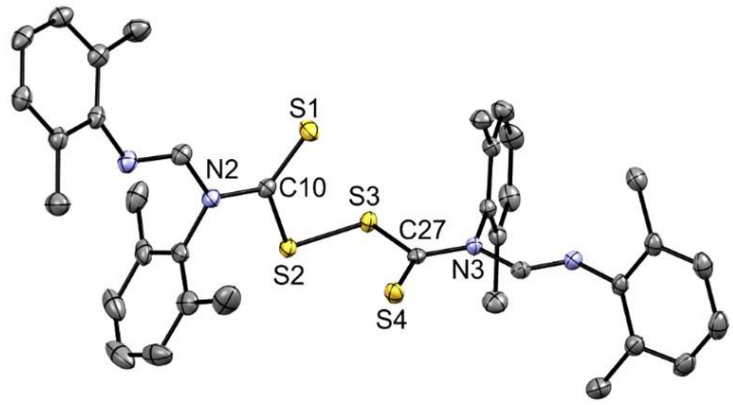

Figure 3.3: ORTEP diagram of **1** drawn at 50 % thermal ellipsoids probability. Hydrogen atoms have been omitted for clarity.

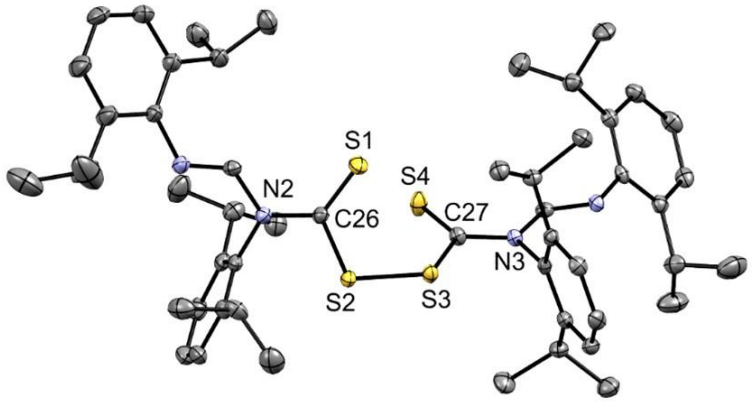

Figure 3.4: ORTEP diagram of **2** drawn at 50 % thermal ellipsoids probability. Hydrogen atoms have been omitted for clarity.

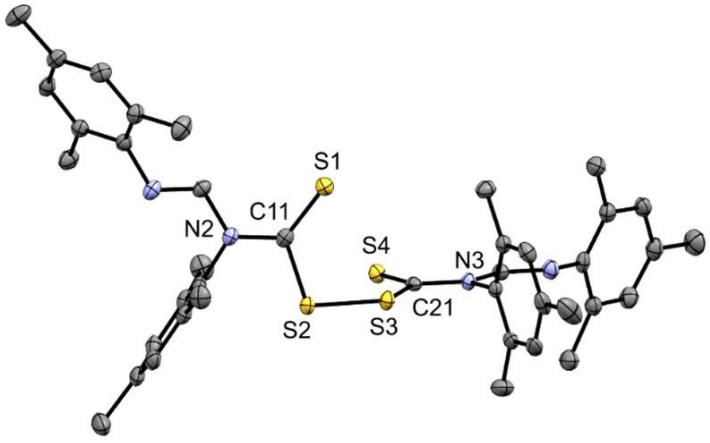

Figure 3.5: ORTEP diagram of **3** drawn at 50 % thermal ellipsoids probability. Hydrogen atoms have been omitted for clarity.

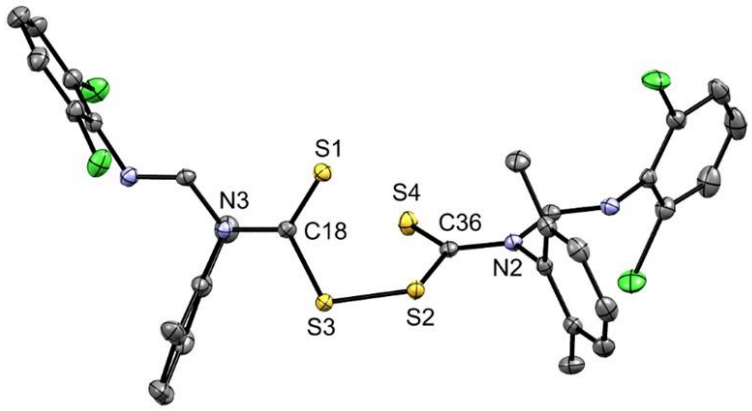

Figure 3.6: ORTEP diagram of **4a** drawn at 50 % thermal ellipsoids probability. Hydrogen atoms and disordered 2,6-dimethylbenzene of one of the dithiocarbamate units have been omitted for clarity.

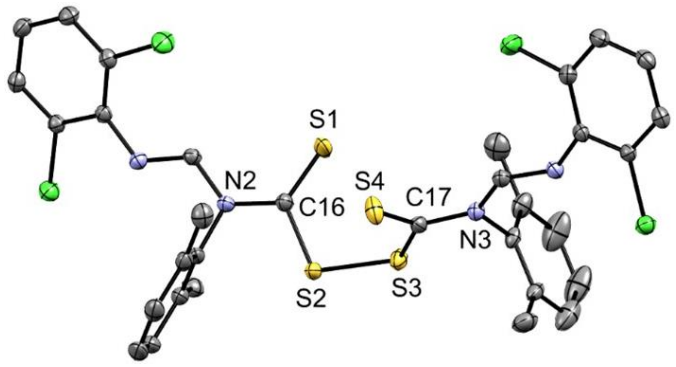

Figure 3.7: ORTEP diagram of **4b** drawn at 50 % thermal ellipsoids probability. Hydrogen atoms and dichloromethane molecule have been omitted for clarity.

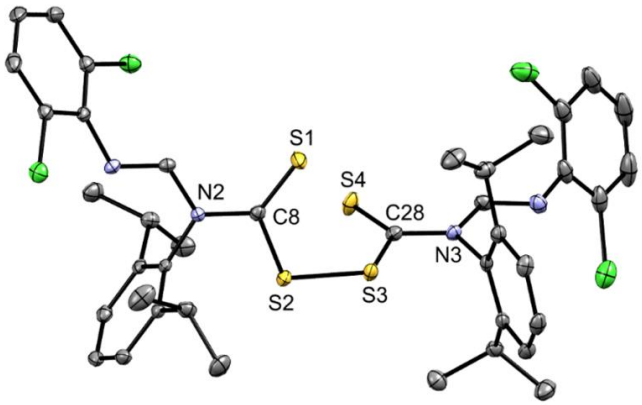

Figure 3.8: ORTEP diagram of **5** drawn at 50 % thermal ellipsoids probability. Hydrogen atoms have been omitted for clarity.

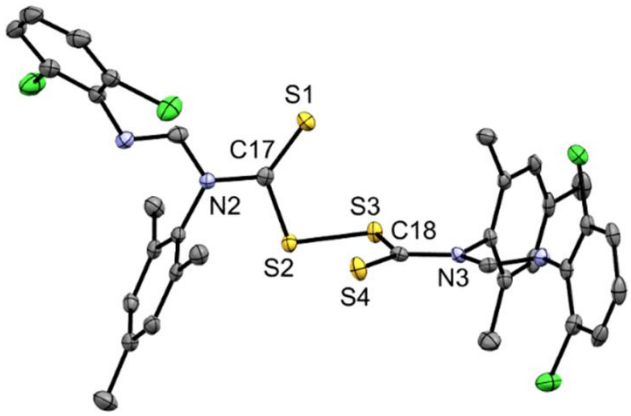

Figure 3.9: ORTEP diagram of **6** drawn at 50 % thermal ellipsoids probability. Hydrogen atoms have been omitted for clarity.

Table 3.2: Selected bond length (Å), bond angles (°) and dihedral angles (°) for thiuram disulfide **1**, **2**, **3**, **4a**, **4b**, **5** and **6.**

Parameters	**1**	**2**	**3**	**4(a)**	**4(b)**	**5**	**6**
Bond distances							
S(2)—S(3)	2.0183(7)	2.0157(11)	2.0176(6)	2.0187(5)	2.0247(5)	2.0171(6)	2.020(1)
C_{dtc}—S(1)	1.636(2)	1.6304(4)	1.638(2)	1.6327(16)	1.6398(15)	1.6296(16)	1.628(3)
C_{dtc}—S(2)	1.799(2)	1.798(4)	1.801(2)	1.8031(16)	1.7970(15)	1.7944(16)	1.806(3)
C_{dtc}—S(3)	1.8014(19)	1.810(3)	1.800(2)	1.7948(16)	1.8030(16)	1.8006(16)	1.801(4)
C_{dtc}—S(4)	1.637(2)	1.630(3)	1.633(2)	1.6341(17)	1.6341(16)	1.6321(16)	1.628(3)
C_{dtc}—N(2)	1.366(2)	1.381(4)	1.368(2)	1.370(2)	1.3723(19)	1.3796(19)	1.381(4)
C_{dtc}—N(3)	1.368(2)	1.370(4)	1.364(3)	1.3692(19)	1.3717(19)	1.376(2)	1.386(4)
Bond angles							
S(1)—C_{dtc}—S(2)	124.17(11)	124.4(2)	124.61	124.69(9)	124.73(9)	124.33(9)	124.4(2)
S(3)—C_{dtc}—S(4)	124.22(11)	123.5(2)	123.9(1)	124.16(9)	124.47(9)	124.39(9)	125.2(2)
Dihedral angle							
C_{dtc}—S(2)—S(3)—C_{dtc}	90.55	87.61	88.35	83.14	85.89	88.90	86.30

3.4 *In silico* insights and cheminformatics evaluation of thiuram disulfides 1 - 6

3.4.1 Identification of potential targets for thiuram disulfide 1 – 6

HitPick and other integrative target-fishing methods have been previously reported and were found to be efficient in the identification of possible target proteins for new synthetic or phytochemical compounds [22, 44]. Often, a combination of these methods is employed to get results that are more reliable. In this study, the *HitPick* webserver and SwissTargetPrediction tools were used to identify and validate potential targets for which compounds **1** to **6** might

have therapeutic effects, See **Section 2.13.1**. **Table 3.3** presents compounds **1** – **6** along with the various predicted targets along with the 3D-structures of the proteins.

Compounds **1** and **4** exhibited potential dual protein selectivity towards COX1 and COX2. COX1 and COX2 are biomolecules that have been extensively implicated in cancer-related inflammation [45, 46]. The two proteins are genetically associated with a number of neoplastic cancer types, including colorectal, pancreatic, breast, skin, head and haematological cancers [62]. Compounds **1** and **4** could therefore be candidates for testing against the above listed cancer types. Compound **2** dually targeted the human sodium (Na^+) channel voltage-gated Nav1.2 and Nav1.4 variants, SCN2A and SCN4A. This is an indication of its therapeutic functionality as a potential subtype blocker for the treatment of Na_v channelopathies [47, 48]. Compound **3** targeted the ubiquitously-expressed cytosolic human carbonic anhydrase II isoform, hCAII [49] while compounds **5** and **6** targeted the human sigma-1 receptor SIGMAR 1 [50]. These are important therapeutically in several neurological disorders, such as depression, neuropathic pain and drug addiction [51]. Therefore, compounds **1** and **4** potentially could have anticancer therapeutic activities compared to **2**, **3**, **5** and **6,** which seemed to target only non-carcinogenic biomolecules. However, additional *in vivo*, *in vitro* and structural (*in silico*) studies are needed to verify and validate the anti-cancer properties of **1** to **6**.

Table 3.3: Predicted protein targets along with the 3D structures, for compounds **1 – 6**

Synthetic compounds	Predicted targets	X-ray crystal structures
1 - N,N''-(disulfanne-1,2-dicarbonothioyl)bis(N,N'-bis(2,6-dimethylphenyl)formimidamide)	*PTSG-1*/COX-1 *PTSG-2*/COX-2	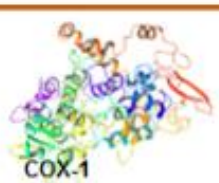 COX-1 PDB ID: 5WBE  COX-2 PDB ID: 5KIR
2 - N,N''-(disulfanne-1,2-dicarbonothioyl)bis(N,N'-bis(2,6-dimethylphenyl)formimidamide)	*SCN2A*/Nav1.2 *SCN4A*/Nav1.4	 Nav1.2 PDB ID: 6J8E  Nav1.4 PDB ID: 5F19
3 - N,N''-(disulfanne-1,2-dicarbonothioyl)bis(N,N'-bis(N,N'-dimesitylformimidamide	CA-II	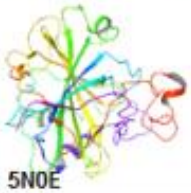 CA-II PDB ID: 5N0E
4 - N,N''-(disulfanne-1,2-dicarbonothioyl)bis(N'-(2,6-dichlorophenyl)-N-(2,6-diisopropylphenyl)formimidamide)	*PTSG-1*/COX-1 *PTSG-2*/COX-2	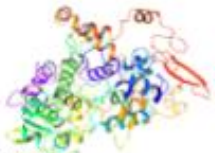 COX-1 PDB ID: 5WBE  COX-2 PDB ID: 5KIR
5 - N,N''-(disulfanne-1,2-dicarbonothioyl)bis(N'-(2,6-dichlorophenyl)-N-(2,6-dimethylphenyl)formimidamide)	SIGMAR-1	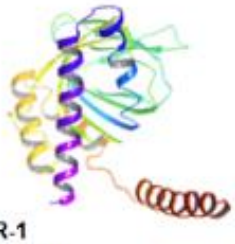 SIGMAR-1 PDB ID: 5HK1
6 - N,N''-(disulfanne-1,2-dicarbonothioyl)bis(N'-(2,6-dichlorophenyl)-N-mesitylformimidamide	SIGMAR-1	

abbreviations: COX-1 → Cyclooxygenase 1, COX-2 → Cyclooxygenase 2, Nav1.2 → voltage-gated sodium (Na+) channel type II, Nav1.4 → voltage-gated sodium (Na+) channel type IV, CA-II → Carbonic anhydrase, SIGMAR-1 → Sigma-1 receptor.

3.4.2: Molecular docking and elucidation of protein-ligand interaction

To provide insights into possible binding interactions of compounds **1** to **6** with the active sites of their respective protein targets, docking refinements were performed. Having identified compounds **1** and **4** as plausible targets for the pro-carcinogenic COX-1 and COX-2, the docking studies were done for only these two compounds. Optimized structures of the compounds used for docking are shown in **Figure 3.10**. In **Figure 3.11**, are presented the best docked poses and their corresponding scores. The selected poses were also superimposed with co-crystallized ligands at the active sites of target proteins, to indicate a degree of accuracy and correctness in the docking method employed in this study. Findings revealed that the selected binding poses for the docked compounds exhibited at least two ring-ring alignments with ligands that were co-crystallized with COX-1 and COX-2, as has previously been reported [49, 52-55].

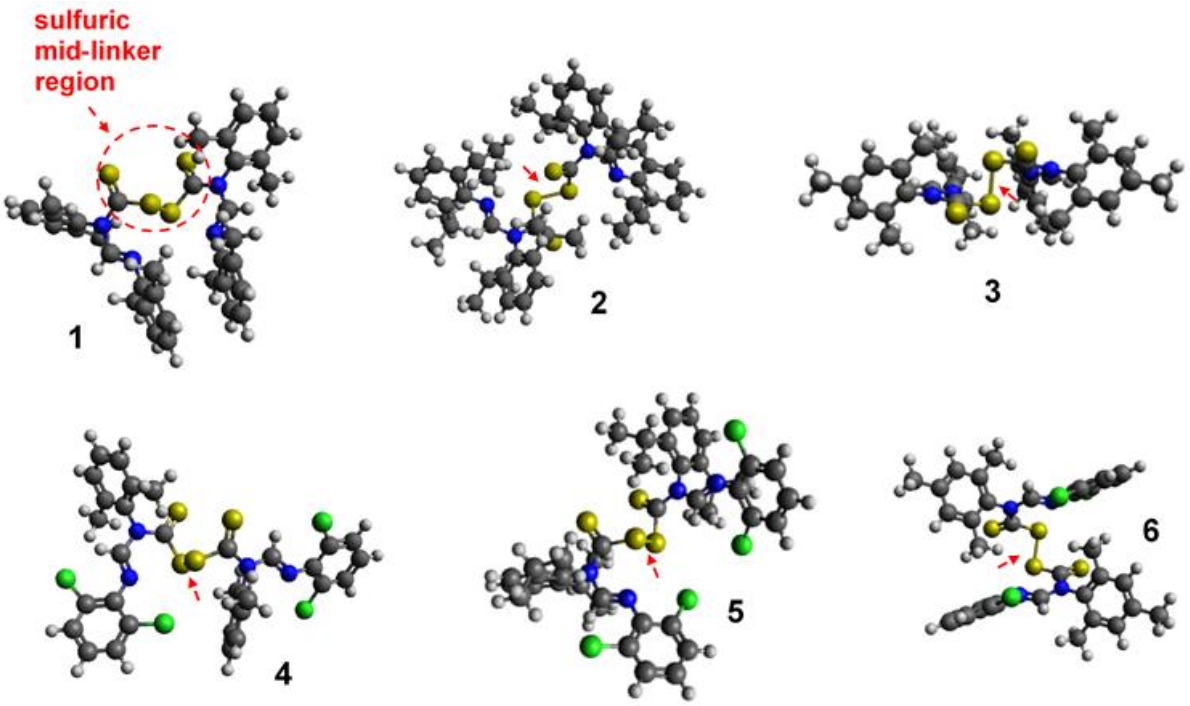

Figure 3.10: Structural and geometrical optimization of the compounds **1** to **6**.

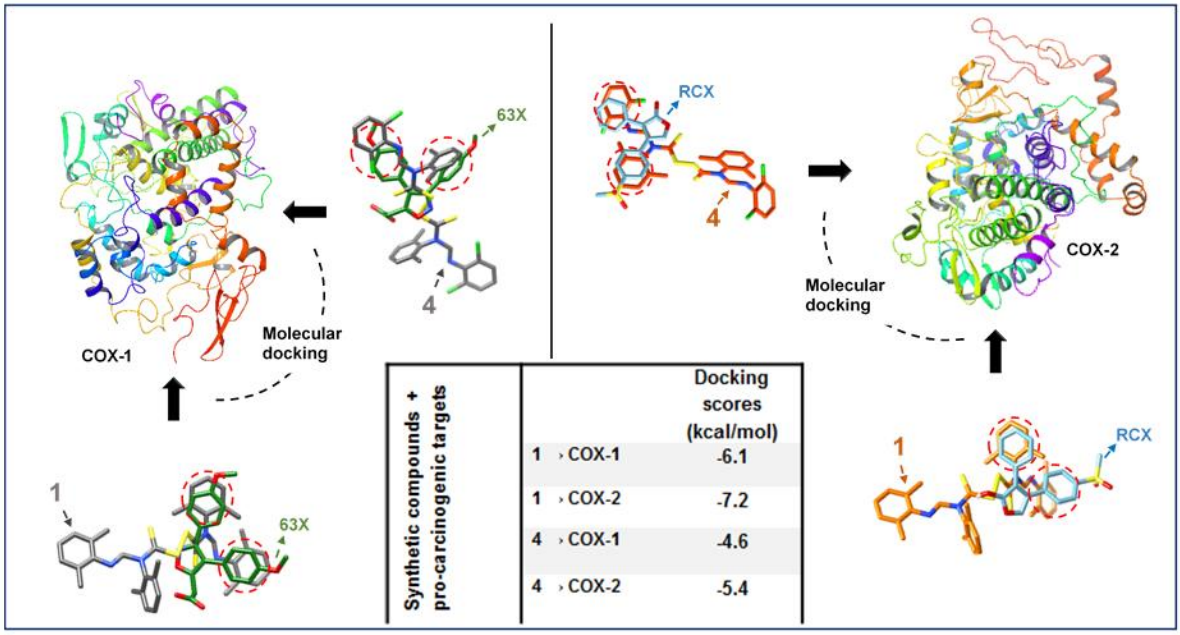

Figure 3.11*:* Docking poses and corresponding scores of **1** and **4** to COX-1/2. Also shown is the superposition of the **1** and **4** with co-crystallized COX-1/2 ligands as retrieved from PDB [56, 57]. 63X is COX-1 co-crystallized ligand while it is RCX for COX-2. Ring alignment between the DS-compounds and the co-crystallized compounds are highlighted in dashed-red circles. These were obtained by post-docking active site superposition.

The near-crystal structure positioning of the ligands could indicate that the docking approaches were correct and relatively valid. Moreover, we observed a similar binding pattern for **1** at the active sites of both COX-1 and COX-2, complemented by the occurrence of strong hydrogen bonds with some key residues such as Tyr355 and Arg120. These residues, according to some previous studies, play major roles in the binding, activities and stabilization of previous COX inhibitors [46].

The binding pattern could suggest the ability of compound **1** to bind dually to both COXs since they have a highly conserved active site. Concerning the patterns of interaction at the COX-1/2 active sites, the mid-linker sulfur atoms of **1** interact with the -OH group of Tyr355 via high-affinity hydrogen bonds, whereas a π-alkyl interaction occurs with Arg120. Thus, it shows that the sulfur-sulfur moiety in the dimer plays a role in anti-cancer activity as reported for disulfiram and indicates the potential that **1** and **4** have as anti-cancer agents [11, 13].

In addition, several other interactions, as shown in **Figures 3.12** and **3.13,** were observed. Compound **4**, showed a number of interactions at the active sites of both COX-1 and COX-2.

The binding involved strong interactions varying from hydrogen bonding to halogen bonding. More quantitative and qualitative theoretical methods such as QM, QM/MM Molecular dynamics (MD), and MM/PBSA-based free binding energy estimations would still be needed to verify the dual mechanistic binding and bonding formation of **1** and **4** at the active sites of COX-1/2. Based on the docking experiments, we can safely say that compounds **1** and **4** have similar binding/bonding patterns and modes at the active sites of COX-1 and COX-2; hence their dual selective targeting effects.

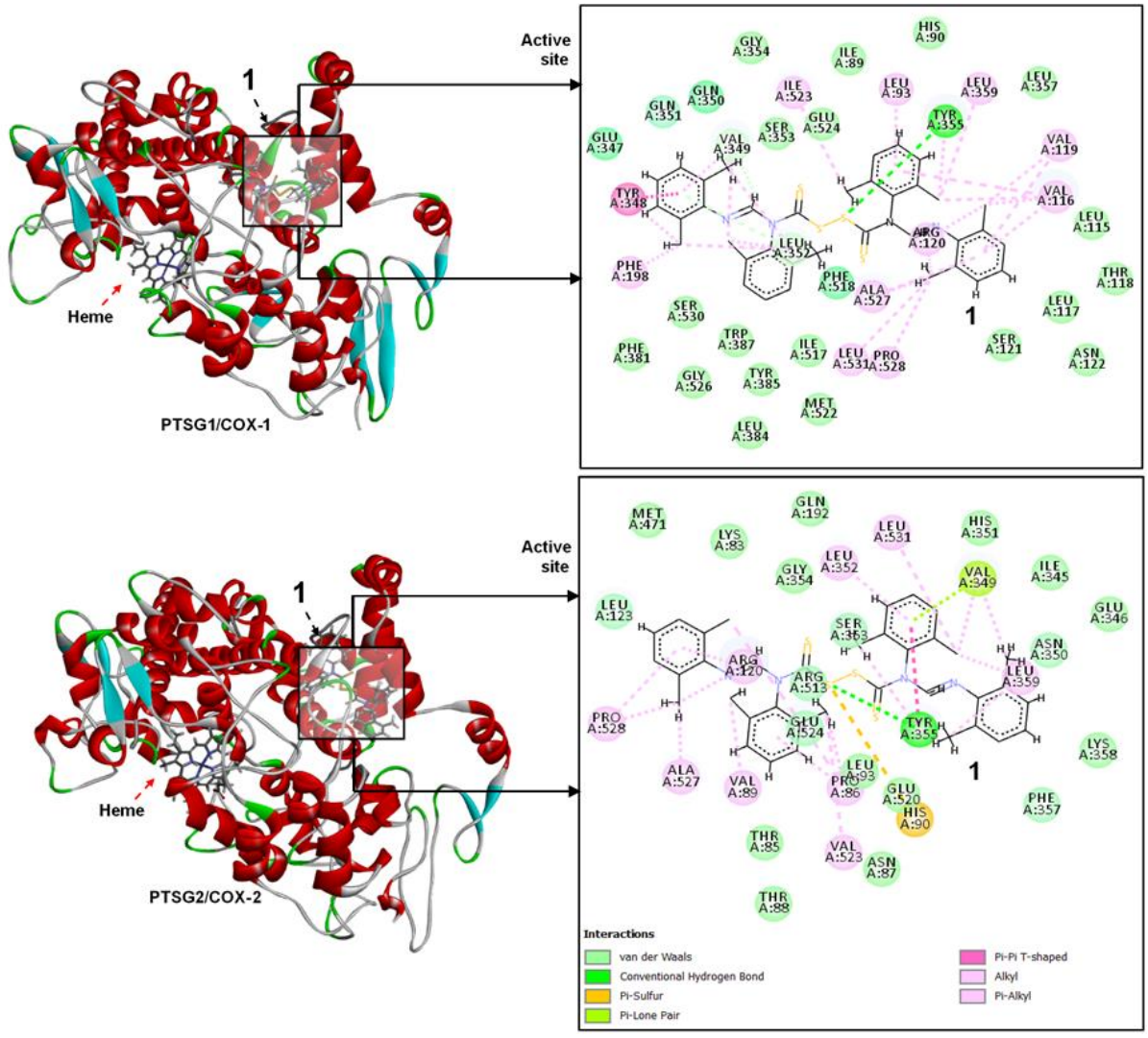

Figure 3.12: Dual binding interactions of **1** at the active sites of COX-1 and COX-2. Interaction nature and types are also shown and properly annotated in accompanying legend.

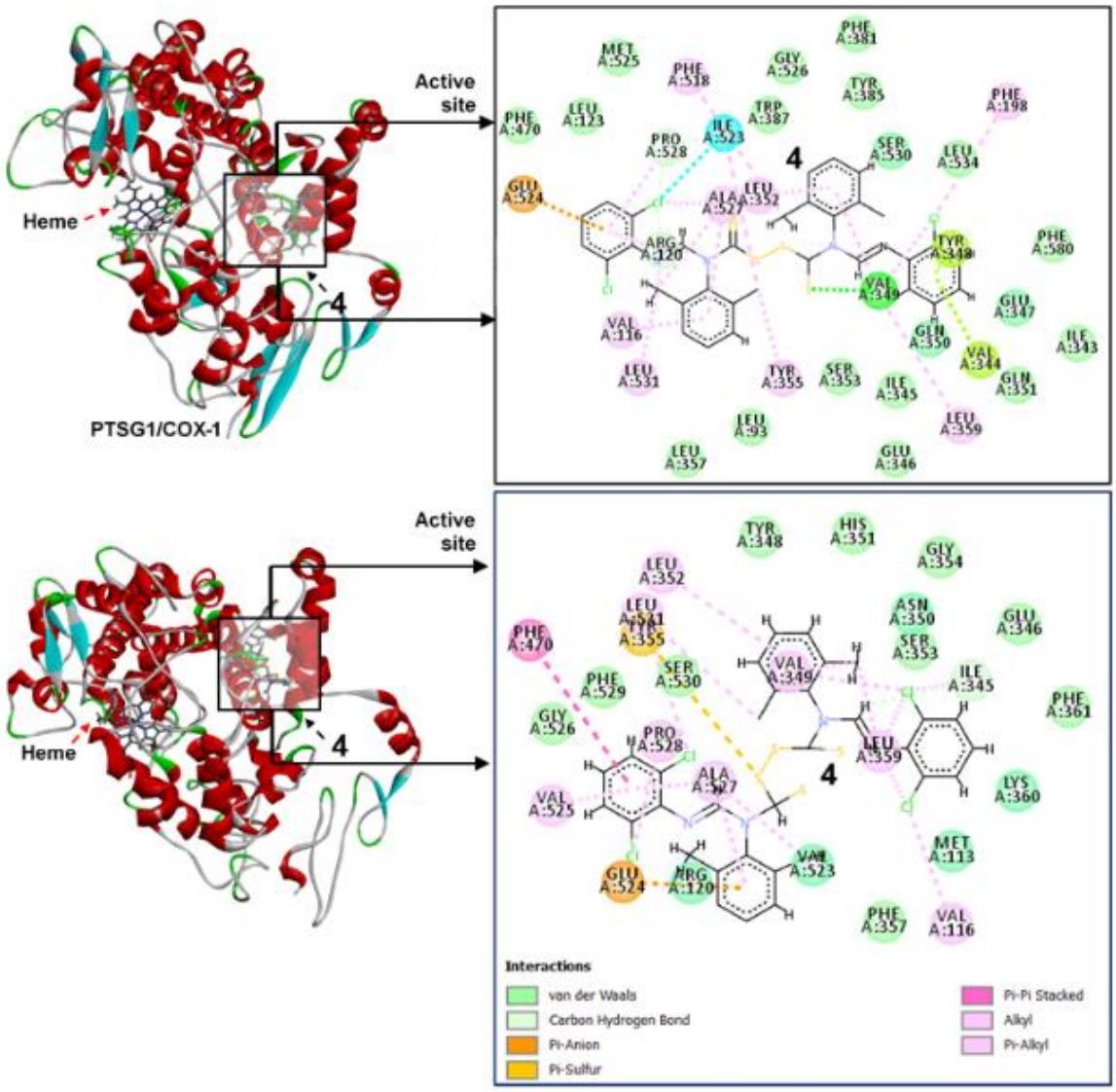

Figure 3.13: Dual binding interactions of 4 at the active sites of COX-1 and COX-2. Interaction nature and types are also shown and properly annotated in accompanying legend.

3.4.3 Estimations of ADMET properties for compounds 1 – 6

The prediction of the pharmacokinetics and pharmacological properties of compounds **1** to **6** was done to pre-determine their drug-likeness and oral bioavailability, which would link to their drug bioactivities. This was achieved using a cohort of cheminformatics tools as described above. In addition, integrative *in silico* modelling and cheminformatics provide a platform for efficient ligand optimization to improve their inhibitory activities and pharmacokinetics [28, 29]. The ADMETS results and physicochemical properties of compounds **1** to **6** are presented in **Table 3.4**. The estimated values were correlated with the standard Lipinski's Ro5 to pin-

point their violations, since active drug molecules are expected to have relatively minimal violations [32, 58, 59].

We estimated molecular weight (MW), lipophilicity (log*P*), aqueous solubility (log*S*), ability to be hydrogen bond donor (HBD) and acceptor (HBA), topological polar surface area (TPSA), rotatable bonds (RotB), ligand efficiency (LE), lipophilic ligand efficiency (LLE) and LD50, which is an important parameter in predicting the degree of toxicity for these compounds when administered orally. It has been revealed that high values of LD50 correlate with high toxicity while relatively lower LD50 values indicate that the compound would be less toxic [60]. Molecular weight of a compound is also an important parameter that can affect its bioavailability in terms of absorption and cellular uptake. A high MW impedes the access of a compound to the target biomolecules while also reducing concentration at the intestinal epithelium surface and to inhibiting eventual absorption [28]. The acceptable concentration for active compounds is ≤500g/mol, according to Lipinski's Ro5. However, as estimated, all the compounds exceeded the threshold, with compound **1** being closest, at 654.2 g/mol. All compounds had an estimated Log*S* value below the 0 – 6 mol/L standard. Likewise, the estimated Log*P* values for all six compounds violated the acceptable threshold of the Lipinski's Ro5 (<5); thus indicating poor lipophilicity. While these findings could imply that the compounds would exhibit poor absorption and permeability, various strategies such as structural fragmentation and nano-encapsulation could be further employed to improve their bio-availabilities [29, 61, 62] and enhance their systemic transport and delivery to cellular target sites. TPSA considers polar atoms on the surface of the compound, such as oxygen and nitrogen together with their added hydrogens [63, 64]. This implies that a compound with a low TPSA has higher propensity for transport across a lipid-bilayer membrane that is tightly packed, such as the GIT, and across the blood-brain barrier (BBB), while compounds with high TPSA demonstrate potential difficulties in permeabilization [65]. Compounds **1** to **6** had a uniform TPSA of 14.3 A^2, which indicates the possiblility of their permeating through the cells, particularly if it further optimized. Compounds **1** to **6** are predictively orally active and bioavailable, based on estimations of RotBs, HBAs and HBDs. RotBs is an important metric in predicting the molecular flexibility of a potential drug compound [66]. RotBs increase with MWs and according to the Lipinski's Ro5, a RotB count of <10 describes an orally active compound. As estimated, all the compounds except **2** and **5** fell within this acceptable threshold, providing room for further optimization relative to improving the oral activities of these two compounds. Overall, these compounds had predicted molecular flexibility values of

0.4 – 0.5, indicating a degree of uniformity in their structural architecture. Hydrogen bond count is also an important descriptor for evaluating solubility because they need to be broken for compounds to permeate a lipid bilayer membrane [67, 68]. Hydrogen bonds, which primarily relates to constituent hydrogen and nitrogen groups, have been correlated with TPSA and altogether they influence permeation by passive diffusion [64, 67]. Hence, a compound with HBDs and HBAs counts of ≤5 and ≤10, respectively, are considered orally active, according to the Lipinski's Ro5. Interestingly, our compounds had a uniform HBA count of 6, with no HBD correlative to the threshold. This further establishes their potentially oral activities and bioavailability. The possibility of these compounds to be orally toxic was deduced by estimating their LD50s. Findings in this regard revealed that, apart from compound **1**, all had relatively low LD50s, indicating their low tendency to induce oral toxicity.

With respect to evaluating drug-likeness and relative binding affinities towards biological targets, ligand efficiency (LE) has become a crucial guide and parameter for lead optimization and selection in drug design [69-71]. As previously proposed, acceptable thresholds for potential drug candidates include an LE > ~ 0.3 kcal/mol/heavy atom. From our findings, LEs for the compounds **1** – **6** were all 0.2 - 0.28 kcal/mol/heavy atom, which presents them as potential drug candidates with functionalities that can be further optimized for improved therapeutic activities. Moreover, with an LE of 0.28 kcal/mol/heavy atom, compound **4** appeared to be the most drug-like among the series. This, along with its ability to dually target COX1/COX2, makes it a compound of interest and possible subject of further investigations. Taken together, **1** and **4** exhibit anti-cancer propensities due to their predicted ability to dually target COX1 and COX2. These compounds, likewise, demonstrate favourable pharmacological and pharmacokinetic tendencies according to acceptable thresholds of Lipinski's Ro5, which entail desirable oral activity and bioavailability, coupled with other inherent properties that could be further enhanced by chemical and structural optimization.

Table 3.4: Estimations of ADMET and physicochemical properties of compounds **1 - 6**. Lipinski's Ro5 violations are indicated in red highlights.

Physicochemical properties	**1**	**2**	**3**	**4**	**5**	**6**	**Acceptable threshold (Ro5)**
Molecular weight (Da)	**654.2**	**878.5**	**710.3**	**734.0**	**846.1**	**762.0**	<500Da
Log*P*	**8.5**	**14.2**	**10.1**	**9.7**	**12.6**	**10.5**	<5
LogS (mol/L)	**-13.9**	**-20.7**	**-14.4**	**-15.1**	**-18.8**	**-15.3**	0 - -6
TPSA (A^2)	14.3	14.3	14.3	14.3	14.3	14.3	≤140
HBA	6	6	6	6	6	6	≤10
HBD	0	0	0	0	0	0	≤5
Rotatable bonds	7	**15**	7	7	**11**	7	<10
Ligand efficiency (kcal/mol/heavy atom)	0.2	0.2	0.25	0.28	0.24	0.26	> ~ 0.3
Oral toxicity prediction							
LD50 (mg/kg)	1000	188	300	160	188	160	
Toxicity class	4	3	3	3	3	3	

3.5 *In vitro* antimicrobial study

Potassium dithiocarbamate salts **DL1** – **DL6,** along with thiuram disulfides **1** – **6,** were screened against two Gram-positive bacteria, viz: MRSA and *S. aureus* and four Gram-negative bacteria, viz: *S. typhimurium*, *P. aeruginosa*, *E. coli* and *K. pneumoniae*. Ciprofloxacin was used as a standard antibiotic for comparison, while DMSO was used as a negative control because, at different concentrations, it showed no antibacterial activity against any of the bacterial strains used for this study. The antimicrobial activity of the compounds was evaluated using their MICs values and results are presented in **Table 3.5**. The higher the MIC values the lower will be the antimicrobial potential [72, 73]. Gram-negative bacteria strains were susceptible to all the compounds, while the compounds displayed no activity against Gram-positive bacteria strains, as seen in **Table 3.4**. Compounds **1 - 6** displayed better antimicrobial activity against *E. coli*, *S. typhimurium* and *P. aeruginosa* than did **DL1** – **DL6**, wheras against *K. pneumoniae* the corresponding potassium dithiocarbamate salts were more active than the thiuram disulfides **1** – **6**.

All the compounds displayed moderate to good antimicrobial activities against *E. coli*, with **6** having almost the same potential as ciprofloxacin. All the compounds were active against *S. typhimurium,* with compounds **4** and **5** outshining the reference drug. However, those that were synthesized from symmetrical formamidine sources were active only at high concentration (1000 µg/mL). All the compounds displayed moderate to good antimicrobial activity against *P. aeruginosa*, but they all exhibited lesser activity than did ciprofloxacin. Of note is that **DL1** – **DL6** showed better activity against *K. pneumoniae* relative to the corresponding compounds **1** – **6,** and **DL3** and **DL5** showed activity that surpassed that of the reference drug. For example, the MICs of potassium dithiocarbamate salts **DL1**, **DL2** and **DL3** were 50, 3.125 and 0.40 µg/mL, respectively, while their thiuram disulfide counterparts **1**, **2** and **3** gave results 50, 25 and 25 µg/mL, respectively.

It was observed that **DL4** – **DL6** and **4** – **6** displayed better activity than did **DL1** – **DL3** and **1** – **3** against all the bacteria strains, except against *K. pneumoniae* where **1** – **3** showed better activity had than **4 - 6**. This might be attributed to the presence of chlorine atoms in **DL4** – **DL6** and **4** – **6** which makes them have better lipophilicity as well as easier penetration into the lipophilic section of the cell membrane than for **DL1** – **DL3** and **1** – **3**, which have no chlorine atoms [74, 75] and this could be corroborated with the lipophilicity (LogP) values in **Table 3.4**. Gram-positive bacteria strains, *S. aureus* and MRSA, were not susceptible to **DL1** – **DL6** nor to **1** – **6** in all concentrations. The incapability of all the compounds to hinder the growth of *S. aureus* and MRSA could be as a result of the compound being modified and so rendered inactive at the surface of the cell wall or as soon as they entered the cell [76].

Table 3.5: Minimum inhibitory concentration of the potassium ditthiocarbamate salts **DL1** – **DL6** and thiuram disulfide **1 - 6** (µg/mL).

Complexes	Gram (-) bacterial				Gram (+) bacterial	
	E. Coli	*S. typhimurium*	*P. aeruginosa*	*K. pneumoniae*	*S. aureus*	MRSA
Symmetrical formamidine dithiocarbamate ligands and their thiuram disulfide **1 - 6**						
DTL1	50	1000	1000	50	NA	NA
DTL2	12.5	1000	1000	3.125	NA	NA
DTL3	12.5	1000	1000	0.40	NA	NA
1	6.25	1000	50	50	NA	NA
2	12.5	1000	25	25	NA	NA
3	12.5	1000	100	25	NA	NA
Unsymmetrical formamidine dithiocarbamate ligands and its cobalt(III) complexes						
DTL4	3.125	12.5	100	6.25	NA	NA
DTL5	6.25	50	1000	0.20	NA	NA
DTL6	1.60	100	1000	12.5	NA	NA
4	1.60	0.20	12.5	100	NA	NA
5	6.25	0.20	12.5	25	NA	NA
6	0.20	3.125	12.5	50	NA	NA
Ciprofloxacin[a]	0.20	0.40	0.8	1.60	25	25

NA = No activity, a = standard

3.6 *In vitro* antioxidant assay

Studies on 2,2-Diphenyl-1-picrylhydrazyl (DPPH) show that it is a stable organic radical compound, which can accept a proton radical or an electron, being then converted into a stable diamagnetic molecule. Its oxidative assay is used extensively in the quantification of the hydrogen-donor or radical-scavenging abilities of samples [77]. DPPH is known to have a strong absorption band in the visible region around 517 nm due to the presence of an odd number of electrons in the molecule. DPPH changes colour from purple to yellow when the unpaired electron present becomes paired with hydrogen from free radical scavenging

antioxidant to form reduced DPP-H [77-79]. Compounds with antioxidant properties always attract researchers' attention because they can be expected to offer protection against inflammation such as in rheumatoid arthritis, which makes them potentially effective drugs [80].

The IC_{50} values of **DL1** – **DL6** and **1** – **6**, as calculated from % free radical scavenging values, are presented in **Table 3.6**. The lower the IC_{50} values the higher will be the 'species' antioxidant activity [81, 82]. Results were compared with the antioxidant activity of ascorbic acid (with IC_{50} value of 1.01×10^{-3} mM). Generally, compared to the ascorbic acid standard, both the potassium dithiocarbamate salts and thiuram disulfide displayed poor antioxidant activity. It was observed that **DL1** – **DL6** were more active that their thiuram disulfide counterparts **1** – **6**, as seen in **Table 3.6.** This could be attributed to the availability of delocalized electron in the $–NCS_2$ moiety of the dithiocarbamates, which can be transferred to the free radical but which is not available in the thiuram disulfides [83]. The antioxidant activity of **DL1 – DL6** and **1 - 6** increases as their concentration increases, as illustrated in **Figures 3.14** and **3.15**.

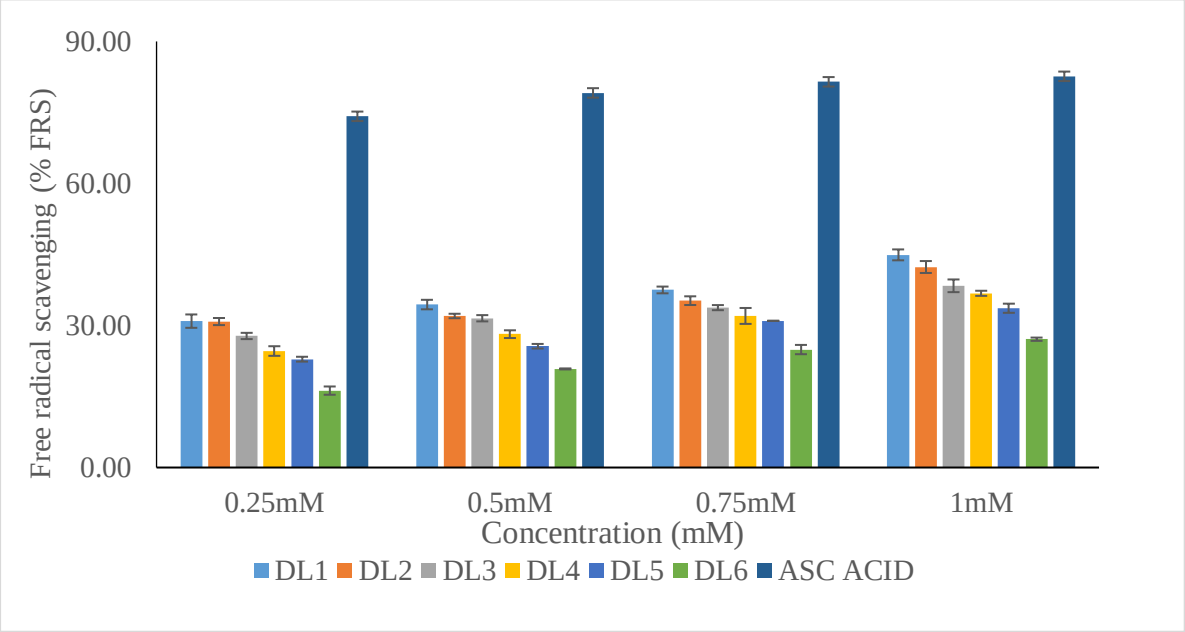

Figure 3.14: % Free radical scavenging vs concentration of potassium dithiocarbamate salts **DL1 – DL6**.

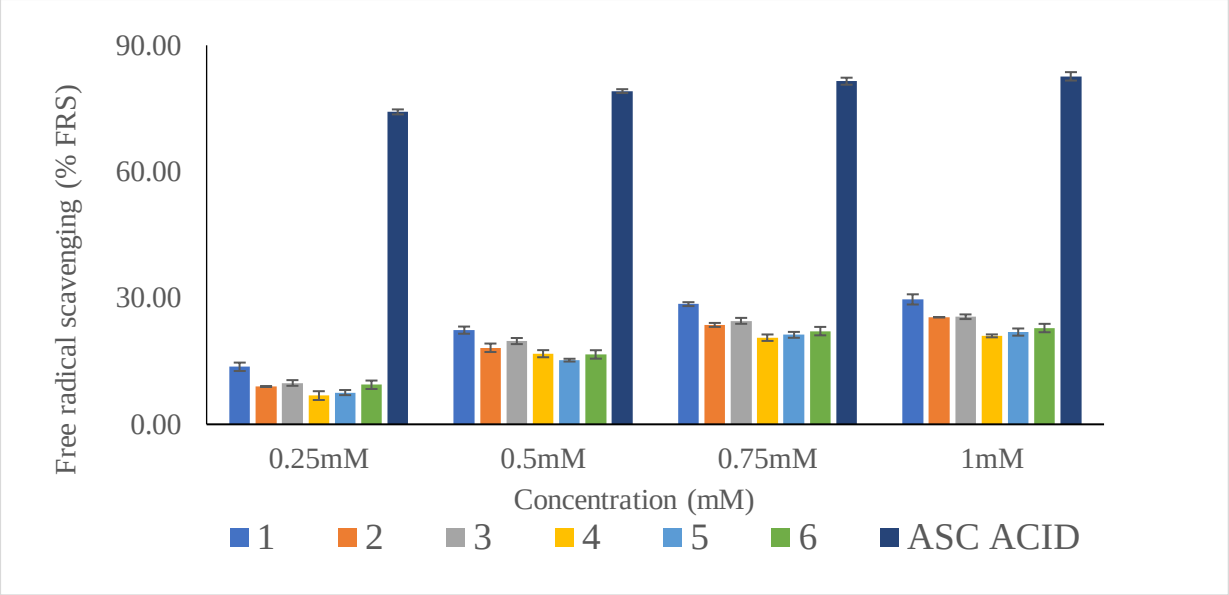

Figure 3.15: Free radical scavenging vs concentration of potassium dithiocarbamate salts **1 – 6**.

Table 3.6: Antioxidant potential of tested compounds at different concentrations using DPPH assay.

Ligands	IC_{50} (mM)	Disulfides	IC_{50} (mM)
DL1	2.14	**1**	5.26
DL2	4.11	**2**	6.97
DL3	6.14	**3**	7.14
DL4	5.71	**4**	>10
DL5	8.69	**5**	>10
DL6	>10	**6**	>10
Ascorbic acid	1.04×10^{-3}	Ascorbic acid	1.04×10^{-3}

Result presented here are the mean values from three independent experiments

Conclusion

Six thiuram disulfides of symmetrical and unsymmetrical N,N'-diarylformamidine-based dithiocarbamates were synthesized and fully characterized. The molecular structures of compounds **1 - 6** showed that two N,N'-diarylformamidine dithiocarbamate moieties are connected via a disulfide bond, and are perpendicular to each other. Of the six compounds, **1** and **4** were found to have possible anti-cancer activity, based on their abilities to dually bind to COX-1 and COX-2, which are crucial pro-carcinogenic targets that mediate cancer inflammation. Compound **1 - 4** exhibited similar binding modes and interacted with crucial residues such as Tyr355 and Arg120 via strong bonds relative to previous co-crystallized inhibitors. Pharmacological analyses revealed that these compounds had minimal violations of Lipinski's Ro5 and they demonstrated tendencies to be orally bioavailable and less toxic. However, it is necessary to employ additional quantitative and qualitative analytical methods to further verify their dual inhibitory prowess, and thereby ascertain more accurately their anti-cancer properties. Compounds **4** and **5** were found to be more active than ciprofloxacin against *S. typhimurium* while **DL3** and **DL5** were also found to display better activity against *K. pneumoniae* when compared to ciprofloxacin and others. All compounds exhibited poor antioxidant activity when compared to ascorbic acid.

REFERENCES

1. A. Kotnis, R. Sarin and R. Mulherkar, *Journal of Biosciences*, **2005**, 30, 93-102.
2. I. Ali, W. A. Wani, K. Saleem and M.-F. Hseih, *Polyhedron*, **2013**, 56, 134-143.
3. A. Jemal, R. Siegel, E. Ward, T. Murray, J. Xu and M. J. Thun, *CA: A Cancer Journal for Clinicians*, **2007**, 57, 43-66.
4. I. Ali, K. Salim, M. A Rather, W. A Wani and A. Haque, *Current Cancer Drug Targets*, **2011**, 11, 135-146.
5. Y. Jung and S. J. Lippard, *Chemical Reviews*, **2007**, 107, 1387-1407.
6. I. Ali, W. A Wani, K. Saleem and A. Haque, *Anti-Cancer Agents in Medicinal Chemistry (Formerly Current Medicinal Chemistry-Anti-Cancer Agents)*, **2013**, 13, 296-306.
7. J. M. Blondeau, *Journal of Antimicrobial Chemotherapy*, **1999**, 43, 1-11.
8. M. Balouiri, M. Sadiki and S. K. Ibnsouda, *Journal of Pharmaceutical Analysis*, **2016**, 6, 71-79.
9. A. Spath and K. Tempel, *Chemico-Biological Interactions*, **1987**, 64, 151-166.
10. M. Wickström, K. Danielsson, L. Rickardson, J. Gullbo, P. Nygren, A. Isaksson, R. Larsson and H. Lövborg, *Biochemical Pharmacology*, **2007**, 73, 25-33.
11. Z. E. Sauna, S. Shukla and S. V. Ambudkar, *Molecular BioSystems*, **2005**, 1, 127-134.
12. H. Lövborg, F. Öberg, L. Rickardson, J. Gullbo, P. Nygren and R. Larsson, *International Journal of Cancer*, **2006**, 118, 1577-1580.
13. J. S. Yakisich, Å. Sidén, P. Eneroth and M. Cruz, *Biochemical and Biophysical Research Communications*, **2001**, 289, 586-590.
14. S.-G. Shian, Y.-R. Kao, F. Y.-H. Wu and C.-W. Wu, *Molecular Pharmacology*, **2003**, 64, 1076-1084.
15. Y. Horita, T. Takii, T. Yagi, K. Ogawa, N. Fujiwara, E. Inagaki, L. Kremer, Y. Sato, R. Kuroishi and Y. Lee, *Antimicrobial Agents and Chemotherapy*, **2012**, 75, 6445-6411.
16. M. Phillips, G. Malloy, D. Nedunchezian, A. Lukrec and R. Howard, *Antimicrobial Agents and Chemotherapy*, **1991**, 35, 785-787.
17. F. K. Keter, M. J. Nell, I. A. Guzei, B. Omondi and J. Darkwa, *Journal of Chemical Research*, **2009**, 20, 322-325.

18. V. Plyusnin, E. Kuznetzova, G. Bogdanchikov, V. Grivin, V. Kirichenko and S. Larionov, *Journal of Photochemistry and Photobiology A: Chemistry*, **1992**, 68, 299-308.
19. V. K. Sharma, J. Aulakh and A. K. Malik, *Journal of Environmental Monitoring*, **2003**, 5, 717-723.
20. J. E. Peachey and C. A. Naranjo, in *Research Advances in Alcohol and Drug Problems*, Springer, **1983**, 397-431.
21. S. K. De and J. R. White, *Rubber technologist's handbook*, iSmithers Rapra Publishing, **2001**, Vol 1.
22. J. M. Rollinger, D. Schuster, B. Danzl, S. Schwaiger, P. Markt, M. Schmidtke, J. Gertsch, S. Raduner, G. Wolber and T. Langer, *Planta Medica*, **2009**, 75, 195-204.
23. M. A. Grant, *Combinatorial Chemistry & High Throughput Screening*, **2009**, 12, 940-960.
24. S. Zahler, S. Tietze, F. Totzke, M. Kubbutat, L. Meijer, A. M. Vollmar and J. Apostolakis, *Chemistry & Biology*, **2007**, 14, 1207-1214.
25. X. Xu, M. Huang and X. Zou, *Biophysics Reports*, **2018**, 4, 1-16.
26. A. Dar and S. Mir, *Journal of Analytical and Bioanalytical Techniques*, **2017**, 8(2) 1-7.
27. V. Salmaso and S. Moro, *Frontiers in Pharmacology*, **2018**, 9.
28. F. A. Olotu, G. Munsamy and M. E. Soliman, *Computational and Structural Biotechnology Journal*, **2018**, 16, 573-586.
29. E. A. Crane and K. Gademann, *Angewandte Chemie International Edition*, **2016**, 55, 3882-3902.
30. M. A. Bakht, M. S. Yar, S. G. Abdel-Hamid, S. I. Al Qasoumi and A. Samad, *European Journal of Medicinal Chemistry*, **2010**, 45, 5862-5869.
31. M. S. Lajiness, M. Vieth and J. Erickson, *Current Opinion in Drug Discovery and Development*, **2004**, 7, 470-477.
32. C. A. Lipinski, F. Lombardo, B. W. Dominy and P. J. Feeney, *Advanced Drug Delivery Reviews*, **1997**, 23, 3-25.
33. A. Gölcü, *Transition Metal Chemistry*, **2006**, 31, 405-412.
34. P. A. Ajibade, J. Z. Mbese and B. Omondi, *Inorganic and Nano-Metal Chemistry*, **2017**, 47, 202-212.
35. D. Onwudiwe and A. Ekennia, *Research on Chemical Intermediates*, **2017**, 43, 1465-1485.

36. A. Z. Halimehjani, S. Torabi, V. Amani, B. Notash and M. R. Saidi, *Polyhedron*, **2015**, 102, 643-648.
37. H. A. Hasan, E. I. Yousif and M. J. Al-Jeboori, *Global Journal of Inorganic Chemistry*, **2012**, 3, 1-7.
38. A. L. Spek, *Acta Crystallographica Section C: Structural Chemistry*, **2015**, 71, 9-18.
39. A. L. Spek, *Acta Crystallographica Section D: Biological Crystallography*, **2009**, 65, 148-155.
40. F. Jian, L. Jiang, H.-K. Fun, K. Chinnakali, I. Razak and X. You, *Acta Crystallographica Section C: Crystal Structure Communications*, **1999**, 55, 573-574.
41. H.-K. Fun, S. Chantrapromma, I. A. Razak, F.-L. Bei, F.-F. Jian, X.-J. Yang, L. Lu and X. Wang, *Acta Crystallographica Section E: Structure Reports Online*, **2001**, 57, 717-718.
42. J. Zhai, H.-D. Yin, F. Li, S.-W. Chen and D.-Q. Wang, *Acta Crystallographica Section E: Structure Reports Online*, **2007**, 63, 1969-1970.
43. P. A. Ajibade, B. C. Ejelonu and B. Omondi, *Acta Crystallographica Section E: Structure Reports Online*, **2012**, 68, 2182-2182.
44. T. Cheng, Q. Li, Y. Wang and S. H. Bryant, *Journal of Chemical Information and Modeling*, **2011**, 51, 2440-2448.
45. M. G Perrone, A. Scilimati, L. Simone and P. Vitale, *Current Medicinal Chemistry*, **2010**, 17, 3769-3805.
46. A. Pannunzio and M. Coluccia, *Pharmaceuticals*, **2018**, 11, 101-107.
47. G. SB Andavan and R. Lemmens-Gruber, *Current Medicinal Chemistry*, **2011**, 18, 377-397.
48. O. K. Steinlein, *Chemical Reviews*, **2012**, 112, 6334-6352.
49. E. Bruno, M. R. Buemi, A. Di Fiore, L. De Luca, S. Ferro, A. Angeli, R. Cirilli, D. Sadutto, V. Alterio and S. M. Monti, *Journal of Medicinal Chemistry*, **2017**, 60, 4316-4326.
50. H. R. Schmidt, S. Zheng, E. Gurpinar, A. Koehl, A. Manglik and A. C. Kruse, *Nature*, **2016**, 532, 527.
51. J. L. Ortega-Roldan, F. Ossa and J. R. Schnell, *Journal of Biological Chemistry*, **2013**, 288, 21448-21457.
52. G. Cingolani, A. Panella, M. G. Perrone, P. Vitale, G. Di Mauro, C. G. Fortuna, R. S. Armen, S. Ferorelli, W. L. Smith and A. Scilimati, *European Journal of Medicinal Chemistry*, **2017**, 138, 661-668.

53. M. J. Lucido, B. J. Orlando, A. J. Vecchio and M. G. Malkowski, *Biochemistry*, **2016**, 55, 1226-1238.
54. H. Shen, Z. Li, Y. Jiang, X. Pan, J. Wu, B. Cristofori-Armstrong, J. J. Smith, Y. K. Chin, J. Lei and Q. Zhou, *Science*, **2018**, 362, 2596-2605.
55. X. Pan, Z. Li, Q. Zhou, H. Shen, K. Wu, X. Huang, J. Chen, J. Zhang, X. Zhu and J. Lei, *Science*, **2018**, 362, 2486-2493.
56. E. F. Pettersen, T. D. Goddard, C. C. Huang, G. S. Couch, D. M. Greenblatt, E. C. Meng and T. E. Ferrin, *Journal of Computational Chemistry*, **2004**, 25, 1605-1612.
57. D. A. Case, T. E. Cheatham III, T. Darden, H. Gohlke, R. Luo, K. M. Merz Jr, A. Onufriev, C. Simmerling, B. Wang and R. J. Woods, *Journal of Computational Chemistry*, **2005**, 26, 1668-1688.
58. C. A. Lipinski, F. Lombardo, B. W. Dominy and P. J. Feeney, *Advanced Drug Delivery Reviews*, **2012**, 64, 4-17.
59. C. A. Lipinski, *Journal of Pharmacological and Toxicological Methods*, **2000**, 44, 235-249.
60. M. N. Drwal, P. Banerjee, M. Dunkel, M. R. Wettig and R. Preissner, *Nucleic Acids Research*, **2014**, 42, 53-58.
61. S. Prasad, A. K. Tyagi and B. B. Aggarwal, *Cancer Research and Treatment: Official Journal of Korean Cancer Association*, **2014**, 46, 2.
62. P. Ma, Q. Zeng, K. Tai, X. He, Y. Yao, X. Hong and F. Yuan, *Food Science and Technology*, **2017**, 84, 34-46.
63. P. Ertl, B. Rohde and P. Selzer, *Journal of Medicinal Chemistry*, **2000**, 43, 3714-3717.
64. S. Prasanna and R. Doerksen, *Current Medicinal Chemistry*, **2009**, 16, 21-41.
65. S. Shityakov, W. Neuhaus, T. Dandekar and C. Förster, *International Journal of Computational Biology and Drug Design*, **2013**, 6, 146-156.
66. Z. Omran and C. Rauch, *European Biophysics Journal*, **2014**, 43, 199-206.
67. L. Di and E. H. Kerns, *Drug-like properties: concepts, structure design and methods from ADME to toxicity optimization*, Academic press, **2015**.
68. M. Abraham, J. Gola, R. Kumarsingh, J. Cometto-Muniz and W. Cain, *Journal of Chromatography. B: Biomedical Sciences and Applications*, **2000**, 745, 103-115.
69. K. D. Freeman-Cook, R. L. Hoffman and T. W. Johnson, *Future Medicinal Chemistry*, **2013**, 5, 113-115.
70. A. L. Hopkins, G. M. Keserü, P. D. Leeson, D. C. Rees and C. H. Reynolds, *Nature Reviews Drug Discovery*, **2014**, 13, 105.

71. C. Abad-Zapatero, *Expert Opinion on Drug Discovery*, **2007**, 2, 469-488.
72. L. S. Kumar, K. S. Prasad and H. D. Revanasiddappa, *European Journal of Chemistry*, **2011**, 2, 394-403.
73. K. Nomiya, A. Yoshizawa, K. Tsukagoshi, N. C. Kasuga, S. Hirakawa and J. Watanabe, *Journal of Inorganic Biochemistry*, **2004**, 98, 46-60.
74. K. Naumann, *EuroChlor Science Dossier November*, **2003**.
75. K. Naumann, *Pest management Science*, **2000**, 56, 3-21.
76. B. L. Batzing, *Microbiology: An Introduction*, Brooks/Cole, **2002**.
77. S. Vartale, N. Halikar, Y. Pawar and K. Tawde, *Arabian Journal of Chemistry*, **2016**, 9, 1117-1124.
78. S. B. Bukhari, S. Memon, M. M. Tahir and M. Bhanger, *Journal of Molecular Structure*, **2008**, 892, 39-46.
79. M. Valko, C. Rhodes, J. Moncol, M. Izakovic and M. Mazur, *Chemico-Biological Interactions*, **2006**, 160, 1-40.
80. M. E. De Leo, A. Tranghese, M. Passantino, A. Mordente, M. M. Lizzio, T. Galeotti and A. Zoli, *The Journal of Rheumatology*, **2002**, 29, 2245-2246.
81. N. Ganji, A. Rambabu, N. Vamsikrishna and S. Daravath, *Journal of Molecular Structure*, **2018**, 1173, 173-182.
82. M. Shabbir, Z. Akhter, I. Ahmad, S. Ahmed, M. Shafiq, B. Mirza, V. McKee, K. S. Munawar and A. R. Ashraf, *Journal of Molecular Structure*, **2016**, 1118, 250-258.
83. S. A. Nami, I. Ullah, M. Alam, D.-U. Lee and N. Sarikavakli, *Journal of Photochemistry and Photobiology B: Biology*, **2016**, 160, 392-399.

CHAPTER FOUR

Synthesis and structural studies of copper(II)-, nickel(II)-, and cobalt(III)-N,N'-diarylformamidine dithiocarbamate complexes as antimicrobial and antioxidant agents

ABSTRACT

A series of six N'N-diarylformamidine dithiocarbamate ligands and their metal complexes of chloride Cu(II), Ni(II) and Co(III) salts have been synthesized. Three symmetrical dithiocarbamate ligands, N,N'-bis(2,6-dimethylphenyl)formamidine dithiocarbamate (**DL1**), N,N'-bis(2,6-disopropylphenyl) formamidine dithiocarbamate (**DL2**), N,N'-mesityl formamidine dithiocarbamate (**DL3**) and three unsymmetrical dithiocarbamate ligands, N'-(2,6-dichlorophenyl-N-(2,6-dimethylphenyl) formamidine dithiocarbamate (**DL4**), N'-(2,6-dichlorophenyl)-N-(2,6-diisopropylphenyl) formamidine dithiocarbamate (**DL5**) and N'-(2,6-dichlorophenyl)-N-mesityl formamidine dithiocarbamate (**DL6**) were reacted with $CuCl_2$, $NiCl_2$ and $CoCl_2$ to give [Ni-(**DL1**)$_2$] (**7**), [Ni-(**DL2**)$_2$] (**8**), [Ni-(**DL3**)$_2$] (**9**), [Ni-(**DL4**)$_2$] (**10**), [Ni-(**DL5**)$_2$] (**11**), [Ni-(**DL6**)$_2$] (**12**), [Cu-(**DL1**)$_2$] (**13**), [Cu-**(DL2**)$_2$] (**14**), [Cu-(**DL3**)$_2$] (**15**), [Cu-(**DL4**)$_2$] (**16**), [Cu-(**DL5**)$_2$] (**17**), [Cu-(**DL6**)$_2$] (**18**), [Co-(**DL1**)$_3$] (**19**), [Co-(**DL2**)$_3$] (**20**), [Co-(**DL3**)$_3$] (**21**), [Co-(**DL4**)$_3$] (**22**), [Co-(**DL5**)$_3$] (**23**) and [Co-(**DL6**)$_3$] (**24**). All ligands and the complexes were characterized using FT-IR, UV-vis, ^{1}H and ^{13}C NMR, mass spectrometry and by elemental analysis. In addition, crystal structures of complexes **7**, **11**, **12**, **14**, **17**, **18**, **19**, **20**, **22** and **23** were determined and confirm the formation of neutral mononuclear species, in which the geometry around the Ni(II) and Cu(II) centres is distorted square planar while the geometry around the Co(III) centre is distorted octahedral. In these coordination structures, the Ni (II) and Cu(II) metal centres are each bound to four sulfur atoms from two dithiocarbamate ligands and the Co(III) centre is bound to six sulfur atoms from three dithiocarbamate ligands. All complexes showed moderate to good antibacterial activities against Gram-negative, *Salmonella typhimurium*, *Pseudomonas aeruginosa*, *Escherichia coli* and *Klebsiella pneumoniae* and Gram-positive, *Staphylococcus aureus* (methicillin resistant) and *Staphylococcus aureus* bacteria. Complexes **10**, **11**, **23** and **24** were found to be more active than ciprofloxacin against *E. coli* and *K. pneumoniae*. In addition, complexes with chloro-substituted ligands displayed higher activities. Antioxidant activities of the dithiocarbamate salts and their metal complexes were also carried out using DPPH and NO assay, respectively, and the complexes were found to be more efficient than the free ligands. The free radical

scavenging potential of complexes with symmetrical formamidine ligands was generally higher than for those with the unsymmetrical formamidine moieties. Notably, complexes **19** and **20** outperformed ascorbic acid with IC_{50} value of 9.93×10^{-4} mM and 2.84×10^{-4} mM, respectively. All the complexes also displayed moderate to good NO scavenging ability.

Keywords: N,N'-diarylformamidine; dithiocarbamates; metal complexes; antioxidant; antibacterial

4.1 Introduction

The increasing number of multi-drug resistant microbial pathogens and the emergence of new ones have presented recent challenges in the treatment of infectious diseases [1]. The presence of multiple intrinsic or acquired mechanisms of bacteria being resistant to antimicrobial agents makes controlling the spread of deadly microbes difficult [2] and for this reason, research on new drugs that can kill drug resistant bacteria is on the increase. Developing new drugs endowed with excellent antimicrobial activities, and particularly those whose mechanism of action is distinct from that of traditional antimicrobial agents to which relevant pathogens are now resistant, is very important [3]. In trying to combat the two issues, metal based antimicrobial agents are increasingly gaining prominence, with a variety of classes of ligands and their transition metals being tested [1, 4, 5].

Drugs serving multiple purposes is another study aspect. There are, for example, drugs preventing transmission of HIV-1 in women while simultaneously averting unintended pregnancies [6, 7]. Similarly, compounds with antimicrobial potential might also be explored as antioxidant agents. Research on antioxidant activity of both synthetic and natural compounds is driven by the health benefits that antioxidants have in protecting organisms and cells from damage induced by oxidative stress [8]. Oxidative stress is caused by the presence of reactive oxygen species (ROS), such as superoxide radical anion ($O_2^{\bullet-}$), hydroxyl radical ($OH^{\bullet}$), and hydrogen peroxide molecule (H_2O_2), which are often formed by the partial reduction of dioxygen (O_2) species [9]. The damage caused by ROS is normally to proteins, lipids and DNA, which can lead to accelerated ageing, cancerous inflammations, and cardiovascular or neurodegenerative diseases [9]. Various methods of analysis have been adopted to study antioxidant activity. One common example of an *in vitro* antioxidant test uses the scavenging activity of DPPH (2,2-diphenyl-1-picrylhydrazyl) assay as a stable free radical to evaluate both natural and synthetic compounds [10].

Dithiocarbamates and their metal complexes have been tested as anticancer [11, 12], antimicrobial [13, 14], and antioxidant agents [15, 16]. Dithiocarbamates are often synthesized by the reaction of either primary or secondary amines with carbon disulfide in the presence of a base, while their metal complexes are prepared via simple ligand displacement reactions following the addition of the dithiocarbamate salt to a metal precursor in the appropriate ratio [17-19]. Dithiocarbamates boast the ability to stabilize transition metals in various oxidation states [20] and in the process form complexes with transition and main group metals [12, 21, 22]. Our interest stems from the properties and structural architectures of the metal complexes, which can be tailored by varying substituents on the ligands sourced from secondary or primary amine [22].

Biological studies of Co(III), Ni(II) and Cu(II) dithiocarbamate complexes have been reported, but with few details [12, 23-25]. Mamba *et al.* [13] reported on *in vitro* antimicrobial studies of cyclohexylamine-N-dithiocarbamate transition metal complexes and their research showed that the antimicrobial activity of the free ligand was enhanced upon chelation with metal ions. In particular, their study showed that Ni(II) complexes displayed antimicrobial activity against *Pseudomonas aeruginosa* and *Staphylococcus aureus*. Antibacterial activities of 2-amino pyridine dithiocarbamate ligand and its Cu(II) and Co(II) complexes was also reported by Gopal *et al*. [26]. Their study showed that the complexes moderately inhibited the growth of *Escherichia coli*, *S. aureus* and *Bacillus subtilis*, with and the Cu(II) complex showing better activity than did the Co(II) complex. Recently, Onwudiwe *et al*. [15] reported on the antioxidant activity of sodium N-ethyl-N-phenyldithiocarbamate and its Cu(II) complexes. Their results showed that the complex had scavenging activity of 75% at 500 µg/ml relative to the ligand which showed 42 % ability at the same concentration.

In a contribution to the search for new compounds with excellent antibacterial and antioxidant properties, we herein report the synthesis, characterization, crystal structures and biological studies (antibacterial and antioxidant) of novel Co(III), Ni(II) and Cu(II) dithiocarbamate metal complexes using symmetrical and unsymmetrical formamidine as the secondary amine.

4.2 Result and discussion

4.2.1 Synthesis of Ni(II), Cu(II) and Co(III) N,N'diarylformamidine-dithiocarbamate complexes.

The synthesis routes for Ni(II) and Cu(II) N,N'-diarylformamidine dithiocarbamate metal complexes **7** – **18** are shown in **scheme 2.3,** while that for Co(III) complexes **19** – **24** are shown in **scheme 2.4**. Complexes **7** – **18** were obtained by the reaction of salts of potassium dithiocarbamates **DL1** – **DL6** with $NiCl_2.6H_2O$ or $CuCl_2.2H_2O$ in a 2:1 ratio, giving air stable purple or red solids for Ni(II) complexes and brown solids for Cu(II) complexes while complexes **19** – **24** were achieved by the reaction of **DL1** – **DL6** with $CoCl_2$ in 3:1 ratios to give air stable green solids. The complexes had decomposition temperatures of 265 – 305 °C; the specific decomposition temperature depending mainly on the substituents on the backbone of the dithiocarbamates. Decomposition temperature was observed to be higher among of the Ni(II) and Cu(II) complexes with symmetrical backbones than for their counterparts with unsymmetrical form. However, in cobalt complexes **19** – **24**, the unsymmetrical formamidine dithiocarbamate backbones were more thermally stable compared to their symmetrical counterparts. All complexes showed good solubility in benzene, toluene, tetrachloromethane, dichloromethane and chloroform, but were only partially soluble in other more polar solvents.

4.2.2 Spectroscopic studies

(i) *Nuclear magnetic resonance*

The ^{1}H NMR data for Ni(II) complexes **7 - 12** and the Co(III) complexes **19** – **24** were obtained in chloroform and peak assignments done using 2D NMR. The azomethine proton (NC(**H**)=N) was used to follow the successful synthesis of the Co(III) and Ni(II) complexes from potassium dithiocarbamates salts where an upfield shift from 9.86 – 10.39 ppm in the spectra of **DL1** – **DL6** to 8.81 – 9.10 ppm in the spectra of **7 - 12** and 8.82 – 9.20 ppm in the spectra of **19 – 24** (**Table 4.1**), which confirmed complexation. Other notable shifts were observed for the aliphatic protons. For example, the signal for the methyl protons (C**H$_3$**-Ar) in **DL1** appeared at 1.99 and 1.90 ppm but upon complexation, a downfield shift to 2.09 and 2.29 ppm in **7** and 2.18 ppm in **19** were observed in their respective spectra. This slight downfield shift in **7 – 12** and **19** – **24** implies the drift of the electron cloud towards the metal ion centre [27, 28]. Also, the peaks of the quaternary thiouride carbon atom (-N*C*S$_2$) in the ^{13}C-NMR spectra of **7 – 12** and **19 - 24** further confirmed complexation from **DL1** – **DL6,** and these were also generally

observed to shift upfield upon complexation (**Table 4.1**). This upfield shift is attributed to the delocalization of the electron cloud from the $–NCS_2$ moiety towards the metal centre, hence lowering the C=S bond strength [29-32].

Table 4.1: The $-NCS_2$ (^{13}C-NMR) and NC(H)=N (^{1}H-NMR) signals for **DL1 – DL6**, **7 – 12** and **19 – 24** and the IR bands of thiouride (C—N) and azomethine (C=N) for ligands and all the complexes **7 – 24.**

Ligands (Complex)	δ ($-NCS_2$) ppm	Δ δ	δ NC(H)=N ppm	Δ δ	υ(C=N) cm^{-1}	Δυ	υ(C—N) cm^{-1}	Δυ
DL1 (7)	217.62 (216.95)	0.69	9.86(8.85)	1.01	1640 (1647)	7	1467 (1472)	7
DL2 (8)	220.94 (206.98)	6.13	10.15(8.88)	1.27	1639 (1651)	12	1452 (1469)	8
DL3 (9)	218.95 (217.92)	1.84	9.92(8.81)	1.11	1629 (1644)	15	1477 (1479)	1
DL4 (10)	218.82 (219.32)	0.50	10.12(8.94)	1.18	1614 (1642)	28	1432 (1474)	3
DL5 (11)	217.02 (218.76)	1.74	10.13(9.10)	1.03	1603 (1639)	36	1430 (1469)	5
DL6 (12)	219.04 (219.49)	0.45	10.39(8.91)	1.48	1612 (1644)	32	1435 (1468)	1
DL1 (13)					1640 (1645)	5	1467 (1470)	3
DL2 (14)					1639 (1663)	24	1452 (1477)	25
DL3 (15)					1629 (1638)	9	1477 (1478)	1
DL4 (16)					1614 (1641)	27	1432 (1471)	39
DL5 (17)					1603 (1640)	37	1430 (1434)	4
DL6 (18)					1612 (1639)	27	1435 (1436)	1
DL1 (19)	217.62(212.97)	4.65			1640(16480	8	1467(1472)	7
DL2 (20)	220.94(214.81)	6.13			1639(1647)	8	1452(1469)	8
DL3 (21)	218.95(213.07)	5.88			1629(1646)	17	1477(1479)	1
DL4 (22)	218.82(213.94)	4.88			1614(1645)	31	1432(1474)	3
DL5 (23)	217.02(215.80)	1.22			1603(1646)	43	1430(1469)	5
DL6 (24)	219.04(213.92)	5.12			1612(1647)	35	1435(1468)	1

(ii) *FT-IR spectroscopy*

The infrared spectra for **7 - 24** exhibit three characteristic vibrational bands; the υ(C—S), υ(N—CS_2), and metal to sulfur bond (M—S) typical of dithiocarbamate complexes [21, 22, 31, 33-35] , and υ(C=Nstr).of the azomethine (C(H)=N) [36, 37]. In dithiocarbamate metal complexes, the υ(C—S) band appears around 950 – 1050 cm^{-1} and because a single peak in this region is typical of bidentate coordination [38], this band defines the bonding mode between the dithiocarbamate moiety and the metal centre. The spectra of all the metal complexes displayed a sharp peak around 999 – 1018 cm^{-1}. The υ(N—CS_2) thiouride band of

7 - 24 was observed at a higher frequency around 1434 - 1479 cm^{-1}, which differs from the results for the dithiocarbamate salts **DL1** – **DL6**, where it was observed around 1430 – 1477cm^{-1}. These values are intermediate of the stretching frequencies associated with C—N single bond (1250 – 1350 cm^{-1}) and C=N double bond (1640 – 1690 cm^{-1}). This is an indication of the partial double bond character of C—N (thiouride band) in **7 – 24**, and the shift to higher frequency in the complex compared to that of the ligand could be due to mesomeric drift of the electron from the dithiocarbamate moiety towards the metal coordination centre [39, 40]. In addition, a strong vibrational band appeared in the region of 1603 **–** 1640 cm^{-1} for all the dithiocarbamate ligands, and this can be associated with υ(C=Nstr).of azomethine in them. It was observed to shift towards higher vibrational frequencies for all the complexes, see **Table 4.1**. The observed shifts could be attributed to an increase in π-electron density in C=Nstr upon coordination, causing the C=N bond vibration at higher frequency. This also confirms that the nitrogen atom in the dithiocarbamate ligand does not coordinate with the metal centre [41-43]. The spectra of the compounds **7 - 24** also show a band in the far infra-red region at 350 **–** 420 cm^{-1}, which can be assigned to the υ(M—S) bond [44].

(iii) *UV-Vis Spectroscopy*

The electronic absorption spectra of the dithiocarbamate ligands and the metal complexes were recorded in DMSO and chloroform, respectively. The UV-Visible spectra of all the ligands **DL1** – **DL6**, and the complexes **7** to **18** are given in Figures **4.1a** – **4.1c**. Generally, transition due to the ligands appeared in the UV region while the d–d transition appeared in the visible region [15]. The spectra of the ligands **DL1 – DL6** showed two absorption bands in the UV region for 289 – 300 nm and for 338 – 345 nm. These absorption bands are assigned to intraligand π→π* associated with an N-C=S group and the π→π* transition within the S-C=S group [45]. In each of the spectra, three absorption bands are observed for the Ni(II) complexes **7** – **12:** 258 – 263 nm, 340 – 343 nm, and 454 – 467 nm. The band between 454 nm and 467 nm can be attributed to a d-d transition while those below 400 nm are assigned to intra-ligand π→π* associated with N-C=S and S-C=S groups of the dithiocarbamate ligand backbone. For the Cu(II) complexes **13** – **18**, two major absorption bands are observed for 300 – 301 nm and 442 – 449 nm.. Highly-intense bands were observed within the range 442 – 449 nm, which were assigned to d-d transitions [21]. There is a possibility of three observable bands in the spectra of **13** – **18** as a shoulder is observed in each, suggesting an overlap of two bands.

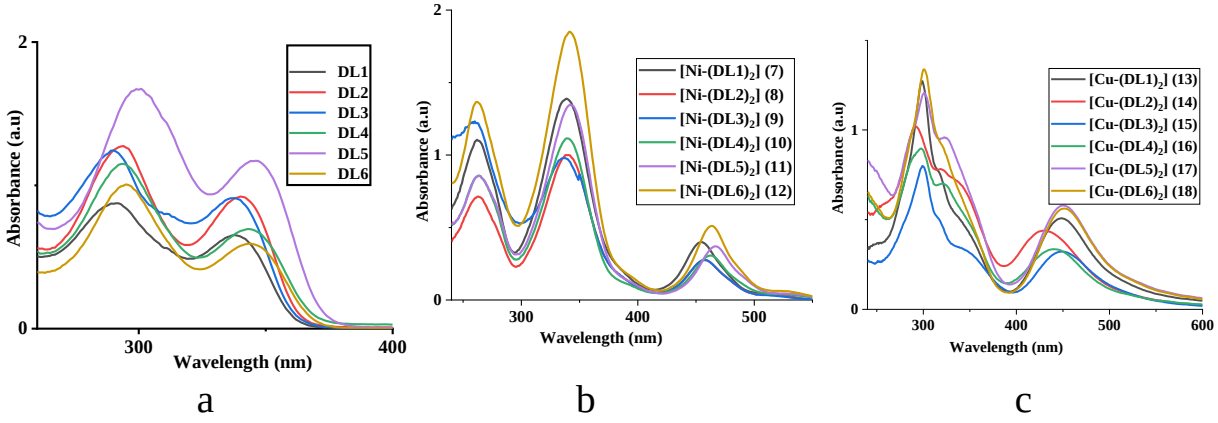

a b c

Figure 4.1: (a): Electronic absorption of **DL1** – **DL6** (b) Electronic absorption spectra of **7** – **12** (c) Electronic absorption spectra of **13 - 18**

A different pattern emerged for the cobalt complexes, **19** – **24,** with five absorption bands being observed in the electronic spectra of each, as seen in Figure **4.2**, for 275 – 278 nm, 305 – 313, 385 – 389, 482 – 494 nm and 618 – 631 nm. The low intensity broad bands around 482 nm and 631 nm are assigned to d—d transition, consistent with the literature [46-48]. Other high-energy absorption bands which appeared around 275 nm, 305 nm and 389 nm are assigned to intraligand charge transfer transitions. Comparing the information from the electronic spectra of **19 – 24** with those ones readily available for $Co(dtc)_3$ [34, 49] suggests an octahedral geometry around their coordination metal centre.

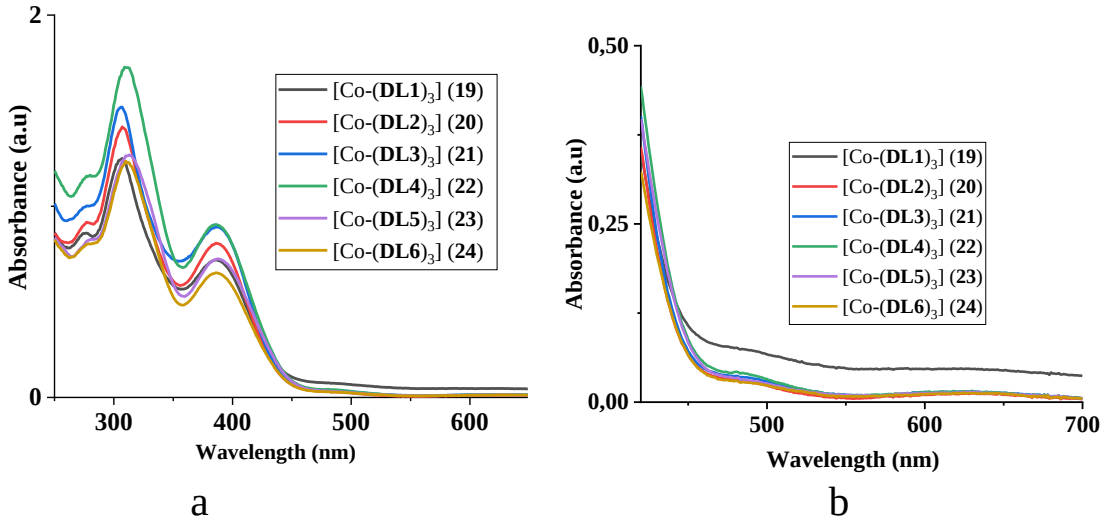

a b

Figure 4.2: (a) Electronic absorption spectra of **19** – **24** (b): Electronic absorption spectra of **19** – **24** showing the broad region of d-d transition.

4.3 X-ray structural analysis

(i) *Ni(II) and Cu(II) complexes*

Suitable crystals for single crystal X-ray diffraction analysis were obtained for complexes **7**, **11**, **12**, **14, 17** and **18** by slow evaporation; crystals of **7**, **14, 17** and **18** were obtained from their solution of toluene, while those of **11** and **12** were obtained from dichloromethane solutions. The molecular structures are given in Figures **4.3 – 4.8,** and selected bond lengths and angles in **Table 4.2**. For complex **7**, the solvent mask was calculated and 48.7 electrons was found in a void with a volume of 203.0 $Å^3$, consistent with the presence of a single $C_6H_5CH_3$ per formula unit, which account for 48.7 electrons. The solvent molecule for complex **7** was toluene, and it was highly disordered. Attempts to model it were unsuccessful and only led to unstable refinement, and it was therefore omitted using the *SQUEZE* [50] option in *PLATON* [51]. The carbon atom of the DCM molecule in complex **11** was also found to be disordered over 2 positions, with the major component having 53.80% site occupancy, while toluene molecules in compound **17** was found to be disordered over an inversion centre and was modelled using PART -1 instruction with a fixed site occupancy factor of 0.5.

Complexes **7, 12, 14** and **18** contain half a molecule of the complex in their asymmetric units while **11** and **17** contain half a molecule together with the solvent in which they were grown; that is dichloromethane and toluene molecules for **11** and **17,** respectively. The structures of both sets of complexes consist of a mononuclear neutral species in which the metal centres, Ni(II) and Cu(II), are coordinated by two pairs of sulfur atoms from two bidentate dithiocarbamate ligands in a distorted square planar geometry fashion around the metal centre. For **7**, **11**, **12**, **14**, **17** and **18,** respectively, the S—M—S bond angles are 79.441(18)°, 79.402(18)°, 79.43°, 76.77(5)°, 77.333(3)° and 77.54°; all of which are smaller than the ideal 90° for square planar geometry. The strained S—C—S angles of all the complexes contribute to the deviation from ideal square planar geometry. In the structures of **7**, **11** and **12**, the Ni—S bond lengths range from 2.2003(5) Å to 2.2090(5) Å while in **14**, **17** and **18** the Cu—S bond lengths range between 2.2597(15) Å and 2.3282(7) Å as seen in **Table 4.2**. These values are consistent with the values reported with mononuclear bis dithiocarbamate complexes [23]. The M—S bond lengths seem not to be influenced much by the electrons of the CS_2 backbone. As expected, the Cu—S bond lengths of **14, 17** and **18** are greater than those for the Ni—S bond of complexes **7, 11** and **12**. The C—S bond lengths seem not to favour single or double bond character in any of the named complexes. They are shorter than the typical single C—S bond

length of 1.82 Å but longer than the C=S double bond length of 1.67 Å [32]. This is an indication of delocalization of electrons along the S—C—S moiety in the complexes. [52]. Also, the C—N bond length in the -NCS_2 moiety of the complexes deviates from the reported value for a single C—N bond, which is 1.47 Å. For complex **7**, C(10)—(N)2 = 1.344(2) Å, C(1)—N(2) = 1.358(2) Å for complex **11**, C(1W)—N(1) = 1.344(7) Å for complex **14** and C(10)—(N)2 = 1.362(4) Å for complex **17**. This indicates the delocalization of π- electrons over the entire S_2CN fragment in the complexes [21].

Table 4.2: Selected bond length (Å) and angles (°) for complexes **7**, **11**, **12**, **14**, **17** and **18**

Parameters	**7**	**11**	**12**	**14**	**17**	**18**
Bond lengths						
M—S	2.2003(5)	2.2023(5)	2.2012	2.2597(15)	2.2643(8)	2.3005
M—S	2.2090(5)	2.2045(3)	2.2055	2.3057(13)	2.3282(7)	2.3183
C—S	1.698(2)	1.696(2)	1.689(2)	1.695(5)	1.688(3)	1.696(2)
C—S	1.711(2)	1.709(2)	1.705(2)	1.731(5)	1.706(3)	1.709(2)
C—N	1.344(2)	1.358(2)	1.354(2)	1.344(7)	1.362(4)	1.398(2)
Bond angles						
S—M—S	79.4421(18)	79.402(18)	79.43	76.77(5)	77.33(3)	77.54
S—C—S	111.50(11)	111.53(11)	112.1(1)	111.70(3)	115.47(17)	116.3(1)

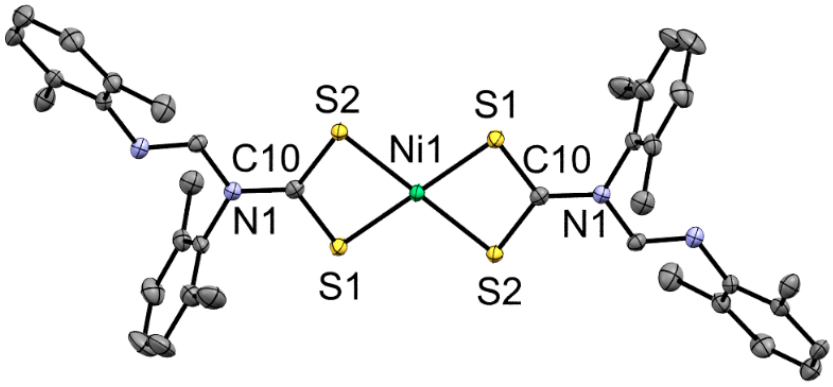

Figure 4.3: ORTEP diagram for complex **7** drawn at 50 % thermal ellipsoids probability. Hydrogen atoms have been omitted for clarity.

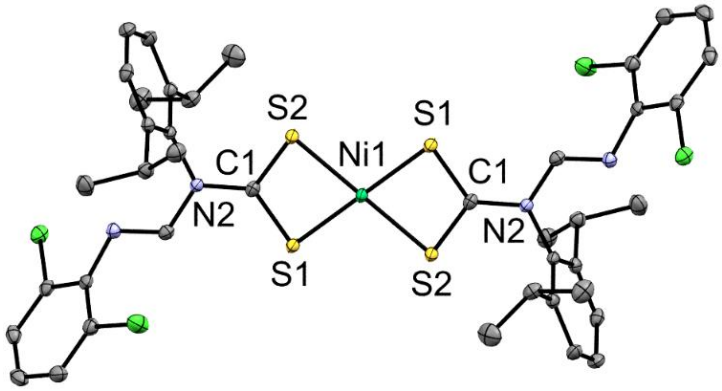

Figure 4.4: ORTEP diagram for complex **11** drawn at 50 % thermal ellipsoids probability. Hydrogen atoms have been omitted for clarity.

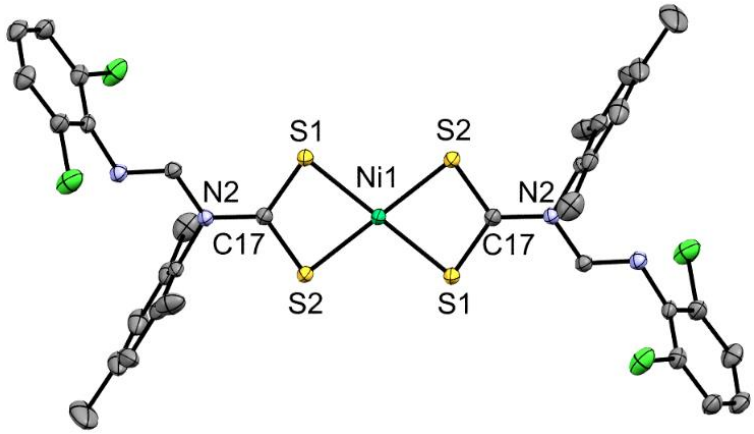

Figure 4.5: ORTEP diagram for complex **12** drawn at 50 % thermal ellipsoids probability. Hydrogen atoms have been omitted for clarity.

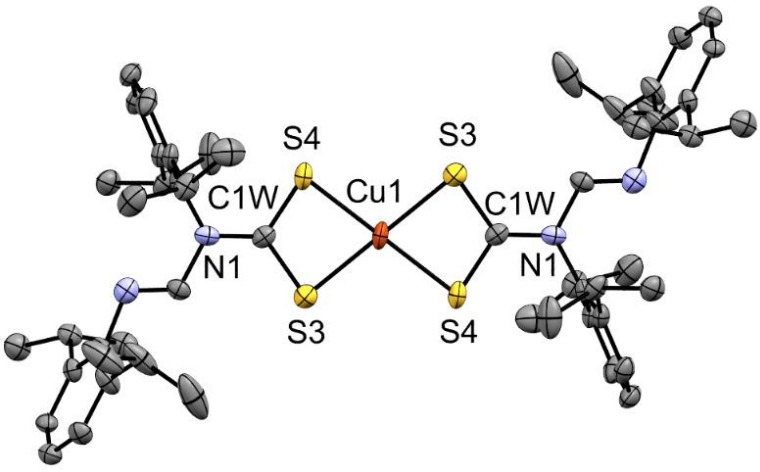

Figure 4.6: ORTEP diagram for complex **14** drawn at 50 % thermal ellipsoids probability. Hydrogen atoms have been omitted for clarity.

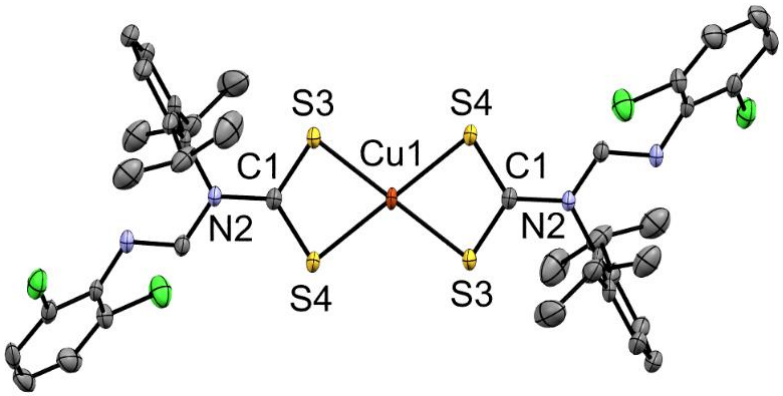

Figure 4.7: ORTEP diagram for complex **17** drawn at 50 % thermal ellipsoids probability. Hydrogen atoms have been omitted for clarity.

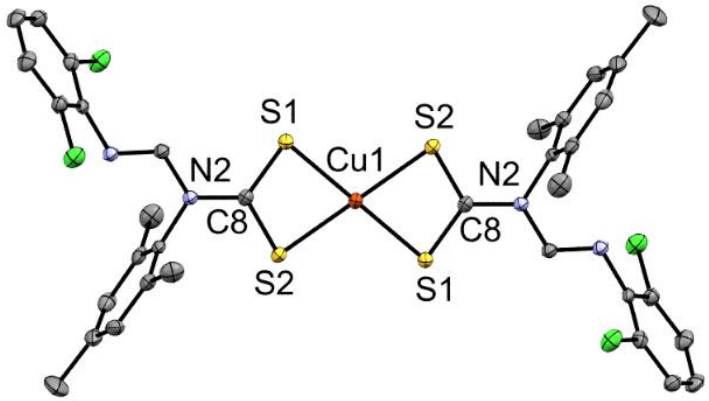

Figure 4.8: ORTEP diagram for complex **18** drawn at 50 % thermal ellipsoids probability. Hydrogen atoms have been omitted for clarity.

(ii) *Cobalt (III) complexes*

For the cobalt complexes, suitable crystals for single X-ray structural analysis were obtained by slow evaporation from a dichloromethane solution for complexes **19a**, **19b**, **20** and **23**, and by vapor diffusion of hexane into the solution of complex **22** in dichloromethane. The molecular structures are given in Figures **4.9** – **4.11,** while selected bond lengths and angles are listed in **Table 4.4**. The asymmetric units of **20**, **22** and **23** each contains a whole molecule of the cobalt dithiocarbamate complex, while that of **19a** has only one-third of the cobalt complex and **19b** has one-third of the cobalt complex together with one molecule of dichloromethane. Complexes **19a** and **19b** are pseudomorphs, as a result of dichloromethane molecule present in **19b** which was not present in **19a**. All five complexes are mononuclear with the Co(III) centre coordinated to six sulfur atoms from three dithiocarbamate ligands, the

ligands coordinating in a bidentate fashion. In that manner, three four-member CS_2Co chelate rings are formed, each with a bite angle of 76.69(17) – 76.97 (17)° (**Table 4.4**). The bite angles around the metal centre show deviation from those of an ideal octahedral geometry [53]. The Co—S bond lengths are non-exceptional and are comparable to those reported in the literature for similar structures, such as $Co(nPr_2dtc)_3$ [54]. As observed in the Ni(II) and Cu(II) complexes, the C—S bond lengths in the cobalt complexes also fall between those for the ideal single or double C—S bonds, indicating partial delocalization of π-electron density over the entire S_2CN fragments [21]. The delocalization is also extended to the C—N bond of the S_2CN fragment in the complexes, similar to what has been reported in the literature [55].

Table 4.3: Selected bond length and angles for complex**es 19a, 19b, 20, 22 and 23**

	19	**19b**	**20**	**22**	**23**
Bond distances					
Co—S(1) (Å)	2.2581(6)	2.2564	2.2642(5)	2.2602(7)	2.2609(5)
Co—S(2) (Å)	2.2581(6)	2.2628	2.2747(5)	2.2708(7)	2.2655(5)
Co—S(3) (Å)	2.2582(6)	2.2564	2.2293(5)	2.2595(9)	2.2510(5)
Co—S(4) (A)	2.2621(6)	2.2628	2.2586(5)	2.2612(7)	2.2802(5)
Co—S(5) (Å)	2.2622(6)	2.2564	2.2414(5)	2.2418(8)	2.2489(5)
Co—S(6) (Å)	2.2621(6)	2.2628	2.2508(5)	2.2764(9)	2.2707(5)
Bond angles					
S(1) - Co(1) - S(2) (°)	76.726(18)	76.81	76.974(17)	76.91(2)	76.761(6)
S(3) - Co(1) - S(4) (°)	76.726(18)	76.81	76.807(17)	76.87(3)	76.758(19)
S(5) - Co(1) - S(6) (°)	76.728(18)	76.81	76.685(17)	76.88(2)	76.691(18)

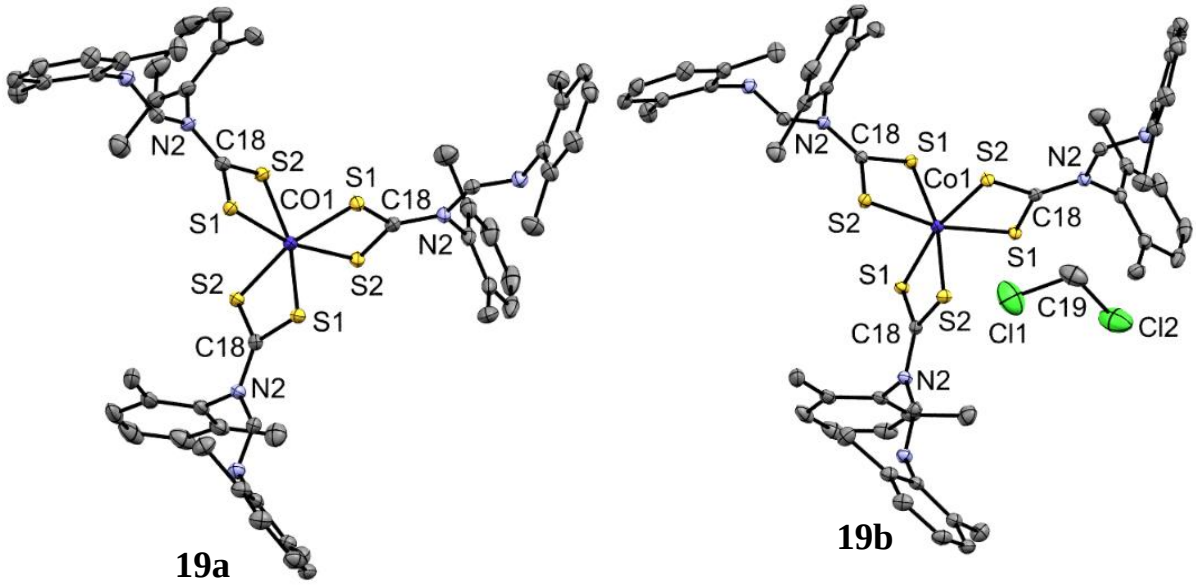

Figure 4.9: ORTEP diagram for complexes **19a and 19b** drawn at 50 % thermal ellipsoids probability. Hydrogen atoms have been omitted for clarity.

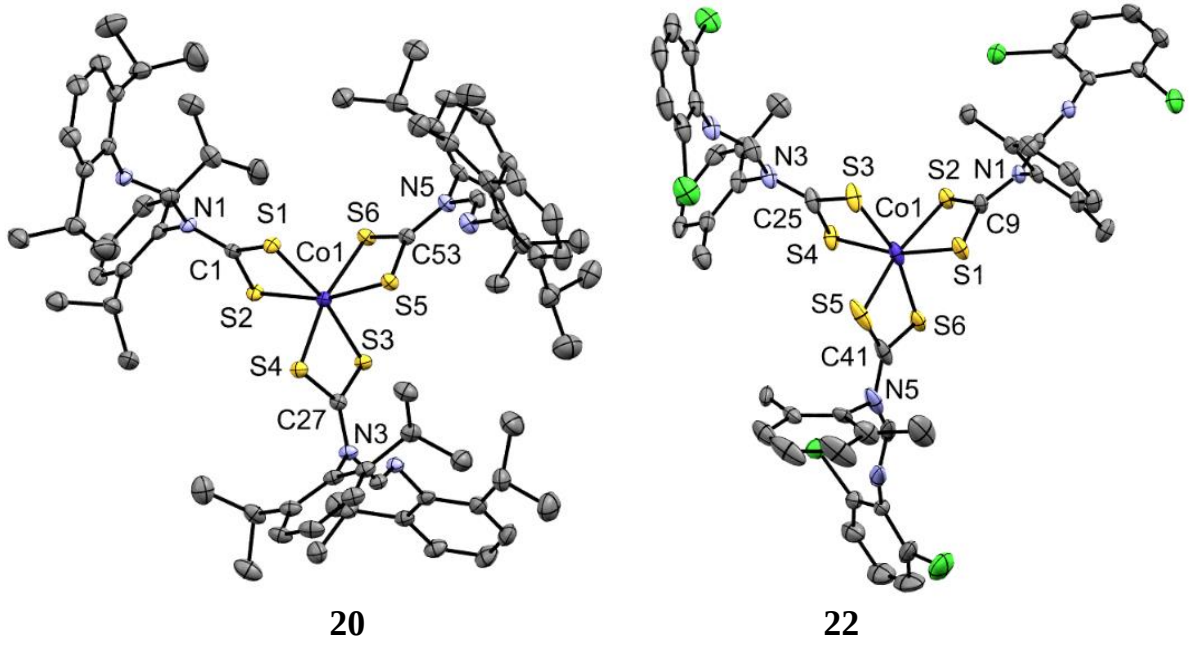

Figure 4.10: ORTEP diagram for complexes **20** and **22** drawn at 50 % thermal ellipsoids probability. Hydrogen atoms have been omitted for clarity.

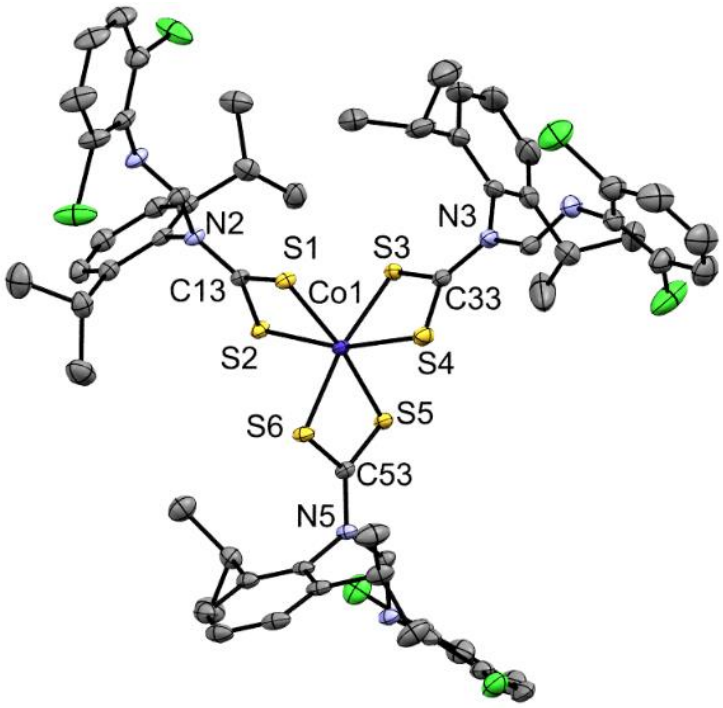

Figure 4.11: ORTEP diagram for complex **23** drawn at 50 % thermal ellipsoids probability. Hydrogen atoms have been omitted for clarity.

4.4 Antimicrobial studies

When designing new compounds to be used as antimicrobial agents, it is desirable for them to be highly capable of killing pathogens, without any negative side effects when used for treatment [56]. Research literature has it that the chelation of ligands with metal ions can, in some instances, increase the ligands' biological activities [25, 57, 58]. This can be explained in terms of chelation theory [59]. One attribute of chelation is that it increases the lipophilic character of the metal chelate, which leads to the greater permeability of complexes through lipid layers of cell membranes. In this study, we observed a similar phenomenon where the metal complexes formed showed enhanced biological activities compared to the free ligands. It may be suggested that the antimicrobial property of these complexes arises either from their deactivating various cellular enzymes with crucial roles in various metabolic pathways of these organisms, or by their denaturing one or more proteins of the cell, which then disrupts normal cellular processes [60]. The results for antimicrobial activities of the Ni(II) complexes **7** – **12**, Cu(II) complexes **13** – **18** and Co(III) complexes **19 - 24** are presented in **Table 4.4**. The activity of these compounds was evaluated against six different types of bacteria; namely, *Staphylococcus aureus*, *Staphylococcus aureus* (methicillin resistant) (MSRA), *Klebsiella pneumoniae*, *Salmonella typhimurium*, *Pseudomonas aeruginosa*, and *Escherichia coli* while

using ciprofloxacin as a reference drug. The MIC values were used to evaluate their antibacterial activity and results were compared with the standard. Lower MIC values indicate a higher antibacterial potential [61-64]. The results based on the MICs shown in **Table 4.4** show that the free ligands exhibited inferior antimicrobial activities against the six bacteria strains when compared to ciprofloxacin, with the exception of **DL3** and **DL5,** which are more active against *Klebsiella pneumoniae* than ciprofloxacin. In contrast to the parent ligands, the complexes show moderate to excellent antimicrobial activity compared with the reference drug, most especially towards Gram-negative bacteria.

Complexes **7**, **10**, **11**, **13**, **16**, **23** and **25** showed better activity against *E. coli* than did free ligands. And, moreover, this activity was even better than shown by the standard ciprofloxacin. The antimicrobial activities of complexes with the symmetrically substituted formamidines, **7 – 9**, **13 – 15** and **19 - 21** were less active compared to those with unsymmetrically substituted formamidine **10 – 12**, **16 – 18**, and **22 - 24** (form). For example, when tested against *E. coli*, the MICs of **7**, **8** and **9** were 0.10 ug/ml, 6.25 ug/ml and 1.6 ug/ml, respectively, while those of **10**, **11** and **12** were 0.025 ug/ml, 0.10 ug/ml and 0.20 ug/ml, respectively (**Table 4.4**). This increased activity in complexes which the formamidine bore an electron withdrawing group (Cl in this instance) can be attributed to better lipophilicity, which allowed easier penetration into the lipophilic section of the cell membrane or lipophilic domains of proteins [65]. A similar trend was observed with the other bacterial strains. The chlorine atoms in Cl-substituted complexes could also help in the fixation of an active molecular conformation, which is necessary for interaction with the protein in the bacteria [66]. While most complexes displayed moderate activities against *S. typhimurium*, **12**, **16**, **23** and **24** showed higher activities compared to the other complexes and ciprofloxacin. The varying degrees of activity of the complexes against *E. coli*, *S. typhimurium* and other bacterial strains could be due to the nature of the metal ion electronic configuration of the complexes, as well as the nature of the cell membrane of each bacteria strain, which determines the permeability of the complexes or the difference in ribosome of the microbial cell [67, 68].

Complexes **14**, **17**, **18**. **21**, **22** and **23** showed better activity against *P. aeruginosa* relative to both the other complexes and to ciprofloxacin. The Cu(II) complex **13** exhibited least activity against *P. aeruginosa* with MIC value of 100 µg/mL, while the Co(III) and Cu(II) complexes **23** and **17**, respectively, displayed the highest activities with MIC value of 0.20 µg/mL. All the complexes showed better activity against *K. pneumonia* relative to ciprofloxacin, except for complexes **7**, **13**, **15**, **16** and **18**. The Cu(II) complexes **14** and **17** together with the Co(III)

complex **23** displayed notably excellent activities, with MIC value as low as 0.00625, which indicates their suitability for clinical trials as an antimicrobial drug against diseases caused by *K. pneumonia*.

It must be noted, however, that all the complexes were inactive against MRSA apart from complexes **10**, **11** and **12,** which were active only at the highest concentration (1000 µg/mL). The failure of the complexes to inhibit MRSA could be due to their inability to penetrate through the bacteria cell wall or the complexes might have been modified or rendered inactive as they entered the cell wall of the MRSA [69]. When comparing activity against *S. aureus,* with the activity against MSRA, all the Cu(II) complexes showed better activity, excluding complex **17,** while all Ni(II) complexes displayed moderate to low activity against it. The cobalt (III) complexes **19** – **24** only displayed activity against *S aureus* at high concentrations (100—1000µg/mL).

Table 4.4: Minimum inhibitory concentration of the Ni (II) complexes (**7-12**), Cu(II) complexes (**13** – **18**) and Co(III) complexes (**19** – **24**) (µg/mL).

	Gram (-) bacteria				**Gram (+) bacteria**	
Complexes	*E. coli*	*S. typhimurium*	*P. aeruginosa*	*K. pneumoniae*	*S. aureus*	MRSA
Ni (II), Cu (II) and Co(III) complexes of symmetrical N,N'-diarylformamidine dithiocarbamate						
7	0.10	100	50	6.25	1000	NA
8	6.25	100	6.25	0.20	1000	NA
9	1.6	50	1.60	0.20	1000	NA
13	0.05	0.80	100	6.25	0.80	NA
14	100	0.40	0.40	0.00625	1.60	NA
15	12.5	1.60	12.5	3.125	0.80	NA
19	12.5	1000	3.125	0.20	1000	NA
20	0.80	1000	12.5	0.025	1000	NA
21	1.60	1.60	3.125	1.60	1000	NA
Ni (II), Cu (II) and Co(III) complexes of unsymmetrical N,N'-diarylformamidine dithiocarbamate						
10	0.025	12.5	1.60	0.20	1000	1000
11	0.10	1.6	6.25	0.20	6.25	1000
12	0.20	0.2	3.125	0.10	50	1000
16	0.025	0.20	1.60	3.125	1.60	NA
17	3.125	0.40	0.20	0.00625	1000	NA
18	0.80	1.60	0.40	1.60	0.025	NA

22	3.125	6.25	0.20	0.80	1000	NA
23	0.025	0.20	0.40	0.00625	100	NA
24	0.10	0.05	0.40	0.10	100	NA
Ciprofloxacin[a]	0.20	0.40	0.80	1.60	25	25

NA = No activity, a = standard

4.5 Antioxidant studies

4.5.1 DPPH Radical scavenging ability

The free radical 2,2-Diphenyl-1-picrylhydrazyl (DPPH) is stable and has an odd number of electrons in its structure [70]. It is usually used for the evaluation of radical scavenging activity because it gives results in a relatively shorter time than do other methods [71]. The ability of antioxidant molecules to scavenge the DPPH radical is due to their hydrogen or electron radical donating capability [72]. We have used DPPH radical scavenging assay for the screening of the antioxidant activity of the Co(III), Ni(II) and Cu(II) dithiocarbamate metal complexes at different concentrations. The antioxidant activity of dithiocarbamates as well as their metal complexes may be explained by the electron donating ability of sulfur and the central metal ions in their various complexes, which lead to free radical stabilization [73]. It has been reported that the presence of the central metal increases the antioxidant activity of the ligand, since the ligand's proton donor capacity is enhanced [8, 74]. The DPPH radical is purple in colour and the odd number of electron electron in its radical gives a strong absorption maximum at 517 nm. The colour turns from purple to yellow when the odd electron of the DPPH radical becomes paired with hydrogen from free radical scavenging antioxidants to form reduced DPP-H [10, 75].

The percentage free radical scavenging ability values were used to calculate the IC_{50} values of complexes **7 - 24** and these are summarized in **Table 4.5**. Results were compared with the antioxidant activity of ascorbic acid (with IC_{50} value of 1.01×10^{-3} mM). The IC_{50} values were used to determine the antioxidant activity, where the lower the IC_{50} value the higher will be the antioxidant activity [76, 77]. The Co(III) complex **20** has the lowest IC_{50} value and therefore the highest antioxidant activity, while Cu(II) complex **18** has the highest IC_{50} value with the least antioxidant activity. The IC_{50} values of complex **19** and **20** are less than that of ascorbic acid, suggesting that, they are better antioxidants than is ascorbic acid. Complexes **7**, **8, 9 13, 14 21**, **22** and **24** also have high value of ascorbic acid equivalent antioxidant capacity

(AEAC),as shown in **Table 4.5**. On the other hand, complexes **12**, **16** and **18** displayed weak antioxidant activity.

The radical scavenging activities of complexes **7 – 9**, **13 – 15** and **19 – 21,** which are rich in electrons due to electron-donating substituents, seem to be better than the activities of the complexes **10 – 12**, **16 – 18** and **22 – 24,** which have an electron withdrawing group. For example, complexes **7**, **8** and **9** have higher activities compared to **10**, **11** and **12,** as seen in **Table 4.5**. A trend was also observed in Cu(II) and Co(III) complexes. It has been shown previously [78, 79] that electronics play a crucial role in enhancing free radical scavenging activity. In **7 – 9**, **13 – 15** and **19 – 21** the presence of an electron donating group increases the electron density at the carbon atoms in the aromatic rings of the complexes; hence, increasing their electron donating capability, which, in turn, leads to their higher antioxidant activity relative to **10 – 12**, **16 – 18** and **22 – 24**, which have electron withdrawing groups. Generally, the antioxidant activity of **7 – 24** increases as the concentration increases and this is illustrated in **Figures 4.11**, **4.12** and **4.13**.

Table 4 5 : Antioxidant potential of tested compounds at different concentrations using DPPH assay.

Complexes	IC_{50} (mM)
7	6.59×10^{-3}
8	1.10×10^{-3}
9	2.99×10^{-3}
10	7.12×10^{-2}
11	1.21
12	1.85
13	1.65×10^{-3}
14	4.50×10^{-3}
15	1.60×10^{-1}
16	2.16
17	1.383
18	2.91
19	9.93×10^{-4}
20	2.84×10^{-4}

21	1.61×10^{-3}
22	8.08×10^{-3}
23	4.71×10^{-2}
24	7.39×10^{-3}
Ascorbic acid	1.04×10^{-3}

Result presented here are the mean values from three independent experiments

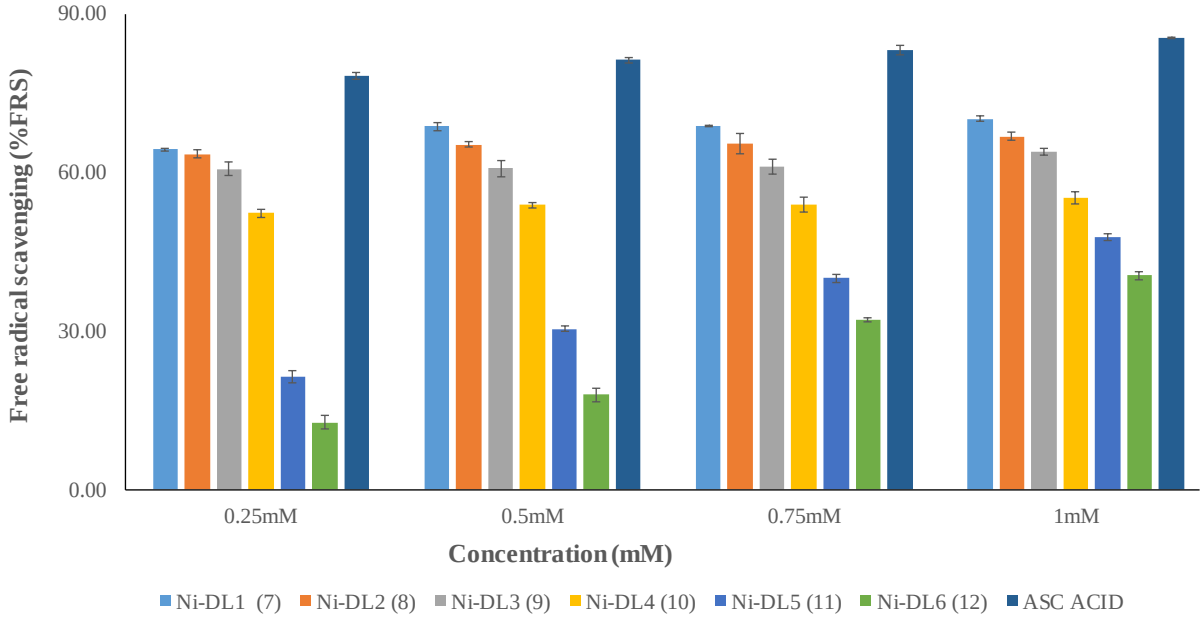

Figure 4.12: % Free radical scavenging vs concentration (mM) of Ni((II) dithiocarbamate metal complexes **7 - 12**

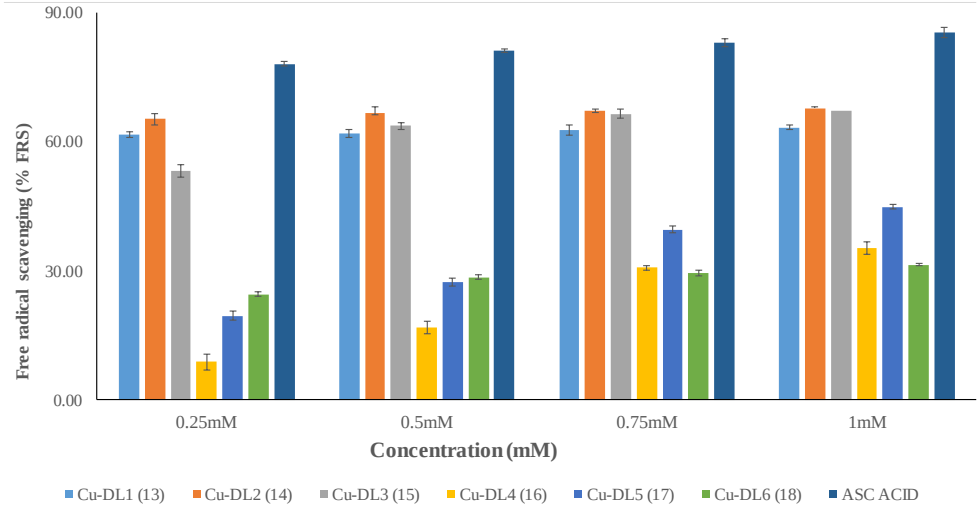

Figure 4.13: % Free radical scavenging vs concentration (mM) of Cu((II) dithiocarbamate metal complexes **13 - 18**

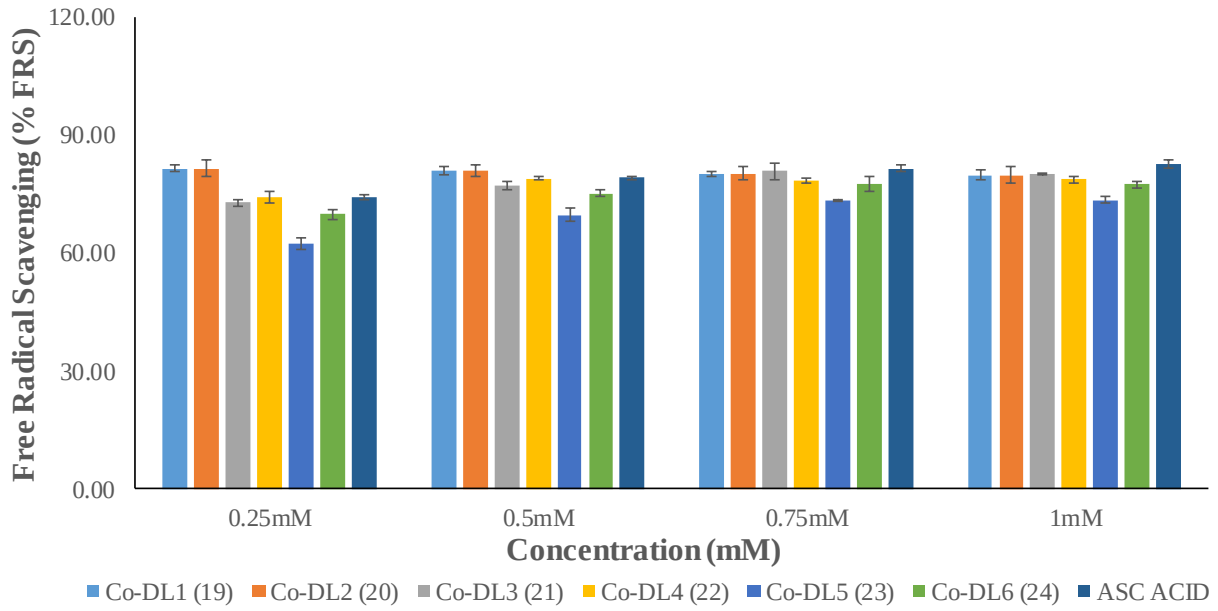

Figure 4.14: % Free radical scavenging vs concentration (mM) of Co(III) dithiocarbamate metal complexes **19 - 24** .

4.5.2 NO Radical scavenging assays

Nitric oxide radical (NO•) is a small molecule that contains one unpaired electron on the antibonding 2π*y orbital [80]. Specific nitric oxide synthases (NOSs) generate nitric oxide radicals (NO•) in biological tissues, which takes place during the metabolism of arginine to citrulline with the aid of five-electron oxidation reaction [81]. The radical NO• plays an important physiological role in processes such as smooth muscle relaxation, defense mechanisms, blood pressure regulation, immune response regulation and neurotransmission [82]. However, overproduction of NO• in the body leads to nitrosylation reactions, which tend to inhibit the normal functions of proteins and even damage them, so its concentration should be regulated in body systems [83].

DTC metal complexes, most especially Fe(II) and Fe(III) of different dithiocarbamate ligands, have been established as good NO-trapping agent [84]. Both complexes form a stable Fe(II)(NO)$(DTC)_2$ when reacted with NO. However, the use of other dithiocarbamate metal complexes is seldom reported. Here, we studied the potential of N,N'-diarylformamidine dithiocarbamates of Ni(II) **7** – **12**, Cu(II) **13** – **18** and Co(III) **19** – **24** as NO trapping agents. The percentage NO radical scavenging ability values were used to calculate the IC_{50} values of complexes **7-24** and reults were compared with the NO scavenging ability of ascorbic acid (with IC_{50} value of 0.23 mM). These are summarized in **Table 4.6**. Potassium dithiocarbamate

salts **DL1** – **DL6** have extremely high IC_{50} values, which indicate their poor NO scavenging ability.

However, the NO scavenging ability increases upon coordination with metal ions, as shown in **Table 4.6**. Complex **20** has the lowest IC_{50} value of 0.27 mM, and has the highest value of ascorbic acid equivalent antioxidant capacity (AEAC), followed by **15**, **13**, **19** and **18,** respectively, On the other hand, complexes **10**, **16**, **17**, **23** and **24** displayed weak NO scavenging ability. The effect of substituents on the dithiocarbamate backbone on the metal complexes seems to have no pronounced effect on their NO scavenging activities. The NO scavenging ability of **7 - 24** increases as the concentration increases and this is illustrated in **Figures 4.14**, **4.15** and **4.16**.

Table 4 6: Antioxidant potential of tested compounds at different concentration using nitric oxide (NO) assay.

Complexes	IC_{50} (mM)
DL1	>10
DL2	>10
DL3	>10
DL4	>10
DL5	>10
DL6	>10
7	1.04
8	0.78
9	2.79
10	6.40
11	1.29
12	>10
13	0.42
14	0.82
15	0.38
16	4.32
17	3.27
18	0.89

19	0.73
20	0.27
21	1.60
22	>10
23	3.38
24	2.11
Ascorbic acid	0.23

Result presented here are the mean values from three independent experiments

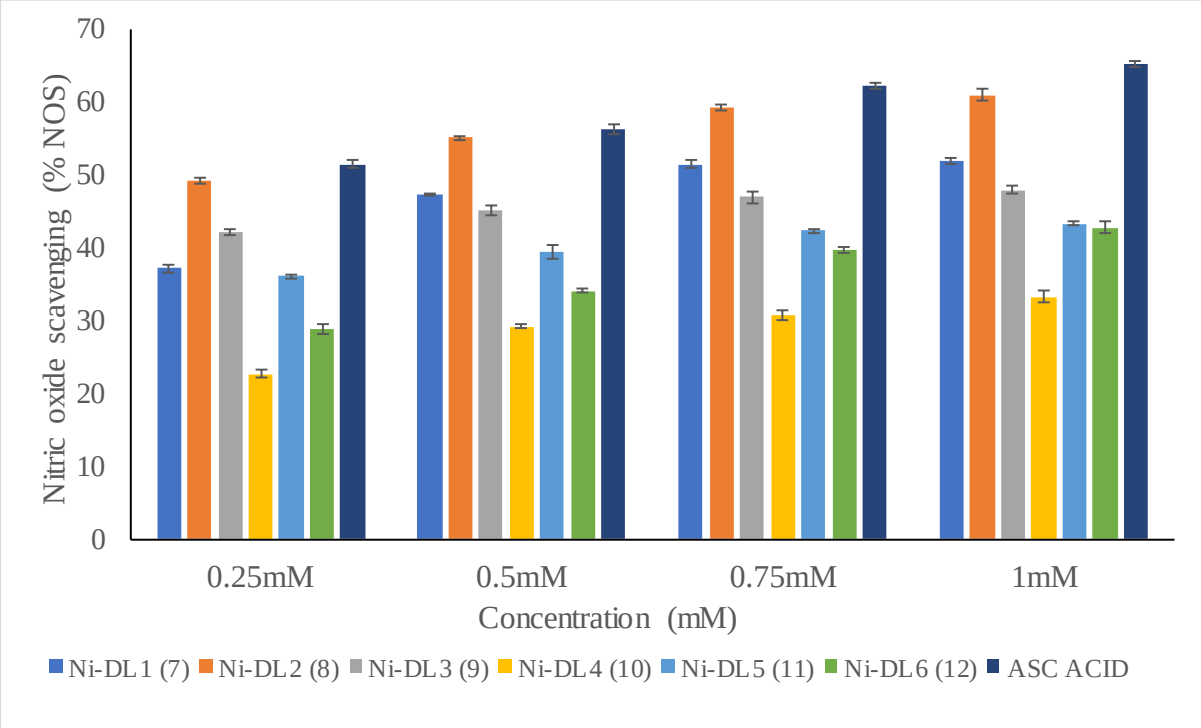

Figure 4.15: % NO radical scavenging vs concentration (mM) of Ni(II) dithiocarbamate metal complexes **7 - 12**

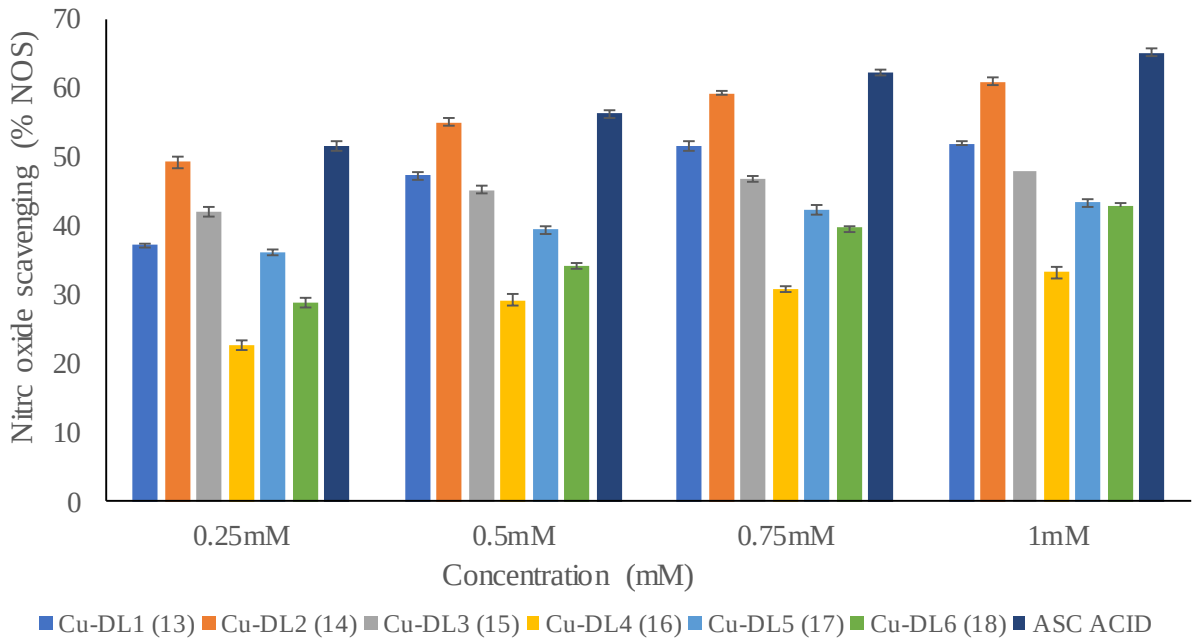

Figure 4.16: % NO radical scavenging vs concentration (mM) of Ni(II) dithiocarbamate metal complexes **13 - 18**

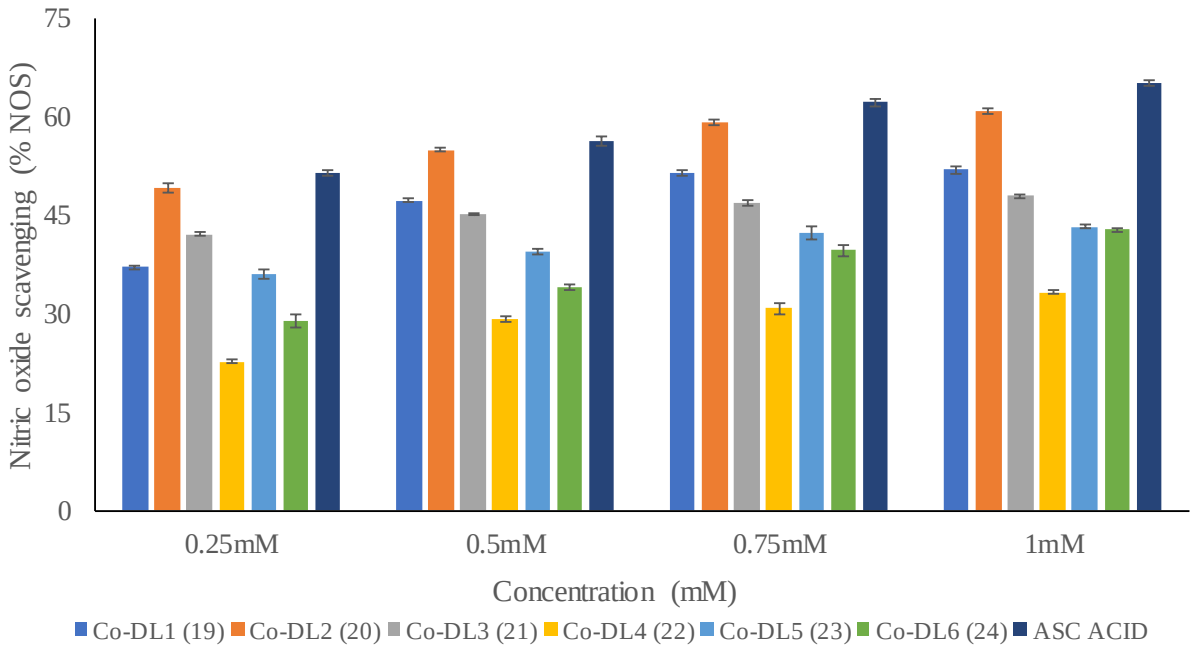

Figure 4.17: % NO radical scavenging vs concentration (mM) of Ni(II) dithiocarbamate metal complexes **19 - 24**

Conclusion

Eighteen Co(III), Ni(II) and Cu(II) complexes of symmetrical and unsymmetrical formamidine-based dithiocarbamate ligands were synthesized and fully characterized by UV-Visible, FT-IR, NMR and Mass spectrometry. X-ray crystal structures of complexes **7**, **11**, **12**, **14**, **17**, **18**, **19**, **20**, **22** and **23** were determined and these confirm the formation of neutral mononuclear species, in which the geometry around Ni(II) and Cu(II) centres is distorted square planar, while the geometry around the Co(III) centre is distorted octahedral. The antibacterial potential of **DL1** – **DL6** increases upon coordination to Co(III), Ni(II) and Cu(II) salts. The MIC values for all the complexes showed that they all had moderate to good antimicrobial activities against all the bacteria strains, except MRSA and *S. aureus*. The presence of chlorine atoms in complexes with unsymmetrical formamidine-based dithiocarbamate ligands enhanced their antibacterial activity, thus showing better activities compared to their symmetrical counterparts. Complexes **10**, **11**, **23** and **24** were found to be more active than ciprofloxacin against *E. coli* and *K. pneumoniae*. All the complexes showed good scavenging activity against NO and the free radical of DPPH compared to their parent ligands, with compounds **19** and **20** having a better antioxidant activity compared to ascorbic acid in terms of free radical scavenging ability.

References

1. M. Rizzotto, in *A search for antibacterial agents*, InTechopen, **2012**, chapter 5.
2. A. Coates, Y. Hu, R. Bax and C. Page, *Nature Reviews Drug Discovery*, **2002**, 1, 895-910.
3. S. K. Verma and V. K. Singh, *RSC Advances*, **2015**, 5, 53036-53046.
4. P. Sadler, *Journal of Inorganic Biochemistry*, **1997**, 67, 1-4.
5. E. Yousif, A. Majeed, K. Al-Sammarrae, N. Salih, J. Salimon and B. Abdullah, *Arabian Journal of Chemistry*, **2017**, 10, 1639-1644.
6. D. R. Friend and G. F. Doncel, *Antiviral Research*, **2010**, 88, 47-54.
7. D. R. Friend, *Expert Opinion on Drug Delivery*, **2012**, 9, 417-427.
8. A. Corona-Bustamante, J. M. Viveros-Paredes, A. Flores-Parra, A. L. Peraza-Campos, F. J. Martínez-Martínez, M. T. Sumaya-Martínez and Á. Ramos-Organillo, *Molecules*, **2010**, 15, 5445-5459.
9. I. Kostova and L. Saso, *Current Medicinal Chemistry*, **2013**, 20, 4609-4632.
10. S. Vartale, N. Halikar, Y. Pawar and K. Tawde, *Arabian Journal of Chemistry*, **2016**, 9, 1117-1124.
11. I. Ali, W. A. Wani, K. Saleem and M.-F. Hseih, *Polyhedron*, **2013**, 56, 134-143.
12. B. Cvek, V. Milacic, J. Taraba and Q. P. Dou, *Journal of Medicinal Chemistry*, **2008**, 51, 6256-6258.
13. S. M. Mamba, A. K. Mishra, B. B. Mamba, P. B. Njobeh, M. F. Dutton and E. Fosso-Kankeu, *Spectrochimica Acta Part A: Molecular and Biomolecular Spectroscopy*, **2010**, 77, 579-587.
14. F. Shaheen, A. Badshah, M. Gielen, M. Dusek, K. Fejfarova, D. de Vos and B. Mirza, *Journal of Organometallic Chemistry*, **2007**, 692, 3019-3026.
15. D. C. Onwudiwe and A. C. Ekennia, *Research on Chemical Intermediates*, **2017**, 43, 1465-1485.
16. S. Khan, W. Ahmad, K. Munawar and S. Kanwal, *Indian Journal of Pharmaceutical Sciences*, **2018**, 80, 480-488.
17. H. Graeme, *Mini-Reviews in Medicinal Chemistry*, **2012**, 12, 1202-1215.
18. B. Macías, M. a. V. Villa, E. Chicote, S. Martín-Velasco, A. Castiñeiras and J. n. Borrás, *Polyhedron*, **2002**, 21, 1899-1904.
19. M. Shahid, T. Rüffer, H. Lang, S. A. Awan and S. Ahmad, *Journal of Coordination Chemistry*, **2009**, 62, 440-445.

20. G. Hogarth, *Progress in Inorganic Chemistry*, **2005**, 53, 71-561.
21. B. Arul Prakasam, M. Lahtinen, A. Peuronen, M. Muruganandham, E. Kolehmainen, E. Haapaniemi and M. Sillanpää, *Inorganica Chimica Acta*, **2015**, 425, 239-246.
22. B. Arul Prakasam, M. Lahtinen, A. Peuronen, M. Muruganandham, E. Kolehmainen, E. Haapaniemi and M. Sillanpää, *Polyhedron*, **2014**, 81, 588-596.
23. F. P. Andrew and P. A. Ajibade, *Journal of Coordination Chemistry*, **2018**, 71, 2776-2786.
24. H. Zhang, J.-s. Wu and F. Peng, *Anti-Cancer Drugs*, **2008**, 19, 125-132.
25. A. Gölcü, *Transition Metal Chemistry*, **2006**, 31, 405-412.
26. K. V. Gopal, P. S. Jyothi, P. A. G. Raju and J. Sreeramulu, *Journal of Chemical and Pharmaceutical Research*, **2013**, 5, 50-59.
27. A. Mohammad, C. Varshney and S. A. Nami, *Spectrochimica Acta Part A: Molecular and Biomolecular Spectroscopy*, **2009**, 73, 20-24.
28. K. Siddiqi, S. Khan, S. A. Nami and M. El-Ajaily, *Spectrochimica Acta Part A: Molecular and Biomolecular Spectroscopy*, **2007**, 67, 995-1002.
29. G. G. Mohamed, N. A. Ibrahim and H. A. Attia, *Spectrochimica Acta Part A: Molecular and Biomolecular Spectroscopy*, **2009**, 72, 610-615.
30. M. Altaf, H. Stoeckli-Evans, S. S. Batool, A. A. Isab, S. Ahmad, M. Saleem, S. A. Awan and M. A. Shaheen, *Journal of Coordination Chemistry*, **2010**, 63, 1176-1185.
31. A. Z. Halimehjani, K. Marjani, A. Ashouri and V. Amani, *Inorganica Chimica Acta*, **2011**, 373, 282-285.
32. A. Z. Halimehjani, S. Torabi, V. Amani, B. Notash and M. R. Saidi, *Polyhedron*, **2015**, 102, 643-648.
33. I. P. Ferreira, G. M. de Lima, E. B. Paniago, J. A. Takahashi, K. Krambrock, C. B. Pinheiro, J. L. Wardell and L. C. Visentin, *Journal of Molecular Structure*, **2013**, 1048, 357-366.
34. G. Gurumoorthy, P. J. Rani, S. Thirumaran and S. Ciattini, *Inorganica Chimica Acta*, **2017**, 455, 132-139.
35. F. P. Andrew and P. A. Ajibade, *Journal of Molecular Structure*, **2018**, 1153, 843-855.
36. T. Peddarao, A. Baishya, M. K. Barman, A. Kumar and S. Nembenna, *New Journal of Chemistry*, **2016**, 40, 7627-7636.
37. E. D. Akpan, S. O. Ojwach, B. Omondi and V. O. Nyamori, *New Journal of Chemistry*, **2016**, 40, 3499-3510.
38. D. Coucouvanis, *Progress in Inorganic Chemistry*, **1970**, 11, 233-371.

39. N. Moloto, N. Revaprasadu, M. Moloto, P. O'Brien and M. Helliwell, *Polyhedron*, **2007**, 26, 3947-3955.
40. N. Moloto, N. Revaprasadu, M. Moloto, P. O'Brien and J. Raftery, *South African Journal of Science*, **2009**, 105, 258-263.
41. F. Bonati and R. Ugo, *Journal of Organometallic Chemistry*, **1967**, 10, 257-268.
42. A. Ziyaei Halimehjani, M. A. Alaei, F. Soleymani Movahed, N. Jomeh and M. R. Saidi, *Journal of Sulfur Chemistry*, **2016**, 37, 529-536.
43. S. H. Dar, S. Thirumaran and S. Selvanayagam, *Polyhedron*, **2015**, 96, 16-24.
44. S. M. Mamba, Masters Thesis, University of Johannesburg, South-Africa, **2010**, pp 20-89 .
45. H. A. Hasan, E. I. Yousif and M. J. Al-Jeboori, *Global Journal of Inorganic Chemistry*, **2012**, 3, 1-7.
46. S. Sibokoza, M. Moloto, N. Moloto and P. Sibiya, *Chalcogenide Letters*, **2017**, 14, 69-78
47. C. K. Jørgensen, *Journal of Inorganic and Nuclear Chemistry*, **1962**, 24, 1571-1585.
48. V. P. Singh, A. Katiyar and S. Singh, *Biometals*, **2008**, 21, 491-501.
49. R. Dulare, M. Bharty, A. Singh and N. Singh, *Polyhedron*, **2012**, 31, 373-378.
50. A. L. Spek, *Acta Crystallographica Section C: Structural Chemistry*, **2015**, 71, 9-18.
51. A. L. Spek, *Acta Crystallographica Section D: Biological Crystallography*, **2009**, 65, 148-155.
52. D. C. Onwudiwe, M. M. Kabanda, E. E. Ebenso and E. Hosten, *Journal of Chemical Sciences*, **2016**, 128, 1081-1093.
53. P. Bharati, A. Bharti, P. Nath, M. Bharty, R. Butcher and N. Singh, *Polyhedron*, **2015**, 102, 375-385.
54. F. Jian, F. Bei, P. Zhao, X. Wang, H. Fun and K. Chinnakali, *Journal of Coordination Chemistry*, **2002**, 55, 429-437.
55. P. J. Rani, S. Thirumaran and S. Ciattini, *Spectrochimica Acta Part A: Molecular and Biomolecular Spectroscopy*, **2015**, 137, 1164-1173.
56. D. C. Onwudiwe and A. C. Ekennia, *Research on Chemical Intermediates*, **2017**, 43, 1465-1485.
57. R. S. Joseyphus and M. S. Nair, *Mycobiology*, **2008**, 36, 93-98.
58. I. Ali, W. A Wani, K. Saleem and D. Wesselinova, *Medicinal Chemistry*, **2013**, 9, 11-21.
59. B. Tweedy, *Phytopathology*, **1964**, 55, 910-914.

60. A. A. Al-Amiery, *Research on Chemical Intermediates*, **2012**, 38, 745-759.
61. L. S. Kumar, K. S. Prasad and H. D. Revanasiddappa, *European Journal of Chemistry*, **2011**, 2, 394-403.
62. H. Lopez-Sandoval, M. E. Londoño-Lemos, R. Garza-Velasco, I. Poblano-Meléndez, P. Granada-Macías, I. Gracia-Mora and N. Barba-Behrens, *Journal of Inorganic Biochemistry*, **2008**, 102, 1267-1276.
63. K. Nomiya, A. Yoshizawa, K. Tsukagoshi, N. C. Kasuga, S. Hirakawa and J. Watanabe, *Journal of Inorganic Biochemistry*, **2004**, 98, 46-60.
64. E. N. Esfahani, M. Mohammadi-Khanaposhtani, Z. Rezaei, Y. Valizadeh, R. Rajabnia, M. Hassankalhori, F. Bandarian, M. A. Faramarzi, N. Samadi, M. R. Amini, M. Mahdavi and B. Larijani, *Research on Chemical Intermediates*, **2019**, 45, 223-236.
65. K. Naumann, *EuroChlor Science Dossier November*, **2003**.
66. K. Naumann, *Pest management science*, **2000**, 56, 3-21.
67. Z. Guo and P. J. Sadler, *Angewandte Chemie International Edition*, **1999**, 38, 1512-1531.
68. K. Mounika, A. Pragathi and C. Gyanakumari, *Journal of Scientific Research*, **2010**, 2, 513-520.
69. B. L. Batzing, *Microbiology: An Introduction*, Brooks/Cole, **2002**.
70. A. C. Ekennia, D. C. Onwudiwe, A. A. Osowole, L. O. Olasunkanmi and E. E. Ebenso, *Journal of Chemistry*, **2016**, 16, 1-12.
71. S. Nithiya, N. Karthik and J. Jayabharathi, *International Journal of Pharmacy and Pharmaceutical Sciences*, **2011**, 3, 254-256.
72. I. Gülçin, Ö. İ. Küfrevioğlu, M. Oktay and M. E. Büyükokuroğlu, *Journal of Ethnopharmacology*, **2004**, 90, 205-215.
73. S. A. Nami, I. Ullah, M. Alam, D.-U. Lee and N. Sarikavakli, *Journal of Photochemistry and Photobiology B: Biology*, **2016**, 160, 392-399.
74. W. Chen, S. Sun, Y. Liang and J. Song, *Journal of Molecular Structure*, **2009**, 918, 194-197.
75. A. Mahajan and V. R. Tandon, *Indian Journal of Rheumatology*, **2004**, 12, 139-142.
76. N. Ganji, A. Rambabu, N. Vamsikrishna and S. Daravath, *Journal of Molecular Structure*, **2018**, 1173, 173-182.
77. A. Fetoh, O. A. El-Gammal and G. M. A. El-Reash, *Journal of Molecular Structure*, **2018**, 1173, 100-110.

78. S. Zara, D. Ahmed, H. Baig and M. Ikram, *Asian Journal of Chemistry*, **2012**, 24, 4345-4351.
79. S. Kwek, L. Leong and R. Bettens, National University of Singapore, *Reports*, **2006**, 1-5.
80. M. Valko, D. Leibfritz, J. Moncol, M. T. Cronin, M. Mazur and J. Telser, *The International Journal of Biochemistry & Cell Biology*, **2007**, 39, 44-84.
81. P. Ghafourifar and E. Cadenas, *Trends in Pharmacological Sciences*, **2005**, 26, 190-195.
82. L. Beneš, Z. Ďuračková and M. Ferenčik, *Life sciences*, **1999**, 65, 1865-1874.
83. P. Klatt and S. Lamas, *European Journal of Biochemistry*, **2000**, 267, 4928-4944.
84. S. Fujii and T. Yoshimura, *Coordination Chemistry Reviews*, **2000**, 198, 89-99.

CHAPTER FIVE

Novel heteroleptic Cu(I) N,N'-diarylformamidine dithiocarbamate PPh_3 complexes: Synthesis, structural characterization, optical properties and *in vitro* biological studies

ABSTRACT

Eight novel heteroleptic copper(I) dithiocarbamate complexes of the general formula **$Cu(PPh_3)_2DL$**, where **DL** represents in turn N,N'-bis(2,6-dimethylphenyl)formamidine dithiocarbamate **DL1** (**25**), N,N'-bis(2,6-disopropylphenyl) formamidine dithiocarbamate **DL2** (**26**), N,N'-dimesitylformamidine dithiocarbamate **DL3** (**27**), N'-(2,6-dichlorophenyl)-N-(2,6-dimethylphenyl)formamidine dithiocarbamate **DL4** (**28**), N'-(2,6-dichlorophenyl)-N-(2,6-diisopropylphenyl)formamidine dithiocarbamate **DL5** (**29**), N'-(2,6-dichlorophenyl)-N-mesitylformamidine dithiocarbamate **DL6** (**30**), N'-(2-bromophenyl)-N-(2,6-dimethylphenyl)formamidine dithiocarbamate **DL7** (**31**) and N'-(2-bromophenyl)-N-mesitylformamidine dithiocarbamate **DL8** (**32**) have been synthesized by metathesis reactions of potassium salt of the dithiocarbamate ligand **DL** and the precursor complex $Cu(PPh_3)_2NO_3$ in an equimolar ratio. These complexes were characterized using ^{1}H, ^{13}C and ^{31}P NMR, FT-IR, UV-vis. and mass spectra and the purity confirmed by elemental analysis. In addition, crystal structures of all the structures were elucidated and confirm the coordination of the copper atom to two sulfur atoms of the dithiocarbamate ligand as well as the two phosphorus atoms of the PPh_3 units, which results in distorted tetrahedral geometry. Complexes **25** – **30** showed a remarkable luminescent property in CH_2Cl_2 at room temperature. Press pellet electrical conductivity (σ_{rt}) values for **25 - 32** are between 3.94×10^{-11} to 9.85×10^{-9} S cm^{-1}, revealing their weak conducting ability. All the complexes showed moderate to low antibacterial activities against Gram-negative bacteria *Escherichia coli*, *Salmonella typhimurium*, *Klebsiella pneumoniae* and *Pseudomonas aeruginosa*, while none of the complexes were active against Gram-positive bacteria *Staphylococcus aureus* (methicillin resistant) and *Staphylococcus aureus*. The antioxidant potential of all the complexes were studied using DPPH and NO assays. We found out that complex **26** has the lowest IC_{50} value of 4.99×10^{-3} mM and has the highest DPPH free radical scavenging ability while **27,** with IC_{50} value of 0.26 mM, has the highest nitric oxide scavenging ability.

Key words: Copper(I) complexes, Dithiocarbamate, Photoluminescence, antioxidant, *in vitro* antibacterial activity

5.1 Introduction

The chemistry of metal dithiocarbamates are well known [1-5] and occupy a vital position among metal dithiolate compounds because of their interesting electrochemical [6], conducting, magnetic [7] and optical properties [8-10]; their use as a single precursor in the syntheses of metal sulfide nanoparticles [11-16], biological applications [17-21] as well as their application in metallurgy [22], vulcanization of rubber and in agriculture as pesticides [23]. The consistent interest in the chemistry of dithiocarbamate ligands arises from the functionalization of the substituents on the dithiocarbamate units, which then leads to a variety of complexes with different structural architectures as well as different physical properties. These differing behaviours can be ascribed to the dominant contribution of the canonical form $\mathbf{R_2N{=}CS_2^-}$ in the dithiocarbamate metal complexes [24, 25].

Copper(I) complexes, both homoleptic as well as heteroleptic, have attracted considerable interest in the past decades, due to their excellent photoluminescence properties [26, 27] with possible application in energy conversion in solar cells [28-32], light emission in electrochemical devices [33-37], imaging in biological cells [38, 39], display devices [40, 41] and in sensors [42, 43]. This photoluminescence property might be associated to the low-energy charge-transfer excited state, which arises due to the $3d^{10}$ system of some Cu(I) complexes [44]. Structurally, copper(I) complexes of the type $[Cu^{I}(DTC)PR_3]_2$, where R represents OMe, Me or Et and DTC represents dithiocarbamates, are dimeric [45] and the cluster form of both homo- as well as heteronuclear Cu(I) complexes of dithiocarbamates and other 1,1-dithiolate ligands had also been reported [46-48].

The ability of dithiocarbamate to stabilize +2 and +3 oxidation state of copper had been reported in literatures [49-51]. Dithiocarbamates in conjunction with strong σ-donor and π-acceptor bulky phosphine ligands, can also stabilize +1 oxidation state of copper and control the coordination sphere around them, favouring tetrahedral geometry [24, 44]. Despite their synthetic versatility and immense practical application, studies on heteroleptic copper(I) dithiocarbamate-phosphine complexes are limited in the literature, particularly regarding their potential biological activity [44]. Nevertheless, previous studies have shown that other complexes with ligands containing phosphorus displayed good biological activities [52-58].

Against this background, it seemed worth undertaking the synthesis of novel heteroleptic copper(I) complexes derived from symmetrical and unsymmetrical N,N'-diarylformamidine functionalized dithiocarbamate and triphenylphosphine to investigate their single crystal structures, electrical conductivity, luminescent and biological activities in antibacterial and antioxidant studies.

5.2 Results and discussion

5.2.1 Synthesis of Cu(I) N,N'-diarylformamidine dithiocarbamate-PPh_3 complexes

Complexes $[Cu(PPh_3)_2DL(n)]$ (**25** – **32**) were synthesized by treating an acetonitrile potassium salt solution of **DL** with a dichloromethane solution of bis(triphenylphosphine)copper(I) nitrate $[Cu(PPh_3)_2]NO]$ in an equimolar ratio at 25°C as was shown in **Scheme 2.5**. All the complexes were obtained as a pale-yellow solid in good yield (70 – 81%); they were air stable and melted within the range 196 – 245 °C. They are all soluble in dichloromethane, tetrahydrofuran, chloroform, dimethyl sulfoxide (DMSO) and N,N-dimethylformamide (DMF).

5.2.2 Spectroscopic studies

Nuclear magnetic resonance

The ^{1}H and ^{13}C NMR data for complexes **25** – **32** were all obtained in in chloroform. The diamagnetic nature of the complexes are confirmed from the NMR spectra and the characteristic resonance of the free ligands correlates perfectly with the corresponding hydrogen atoms. The azomethine proton (NC(*H*)=N) gives an insight into the successful synthesis of the copper(I) dithiocarbamate phosphine complexes from the free ligands where an upfield shift from 9.53 – 10.02 ppm in the spectra **DL1** – **DL8** to 8.82 – 9.20 ppm in the spectra of **25 – 32** confirmed complexation (see **Table 5.1**). Generally, there were downfield shifts in the signal of aliphatic protons between the potassium dithiocarbamate salts and the complexes. For example, the peak for the methyl protons (CH_3-Ar) in **DL4** appeared at 2.13 ppm but upon complexation, it was deshielded and appeared at 2.23 ppm in complex **28**. This noticeable downfield shift can be attributed to the drift of electron density towards the positive Cu(I) centre in the heteroleptic complexes [23, 59]. In addition, the aromatic protons of the PPh_3 moiety and the ligands in the complexes appeared in the range 6.83 – 7.41 ppm. In the ^{13}C-NMR spectra of the complexes, a noticeable upfield shift (δ = 1.42 – 3.50 ppm) in the resonances for the carbon atom of -NCS_2 in all the complexes compared to that for the dithiocarbamate ligands substantiates the metal to sulfur bonding in the complexes. In the ^{13}P-

NMR spectra of the complexes, the presence of a single peak around -0.85 – 0.20 ppm indicates the nature of triphenylphosphine ligand bonded to a Cu atom, with values being like those reported in literature [24, 44].

Table 5.1: The -NCS_2 (^{13}C-NMR) and NC(H)=N (^{1}H-NMR) signals for **DL1** – **DL8** and **25** – **32**, and the IR bands of thiouride (C—N) and azomethine (C=N_{str}) for ligands and the complexes.

Ligands (Complex)	**δ (-NCS_2) ppm**	**Δ δ**	**δ** NC(H)=N ppm	**Δ δ**	**υ(C=N) cm^{-1}**	**Δυ**	**υ(C—N) cm^{-1}**	**Δυ**
DL1 (25)	217.62 (215.90)	1.72	9.86(9.56)	0.30	1640 (1643)	3	1467 (1476)	9
DL2 (26)	220.94 (217.47)	3.47	10.15(9.77)	0.38	1639 (1643)	4	1452 (1476)	24
DL3 (27)	218.95 (216.05)	2.90	9.92(9.53)	0.39	1629 (1633)	4	1477 (1478)	1
DL4 (28)	218.82 (215.30)	3.52	10.12(9.67)	0.45	1614 (1632)	18	1432 (1477)	45
DL5 (29)	217.03 (218.04)	1.01	10.13(10.0)	0.13	1603 (1632)	29	1430 (1479)	49
DL6 (30)	219.04 (216.58)	2.46	10.39(9.69)	0.70	1612 (1633)	21	1435 (1479)	44
DL7 (31)	219.19 (216.09)	3.10	10.08(9.53)	0.55	1613 (1616)	3	1467 (1468)	1
DL8 (32)	219.43 (216.22)	3.21	10.07(9.67)	0.40	1614 (1625)	11	1465 (1479)	14

Fourier transform infra-red spectroscopy

The IR spectra of complexes **25** – **28** displayed υ(C—NCS_2), υ(C—S), and metal to sulfur bond (M—S) vibrational bands, which are diagnostic of dithiocarbamate salts coordination [3, 24, 60, 61] and υ(C=Nstr).of the azomethine (C(H)=N) [62-64]. In the spectra of heteroleptic Copper(I) dithiocarbamate-phosphine complexes **25 - 32**, the thiouride band was observed at higher wave number, around 1468 – 1479 cm^{-1}, than for those of dithiocarbamate ligands, which appeared around 1430 – 1477 cm^{-1}; this shift to higher wavenumber in the complexes could be due to a mesomeric drift of electrons from the dithiocarbamate moiety towards the metal coordination centre [65]. The noticeable enhancement in the υ(C—N) frequency of **25** – **32** relative to the potassium salts of the free ligands **DL1** – **DL8** indicates that the dithiocarbamate ligands coordinate in a symmetrical bidentate manner due to the dominance of the canonical form $R_2N{=}CS_2^-$, thereby indicating the partial double bond character in the thiouride band. A single band around 1024 – 1092cm^{-1} indicates υ(C—S) and thus alludes to

the bidentate coordination mode of the dithiocarbamate ligands to the metal centre [50, 65-67]. The vibrational bands for υ(C=Nstr) of the azomethine (C(H)=N) were observed at higher frequency, around 1616 – 1643 cm^{-1}, than those for the ligands, which appeared around 1603 – 1640 cm^{-1}. The Cu—P and Cu—S vibrational bands were assigned to the bands that appeared at the far infrared region, that is around 429 - 445 cm^{-1} and 492 - 500 cm^{-1}, respectively.

Electronic absorption and emission spectroscopy

The UV-Visible spectra of complexes **25** – **32** in dichloromethane solution are given in **Figure 5.1a.** The free dithiocarbamate ligands **DL1** – **DL8** exhibited two strong absorption bands in the UV region at 289 – 300 nm and 338 – 345 nm. The absorption bands of all the heteroleptic Cu(1) complexes **25** – **32** have the same features as their parent ligands, with two strong absorption bands, but shifted to shorter wavelength (blue shift) and appeared at 272 - 277 nm and 330 - 336 nm. These bands can be assigned to metal-perturbed $\pi \rightarrow \pi^*$ intraligand charged transfer transitions within dithiocarbamate and PPh_3 ligands [44].

When excited at 380 nm in dichloromethane solution at room temperature, **25** – **30** showed an unstructured emission band at about 464 and 465 nm (**Figure 5.1b**) emitting a bluish-green light with a large stoke shift, averaging 84 – 85 nm, which emanates from the admixture of π—π^* IL and MLCT in the perturbed coordination environment about the metal atoms [44, 68, 69]. Previous reports have suggested that there is tendency for the complexes to have slight structural changes in the excited state, as compared to the ground state, due to a small force imposed on them from the bulkiness of the substituents on the dithio ligands together with the phosphine ligands. For example, a tetrahedral geometry is transformed to a flattened structure as reported in the case of Cu(I), a d^{10} system, and this influences the luminescent pattern after metal ligand charge transfer transition [70-72].

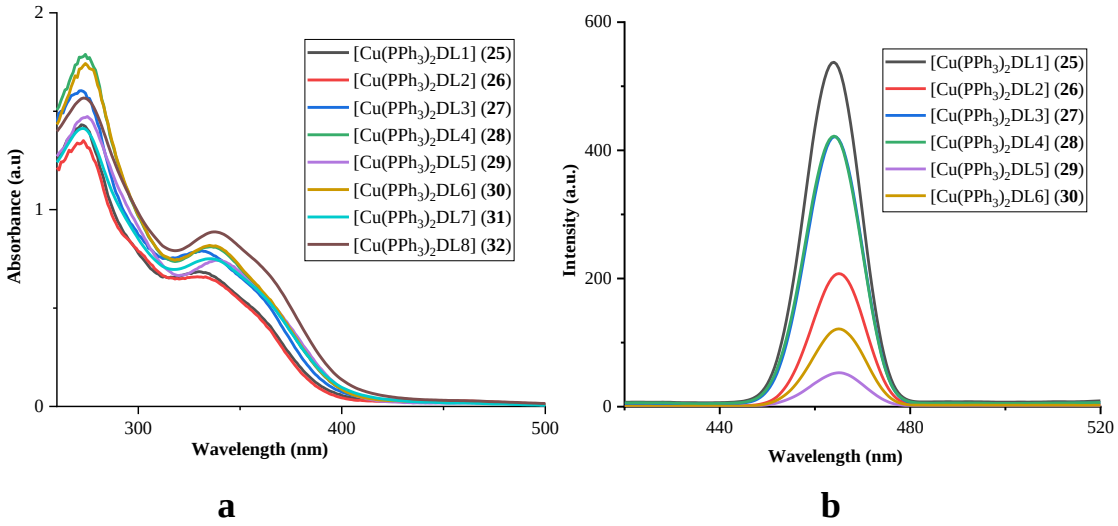

Figure 5 1: (a) Electronic absorption spectra of **25 – 32** in CH_2Cl_2 (b) Emission spectra of **25 – 30** in CH_2Cl_2

5.3 X-ray crystal structures of 25 - 32

Suitable crystals of **25** – **32** were grown by slow evaporation of a dichloromethane/methanol solution of each complex. The molecular structures are illustrated in **Figures 5.2 –** 5.5 while selected bond lengths and angles are given in **Table 5.3**. In complex **27**, a dichloromethane molecule is disordered over an inversion centre with 50% site occupancy while, in complex **32**, the bromine atom is disordered over two positions with a major component having 94% site occupancy. Also, the 2-bromophenyl substituent in complex **31** is disordered over three positions. The specific site occupancies for each atom of this molecule are listed in **Table 5.2**.

Table 5.2: Atomic site occupancies of disordered 2-bromophenyl substituent in complex **31**

Atom	Occupancy	Atom	Occupancy	Atom	Occupancy
C53	0.55(2)	C47	0.49(3)	C49	0.54(2)
C48	0.45(18)	Br2	0.52(3)	C1AA	0.60(14)
C0AA	0.51(14)	C1F	0.10	C1A	0.26(18)
C1B	0.21(13)	C1C	0.11(2)	C1D	0.16
C1E	0.05(2)	Br1	0.12(15)	C1G	0.32(2)
C1H	0.47(3)	C1I	0.42(2)	C1J	0.34(15)
C1K	0.37(14)	C1L	0.36(14)	Br0A	0.09(3)

The asymmetric units of all the complexes contain a whole molecule of the Cu(I) dithiocarbamate phosphine complexes. The geometry of all the complexes entails the coordination of the copper atom to two sulfur atoms of the dithiocarbamate ligand as well as the two phosphorus atoms of the PPh_3 units. The CuP_2S_2 core centre in all the complexes has a distorted tetrahedral geometry, as is evident from the bond angles shown in **Table 5.3**, can be accounted for as follows. Firstly, the deviation from the ideal geometry arises mainly as a results of the constraint imposed by $CS_2Cu(I)$ chelate rings, which leads to small S(1)—Cu—S(2) bite angles ranging from 74.61(2)° to 75.03(2)° [24].Another factor that might be responsible for the distortion is the steric restrictions of the bulky phosphine ligands. In all the complexes, the Cu(1)—S(1) and Cu(1)—S(2) bond lengths differ significantly, with the Cu(1)—S(2) being clearly and consistently longer than Cu(1)—S(1), whereas there are no noticeable differences in the various C—S bond lengths. The angle between the two least-square planes formed by Cu(1), S(1), S(2) and C_{dtc} and P(1), Cu(1) and P(2) for **25** to 32 are, respectively, 86.95°, 87.61°, 87.16°, 87.33° 88.28°, 86.72°, 85.89° and 82.73°; thus indicating that the two planes are almost perpendicular to each other. The CS_2Cu chelate ring in **25**, **26**, **27**, **28**, **29**, **30**, **31** and **32** deviates from planarity with root mean square (r.m.s) values of 0.0530, 0.0171, 0.0404, 0.0297, 0.0236, 0.0355, 0.0256 and 0.0213 Å, respectively.

The Cu—P and Cu—S bond lengths disussed above are not exceptional and, moreover, are comparable to those found in analogous Cu(1) complexes [73, 74]. The values for the C—N bond in each complex, as shown in **Table 5.3,** are intermediate between those published for C=N (1.28 Å) and C—N (1.47 Å) [75]. This indicates the delocalization of π-electrons over the entire S_2CN fragment in the complexes and affirm the contribution of resonance form $R_2N{=}CS_2^-$ of the dithiocarbamates, bringing about the partial double-bond character of the C—N bond [24]. The C—S bond lengths in all the complexes have a range 1.687(2) – 1.704(2) Å and so are significantly shorter than the standard single C—S bond length of 1.81Å, due to π-electron delocalization over the —NCS_2 unit [24]. The packing diagrams of all the complexes, although not shown here, indicate no prominent S•••S intermolecular stacking involving dithiocarbamate ligands, as is common among such complexes [76]. This is as due to steric hindrances imposed by the bulky phosphine ligands in the complexes [24, 44].

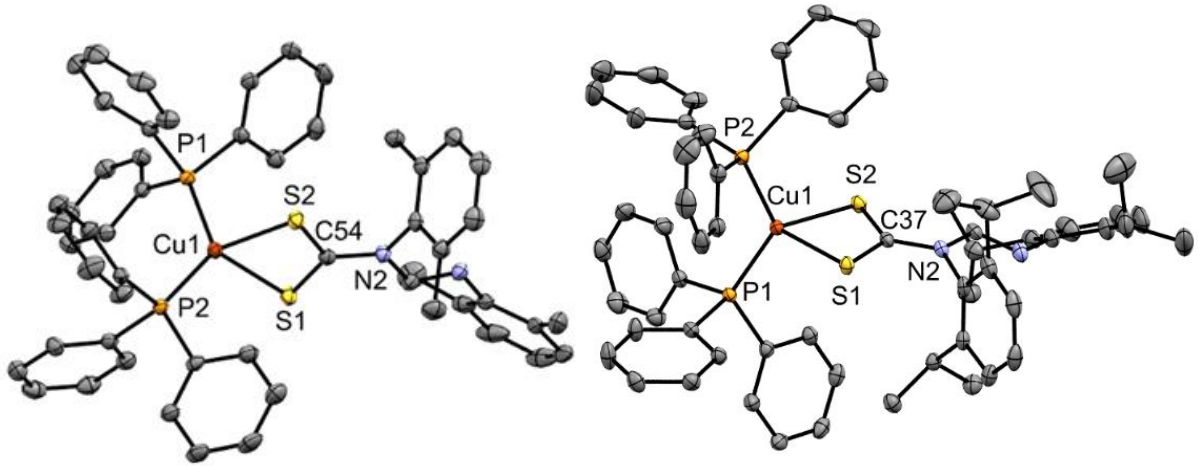

25 **26**

Figure 5.2: ORTEP diagram of complexes **25** and **26** drawn at 50 % thermal ellipsoids probability. Hydrogen atoms have been omitted for clarity.

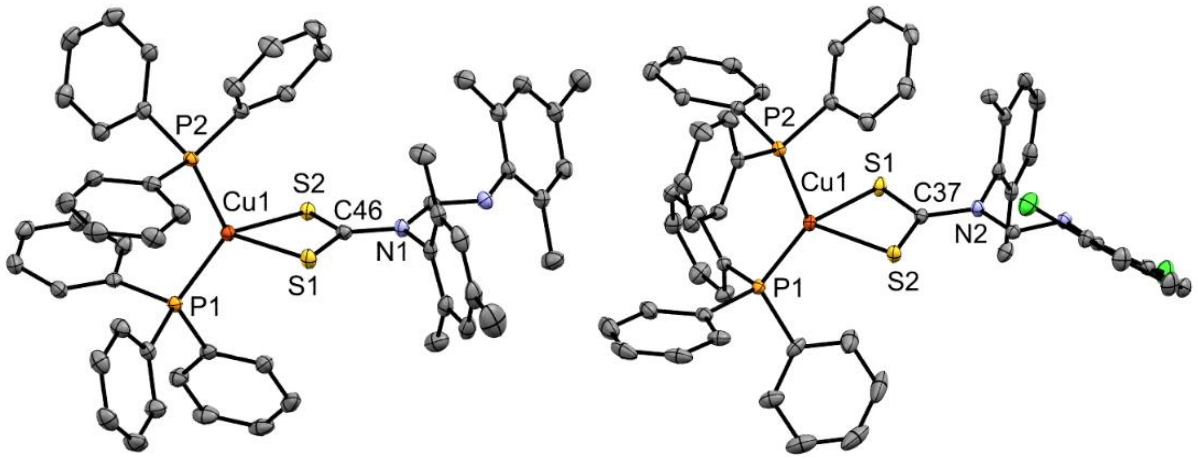

27 **28**

Figure 5.3: ORTEP diagram of complexes **27** and **28** drawn at 50 % thermal ellipsoids probability. Hydrogen atoms have been omitted for clarity in both complexes. One molecule of methanol and two molecules of disordered dichloromethane were also omitted in **27,** and one molecule of dichloromethane was omitted in **28**.

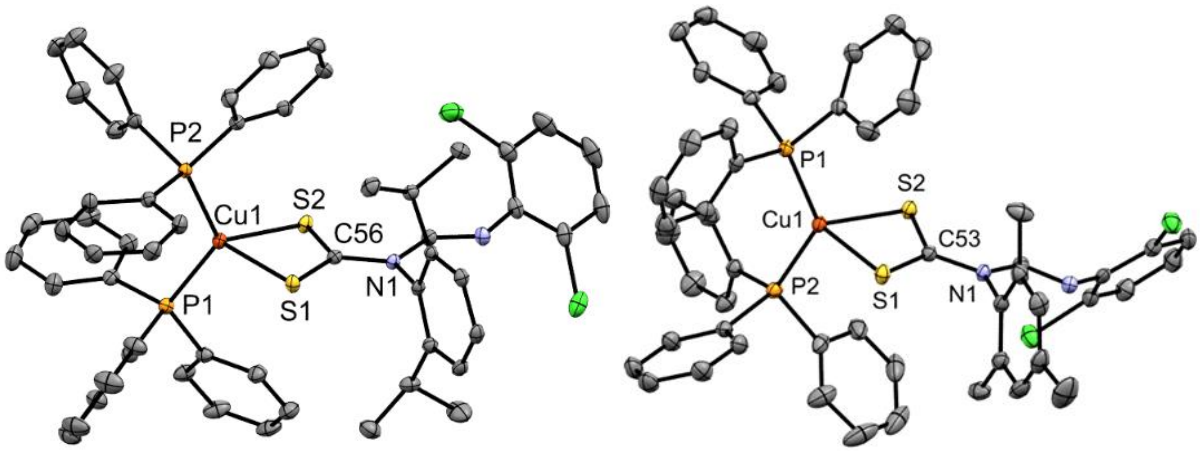

29 **30**

Figure 5.4: ORTEP diagram of complexes **29** and **30** drawn at 50 % thermal ellipsoids probability. Hydrogen atoms have been omitted for clarity in both complexes. One molecule of dichloromethane was also omitted in **30**.

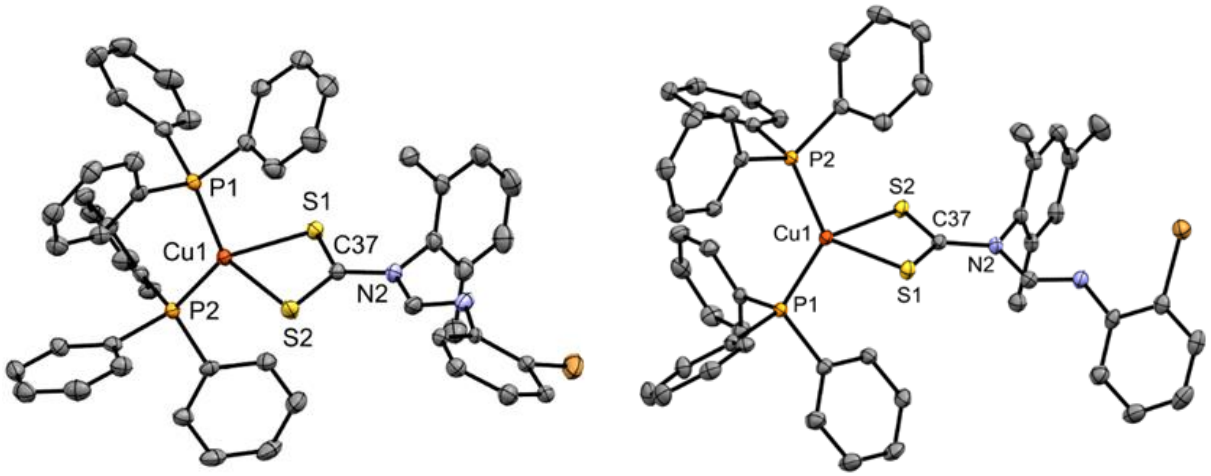

31 **32**

Figure 5.5: ORTEP diagram of complexes **31** and **32** drawn at 50 % thermal ellipsoids probability. Hydrogen atoms have been omitted for clarity in both complexes. A disordered bromine atom was also omitted in **7**, and a disordered 2-bromophenyl molecule was omitted in **8**.

Table 5 3: Selected bond length (Å) and angles (°) for complexes **25 - 32**

Parameters	**25**	**26**	**27**	**28**	**29**	**30**	**31**	**32**
Bond lengths								
Cu—P(1)	2.2509(5)	2.2307(5)	2.2393(5)	2.2307(5)	2.2370(4)	2.2353(5)	2.2475(7)	2.2427(8)
Cu—P(2)	2.2351(7)	2.2472(7)	2.2525(5)	2.2472(7)	2.2415(5)	2.2470(7)	2.2335(7)	2.2428(7)
Cu—S(1)	2.3891(9)	2.2472(7)	2.4060(5)	2.4181(7)	2.3793(6)	2.4194(7)	2.4215(7)	2.4173(5)
Cu—S(2)	2.4186(7)	2.3915(8)	2.4165(4)	2.3915(8)	2.4297(5)	2.3934(5)	2.3840(9)	2.3920(6)
C—S(1)	1.696(2)	1.692(3)	1.687(2)	1.692(3)	1.691(2)	1.689(2)	1.694(3)	1.691(2)
C—S(2)	1.697(2)	1.697(3)	1.704(2)	1.697(3)	1.698(2)	1.698(3)	1.696(3)	1.696(2)
C—N	1.376(3)	1.384(2)	1.395(2)	1.396(3)	1.393(2)	1.393(3)	1.384(3)	1.391(2)
Bond angles								
P(1)—Cu—P(2)	125.73(3)	126.55(3)	121.81(2)	126.55(3)	124.56(2)	129.91(3)	125.48(3)	127.78(3)
P(1)—Cu—S(1)	111.30(3)	112.60(2)	115.55(2)	112.60(2)	111.94(2)	111.87(2)	105.39(3)	109.23(2)
P(1)—Cu—S(2)	105.10(2)	115.71(3)	115.17(2)	115.71(3)	111.52(5)	112.34(2)	111.46(3)	112.89(2)
P(2)—Cu—S(1)	112.74(3)	107.92(2)	105.14(2)	103.59(2)	104.46(2)	104.60(2)	115.57(3)	116.18(2)
P(2)—Cu—S(2)	115.65(2)	108.10(2)	114.51(2)	110.63(3)	117.48(2)	109.37(2)	112.72(3)	102.79(2)
Cu—S(1)—C	83.09(8)	82.70(5)	83.34(6)	82.03(9)	81.90(5)	82.08(8)	81.98(9)	82.27(9)
Cu—S(2)—C	82.17(17)	83.87(5)	82.67(6)	82.76(9)	83.32(5)	82.70(8)	83.11(9)	82.95(9)
S(1)—C—S(2)	119.0(1)	118.72(9)	119.1(1)	119.80(1)	119.58(9)	119.8(1)	119.3(3)	119.7(1)
S(1)—Cu—S(2)	75.03(2)	74.62(1)	74.61(2)	75.12(2)	75.03(2)	75.03(2)	74.99(3)	74.99(2)

5.4 Pressed-pellet electrical conductivity

The electrical conductivity of all the complexes **25** – **32** was measured with a Keithley 236 source measure unit using the four-probe techniques and the results are summarized in **Table 5.4**. The electrical conductivity (σ_{rt}) of all the complexes ranged between 3.94 x 10^{-11} Scm^{-1} and 9.85 x 10^{-9} Scm^{-1}, with complexes **31** and **27** having the least and highest electrical conductivities, respectively. The weak conducting ability of the complexes can be attributed to the lack of S•••S intermolecular stacking (as discussed in the crystallography section), which is prevented by bulky PPh_3 ligands [24, 44].

Table 5.4: Electrical resistivity and conductivity of complexes **25** – **32**

Complexes	Resistivity (Ω cm)	Conductivity (S cm^{-1})
25	1.64 x 10^{9}	5.94 x 10^{-10}
26	2.77 x 10^{9}	3.62 x 10^{-10}
27	1.01 x 10^{8}	9.85 x 10^{-9}
28	2.74 x 10^{9}	3.65 x 10^{-10}
29	2.55 x 10^{9}	3.92 x 10^{-10}
30	9.69 x 10^{9}	1.03 x 10^{-10}
31	2.54 x 10^{10}	3.94 x 10^{-11}
32	2.84 x 10^{10}	3.52 x 10^{-11}

5.5 Antimicrobial activities evaluation

The novel synthesized heteroleptic complexes **25** – **28** were tested for their antibacterial potential against six bacterial strains. *Klebsiella pneumoniae*, *Pseudomonas aeruginosa*, *Salmonella typhimurium*, *Escherichia coli*, *Staphylococcus aureus* (methicillin resistant) (MSRA) and *Staphylococcus aureus* were employed for the study, while ciprofloxacin was used as a standard drug. The minimum inhibitory concentration (MIC) values were used to evaluate the antimicrobial activities of the complexes and are summarized in **Table 5.4**. The higher the MIC values the lower will be the antibacterial potency [77-79]. It was observed that the complexes exhibited moderate to fairly good antimicrobial activities against the Gram-negative bacteria strains *K. pneumoniae, P. aeruginosa and S. typhimurium* but none was active against the Gram-positive bacteria strains, *S. aureus* and MRSA. This difference in the activity

of all the complexes against the two types of bacteria might be due to the differing natures of their cell membranes, which determines the degree to which compounds can penetrate the bacteria [20, 80, 81]. The non-toxicity of the complexes towards the Gram-positive bacteria might therefore be attributed to the compounds being damaged or modified as they enter the cell wall of *S. aureus* and *S. aureus* (methicillin resistant) [82].

Complexes **25** and **31** showed good activity against *E. coli* while others exhibited moderate to low activity against it. Against *S. typhimurium*, complex **32** showed good antimicrobial activity with MIC value almost the same as for ciprofloxacin (standard used), while **25**, **26** and **31** showed moderate activity, and the others showed activity only at high concentration. Against *P aeruginosa*, complex **26** showed moderate activity with MIC value of 50 µg/mL whilst **25**, **27**, **28** and **29** were active at only highest concentration (1000 µg/mL) and **30**, **31** and **32** were completely inactive. Against *K. pneumonia*, the complexes were active only at 1000 µg/mL, except for **30**, **31** and **32**, which displayed no activity at any concentration.

Table 5 5: Minimum inhibitory concentration of the metal complexes **25 - 32** (µg/mL).

Complexes	**Gram (-) bacteria**				**Gram (+) bacteria**	
	E. coli	*S. typhimurium*	*P. aeruginosa*	*K. pneumoniae*	*S. aureus*	MRSA
25	3.125	12.50	1000	1000	NA	NA
26	100	25	50	100	NA	NA
27	25	100	1000	1000	NA	NA
28	1000	1000	1000	1000	NA	NA
29	1000	100	1000	1000	NA	NA
30	1000	1000	NA	NA	NA	NA
31	1.60	3.125	NA	NA	NA	NA
32	50	0.80	NA	NA	NA	NA
Ciprofloxacin[a]	0.20	0.40	0.80	1.60	25	25

NA = no activity and a = standard

5.6 Antioxidant studies

5.6.1 DPPH Radical scavenging ability

The ability of complexes to react with stable free radicals can be determined by DPPH assay. It has earlier been reported that the strong absorption band at 517 nm in visible spectrophotometry of DPPH results from the presence of an unpaired electron [83-85]. This absorption band disappears when hydrogen or an electron from free radical scavengers pairs with this electron to form reduced DPP-H, which leads to the abrupt change of DPPH colour from purple to yellow [85]. Compounds with DPPH scavenging ability are receiving tremendous attention due to their anticancer, anti-aging and anti-inflammatory activities [86]. Therefore, compounds with antioxidant activities may offer protection in inflammatory conditions such as rheumatoid arthritis [84]. In this study, we assessed the antioxidant activities of the complexes using IC_{50} values as calculated from their % free radical scavenging ability. Ascorbic acid (with IC_{50} value of 1.01×10^{-3} mM) was used as a standard to evaluate the antioxidant property of the complexes. Results are summarized in **Table 5.5.**. The higher the IC_{50} value the lower the antioxidant activity potency [87, 88].

We found, as shown in **Table 5.5,** that, on the one hand, complex **26** has the least IC_{50} value of 4.99×10^{-3} mM and the highest value of ascorbic acid equivalent antioxidant capacity (AEAC), followed, respectively, by **27**, **25** and **29** . On the other hand, complexes **28**, **30**, **31** and **32** all displayed weak antioxidant activity. It was observed that the ligands' associated electronic factor seems to influence the antioxidant potential of the complexes. In other words, those having rich electron density, from their electron-donating substituents, being more active as antioxidants than were the complexes with a electron-withdrawing group [89]. For example, complexes **25**, **26** and **27** have better activities compared to others, as seen in **Table 5.5**. Generally, the antioxidant activity of **25 – 32** increases as the concentration increases, which is illustrated in **Figure 5.6**.

Table 5 6: Antioxidant potential of tested compounds **25 - 32** at different concentration using DPPH assay.

Complexes	IC_{50} (mM)
25	6.29×10^{-2}
26	4.99×10^{-3}
27	5.66×10^{-3}
28	4.49×10^{-1}
29	2.45×10^{-2}
30	4.36×10^{-1}
31	7.59×10^{-1}
32	4.62×10^{-1}
Ascorbic acid	1.04×10^{-3}

Result presented here are the mean values from three independent experiments

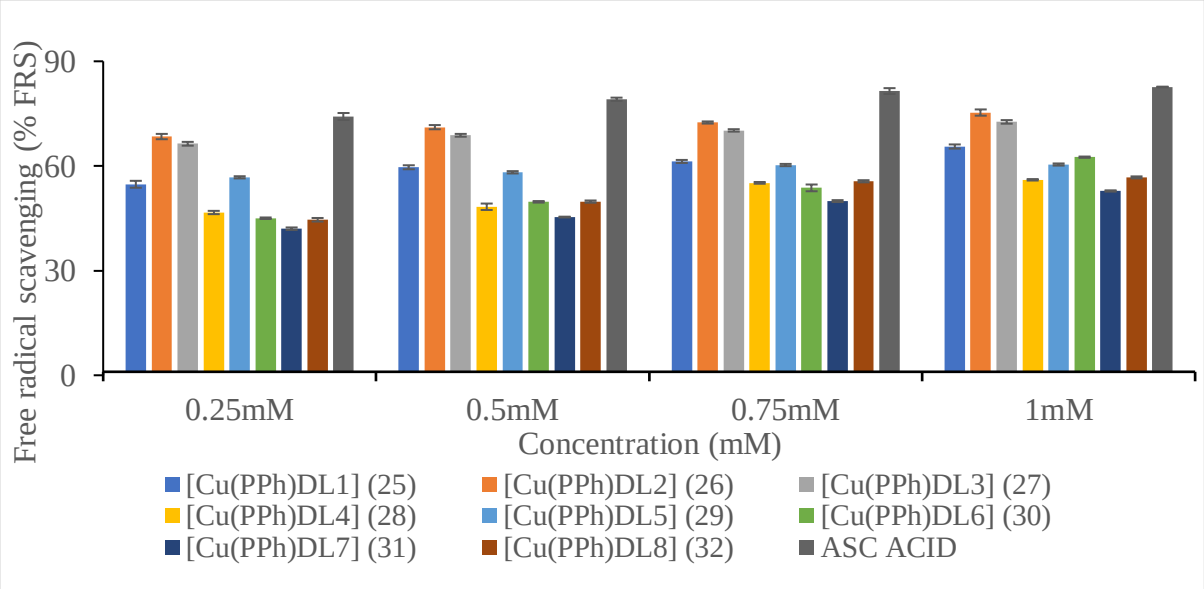

Figure 5.6: Free radical scavenging (%) vs concentration (mM) of Cu(I) dithiocarbamate-PPh_3 complexes (**25 - 32**).

5.6.2 Nitric oxide (NO) scavenging ability

The beneficial role of nitric oxide radical ($NO^{\bullet}$) as an important oxidative biological indicating molecule in various physiological processes such as immune regulation, defense mechanism,

blood pressure regulation and neurotransmission have been reported [90-92]. NO• is a reactive nitrogen species that contain one unpaired electron on the antibonding of $2\pi^*y$ orbital [92]. The excess production of nitric oxide radical as well as other reactive nitrogen species is called nitrosative stress [94]. This may lead to nitrosylation reactions, which alter protein structures and so have an adverse effect on body systems.

Compounds such as flavonoids [95], green tea [96], dithiocarbamates [97], and metal complexes [97-99] have been reported to display good NO• scavenging ability. Herein, we study the ability of Cu(I) dithiocarbamate-PPh_3 complexes, **25** – **32,** to scavenge NO•. The percentage nitric oxide radical scavenging activity values were used to calculate the IC_{50} of all the complexes and these are summarized in **Table 5.6**. When compared to the standard IC_{50} value of 0.23 mM for ascorbic acid, compounds **25** – **32** exhibited moderate to good NO• scavenging ability with complex **27** having the least IC_{50} value of 0.26 mM, which is almost the same antioxidant capacity as ascorbic acid. Complexes **26**, **31** and **32,** with IC_{50} values of 1.56 mM, 1.72 mM and 1.21 mM, respectively, exhibited moderate NO• scavenging activity, while **25**, **28**, **29** and **30** displayed poor activity. The nitric oxide scavenging ability of **25 - 32** increases as the concentration increases and this is illustrated in **Figure 5.7.**

Table 5 7: Antioxidant potential of tested compounds **25 - 32** at different concentration using nitric oxide (NO) assay.

Complexes	IC_{50} (mM)
25	>10
26	1.56
27	0.26
28	>10
29	>10
30	>10
31	1.72
32	1.21
Ascorbic acid	0.23

Results presented here are the mean values from three independent experiments

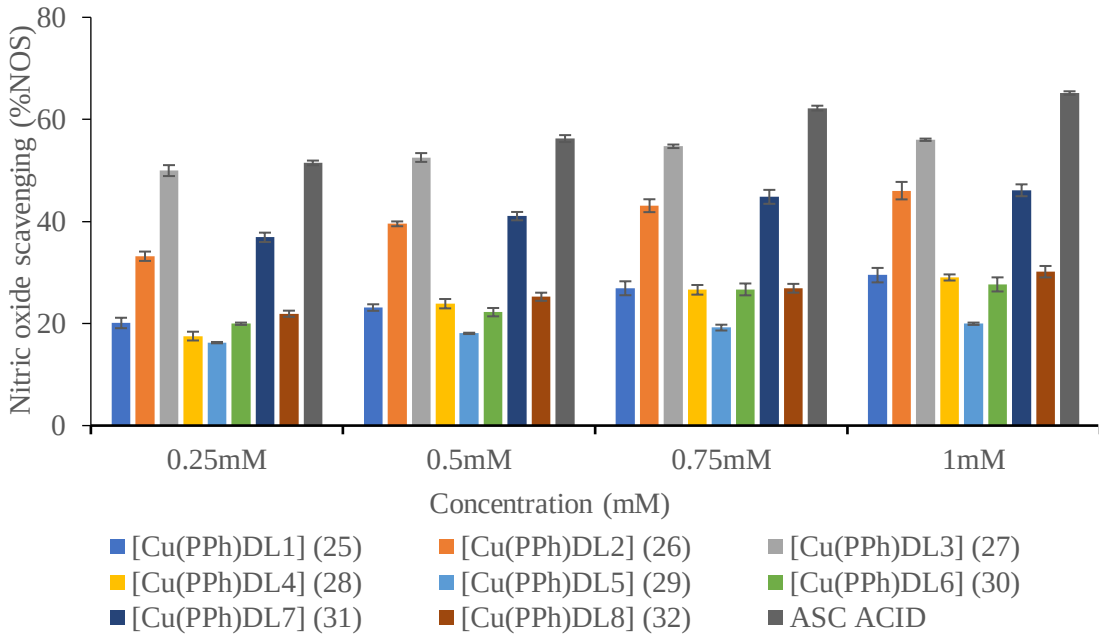

Figure 5.7: % Nitric oxide scavenging vs concentration (mM) of Cu(I) dithiocarbamate-PPh_3 complexes (**25 - 32**).

5.0 Conclusion

In conclusion, eight new heteroleptic copper(I) dithiocarbamate-PPh_3 complexes (**25** – **30**) have been synthesized and fully characterized by elemental analysis and spectroscopy techniques. Crystal structures of **25** – **32** showed that the geometry around the CuS_2P_2 core is distorted tetrahedral. At room temperature, complexes **25** – **30** displayed interesting luminiscent in dichloromethane solution as a result of an admixture of ILCT and MLCT states. All the complexes conduct poorly at room temperature due to absence of prominent S•••S intermolecular stacking in the solid state. The MIC values for all the complexes showed that they all had moderate to low antimicrobial activities against Gram-negative bacteria and displayed no activity against the Gram-positive bacteria used in this study. All the complexes showed good to moderate antioxidant activities, with **26** and **30** having the highest and lowest, respective, free radical scavenging abilities while complex **27** had the highest nitric oxide scavenging ability.

REFERENCES

1. V. Barba, B. Arenaza, J. Guerrero and R. Reyes, *Heteroatom Chemistry*, **2012**, 23, 422-428.
2. D. Cardell, G. Hogarth and S. Faulkner, *Inorganica Chimica Acta*, **2006**, 359, 1321-1324.
3. H. Graeme, *Mini-Reviews in Medicinal Chemistry*, **2012**, 12, 1202-1215.
4. A. Z. Halimehjani, K. Marjani, A. Ashouri and V. Amani, *Inorganica Chimica Acta*, **2011**, 373, 282-285.
5. A. Z. Halimehjani, S. Torabi, V. Amani, B. Notash and M. R. Saidi, *Polyhedron*, **2015**, 102, 643-648.
6. J. D. Wilton-Ely, D. Solanki, E. R. Knight, K. B. Holt, A. L. Thompson and G. Hogarth, *Inorganic Chemistry*, **2008**, 47, 9642-9653.
7. T. Okubo, N. Tanaka, K. H. Kim, H. Yone, M. Maekawa and T. Kuroda-Sowa, *Inorganic Chemistry*, **2010**, 49, 3700-3702.
8. V. Kumar, V. Singh, A. N. Gupta, K. K. Manar, M. G. Drew and N. Singh, *CrystEngComm*, **2014**, 16, 6765-6774.
9. Y. S. Tan, A. L. Sudlow, K. C. Molloy, Y. Morishima, K. Fujisawa, W. J. Jackson, W. Henderson, S. N. B. A. Halim, S. W. Ng and E. R. Tiekink, *Crystal Growth & Design*, **2013**, 13, 3046-3056.
10. R. F. Semeniuc, T. J. Reamer, J. P. Blitz, K. A. Wheeler and M. D. Smith, *Inorganic Chemistry*, **2010**, 49, 2624-2629.
11. K. Ramasamy, V. L. Kuznetsov, K. Gopal, M. A. Malik, J. Raftery, P. P. Edwards and P. O'Brien, *Chemistry of Materials*, **2013**, 25, 266-276.
12. P. A. Ajibade, J. Z. Mbese and B. Omondi, *Inorganic and Nano-Metal Chemistry*, **2017**, 47, 202-212.
13. P. Bera, C.-H. Kim and S. I. Seok, *Solid State Sciences*, **2010**, 12, 1741-1747.
14. J. C. Bruce, N. Revaprasadu and K. R. Koch, *New Journal of Chemistry*, **2007**, 31, 1647-1653.
15. S. K. Maji, A. K. Dutta, S. Dutta, D. N. Srivastava, P. Paul, A. Mondal and B. Adhikary, *Applied Catalysis B: Environmental*, **2012**, 126, 265-274.
16. T. Mthethwa, V. R. Pullabhotla, P. S. Mdluli, J. Wesley-Smith and N. Revaprasadu, *Polyhedron*, **2009**, 28, 2977-2982.

17. F. F. Bobinihi, D. C. Onwudiwe, A. C. Ekennia, O. C. Okpareke, C. Arderne and J. R. Lane, *Polyhedron*, **2019**, 158, 296-310.
18. Ö. Güzel and A. Salman, *Bioorganic & Medicinal Chemistry*, **2006**, 14, 7804-7815.
19. S. I. Islam, S. B. Das, S. Chakrabarty, S. Hazra, A. Pandey and A. Patra, *Advances in Chemistry*, **2016**, 9, 524-530.
20. D. C. Onwudiwe, A. C. Ekennia and E. Hosten, *Journal of Coordination Chemistry*, **2016**, 69, 2454-2468.
21. P. J. Rani, S. Thirumaran and S. Ciattini, *Journal of Sulfur Chemistry*, **2014**, 35, 106-116.
22. A. Abramov and K. Forssberg, *Mineral Processing & Extractive Metall. Rev.*, **2005**, 26, 77-143.
23. A. Mohammad, C. Varshney and S. A. Nami, *Spectrochimica Acta Part A: Molecular and Biomolecular Spectroscopy*, **2009**, 73, 20-24.
24. A. N. Gupta, V. Singh, V. Kumar, L. B. Prasad, M. G. Drew and N. Singh, *Polyhedron*, **2014**, 79, 324-329.
25. K. K. Manar, M. K. Yadav, M. G. Drew and N. Singh, *Polyhedron*, **2016**, 117, 592-599.
26. P. C. Ford, E. Cariati and J. Bourassa, *Chemical Reviews*, **1999**, 99, 3625-3648.
27. C. Kutal, *Coordination Chemistry Reviews*, **1990**, 99, 213-252.
28. M. Sandroni, L. Favereau, A. Planchat, H. Akdas-Kilig, N. Szuwarski, Y. Pellegrin, E. Blart, H. Le Bozec, M. Boujtita and F. Odobel, *Journal of Materials Chemistry A*, **2014**, 2, 9944-9947.
29. M. Sandroni, M. Kayanuma, A. Planchat, N. Szuwarski, E. Blart, Y. Pellegrin, C. Daniel, M. Boujtita and F. Odobel, *Dalton Transactions*, **2013**, 42, 10818-10827.
30. C. E. Housecroft and E. C. Constable, *Chemical Society Reviews*, **2015**, 44, 8386-8398.
31. T. E. Hewat, L. J. Yellowlees and N. Robertson, *Dalton Transactions*, **2014**, 43, 4127-4136.
32. B. Bozic-Weber, S. Y. Brauchli, E. C. Constable, S. O. Fürer, C. E. Housecroft and I. A. Wright, *Physical Chemistry Chemical Physics*, **2013**, 15, 4500-4504.
33. N. Armaroli, G. Accorsi, M. Holler, O. Moudam, J. F. Nierengarten, Z. Zhou, R. T. Wegh and R. Welter, *Advanced Materials*, **2006**, 18, 1313-1316.
34. R. D. Costa, D. Tordera, E. Ortí, H. J. Bolink, J. Schönle, S. Graber, C. E. Housecroft, E. C. Constable and J. A. Zampese, *Journal of Materials Chemistry*, **2011**, 21, 16108-16118.

35. Y.-M. Wang, F. Teng, Y.-B. Hou, Z. Xu, Y.-S. Wang and W.-F. Fu, *Applied Physics Letters*, **2005**, 87, 233512.
36. M. Elie, F. Sguerra, F. Di Meo, M. D. Weber, R. Marion, A. l. Grimault, J.-F. o. Lohier, A. l. Stallivieri, A. Brosseau and R. B. Pansu, *ACS Applied Materials & Interfaces*, **2016**, 8, 14678-14691.
37. R. D. Costa, E. Orti, H. J. Bolink, F. Monti, G. Accorsi and N. Armaroli, *Angewandte Chemie International Edition*, **2012**, 51, 8178-8211.
38. M. H. Lim, D. Xu and S. J. Lippard, *Nature Chemical Biology*, **2006**, 2, 375.
39. X.-L. Xin, M. Chen, Y.-b. Ai, F.-l. Yang, X.-L. Li and F. Li, *Inorganic Chemistry*, **2014**, 53, 2922-2931.
40. M. Hashimoto, S. Igawa, M. Yashima, I. Kawata, M. Hoshino and M. Osawa, *Journal of the American Chemical Society*, **2011**, 133, 10348-10351.
41. D. M. Zink, D. Volz, T. Baumann, M. Mydlak, H. Flügge, J. Friedrichs, M. Nieger and S. Bräse, *Chemistry of Materials*, **2013**, 25, 4471-4486.
42. L. Yang, R. McRae, M. M. Henary, R. Patel, B. Lai, S. Vogt and C. J. Fahrni, *Proceedings of the National Academy of Sciences*, **2005**, 102, 11179-11184.
43. D. W. Domaille, L. Zeng and C. J. Chang, *Journal of the American Chemical Society*, **2010**, 132, 1194-1195.
44. G. Rajput, V. Singh, S. K. Singh, L. B. Prasad, M. G. Drew and N. Singh, *European Journal of Inorganic Chemistry*, **2012**, 24, 3885-3891.
45. M. Afzaal, C. L. Rosenberg, M. A. Malik, A. J. White and P. O'Brien, *New Journal of Chemistry*, **2011**, 35, 2773-2780.
46. F. Sabin, C. Ryu, P. Ford and A. Vogler, *Inorganic Chemistry*, **1992**, 31, 1941-1945.
47. J. Fackler, R. J. Staples, C. W. Liu, R. T. Stubbs, C. Lopez and J. T. Pitts, *Pure and Applied Chemistry*, **1998**, 70, 839-844.
48. N. Zhu, S. Du, P. Chen and X. Wu, *Journal of Cluster Science*, **1992**, 3, 201-218.
49. G. Hogarth, *Progress in Inorganic Chemistry,* **2005**, 53 71-561.
50. D. Coucouvanis, *Progress in Inorganic Chemistry,* **1970**, 11, 233-371.
51. D. Coucouvanis, *Progress in Inorganic Chemistry,* ,**2007**, 26, 301-469.
52. M. Fereidoonnezhad, M. Niazi, M. Shahmohammadi Beni, S. Mohammadi, Z. Faghih, Z. Faghih and H. R. Shahsavari, *ChemMedChem*, **2017**, 12, 456-465.
53. M. Frezza, Q. P. Dou, Y. Xiao, H. Samouei, M. Rashidi, F. Samari and B. Hemmateenejad, *Journal of Medicinal Chemistry*, **2011**, 54, 6166-6176.

54. H. Samouei, M. Rashidi and F. W. Heinemann, *Journal of the Iranian Chemical Society*, **2014**, 11, 1207-1216.
55. H. Samouei, M. Rashidi and F. W. Heinemann, *Journal of Organometallic Chemistry*, **2011**, 696, 3764-3771.
56. T. S. Kamatchi, N. Chitrapriya, H. Lee, C. F. Fronczek, F. R. Fronczek and K. Natarajan, *Dalton Transactions*, **2012**, 41, 2066-2077.
57. A. A. Nazarov and P. J. Dyson, *Phosphorus Compounds*, Springer, **2011**.
58. K. Sampath, S. Sathiyaraj, G. Raja and C. Jayabalakrishnan, *Journal of Molecular Structure*, **2013**, 1046, 82-91.
59. K. Siddiqi, S. Khan, S. A. Nami and M. El-Ajaily, *Spectrochimica Acta Part A: Molecular and Biomolecular Spectroscopy*, **2007**, 67, 995-1002.
60. A. Gölcü, *Transition Metal Chemistry*, **2006**, 31, 405-412.
61. P. J. Heard, *Progress in Inorganic Chemistry*, **2005**, 53, 1-69.
62. A. Mekhalfia, R. Mutter, W. Heal and B. Chen, *Tetrahedron*, **2006**, 62, 5617-5625.
63. M. Sheykhan, M. Mohammadquli and A. Heydari, *Journal of Molecular Structure*, **2012**, 1027, 156-161.
64. E. D. Akpan, S. O. Ojwach, B. Omondi and V. O. Nyamori, *New Journal of Chemistry*, **2016**, 40, 3499-3510.
65. N. Moloto, N. Revaprasadu, M. Moloto, P. O'Brien and J. Raftery, *South African Journal of Science*, **2009**, 105, 258-263.
66. F. P. Andrew and P. A. Ajibade, *Journal of Molecular Structure*, **2018**., 1153, 843-845.
67. F. Bonati and R. Ugo, *Journal of Organometallic Chemistry*, **1967**, 10, 257-268.
68. D. P. Segers, M. K. DeArmond, P. A. Grutsch and C. Kutal, *Inorganic Chemistry*, **1984**, 23, 2874-2878.
69. H. Kunkely and A. Vogler, *Journal of the American Chemical Society*, **1995**, 117, 540-541.
70. D. R. McMillin and K. M. McNett, *Chemical Reviews*, **1998**, 98, 1201-1220.
71. C. T. Cunningham, K. L. Cunningham, J. F. Michalec and D. R. McMillin, *Inorganic Chemistry*, **1999**, 38, 4388-4392.
72. C. T. Cunningham, J. J. Moore, K. L. Cunningham, P. E. Fanwick and D. R. McMillin, *Inorganic Chemistry*, **2000**, 39, 3638-3644.
73. C. Bianchini, C. A. Ghilardi, A. Meli, S. Midollini and A. Orlandini, *Inorganic Chemistry*, **1985**, 24, 932-939.

74. I. Haiduc, R. Cea-Olivares, R. A. Toscano and C. Silvestru, *Polyhedron*, **1995**, 14, 1067-1071.
75. D. J. Halls, *Microchimica Acta*, **1969**, 57, 62-77.
76. B. Singh, M. G. Drew, G. Kociok-Kohn, K. C. Molloy and N. Singh, *Dalton Transactions*, **2011**, 40, 623-631.
77. N. A. Mathews, A. Jose and M. P. Kurup, *Journal of Molecular Structure*, **2019**, 1178, 544-553.
78. L. S. Kumar, K. S. Prasad and H. D. Revanasiddappa, *European Journal of Chemistry*, **2011**, 2, 394-403.
79. H. Lopez-Sandoval, M. E. Londoño-Lemos, R. Garza-Velasco, I. Poblano-Meléndez, P. Granada-Macías, I. Gracia-Mora and N. Barba-Behrens, *Journal of Inorganic Biochemistry*, **2008**, 102, 1267-1276.
80. A. Osowole, G. Kolawole and O. Fagade, *Journal of Coordination Chemistry*, **2008**, 61, 1046-1055.
81. K. Mounika, A. Pragathi and C. Gyanakumari, *Journal of Scientific Research*, **2010**, 2, 513.
82. B. L. Batzing, *Microbiology: An introduction*, Brooks/Cole, **2002**.
83. A. Mahajan and V. R. Tandon, *Indian Journal of Rheumatology*, **2004**, 12, 139-142.
84. F. Dimiza, A. N. Papadopoulos, V. Tangoulis, V. Psycharis, C. P. Raptopoulou, D. P. Kessissoglou and G. Psomas, *Dalton Transactions*, **2010**, 39, 4517-4528.
85. S. Vartale, N. Halikar, Y. Pawar and K. Tawde, *Arabian Journal of Chemistry*, **2016**, 9, 1117-1124.
86. C. Kontogiorgis and D. Hadjipavlou-Litina, *Journal of Enzyme Inhibition and Medicinal Chemistry*, **2003**, 18, 63-69.
87. A. Fetoh, O. A. El-Gammal and G. M. A. El-Reash, *Journal of Molecular Structure*, **2018**, 1173, 100-110.
88. S. Zara, D. Ahmed, H. Baig and M. Ikram, *Asian Journal of Chemistry*, **2012**, 24, 4345-4351.
89 Segun D. Oladipo, Bernand Omondi and Chunderika, *Polyhedron*, **2019**,170, 712-722.
90. S. Archer, *The FASEB journal*, **1993**, 7, 349-360.
91. W. K. Alderton, C. E. Cooper and R. G. Knowles, *Biochemical Journal*, **2001**, 357, 593-615.
92. L. Beneš, Z. Ďuračková and M. Ferenčik, *Life Sciences*, **1999**, 65, 1865-1874.

93. M. Valko, D. Leibfritz, J. Moncol, M. T. Cronin, M. Mazur and J. Telser, *The International Journal of Biochemistry & Cell Biology*, **2007**, 39, 44-84.
94. M. Valko, C. Rhodes, J. Moncol, M. Izakovic and M. Mazur, *Chemico-Biological Interactions*, **2006**, 160, 1-40.
95. S. A. Vanacker, M. N. Tromp, G. R. Haenen, W. Vandervijgh and A. Bast, *Biochemical and Biophysical Research Communications*, **1995**, 214, 755-759.
96. T. Nakagawa and T. Yokozawa, *Food and Chemical Toxicology*, **2002**, 40, 1745-1750.
97. S. Fujii and T. Yoshimura, *Coordination Chemistry Reviews*, **2000**, 198, 89-99.
99. S. Fricker, E. Slade, N. Powell, O. Vaughan, G. Henderson, B. Murrer, I. Megson, S. Bisland and F. Flitney, *British Journal of Pharmacology*, **1997**, 122, 1441-1449.
100. L. Morbidelli, S. Donnini, S. Filippi, L. Messori, F. Piccioli, P. Orioli, G. Sava and M. Ziche, *British Journal of Cancer*, **2003**, 88, 1484-1491.

CHAPTER 6

General conclusions and future prospects

The major goal of this research work was to synthesize, characterize and study the biological applications of N,N'-diarylformamidine dithiocarbamate based thiuram disulfide, metal complexes and Cu(I) heteroleptic-PPh_3 complexes. We also sought insight into the *in silico* behaviour of the thiuram disulfide as a potential anticancer drug. The research effort was directed mainly towards developing new compounds with better antimicrobial and antioxidant activities than those in existence and to evaluate the anticancer potential of the thiuram disulfide using computational tools. This was done by varying the substituents on the dithiocarbamate backbone so as to fine-tune the electronic and steric environment and using the less toxic metal complexes of, nickel, copper and cobalt.

6.1 Research summary

A series of symmetrical and unsymmetrical N,N'-diarylformamidine compounds (**L1** – **L8**) were synthesized in good yield, and used as a source of secondary amine to prepare their respective potassium dithiocarbamate salts. An equimolar ratio of N,N'-diarylformamidine, carbon disulfide and KOH were reacted together over an ice bath to afford potassium dithiocarbamate (**DL1** – **DL8**) in good yield. The disappearance of the amine proton, which appears in the region 5.43 – 5.60 ppm in the ^{1}H-NMR spectra of **L1** – **L8,** and the appearance of quaternary thiouride carbon peak at a downward field region marked the successful synthesis of **DL1** – **DL8**.

Compounds **DL1** – **DL6** were reacted with iodine in a 2 : 1 ratio to give thiuram disulfides **1** – **6,** as stable yellow solids. The single crystal structures of **1** – **6** confirm the coupling of N,N'-diarylformamidine dithiocarbamates moieties in **1** – **6**. The antimicrobial and antioxidant studies of both **DL1** – **DL6** and **1** – **6** were investigated. Compounds **1** – **6** showed better activities towards *E. coli*, *S. typhimurium* and *P. aeruginosa* than did **DL1** – **DL6** while **DL1** – **DL6** displayed better activities against *K. pneumoniae* than **1** – **6**. None of the compounds were active against Gram-positive bacteria, *S. aureus* and MRSA. Both the potassium dithiocarbamate salts and thiuram disulfide exhibited poor antioxidant activities when compared to ascorbic acid and it was observed that **DL1** – **DL6** showed better DPPH free radical scavenging activities than **1** – **6**. Using efficient computational tools for *in silico* investigations predicted, and affirmed that, **1** and **4** exhibited dual selective inhibitory activities

towards the inflammatory mechanisms of cancer, cyclooxygenase -1 and 2. Pharmacological estimations of **1 - 6** revealed that they had minimal violations of Lipinski's rule but exhibited inclinations to be orally bioavailable . (**Chapter 3**).

This research was extended in Chapter 4 to synthesize Ni(II), Cu(II) and Co(III) dithiocarbamate metal complexes **7** – **24** so as to improve the antibacterial and antioxidant activities of **DL1** – **DL6** and **1** – **6** in the previous chapter. The literature on chelation of ligands with metal ions has shown increased biological activities of respective ligands, based on chelation theory. The metal complexes were synthesized by reacting **DL1** – **DL6** with their respective salts and all were obtained in good yield. Single crystal structures of the complexes established distorted square planar geometry for the Ni(II) and Cu(II) complexes and distorted octahedral geometry for the Co(III) complexes. As projected, the antimicrobial activities of the **DL1** – **DL6** were greatly enhanced upon complexation, which can be attributed to increased lipophilicity of the metal complexes thereby enhancing permeability through lipid layers of the cell membrane. Cobalt complexes **23** and **24** were found to show broad spectrum action against the Gram-negative bacteria used in this study, namely *E. coli, S. typhimurium, K. pneumoniae* and *P. aeruginosa*. Moreover, they were more active than the reference drug ciprofloxacin, which makes them a potential antimicrobial drugs. Cu(II) complexes **13 - 19** were found to display excellent activity against *S. aureus* which again was even better than ciprofloxacin, while others were active only at high concentration or not even active at all. We observed that complexes in which the formamidine bore an electron withdrawing group (Cl in this instance) were more active than those with no chlorine atoms and their activities can be attributed to better lipophilicity allowing easier penetration into the lipophilic section of the cell membrane or lipophilic domains of proteins. All the complexes were non active against MRSA, apart from **10**, **11** and **12,** which were active against MRSA at high concentration (chapter 4)

As predicted, the antioxidant activities of **DL1** – **DL6** were highly improved upon chelation. Co(III) complexes **19** and **20** displayed better free DPPH radicals scavenging activities than ascorbic acid and the other complexes. Compounds **7** – **24** exhibited moderate to good nitric oxide (NO) radical scavenging activities but none of them outshone ascorbic acid. We observed that complexes in which formamidine bore electron-donating group showed better antioxidant activities than those that bore an electron-withdrawing group (Chapter 4).

Finally, a series of eight heteroleptic Cu(I) dithiocarbamate PPh_3 complexes, **25** – **32,** were synthesized and screened for their antimicrobial and antioxidant activities. Crystal structures

of all the complexes confirmed the coordination of the copper atom to two sulfur atoms of the dithiocarbamate ligand as well as the two phosphorus atoms of the PPh_3 units, which resulted in distorted tetrahedral geometry. Our intention in these preparations arose from complexes with ligands containing phosphorus having been reported to display excellent activities. However, our studies showed that the heteroleptic Cu(I) complexes **25** – **32** showed only moderate to low antimicrobial activities against Gram-negative bacteria and none of them were active against Gram-positive positive bacteria. They were less active when compared to Ni(II), Cu(II) and Co(III) dithiocarbamate complexes **7** – **24** and to ciprofloxacin. The ligands' associated electronic factor seems to not have affected the antimicrobial activities of the complexes **25 - 32**. The heteroleptic Cu(I) complexes displayed better antioxidant activities than **DL1** – **DL8** but were still less effective than **7** – **24**. Compounds **26** and **30** had the highest and lowest free radical scavenging activities, respectively, while **27** had the highest nitric oxide scavenging activity. Complexes **25** – **30** showed a remarkable luminescent property in CH_2Cl_2 at room temperature, but displayed poor electrical conductivities.

6.2 General conclusion

The outcomes of this research work are stated below;

- The N,N'-diarylformamidine dithiocarbamate based thiuram disulfide, metal complexes and Cu(I) heteroleptic PPh_3 complexes were successfully synthesized as shown by the results of FT-IR, UV, NMR and Mass spectroscopic studies, elemental analysis and single crystal structures.
- The thiuram disulfides **1** – **6** displayed better antimicrobial activities against Gram-negative bacteria strains, *Pseudomonas aeruginosa, Salmonella typhimurium, E coli* than did the potassium dithiocarbamate salts, while the dithiocarbamate salts displayed better antimicobial activies against *K. pneumoniae*.than did 1 – 6.
- Cheminformatic evaluation and *in silico* investigation using efficient computational tools on the thiuram disulfide **1 - 6** revealed that all the compounds had minimal violations of Lipinski's rule but exhibited inclinations to be orally bioavailable and less toxic. Only compounds **1** and **4** exhibited dual selective inhibitory activities towards the inflammatory mechanism of cancer, cyclooxygenase -1 and 2.
- Potassium dithiocarbamate salts **DL1** – **DL6** and thiuram disulfide **1** – **6** displayed poor antioxidant activity. However, **DL1** – **DL6** exhibited better antioxidant action than did **1** – **6**.

- ❖ All the metal complexes showed better antimicrobial activities than did the corresponding ligands. In particular Co(III) complexes **23** and **24** showed broad spectrum antimicrobial activities against Gram-negative bacteria strains, with better activities than even the reference drug ciprofloxacin.
- ❖ All the complexes displayed poor activity against Gram-positive bacteria strains *S. aureus* and MRSA. An exception was the Cu(II) complexes **13** – **18,** which showed excellent activities against *S. aureus* where it was even more active than ciprofloxacin.
- ❖ Complexes which formamidine that bore chlorine atoms showed better activities than those that bore no chlorine atom.
- ❖ All the complexes displayed moderate to good antioxidant activities. Compounds **19** and **20** displayed the highest DPPH free radical activities of all the compounds tested and exhibited better activities than even ascorbic acid.
- ❖ The complexes **25 - 32** did not exhibit good bacterial growth inhibitory and only displayed moderate antioxidant activities. However, they showed a remarkable luminescent property.

6.3 Future work

- ❖ More quantitative and qualitative theoretical methods such as Quantum mechanism (QM), Molecular mechanism (MM), Molecular dynamics (MD), and MM/PBSA-based free binding energy estimations should be carried out on compounds **1** and **4** to verify and validate their dual mechanistic binding and bonding formation at the active sites of COX-1/2. Also, both compounds should be screened against cancer cells in vitro so as to affirm their anticancer properties that has been projected computationally.
- ❖ Some of the metal complexes showed promising antimicrobial activities, it is therefore necessary to carry out cytotoxicity tests with them, to ascertain whether they are damaging or not to tissue cells.
- ❖ All the dithiocarbamate metal complexes and heteroleptic Cu(I) dithiocarbamate PPh_3 complexes should be screened for their anticancer activities.
- ❖ Ruthenium-based compounds have been gaining interest due to their excellent antimicrobial and anticancer activities. It would be of interest to synthesize ruthenium dithiocarbamate complexes using **DL1** – **DL8** and to test them for their antimicrobial and anticancer activities.

❖ The unsymmetrical N,N'-diarylformamidine ligands can be modified by introducing fluorine and bromine atoms as depicted in Figures **6.1a** and **6.1b** to establish how these elements would affect the antimicrobial activities of the complexes compared to the chloro derivatives reported in this research work.

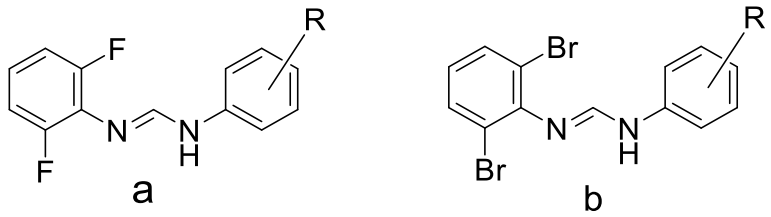

Figure 6.1: Modified unsymmetrical N,N'-diarylformamidine.

❖ The use of ferrocenyl aniline derivatives during the synthesis of formamidine could afford N,N'-diarlyferrocene formamidine, which could be used to synthesize dithiocarbamate bimetallic complexes that might improve the antimicrobial and the antioxidant activities of those complexes reported in this research work. The reaction scheme is given below:

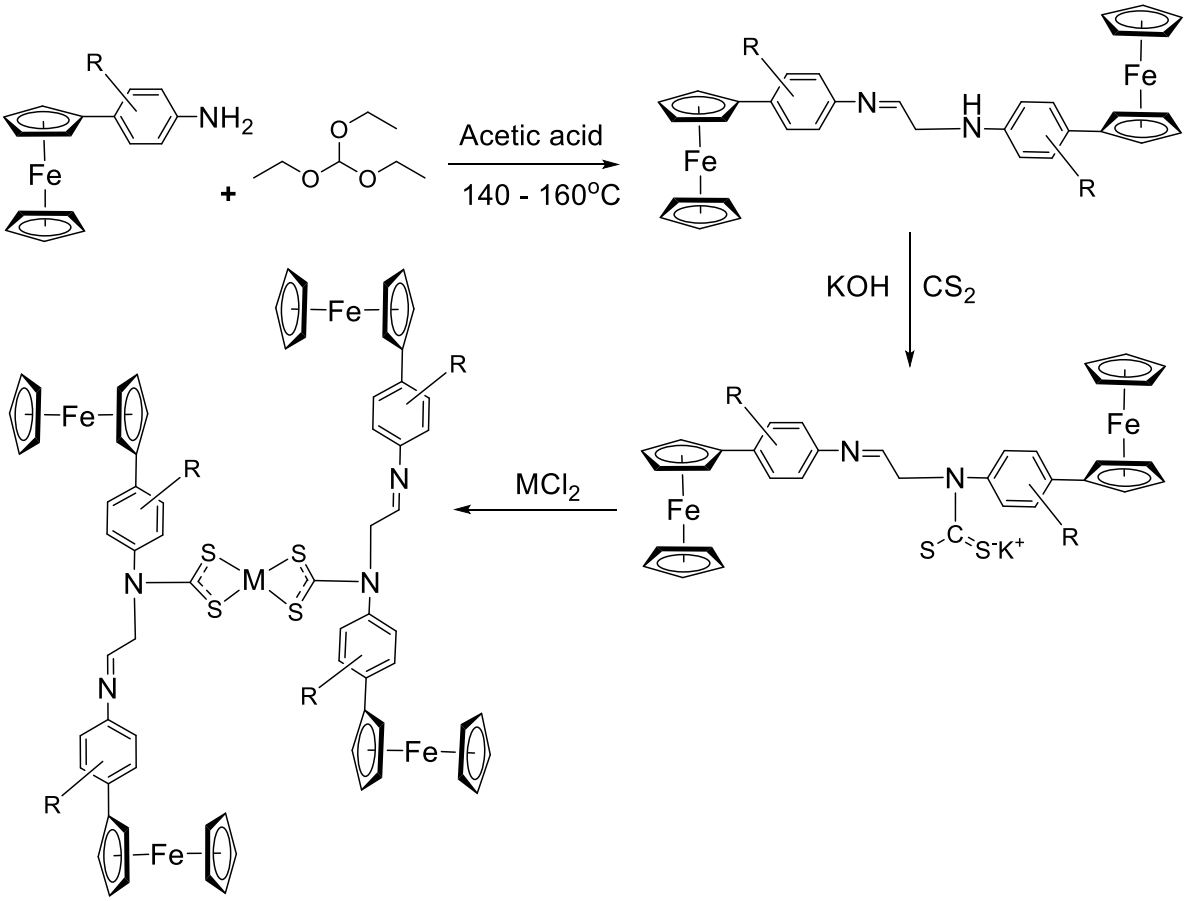

Scheme 6.1: Synthesis of N,N'-diarylferrocene dithiocarbamate metal complexes.